
THE UNIVERSITY *of* EDINBURGH

# Chlorometallate Extraction (Base Metals)

**Ross Johannes Ellis**


**Doctor of Philosophy**

**University of Edinburgh**

**September 2009**

## Preface and Declaration

The author graduated from the University of Edinburgh in 2006 with a BSc. (Hons) degree in Chemistry, and since then has been engaged in a programme of full time research under the supervision of Professor Peter A. Tasker at the University of Edinburgh.

The work presented in this document is the original work of the author, except where references are made to other sources. It has been composed by the author and has not been submitted previously in whole or in part for another degree or qualification from this or any other university or institute of learning. In accordance with the regulation, this thesis does not exceed 70,000 words in length.

Ross Johannes Ellis
September 2009

## Abstract

The work outlined in this thesis was sponsored, in part, by Anglo American and concerns the development of new technologies to achieve the *concentration* and *separation* of base metal values in chloride hydrometallurgical circuits. New processes for the production of zinc, cobalt and nickel aim to use solvent extraction to achieve the separation of metal values in highly concentrated acid chloride feeds containing iron and this thesis involves new extractants for potential use in these circuits. Anion exchange solvent extraction was chosen as the most practical approach and so a range of new reagents are described which remove zinc(II), cobalt(II) and iron(III) chlorometallates from acid chloride solutions via the reaction:

$$nL_{(org)} + nH^+ + MCl_x^{n-} \rightleftharpoons [(LH)_nMCl_x]_{(org)}$$

Chapter 1 reviews the literature which concerns base metal chloride hydrometallurgy, presents a range of commercial processes and discusses the chemistry which underpins them. This chapter also outlines the new Anglo American circuits and the general approach to the design of base metal chlorometallate extractants.

In Chapter 2, the analytical methods are discussed. These methods include the solvent extraction experiments that were used to define the behaviour of the new ligands and the techniques that were employed to examine the interactions between an extractant and a chlorometallate anion.

Chapter 3 presents a series of five new amido-functionalised pyridine reagents that were designed to investigate the affect of hydrogen bond donor functionality on the extraction of zinc, cobalt and iron chlorometallates. The pyridine nitrogen atom is sterically hindered in the new reagents to suppress formation of inner-sphere complexes. Solvent extraction performance was found to vary considerably with hydrogen bond donor functionality and ligand structure. The ligand 2-(4,6-di-*tert*-butylpyridin-2-yl)-*N*,*N'*-dihexylmalonamide ($\mathbf{L^2}$) was the *strongest* and most *efficient*

extractant in this series and this was attributed to a 'proton chelate' six-membered ring interaction between the malonamide oxygens and the protonated pyridine nitrogen that resulted in a pre-organised array of N-H and C-H donors that could interact favourably with the chlorometallate anion.

Chapter 4 explores a series of six new tertiary amine-based ligands which contain varying amido-functionality, e.g. 3-(di-2-ethylhexylamino)-*N*-hexylpropanamide (**MAA**). Zinc, cobalt and iron chlorometallate extraction studies show the amide and malonamide-functionalised ligands are notably stronger than the tertiary alkylamine control, tris-2-ethylhexylamine (**TEHA**). Platinum(IV) extraction is also discussed, showing that some of the new reagents are more *efficient* than the tren-based ligands previously described,{Bell Katherine, 2008 #93} which were the most *efficient* known. The enhanced extraction performance of the new 'MAA-type' ligands was again attributed to the formation of a 'proton chelate' six-membered ring forming $[(LH)_2MCl_4]$ assemblies in the organic phase. Conditions have been identified which would allow separation of Fe(III), Co(II) and Zn(II) in circuits which use the 'MAA-type' reagents.

Chapter 5 explores a series of three new malonamide reagents which contain varying alkyl-chain functionality, e.g. *N,N*'-dimethylhexylpentadecylmalonamide ($\mathbf{M^1}$), which are thought to extract chlorometallate anions via protonation of the carbonyl oxygens. Zinc, cobalt and iron chlorometallate extraction studies demonstrate that the malonamide ligands show high *efficiency* and *selectivity* for iron over zinc and cobalt.

Performance as chlorometallate extractants was found to vary considerably with ligand structure and hydrogen bond donor functionality in all three ligand series, with a number of ligands showing potential for commercial application. Analysis of anion-host interactions suggests that chlorometallate binding in the organic phase probably proceeds via an array of both N-H and C-H weak hydrogen bonding interactions between the extractant and the outer-sphere of the metallate complex.

## Acknowledgements

First and foremost I would like to thank Peter for his patience (he probably should have fired me ages ago for missing so many group meetings), guidance (an excellent teacher), inspiration (I'd walk into his office thinking that I hate chemistry and walk out loving it!) and just for being a great boss!

Thanks to the post docs (in chronological order): Arjan (for showing me the ropes early on), Jy (it was a privilege working with you, I genuinely think I would have still been trying to make the first ligand if it wasn't for you!), Christine (for showing me how to use a computer, otherwise I wouldn't have been able to write this. Also for popcorn and sweets), Tim (for taking up where Christine left off and being generally ace to work with), John (you came late on but still managed to supply some great advice), Dave (you've always been there, buddy, for all those questions a PhD student needs to ask!) A very special thanks to Fraser (for all of the crystallography and pretty pictures), Patricia (the comp. chem. wiz-kid!) and Marika (for lots of NMR help!).

Thanks to Kathy for giving me a taste of industrial research. You gave me a great opportunity! (and I'm really sorry for standing on your toe line dancing at Tucson, people like me shouldn't be aloud to wear shoes)

I thank the rest of the Tasker group, past and present, for listening patiently to my awful presentations and then shooting me down in flames. You guys made my time here great. I'll especially miss football and pub quiz night!

Project students: Evan, James and Matt. You guys were a great help! (apart from Matt who was much more of a hindrance ; . ) ).

Thanks to my mates who tried their best to lead me astray but didn't manage! ;.)

And last but not least I thank my family: Antonia (for being a great sister and making life interesting), Remke, Arnout, Ruthie, Mum, Clem, Dad, Charlotte, Opa and Oma, and Grandad. I dedicate this thesis to you, my family (I expect you all to read it).

# Contents

## Abbreviations

| | |
|---|---|
| Δ | change in |
| δ | chemical shift |
| Σ | sum of |
| ° | degrees |
| °C | degree centigrade |
| $ | dollars |
| £ | Great British pounds |
| = | equal to |
| < | less than |
| ≤ | less than or equal to |
| > | greater than |
| ≥ | greater than or equal to |
| % | percent |
| 1D | one-dimensional |
| 2D | two-dimensional |
| Å | Angstrom |
| aq | aqueous phase |
| anal. | analysis |
| Ar | aromatic; aryl |
| b.p. | boiling point |
| BE | binding energy |
| Bu | butyl |
| ca. | *circa* (around) |
| calc. | calculated |
| CHN | carbon, hydrogen and nitrogen |
| CLP | Chlorine Leach Process |
| CLX50 | Pyridine-3, 5-dicarboxylic acid diisodecyl ester |
| COSY | Correlated Spectroscopy |
| d | doublet (NMR) |
| D2EHPA | di(2-ethyl hexyl)phosphoric acid |

| | |
|---|---|
| DBBP | dibutyl butyl phosphonate |
| DCM | dichloromethane |
| DFT | Density Functional Theory |
| DMSO | dimethylsulfoxide |
| E | energy |
| *e.g.* | for example |
| ESI | electrospray (MS) |
| *et al* | *et alli* (and others) |
| *etc* | *et cetera* (and so on) |
| EtO | ethoxy |
| EtOH | ethanol |
| g | gram; gaseous |
| HF | Hartree-Fock |
| HSQC | Heteronuclear Single Quantum Correlation |
| hr | hour |
| ICP-OES | inductively coupled plasma optical emission spectroscopy |
| *i.e.* | that is |
| IE | interaction energy |
| *in vacuo* | under vacuum |
| IR | infrared |
| K | degree Kelvin |
| $K_a$ | association constant |
| L | ligand |
| m | multiplet (NMR), metre |
| *m* | *meta* |
| M | metal |
| M | molar |
| mM | millimolar |
| Me | methyl |
| MeO | methoxy |
| MeOH | methanol |
| $MH^+$ | positively charged parent molecular ion (MS) |

| | |
|---|---|
| MHz | frequency (NMR) |
| mg | milligram |
| ml | millilitre |
| mmol | millimole |
| mol | mole |
| MS | mass spectrometry |
| *m/z* | mass to charge ratio |
| NBO | natural bond order |
| nm | nanometres |
| NMR | nuclear magnetic resonance |
| NOE | nuclear Overhauser effect |
| NOESY | Nuclear Overhauser Effect Spectroscopy |
| *o* | *ortho* |
| org | organic phase |
| *p* | *para* |
| PA | proton affinity |
| PGM | platinum group metal |
| pH | $-\log_{10}[H^+]$ |
| $pH_{0.5}$ | pH when D = 0 |
| $pK_a$ | $-\log_{10}K_a$ |
| PLS | pregnant leach solution |
| ppm | parts per million |
| q | quartet (NMR) |
| s | singlet (NMR); solid |
| SX | solvent extraction |
| t | triplet (NMR) |
| *t* | tertiary |
| T | temperature |
| TBP | tri-*n*-butylphosphate |
| *tert* | tertiary |
| TMS | Tetramethylsilane |
| TOA | tri-n-octylamine |

| | |
|---|---|
| UV-Vis | ultraviolet-visible |
| *via* | by way of |
| *vs.* | versus |
| ZPE | zero point energy correction |

## Ligands

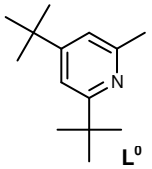
L⁰

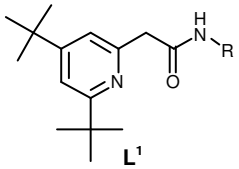
L¹

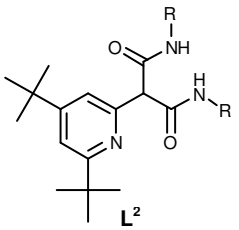
L²

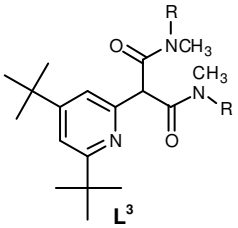
L³

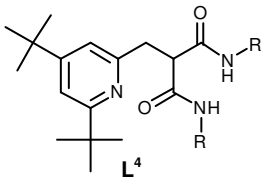
L⁴

Chapter 3 ligands
R = n-hexyl

---

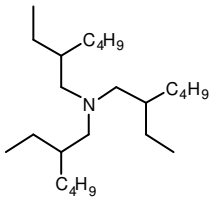
TEHA

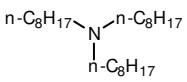
TOA

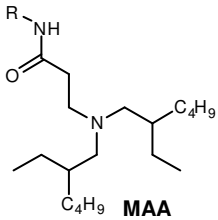
MAA

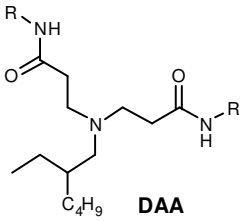
DAA

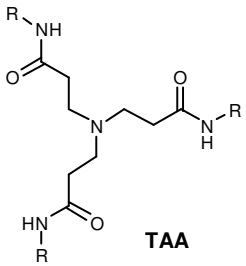
TAA

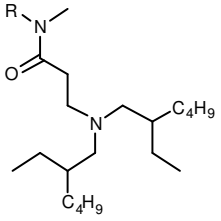
M*t*AA

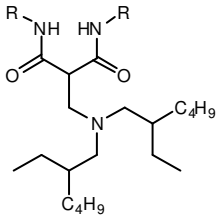
MalA¹

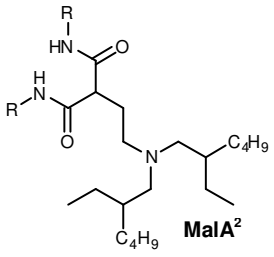
MalA²

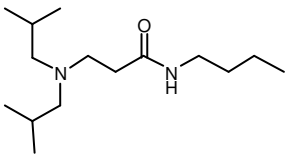
MAAX

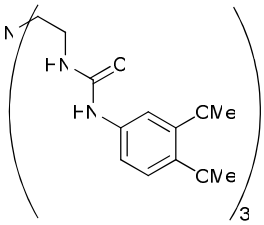
15

Chapter 4 ligands R = n-hexyl

---

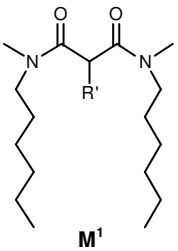
M¹

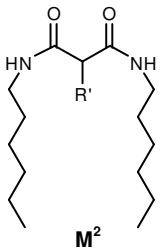
M²

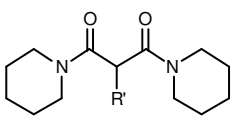
M³

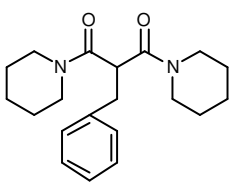
M³X

Chapter 5 ligands R' = n-pentadecyl

# CHAPTER 1

# INTRODUCTION

## 1.1. General Aims

The work outlined in this thesis focuses on the development of new technologies to achieve the *concentration* and *separation* of base metal values in chloride hydrometallurgical circuits. New processes developed by Anglo American for the production on zinc, cobalt and nickel aim to use solvent extraction to achieve the separation of metal values in feeds containing iron and this study investigates new extractants for potential use in these circuits.

## 1.2. The Origins of Chloride Hydrometallurgy

Chloride hydrometallurgy first found application in the production of platinum group metals (PGMs) when, in 1810, W. H. Wollaston established a process involving the dissolution of raw materials containing platinum values in aqua regia.[1] Wollaston's process involved the precipitation of ammonium hexachloroplatinate from the acidic solution, followed by the heating of the resulting solid to form platinum sponge (a porous form of platinum metal). This breakthrough lead to the establishment of Johnson, Matthey & Co., London in 1817, laying the foundation of modern PGM production and chloride hydrometallurgy.[2]

Traditionally, chloride hydrometallurgy has been confined to the PGM sector. However, certain base metal ore types have also been identified as being well-suited to chloride hydrometallurgical treatment and a number of processes have been developed.[3-6] This chapter reviews some of the more elegant and important chloride hydrometallurgical processes for the treatment of these ore types, along with the fundamental chemistry which underpins them.

## 1.3. Leaching

Base metal oxides and sulfides can be transferred into aqueous chloride media by either an oxidative or non-oxidative lixiviant. Although the precise mechanisms for leaching are often complex and specific to the ore type, some general observations can be made.[7]

### 1.3.1. Non-Oxidative Acid Chloride Leaching

A non-oxidative acid chloride lixiviant usually consists of a high strength brine containing HCl that dissolves the metal sulfides or oxides according to:

**Equation 1.1**

$$MO_{(s)} + 2H^+ \rightleftharpoons M^{2+} + H_2O$$

or

**Equation 1.2**

$$MS_{(s)} + 2H^+ \rightleftharpoons M^{2+} + H_2S$$

The acid leaching of pure base metal oxide according to Equation 1.1 is thermodynamically very favourable; however metal oxides are present in ores as part of a silicate lattice so that aggressive leaching conditions (high heat and/or high acidity) are needed to break it down.[7]

The leaching of sulfide ore according to Equation 1.2 is less thermodynamically favourable than leaching oxide ore.[7] Indeed, the dissolution of zinc sulfide (sphalerite) with 1 M HCl yields a solution with a zinc concentration of only about 0.0007 M, which is far too low to be practical in a hydrometallurgy circuit.[8] The leaching of base metal sulfides with HCl, without the aid of an oxidising agent, therefore requires very high acidity in order to force the equilibrium in Equation 1.2 to the right.

A mechanism involving the adsorption of proton and chloride onto the surface of the sulfide or oxide ore has been suggested by several authors.[9-11] Sananayake suggested

a surface reaction mechanism for the leaching of copper oxide, involving the adsorbed species defined in Equation 1.3 and Equation 1.4.[12]

**Equation 1.3**

$$CuO_{(s)} + HCl \rightleftharpoons Cu(OH)Cl_{(ads)}$$

**Equation 1.4**

$$Cu(OH)Cl_{(ads)} + HCl \rightarrow CuCl_2 + H_2O$$

Non-oxidative acid chloride leaching is very effective in high strength brines as the adsorption of HCl is very efficient due to the elevated proton activity.[13]

According to hydration theory, proton activity is a function of both the concentration of acid and the activity of water in solution.[14] Hence, a solution containing low concentrations of acid can still have high proton activity if the activity of water is low. The activity of water can be greatly perturbed by addition of electrolyte and the magnitude of the perturbation is dependent on the hydration number of the electrolyte salt. Hydration numbers of common salts that are used in leach solutions vary according to:

NaCl (3.5) < HCl (8) < $CaCl_2$ (12) < $NiCl_2$ (13) < $MgCl_2$ (14)

A high hydration number creates a greater reduction in the activity of water and, therefore, a larger increase in proton activity.[15] The effect that the concentration of different metal chloride salts has on proton activity in HCl solution was studied by Majima and Awakura, who found that proton activity increased three-fold in 1 M NaCl and twenty-fold in 3 M NaCl, while $CaCl_2$ was found to be twice as effective at increasing proton activity than NaCl due to its higher hydration number.[16] The elevated proton activity in high strength brines is key to making non-oxidative acid chloride leaching effective.

### 1.3.2. Oxidative Chloride Leaching

The oxidative chloride leaching of base metal sulfides is of particular interest in metallurgy as it results in the deposition of elemental sulfur (Equation 1.5) and avoids the generation of sulfur dioxide or sulfates.

**Equation 1.5**

$MS_{(s)} + 2ox \rightarrow M^{2+} + 2ox^{-} + S_{(s)}$

Common oxidants (ox) that are used in commercial processes include $Cl_2$, or Fe(III) and Cu(II) ions. Ferric and cupric oxidants may also be used in sulfate media, although they are more effective in chloride media due to more favourable redox couples.[13] $CuCl_2$ is particularly effective as an oxidising agent as Cu(I) forms stable complexes with chloride which lowers its activity and displaces the reduction equation towards formation of $Cu_{(s)}$ as in Equation 1.6.[13]

**Equation 1.6**

$Cu(II) + e^{-} \rightarrow Cu(I)$

Detailed investigations into the oxidative chloride leaching mechanisms of a range of sulfide minerals have been undertaken and it is clear that the mechanisms are often complex and specific to the ore and oxidant type.[17-19] In general, the transference of metal values from the sulfidic ore into solution, coupled with the deposition of sulfur, is thought to proceed via an acid catalysed mechanism that involves the initial dissolution of sulfur as $H_2S$, followed by oxidation to precipitate $S^0$ (Equation 1.7 and Equation 1.8). This mechanism is supported by investigations into the morphology of the deposited sulfur and the dependence of leaching rate on proton activity.[17, 19]

**Equation 1.7**

$MS_{(s)} + 2HCl \rightarrow MCl_2 + H_2S$

**Equation 1.8**

$H_2S + 2FeCl_3 \rightarrow 2FeCl_2 + 2HCl + S_{(s)}$

Sulfidic ores often contain mixed metal concentrates and this has certain implications on the specific leaching of individual ores types. For example, Crundwell has shown

that the leaching rate of sphalerite (mixed ZnS, FeS ore) is directly dependent on its iron content.[20, 21]. Lead sulfide (galena) is very susceptible to oxidative chloride leaching due to the formation of stable lead chlorometallate complexes that are highly soluble in aqueous media (Equation 1.9). This allows for the selective leaching of galena from mixed sulfidic ore at low temperature.[22]

**Equation 1.9**

$$PbS_{(s)} + 2FeCl_3 \rightarrow PbCl_2 + 2FeCl_2 + S_{(s)}$$
$$\Big\downarrow +2Cl^-$$
$$PbCl_4^{2-}$$

## 1.4. Speciation and Solubility

The speciation of base metal complexes in chloride media can be manipulated by varying the free chloride activity and the pH of the system. This has important implications in the *concentration* and *separation* processes for base metal values through precipitation and solvent extraction mechanisms.

### 1.4.1. The Activity of Chloride

The formation of metal chloro-complexes in aqueous media depends on the activity of chloride ion and the nature of the metal cations in solution. When a metal chloride salt, $MCl_{n(s)}$, is dissolved in aqueous chloride media, free chloride activity changes depending on the chloride 'accepting' or 'donating' ability of $MCl_n$.[6] Berger and Winand proposed the following series to define the chloride accepting ability of various metal chloride salts:[23]

$CuCl > PbCl_2 > ZnCl_2 > CuCl_2 > FeCl_3 > FeCl_2 > NiCl_2 > HCl, NaCl, KCl.$

Strong chloride acceptors, like CuCl, may interact with free chloride in solution to form chloro-complexes (e.g. $CuCl_4^{3-}$), thus decreasing free chloride activity. Metal chloride salts that fully dissociate in aqueous solution (like KCl) are chloride donors and increase free chloride activity by increasing the concentration of free chloride ions and decreasing the activity of water.

The speciation of base metal chloro-complexes in solution depends on free chloride activity. Figure 1.1 shows how the distribution of cobalt chloro-complexes in aqueous media varies according to HCl concentration. At low HCl concentrations (low chloride activity), the cobalt values in solution are cationic complexes, whereas at high HCl concentration (high chloride activity) the cobalt values are anionic complexes. An understanding of the speciation of metal chloro-complexes in solution is crucial for the design of solvent extraction processes for the *concentration* and *separation* of base metal values.

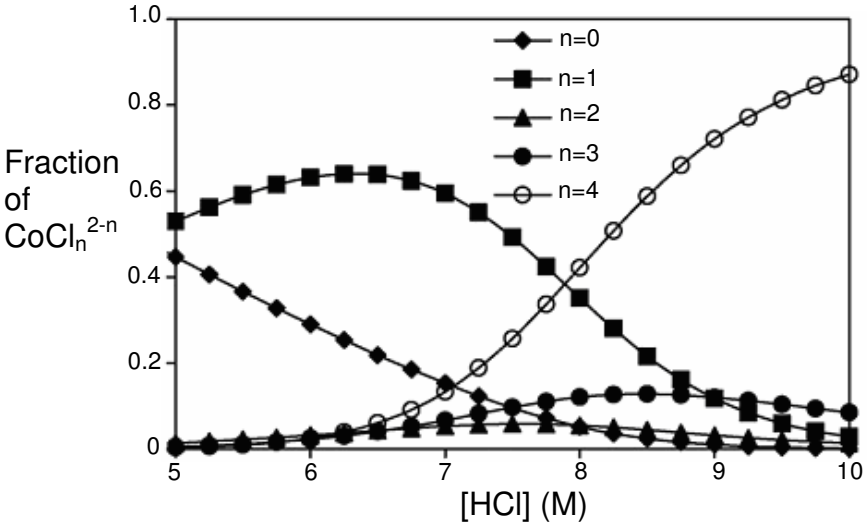


**Figure 1.1: A speciation diagram for Co(II) in aqueous chloride media.[24]**

As the saturated solubility of some base metal chloride salts in aqueous media is quite low, free chloride activity may be manipulated to remove base metal values from aqueous chloride media via precipitation of $MCl_n$. For metal chloride donors (e.g. $NiCl_2$), dissolution in aqueous chloride media may be described by Equation 1.10.

**Equation 1.10**

$$MCl_{2(s)} \rightleftharpoons M^{2+} + 2Cl^-$$

According to Equation 1.10, high free chloride activity will disfavour $NiCl_{2(s)}$ dissolution so, as free chloride activity is increased, the saturated solubility of Ni(II) decreases (Figure 1.2), facilitating the precipitation of $NiCl_{2(s)}$ from solution.[15]

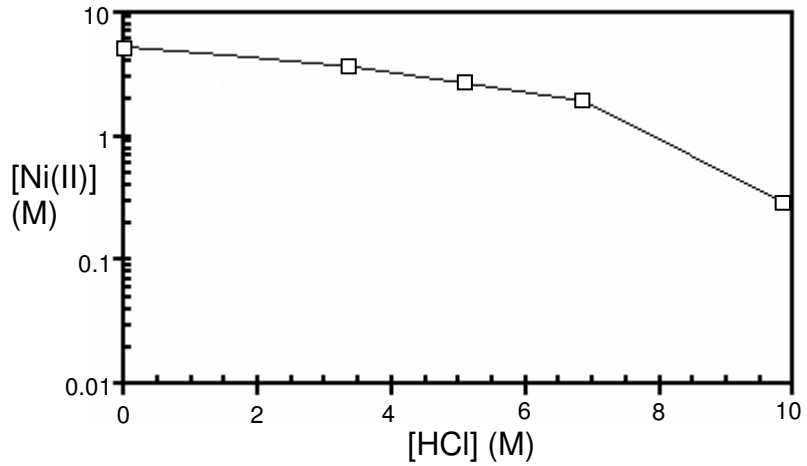


**Figure 1.2: The solubility of Ni(II) in chloride media at 25$^0$C.[15]**

For the dissolution of metal chloride acceptors (like $PbCl_{2(s)}$) that form chloro-complexes of the type $[MCl_n]^{(2-n)}$, the saturated solubility is described by the sum of Equation 1.10 and Equation 1.11.

**Equation 1.11**

$$MCl_{2(s)} + (n-2)Cl^- \rightleftharpoons [MCl_n]^{(2-n)}$$

The saturated solubility of $PbCl_2$ in aqueous solution is described in Figure 1.3.

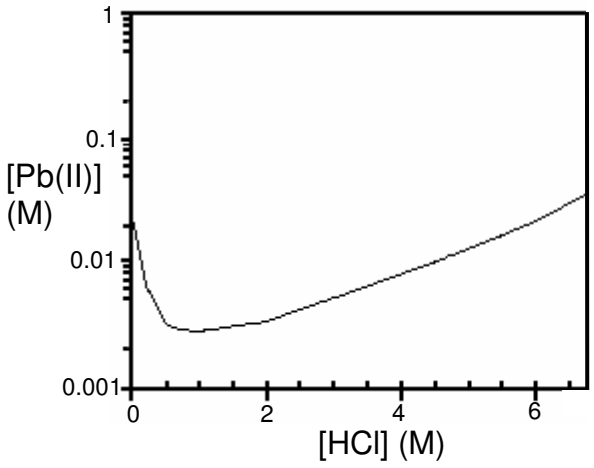


**Figure 1.3: The solubility of Pb(II) in chloride media at 25$^0$C.[15]**

At low free chloride activity, $PbCl_2$ dissolves and forms the soluble $Pb^{2+}$ and $PbCl^+$ cations. As the activity of free chloride is increased, the less soluble $PbCl_2$ species forms and precipitates out of solution. At higher free chloride activity, soluble anionic species such as $PbCl_3^-$ and $PbCl_4^{2-}$ begin to form and so the concentration of Pb(II) in solution increases. Hence the saturated solubility profile of $PbCl_2$ with

respect to free chloride activity (Figure 1.3) shows a minimum where the precipitation of $PbCl_{2(s)}$ is favourable.

### 1.4.2. Activity of Proton

Speciation in aqueous chloride feeds is sensitive to pH and the precipitation of impurities through hydrolysis is useful in hydrometallurgical processes. Antimony and bismuth are common impurities that, when leached into acidic chloride media, form anionic chloro-complexes.[13] The removal of these impurities from the liquor can be achieved by raising the pH above 1 to promote hydrolysis, resulting in the precipitation of the oxychlorides according to Equation 1.12.[13]

**Equation 1.12**

$$BiCl_4^- + H_2O \rightarrow BiOCl_{(s)} + 2H^+ + 3Cl^-$$

Due to its high solubility in acid chloride media, usage as an oxidising agent and great abundance in the earths crust, ferric iron is a common and prolific impurity in base metal leach liquors. Ferric iron is more sensitive to hydrolysis than base metals and can, therefore, be selectively precipitated from solution by careful pH adjustment. Figure 1.4 is an Eh-pH diagram for copper and iron in aqueous chloride media and it clearly shows that, in mildly oxidising conditions, iron will hydrolyse at lower pH than copper. The area marked '**X**', shows conditions where iron precipitates as jarosite (FeOOH) and copper reports in solution as $CuCl_2^-$; a phenomenon that forms the basis of iron removal from the leach liquor in the CLEAR process (discussed in Section 1.7.1).[25]

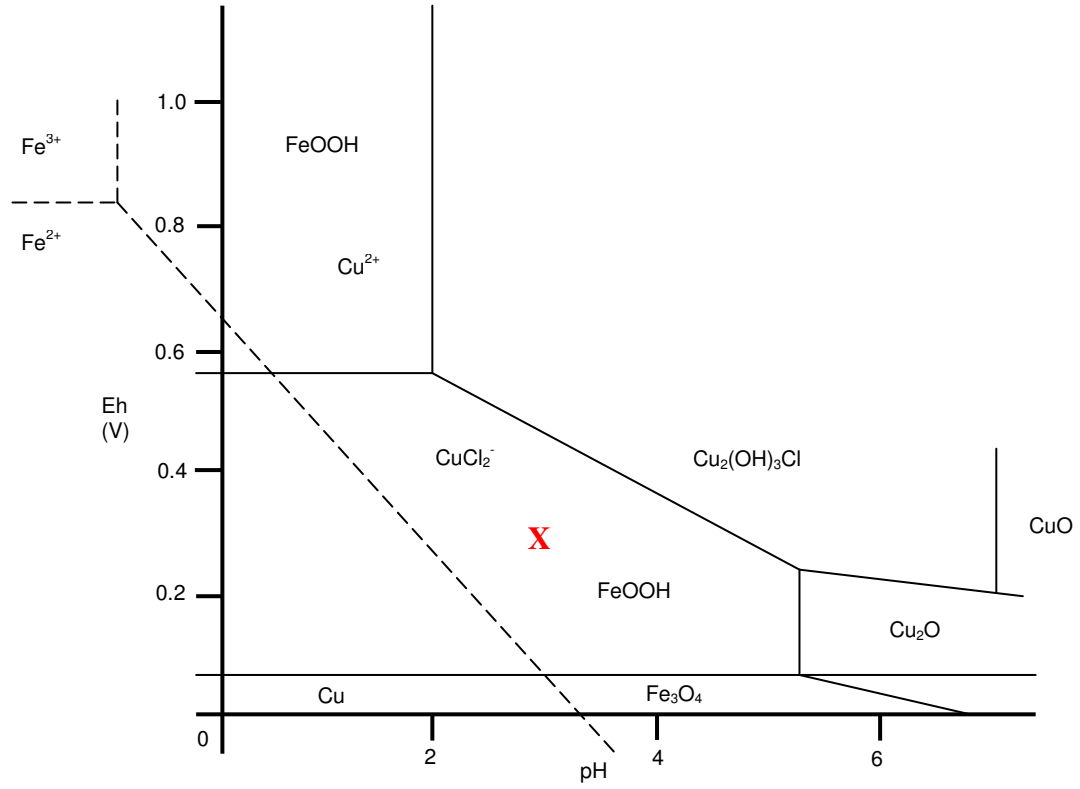


**Figure 1.4: Eh-pH diagram of a Cu-$H_2O$-$Cl^-$ and Fe-$H_2O$ system (3 M NaCl, $90^0$C)** [25]

## 1.5. Solvent Extraction

The high efficiency of chloride leaching ensures that many different metal values report in pregnant leach solutions, warranting efficient and selective processes to achieve the *concentration* and *separation* of the desired metal values prior to electrowinning. Solvent extraction is a versatile and diverse technique that can be used to selectively remove a desired metal value from the leach liquor into a water immiscible organic phase to generate pure electrolyte from which the metal can be obtained. A large number of solvent extraction reagents have been developed for the *concentration* and *separation* of base metal values in chloride media and these have been reviewed.[26]

Solvent extractants can be categorized into three major groups: those that transport metal cations; those that transport metal salts; and those that transport metal complex

anions. This section will focus on the chemistry of some of the reagents which are used in the commercial processes discussed in Section 1.7.

## 1.5.1. Metal Cation Extractants

Base metal cations can be extracted into an organic phase from aqueous chloride media by organic acids according to Equation 1.13.

**Equation 1.13**

$$2LH_{(org)} + M^{2+} \rightleftharpoons [L_2M]_{(org)} + 2H^+$$

The extraction equilibrium is dependent on pH, with loading of the organic phase being favoured when the aqueous feed solution is weakly acidic and stripping can be accomplished by contacting the loaded organic phase with strong acid.

A well studied class of organic acid used in the extraction of base metal cations is the phenolic oximes.[27] Such reagents have been shown to form dimers (see Figure 1.5) with a *pseudo*-macrocyclic structure in solution.[28, 29] Metal cations with planar donor sets, such as Cu(II) and Ni(II), insert into the centre of the *pseudo*-macrocycle as shown in Figure 1.5 with relatively small changes in the geometry of the donor set.

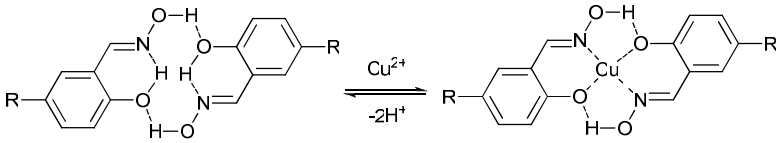


**Figure 1.5: Favourable insertion of Cu(II) into a bis-salicylaldoxime *pseudo*-macrocycle.**

Phenolic oxime extractants have a special selectivity for Cu(II), which is thought to arise from the goodness-of-fit size of the nucleophilic cavity.[28] These reagents have proved so successful that, in 2002, approximately a third of the world's copper was produced using hydrometallurgical processes involving solvent extraction with phenolic oximes.[30]

Organophosphorus acids, such as di-2-ethylhexyl phosphoric acid (D2EHPA, Table 1.1), are also important extractants for metal cations and have recently seen an increase in use in new base metal refining operations such as in Anglo American's large Skorpion zinc plant in Namibia.[31]

| Structure | R | Reagents |
|---|---|---|
| 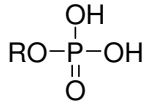 (phosphoric) | $CH_2CH(C_2H_5)C_4H_9^{n}$<br>$C_{18}H_{37}^{iso}$ | MEHPA<br>SBX50 |
| 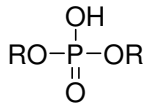 (phosphoric) | $CH_2CH(C_2H_5)C_4H_9^{n}$<br>$C_{10}H_{21}^{iso}$<br>$C_{18}H_{37}^{iso}$ | D2EHPA, DP-8R,<br>Hostarex PA216<br>P204<br>DP10-R<br>TR-63 |
| 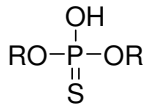 (mono-thio phosphoric) | $CH_2CH(C_2H_5)C_4H_9^{n}$ | Hoe F 3787 |
| 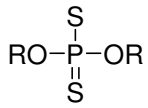 (di-thio phosphoric) | $CH_2CH(C_2H_5)C_4H_9^{n}$ | DEHTPA |
| 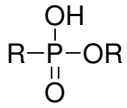 (phosphonic) | $CH_2CH(C_2H_5)C_4H_9^{n}$ | PC-88A, SME, YP-AC,<br>4050-MOOP |
| 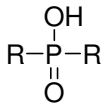 (phosphinic) | $CH_2CH(CH_3)CH_2C_4H_9^{t}$<br>$CH_2CH(C_2H_5)CH_2C_4H_9^{n}$ | Cyanex 272<br>PIA-8 |

| | | |
|---|---|---|
| 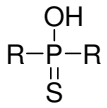 (mono-thio phosphinic) | $CH_2CH(CH_3)CH_2C_4H_9^t$ | Cyanex 302 |
| 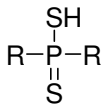 (di-thio phosphinic) | $CH_2CH(CH_3)CH_2C_4H_9^t$ | Cyanex 301 |
| 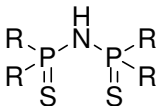 | R= aryl or aryloxy | DS 5968 DS 6001 |

**Table 1.1: The commercial names and structures of phosphorus(V) acid extractants.[26]**

The extraction behaviour of phosphorous acids is influenced by the formation of strong ligand-ligand hydrogen bonds which result in the formation of 8-membered rings which are preserved when metal complexes are formed (Figure 1.6).[32]

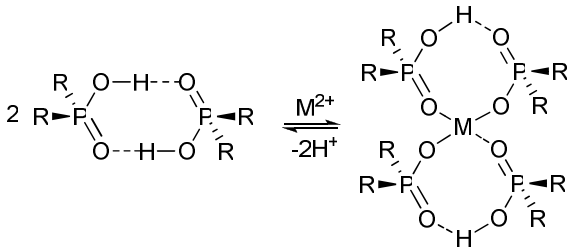

**Figure 1.6: Favourable insertion of $M^{2+}$ into an organophosphorous acid *pseudo*-macrocycle.**

The bite angle in the 8-membered *pseudo*-macrocycle favours metals with tetrahedral coordination geometries, such as Zn(II) and Co(II), over metals with other geometries, such as Cu(II) and Ni(II), and gives rise to unusual anti-Irving-Williams orders of stability.[32]

## 1.5.2. Metal Chloride Salt Extractants

In this type of process, both the metal cation and its attendant anion(s) are transferred into the organic phase. The reagents which facilitate this have often been referred to as 'solvating reagents' because they apparently replace some or all of the water molecules associated with hydration to generate an organic soluble form of the salt.[26]

Chloride activity in organic solvents is high relative to aqueous solutions so that stable metal chloro-complexes are formed in the organic solvents commonly used in extractive metallurgy.[13] Consequently, metal chloride salt extraction usually proceeds via the displacement of some, or all, of the water molecules in the coordination sphere of the metal cation by both chloride ions and by neutral organic electron donors according to Equation 1.14:[26]

**Equation 1.14**

$$MCl_2 + 2L_{(org)} \rightleftharpoons L_2MCl_{2(org)}$$

The organic donors are usually weak bases, limiting protonation, so that extraction is selective for $MCl_2$ over HCl. Tri-*n*-butylphosphate (TBP, Table 1.2) is a neutral ligand that coordinates to metal centres via the oxygen lone pairs of the 'soft' P=O donor. Other weak bases, such as ester-substituted pyridine ligands, like CLX 50 (Table 1.2), are also capable of base metal salt extraction from acid chloride media. The electron withdrawing ester groups lower the basicity of the pyridyl nitrogen.

To optimise extraction of the desired metal value, aqueous phase conditions are adjusted so that free chloride activity favours formation of the neutral $MCl_2$ species of the target metal. Stripping can be achieved by contacting the loaded organic phase with an aqueous phase of low chloride activity so that the metal chloride salt dissociates into the aqueous phase according to Equation 1.15.

**Equation 1.15**

$$[L_2MCl_2]_{(org)} \rightleftharpoons 2L_{(org)} + M^{2+} + 2Cl^-$$

| Structure | R | R' | Reagent |
|---|---|---|---|
| | | | TBP |
| 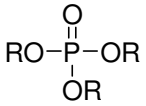 | $C_4H_9^n$ | - | |
| | $C_8H_{17}$ | - | TOPO, Hostarex PX 324, Cyanex 921[a] VP-AC 4046 DBBP |
| 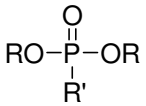 | $C_4H_9^n$ | $C_4H_9^n$ | |
| | $C_2H_5$ | $C_5H_{11}$ | VP-AC 4014 DPPP |
| | $C_2H_5$ | $C_{12}H_{23}$ | DEDP VP A1 4059 |
| 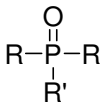 | $C_8H_{17}^n$ | $C_4H_9^{sec}$ | Hostarex 320 |
| 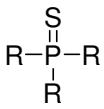 | $C_4H_9^i$ | - | Cyanex 471 |
| 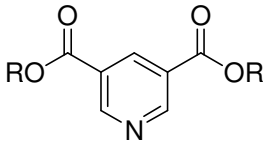 | $C_{10}H_{21}^i$ | - | CLX50 |
| 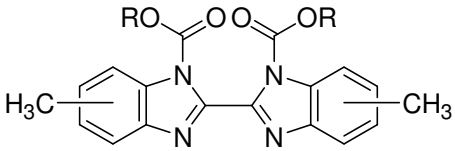 | $C_{13}H_{27}$ | - | ZNX50 |
| RSR | $C_8H_{17}^n$ | - | - |
| | $C_6H_{13}^n$ | - | HOE F 3440, SFI-6 |

**Table 1.2: The structures of some neutral (solvating) extractants. [a]Cyanex 923 contains a mixture of *n*-octyl and *n*-hexyl groups and Cyanex 925 a mixture of normal and branched octyl groups.[26]**

### 1.5.3. Anionic Metal Chloro-Complex Extractants

Base metal values can be separated in chloride streams using 'anion exchange' solvent extraction. This method of solvent extraction can be used to separate metals which form anionic chlorometallate complexes from those that do not.[26] Most chlorometallate solvent extraction processes use alkyl ammonium chloride salts, such as tri-*n*-octylamine hydrochloride (**TOA**·HCl). The solvent extraction mechanism for base metal chlorometallate complexes depends on the system. One possible mechanism results in the protonation of an organic base coupled with direct extraction of the chlorometallate according to Equation 1.16.[33]

**Equation 1.16**

$$2L_{(org)} + 2H^+ + [MCl_4]^{2-} \rightleftharpoons [(LH)_2MCl_4]_{(org)}$$

Other possible mechanisms proceed via reaction of the metal chloro-complex with a chloride salt of the organic base. This may be described as an 'anion exchange' mechanism according to Equation 1.17 and Equation 1.18,[33]

**Equation 1.17**

$$[MCl_4]^{2-} + 2LHCl_{(org)} \rightleftharpoons [(LH)_2MCl_4]_{(org)} + 2Cl^-$$

**Equation 1.18**

$$[MCl_3]^- + LHCl_{(org)} \rightleftharpoons [LHMCl_3]_{(org)} + Cl^-$$

or by chelation of a neutral $MCl_2$ moiety according to Equation 1.19.[33]

**Equation 1.19**

$$MCl_2 + 2LHCl_{(org)} \rightleftharpoons [(LH)_2MCl_4]_{(org)}$$

The competitive equilibria described in Equation 1.17 and Equation 1.18 lie far to the right due to the *Hofmeister bias.*[34, 35] The *Hofmeister bias* is used to relate the effects of anion solvation to extraction. Anions that have a high hydrophilicity are highly solvated in the aqueous phase and are, therefore, harder to extract into water immiscible solvents. Table 1.3 shows the hydration enthalpies of a selection of anions. In solvent extraction, these anions show the following selectivity (most readily extracted anions on the left), demonstrating that lower hydration enthalpies favours extraction:[36]

$$ClO_4^- > I^- > NO_3^- > Br^- > Cl^- >> SO_4^{2-} > CO_3^{2-} > PO_4^{3-}$$

| Anion | $ClO_4^-$ | $I^-$ | $NO_3^-$ | $Br^-$ | $Cl^-$ | $SO_4^{2-}$ | $CO_3^{2-}$ | $PO_4^{3-}$ |
|---|---|---|---|---|---|---|---|---|
| $\Delta_{hyd}H^o$ (kJ/mol) | -205 | -287 | -316 | -328 | -359 | -1099 | -1486 | -2921 |

**Table 1.3: Standard absolute molar hydration enthalpies of selected anions.**[37]

In general, large and more charge diffuse anions have lower hydration enthalpies than small and highly charged anions. This means that large, charge diffuse chlorometallate anions extract more favourably into water immiscible organic solvents than small, charge localised ions, like chloride.

Stripping the chlorometallate from the water immiscible organic phase is possible by raising the pH of the aqueous phase to deprotonate the extractant (Equation 1.20) or by decreasing the chloride activity so that formation of anionic chlorometallate species is disfavoured and the metal values are recovered from the organic phase as neutral or cationic complexes (Equation 1.21).

**Equation 1.20**

$$[(LH)_2MCl_4]_{(org)} + 2NaOH \rightarrow 2L_{(org)} + MCl_2 + 2NaCl + 2H_2O$$

**Equation 1.21**

$$[(LH)_2MCl_4]_{(org)} \rightarrow 2LHCl_{(org)} + MCl_2$$

The charge-charge electrostatic 'ion-pairing' interaction between the ligand and chlorometallate complex is usually considered to be the dominant force in anion extraction.[32] However, it has been shown recently that multiple N-H and C-H hydrogen bonding interactions between the ligand and the outer-sphere of the chlorometallate anion is important both in stabilising the assembly in the organic phase and in extraction selectivity for chlorometallate over chloride.[38, 39]

## 1.6. Reduction and Regeneration

Of great importance in hydrometallurgical circuits are the processes used for reducing the cationic metal values and regenerating the reagents consumed in the leaching of the ore. An insight into the chemistry underlying the reduction and regeneration techniques is key to our understanding of chloride hydrometallurgical processes.

### 1.6.1. Reduction

At the heart of hydrometallurgy is the ability to reduce metal values using relatively clean methods that do not require large amounts of heat and carbon. In the production of base metals, it is common to reduce the metal values in aqueous solution using electrolysis.

The electrolytic reduction of base metal cation, $M^{2+}$, in aqueous chloride media yields chlorine gas and the metallic solid (Equation 1.22 and Equation 1.23).

**Equation 1.22**

$$M^{2+} + 2e^- \rightarrow M^0_{(s)}$$

**Equation 1.23**

$$2Cl^- \rightarrow Cl_{2(g)} + 2e^-$$

On thermodynamic grounds, oxygen has a lower reduction potential than chlorine and should, therefore, be evolved instead. However, chlorine discharge is kinetically favoured due to efficient adsorption of chloride onto the surface of the electrode.[13] The reduction mechanism of the metal is also thought to proceed via an adsorbed chloride species. For example, for the reduction of Ni(II) in chloride solution, the following mechanism was proposed (Equation 1.24 and Equation 1.25):[40]

**Equation 1.24**

$$NiCl^+ + e^- \rightarrow NiCl_{(ads)}$$

**Equation 1.25**

$$NiCl_{(ads)} + e^- \rightarrow Ni^0_{(s)} + Cl^-$$

The metallic structure of the reduced deposits and reduction overpotential are important factors to consider in hydrometallurgical processes and are dependent on the type of metal cation and background electrolyte. The overpotential for base metal reduction from chloride media is generally lower than for sulfate media due to the higher conductivity of chloride electrolytes.[6] For copper ions, the reduction overpotential in chloride media can be significantly lower than in sulfate as the one-electron reduction/oxidation of the $Cu^{+}$ ion is possible in chloride solutions and this has important implications in hydrometallurgical processes, such as in the CLEAR process (Section 1.7.1). However, reduction of copper values in chloride media yields a granular, crystalline product which is undesirable compared to the uniform sheets that report from sulfate media.[41] Reduction of zinc in chloride media gives a 'sponge-like' product which is undesirable in comparison to the uniform sheets gained from sulfate solution.[42] In contrast, cobalt and nickel give a better metallic product when reduced in chloride media, compared to the nodular deposits achieved in sulfate media, which is, in part, responsible for the success of chloride hydrometallurgy in the treatment of nickel-cobalt mattes (see Section 1.7.3).[6]

An important factor that affects the overpotential in the electrolytic reduction of base metal values is the concentration of chloride in the electrolyte. In chloride solutions, free chloride activity affects the reduction overpotential of the metal cation depending on whether it is a chloride donor or acceptor. For strong chloride donors, like Ni(II), a high free chloride activity decreases the activity of water and, therefore, increases the activity of the metal cation resulting in a lower reduction overpotential. For chloride acceptors, such as Zn(II), a high chloride activity increases chloro-complex formation and therefore decreases the activity of metal cation resulting in a higher reduction overpotential.[43]

An alternative to the electrolytic reduction of base metal values is chemical reduction. In hydrometallurgy, the chemical reduction of base metal cations has been used for a long time, for example, in the 1670s mine waters were treated with scrap iron to precipitate or 'cement' out copper.[44] Cementation is also used in more modern processes to facilitate the selective reduction of metal values from solution,

such as in the processes discussed in Section 1.7.2. In other processes (see Section 1.7.3.1) hydrogen gas is used as a reducing agent to produce metal from metal oxides according to Equation 1.26:[7]

**Equation 1.26**

$MO_{(s)} + H_{2(g)} \rightarrow M^{0}_{(s)} + H_2O$

## 1.6.2. Regeneration

Efficient on-site regeneration of materials consumed during the hydrometallugical process makes the system more sustainable and cost effective. The acid chloride leaching of base metal ores results in the consumption of proton and the build-up of undesired metal chloride salts, such as $MgCl_2$ and $FeCl_2$. A useful method for the removal of these unwanted metal chloride salts, while simultaneously regenerating hydrochloric acid, is pyrohydrolysis. In general terms, pyrohydrolysis is the high temperature reaction of water vapour and oxygen with the metal chloride to produce hydrochloric acid and metal oxide as shown in Equation 1.27.[45]

**Equation 1.27**

$2FeCl_2 + 2H_2O_{(g)} + ½O_{2(g)} \rightarrow Fe_2O_{3(s)} + 4HCl$

The growing demand for HCl as a lixiviant in the base metal industry is stimulating the development of new, and more efficient, pyrohydrolysis techniques.[46]

Another way of regenerating materials consumed in chloride hydrometallurgical processes is via a chloralkali cell (Figure 1.7).

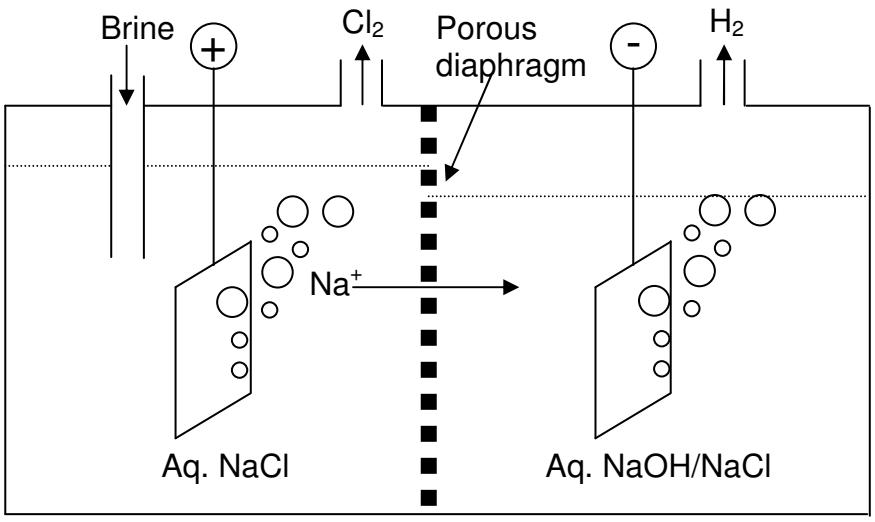


**Figure 1.7: A simplified diagram of a chloralkali cell, showing the major functions.[47]**

The chloralkali cell produces $Cl_2$ and $H_2$ from brine using electrical power and the main reactions are described by Equation 1.28, Equation 1.29 and Equation 1.30.

**Equation 1.28: Anodic reaction**

$$Cl^- \rightarrow \tfrac{1}{2}Cl_{2(g)} + e^-$$

**Equation 1.29: Cathodic reactions**

$$Na^+ + e^- \rightarrow Na + H_2O \rightarrow Na^+ + OH^- + \tfrac{1}{2}H_{2(g)}$$

**Equation 1.30: Overall reaction**

$$NaCl + H_2O \rightarrow NaOH + \tfrac{1}{2}Cl_{2(g)} + \tfrac{1}{2}H_{2(g)}$$

The porous diaphragm is of key importance to chloralkali cell technology as it must only be permeable to $Na^+$ and not $Cl^-$. The 'poisoning' of the diaphragm with other metals, such as $Mg^{2+}$, can be problematic.

## 1.7. Processes for the Recovery of Base Metals from Chloride Media

For certain base metal ore types, hydrometallurgical treatment in chloride media is thought to be more advantageous than treatment in sulfate media. This section discusses some of the most elegant and important processes that have been developed for the commercial treatment of these ore types in chloride media.

### 1.7.1. Copper Production from Sulfidic Ore

It is estimated that about 50% of the world's copper deposits exist in the form of sulfidic copper ores such as chalcopyrite ($CuFeS_2$).[48] Leaching sulfidic copper ore into sulfate media involves oxidative leaching at high temperature and pressure, resulting in a build-up of sulfuric acid in the circuit and release of $SO_2$.[27] High energy consumption and poor materials balance makes the hydrometallurgical treatment of sulfidic copper in sulfate media uneconomical in comparison to traditional smelting techniques.[27] On the other hand, oxidative chloride leaching of sulfidic copper ore offers several advantages relating to metal purification and recovery options, sulfur control and process economics.[3]

One of the earliest processes designed for the chloride hydrometallurgical treatment of chalcopyrite ore was developed during the late 1970s and early 1980s by the Duval Corporation.[49] Duval's 'CLEAR' process (Copper Leaching, Electrowinning and Recycle) remains the only example of large-scale commercial production of copper from chalcopyrite ore in chloride media. The CLEAR process used a two-stage leach to obtain an electrolyte containing cuprous chloride followed by the removal of iron from solution. Sulfur is generally precipitated in its elemental form, although some sulfate is evolved.[3]

In the first leach stage of the CLEAR process, the chalcopyrite ore is *partially* leached into strong brine according to Equation 1.31.[6]

**Equation 1.31**

$2CuFeS_{2(s)} + 3CuCl_2 \rightarrow 4CuCl + FeCl_2 + 2S_{(s)} + CuFeS_{2(s)}$

The sulfur and chalcopyrite solids are removed and the clarified solution is sent to the electrolysis unit where copper metal is deposited from the solution according to Equation 1.32 and Equation 1.33.[3]

**Equation 1.32**

$Cu^+ + e^- \rightarrow Cu^0_{(s)}$ (cathode)

**Equation 1.33**

$Cu^+ - e^- \rightarrow Cu^{2+}$ (anode)

The reduction and oxidation reactions described in Equation 1.32 and Equation 1.33 happen at low voltage which means that copper can be electrowon selectively over other metal values. The $Cu^{2+}$ that forms at the anode is recycled into the second leaching stage.

The second leaching stage involves treating the sulfur-chalcopyrite residue from the first leaching stage with the spent electrolyte under oxygen pressure to precipitate iron and generate more $CuCl_2$ lixiviant (Equation 1.34).[6]

**Equation 1.34**

$CuFeS_{2(s)} + 2S_{(s)} + 2CuCl_2 + FeCl_2 + 1½O_2 + 3H_2O \rightarrow 3CuCl_2 + 2Fe(OH)_{3(s)} + 4S_{(s)}$

The CLEAR process demonstrated that copper could be produced commercially using a chloride hydrometallurgical process. However, the electrowon product was granular in nature and contained impurities, necessitating further refining which, along with low copper prices, caused the plant to close in 1982.[3]

Various processes to circumvent the problems experienced in the CLEAR process have been developed and tested on pilot plant scale.[3] One such process, the CUPREX process, uses solvent extraction to produce very high purity copper from chloride media. The solvent extraction step involves a pyridine di-ester ligand, CLX50 (Table 1.2), which is very selective for $CuCl_2$ over other metal values, allowing the production of very high purity copper crystals after electrowinning.[50]

The CUPREX process claims to produce copper from sulfidic ores with a very favourable materials balance as shown in Scheme 1.1.

| | | | |
|---|---|---|---|
| $Cu_2S_{(s)} + 4FeCl_3$ | → | $2CuCl_2 + 4FeCl_2 + S_{(s)}\downarrow$ | Leach |
| $2CuCl_2 + 4L_{(org)}$ | → | $2[CuL_2Cl_2]_{(org)}$ | Extract (high $a_{Cl^-}$) |
| $2[CuL_2Cl_2]_{(org)}$ | → | $2CuCl_2 + 4L_{(org)}$ | Strip (low $a_{Cl^-}$) |
| $2CuCl_2$ | → | $2Cu_{(s)} + 2Cl_{2(g)}$ | Electrowin |
| $4FeCl_2 + 2Cl_{2(g)}$ | → | $4FeCl_3$ | Lixiviant regeneration |
| **$Cu_2S$** | → | **$2Cu_{(s)} + S_{(s)}$** | **Overall** |

**Scheme 1.1: The materials balance for copper production in the CUPREX process.**

Although the CUPREX process is an attractive system in terms of product purity and materials balance, electrowinning from chloride media results in an unattractive granular product which is undesirable to the consumer.

The Henkel Corporation (now Cognis) developed a process that leaches sulfidic copper ore into chloride media and transfers the copper values into sulfate media prior to electrowinning.[51] This process involves a ferric chloride lixiviant, similar to that which is used in the Cuprex process, to produce a pregnant leach solution containing $CuCl_2$. This is extracted into an organic phase containing a mixture of two extractants, with the copper values being transferred from one extractant to the other via a scrubbing step. Initially, the $CuCl_2$ salt is extracted from the aqueous phase by a pyridine ester and, by contacting the loaded organic phase with a solution of NaOH, the copper values are transferred from the neutral pyridine ester to the acidic LIX 860 extractant (Figure 1.8), removing chloride from the organic phase. Finally, the organic phase is contacted with $H_2SO_4$ solution to release the copper values back into the aqueous phase from which copper metal is electrowon. This process is described in Scheme 1.2.

| | | |
|---|---|---|
| $Cu_2S_{(s)} + 4FeCl_3$ | $\rightarrow 2CuCl_2 + 4FeCl_2 + S_{(s)}\downarrow$ | Leach |
| $2CuCl_2 + 4L_{(org)}$ | $\rightarrow 2[CuL_2Cl_2]_{(org)}$ | Extract (high $a_{Cl^-}$) |
| $2[CuL_2Cl_2]_{(org)} + 4L'H_{(org)} + 4NaOH$ | $\rightarrow 2CuL'_{2(org)} + 4NaCl + 4L_{(org)} + 4H_2O$ | Scrub |
| $2CuL'_{2(org)} + 2H_2SO_4$ | $\rightarrow 2CuSO_4 + 2L'H_{(org)}$ | Strip |
| $2CuSO_4 + 2H_2O$ | $\rightarrow 2Cu_{(s)} + O_{2(g)} + 2H_2SO_4$ | Electrowin |
| **$Cu_2S_{(s)} + 4FeCl_3 + 4NaOH$** | **$\rightarrow O_2 + 4NaCl + 4FeCl_2 + 2H_2O + 2Cu + S$** | **Overall** |

**Scheme 1.2: The materials balance for copper production in the Henkel Corporation process.[51]**

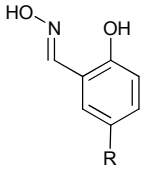


**Figure 1.8: LIX 860 (R = alkyl)**

This process, although producing a high purity copper cathode product, requires the consumption of NaOH and the need for $Cl_2$ to regenerate the $FeCl_3$ lixiviant, necessitating the use of a chloralkali cell which significantly elevates running costs.[3]

## 1.7.2. Base Metal Production from Complex Sulfide Ores

Complex sulfide ores are mixed base metal deposits that generally consist of large amounts of pyrite ($FeS_2$) and sphalerite (mixed FeS, ZnS) combined with smaller amounts of chalcopyrite, galena (PbS) and some silver minerals. The chloride hydrometallurgical treatment of these ores offers considerable advantages over treatment in sulfate media and traditional smelting processes due to better overall metal recovery, metal separation options, sulfur control and selective leaching over pyrite.[4]

Figure 1.9 is a general outline of a hydrometallurgical process for the chloride treatment of complex sulfide ore where precipitation, cementation and solvent

extraction techniques are used to achieve the *concentration* and *separation* of the various metal values.[4]

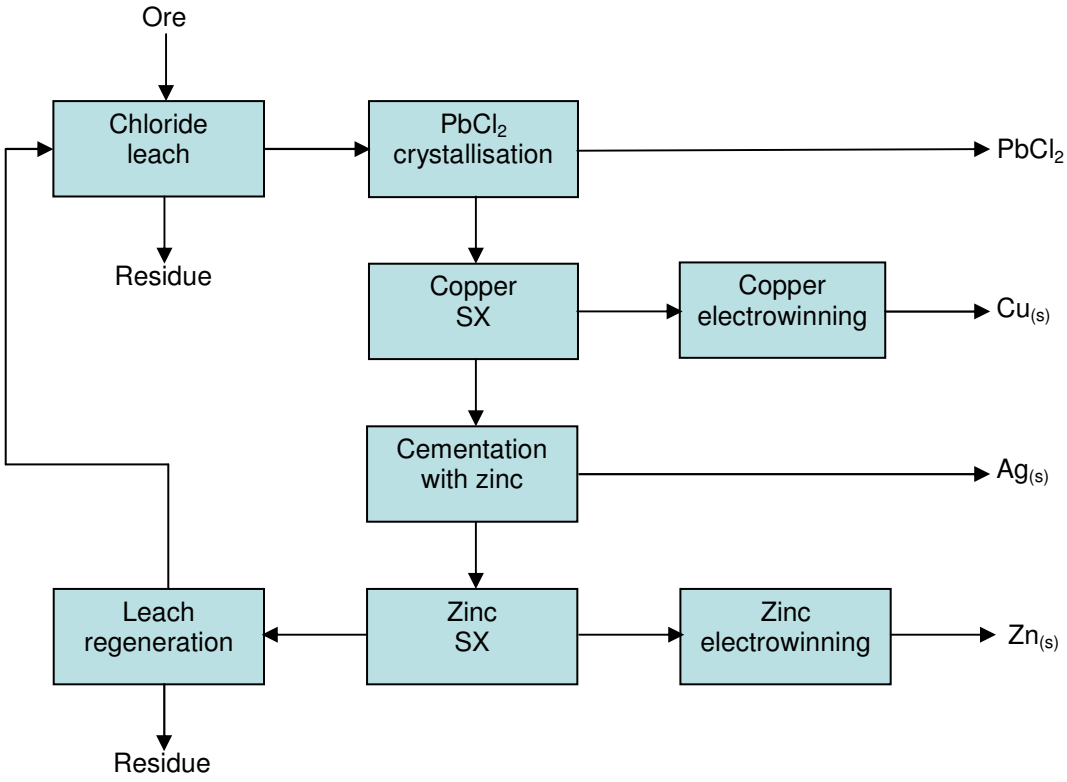


**Figure 1.9: General process outline for the chloride hydrometallurgical treatment of complex sulfide ore.** [4]

In the majority of the processes discussed in the literature that treat complex sulfide ore, an oxidative chloride leach is applied to the ore, transferring the base metal values into solution whilst leaving elemental sulfur and pyrite in the residue (Equation 1.35 and Equation 1.36, M = Zn, Fe, Pb):[3]

**Equation 1.35**

$$CuFeS_{2(s)} + 4ox \rightarrow Cu^{2+} + Fe^{2+} + 2S_{(s)} + 4ox^{-}$$

**Equation 1.36**

$$MS_{(s)} + 2ox \rightarrow M^{2+} + S_{(s)} + 2ox^{-}$$

The Zincex® process was originally a chloride hydrometallurgical process developed by Tecnicas Reunidas in 1976 for the production of zinc from complex sulfide ore.[52] This process circumvented the problems associated with electrowinning zinc from chloride solution by using a two-stage solvent extraction system (Figure 1.10) to

produce a highly pure zinc sulfate electrolyte from a chloride leach liquor. In the first stage, zinc and a small amount of cadmium, iron and copper are extracted from the pregnant leach solution (PLS) as anionic chlorometallate complexes using a secondary amine according to Equation 1.37. The metal values are then all stripped into water to produce a mixed metal chloride solution from which iron and zinc are selectively extracted using D2EHPA (Table 1.1) according to Equation 1.38. The loaded organic phase is then stripped with sulfuric acid to selectively recover the zinc to produce the high purity zinc sulfate electrolyte. The iron is then recovered by contacting the loaded organic with strong hydrochloric acid. Two plants using the original Zincex process operated in Spain and Portugal in the late 1970s and early 1980s.[53] However, the original process has since been simplified, becoming the Modified Zincex Process or MZP, which involves only one solvent extraction step using D2EHPA and can be applied to both chloride and sulfate feeds.[53, 54] The MZP has been so successful that it is used in processes ranging from the recycling of zinc in batteries[55] to the production of zinc at one of the world's biggest mines; Anglo American's Skorpion Zinc facility.[31]

**Equation 1.37: SX 1**

$$2L_{(org)} + 2H^+ + [MCl_4]^{2-} \rightleftharpoons [(LH)_2MCl_4]_{(org)}$$

**Equation 1.38: SX 2**

$$2LH_{(org)} + M^{2+} \rightleftharpoons [L_2M]_{(org)} + 2H^+$$

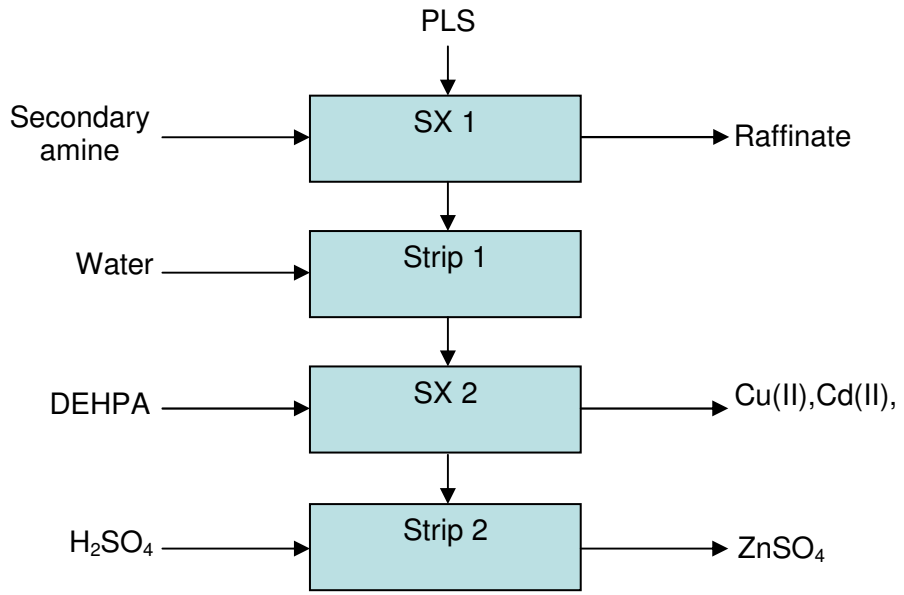


**Figure 1.10: A diagram summarising the two-stage solvent extraction system used to refine zinc in the original Zincex process.**

Another process that has been developed for the treatment of complex sulfide ores in chloride media (but never applied to large-scale refining) has been developed by Minemet Recherche.[56, 57] In this process the ore is oxidatively leached with hot cupric chloride and chlorine in brine. Silver, bismuth and other impurities are then removed from solution by cementation on lead followed by iron hydrolysis and precipitation as goethite. Lead precipitates from the cooled solution as $PbCl_2$ which is then collected, re-dissolved and electrowon. Zinc and copper are extracted and separated by contacting the solution with D2EHPA (Table 1.1) and selectively stripping the copper values with dilute $H_2SO_4$ followed by stripping the zinc values with concentrated $H_2SO_4$.

A process similar to the Minemet Recherche process has been developed by CANMET and has been demonstrated to be economically viable for zinc production.[58] In the CANMET process, the ore body is leached oxidatively into chloride solution with ferric chloride. After leaching, the solution is rapidly cooled to remove the lead via $PbCl_2$ precipitation. The addition of iron powder removes copper and silver from solution via cementation, leaving a liquor from which zinc can be

selectively extracted as $ZnCl_2$ using TBP (Table 1.2). The zinc is stripped into a chloride electrolyte and the small amount of Fe(III) that is also transported into the electrolyte is cemented onto zinc dust prior to electrowinning. The chlorine gas which is produced during electrowinning is used to regenerate the ferric chloride lixiviant according to Equation 1.39.

**Equation 1.39**

$$2FeCl_2 + Cl_2 \rightarrow 2FeCl_3$$

## 1.7.3. Production of Nickel and Cobalt from Sulfide Mattes

Nickel containing sulfidic ores typically contain cobalt, copper, PGMs and large amounts of sulfur and iron. Partial smelting of these ores removes much of the iron and sulfur to produce a nickel-cobalt-copper-PGM sulfidic 'matte' which can then be refined using hydrometallurgy.

### 1.7.3.1. The Falconbridge Nikkelverk Refinery

Perhaps the biggest commercial success in base metal chloride hydrometallurgy is the Falconbridge Nikkelverk refinery in Norway. This is one of the world's largest cobalt/nickel production plants and, over the last 30 years, has seen significant increases in output.[59]

Until 1978, the Falconbridge Nikkelverk refinery used a process to treat nickel-cobalt matte that involved a sulfuric acid leach and inefficient refining.[60] This was replaced by a chloride hydrometallurgical process which has developed to become more efficient and has been well documented.[59, 61-63]

The original chloride Matte-Leach Process (MLP) used at the Nikkelverk refinery involved using concentrated HCl for the acid leaching of the matte, releasing nickel, cobalt and small amounts of copper into solution. Equation 1.40 describes the leaching of the nickel values from the matte.[64]

**Equation 1.40**

$$Ni_3S_{2(s)} + 6HCl \rightarrow 3NiCl_2 + 2H_2S + H_{2(g)}$$

$H_2$ is produced due to the low oxidation state of the nickel in the matte. The small amount of copper in the leach liquor is precipitated as a sulfide by reacting the leach liquor with excess matte according to Equation 1.41.[7]

**Equation 1.41**

$$Ni_3S_{2(s)} + 3Cu^{2+} \rightarrow 3Ni^{2+} + CuS_{(s)} + Cu_2S_{(s)}$$

After the initial leach, the solids containing the copper values and PGMs are collected and leached with $H_2SO_4$; dissolving the copper and leaving the PGMs in the residue for further refining. The chloride leach liquor, containing mainly cobalt and nickel with small amounts of iron and $H_2S$, is further purified first by air oxidation, converting $H_2S$ to elemental sulfur and oxidising all of the iron to Fe(III), followed by solvent extraction with TBP (Table 1.2) for Fe(III) removal according to Equation 1.42.

**Equation 1.42**

$$FeCl_3 + 3TBP_{(org)} \rightleftharpoons TBP_3FeCl_{3(org)}$$

Cobalt is removed from the leach liquor as a chlorometallate anion according to Equation 1.16 by solvent extraction with tri-*n*-octylamine (TOA), and stripped into dilute HCl to produce a $CoCl_2$ electrolyte for electrowinning. $NiCl_2$ crystals are precipitated from the leach liquor by introducing gaseous HCl, which raises free chloride activity, effectively salting out the nickel values (see Figure 1.2). Pyrohydrolysis of the $NiCl_2$ crystals regenerates the HCl lixiviant and produces NiO which is subsequently reduced with hydrogen gas to produce the nickel metal.[63] A diagram summarising the major unit operations of the MLP is shown below (Figure 1.11).

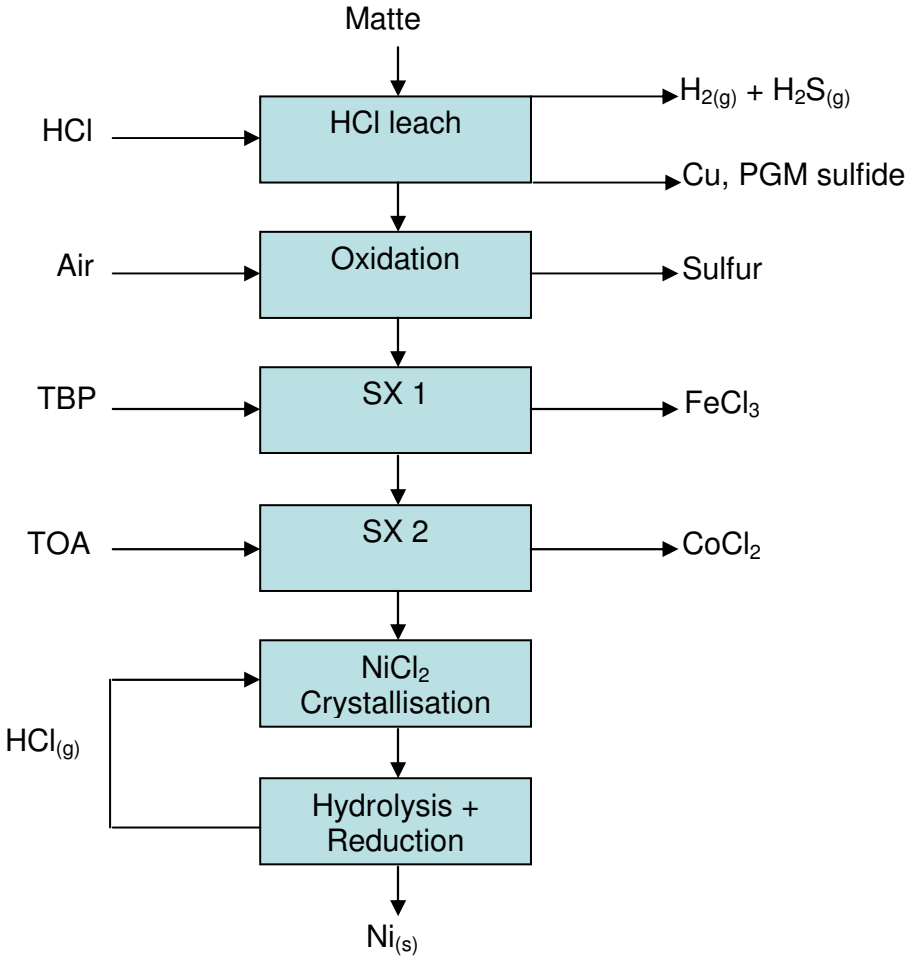


**Figure 1.11: A simplified diagram of the Falconbridge Matte-Leach Process.**

The MLP at the Falconbridge Nikkelverk refinery was not expanded above pilot plant scale as it was quickly superseded by the Chlorine Leach Process (CLP).[61] The CLP is more fuel efficient with a more favourable materials balance compared with the MLP, and was responsible for the expansion of the Nikkelverk plant into one of the world's largest cobalt-nickel refineries.[64]

The CLP uses a copper-catalysed oxidative chloride leach in which $Cl_2$ is consumed as the oxidant (Equation 1.43), releasing the nickel and cobalt values into solution and depositing elemental sulfur (Equation 1.44 and Equation 1.45).

**Equation 1.43**

$$2Cu^{+} + Cl_2 \rightarrow 2Cu^{2+} + 2Cl^{-}$$

**Equation 1.44**

$$Ni_3S_{2(s)} + 2Cu^{2+} \rightarrow 2NiS_{(s)} + Ni^{2+} + 2Cu^{+}$$

**Equation 1.45**

$$NiS_{(s)} + 2Cu^{2+} \rightarrow Ni^{2+} + 2Cu^{+} + S_{(s)}$$

This is an exothermic process, raising the temperature of the solution to near-boiling which is beneficial to leaching kinetics and energy consumption.[64]

After the initial leach, the liquor is contacted with excess matte to remove copper from solution by precipitating copper sulfides, which are separated from the PGM values by leaching the residue with $H_2SO_4$ as described in the MLP. Iron removal in the CLP is achieved by raising the pH of the leach liquor by addition of nickel carbonate which results in precipitation of iron hydroxide. Cobalt is solvent extracted and electrowon in the CLP in the same way as described in the MLP. After cobalt removal, the nickel chloride liquor is electrowon to produce nickel metal.[59] A diagram summarising the main unit operations of the CLP is shown Figure 1.12.

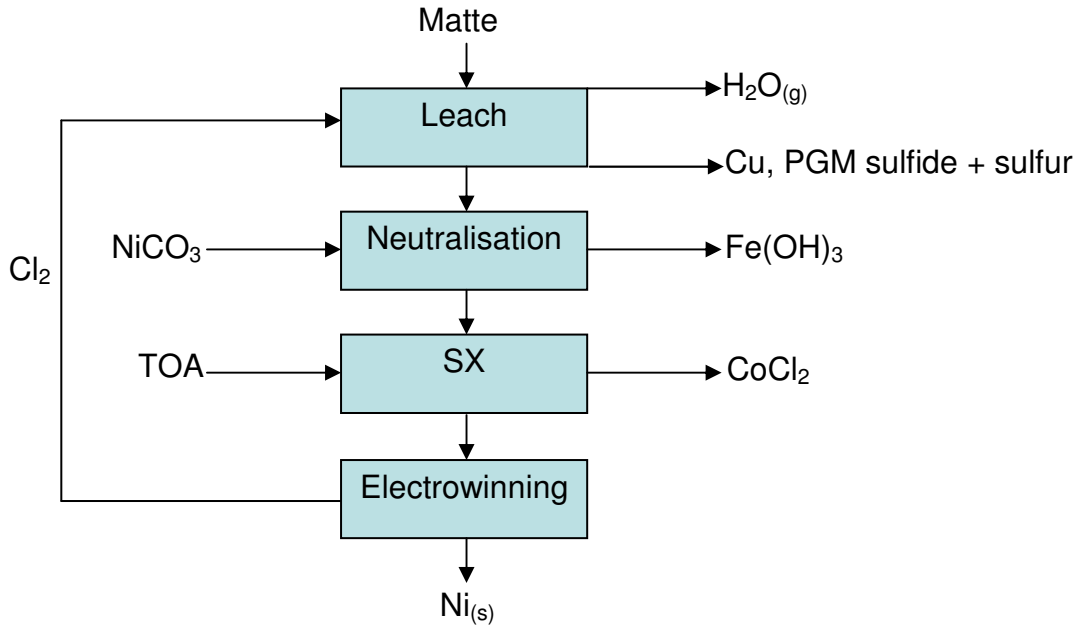


**Figure 1.12: A simplified diagram of the Falconbridge Chlorine-Leach Process.**

### 1.7.3.2. The Sumitomo Metal Mining Co. Nickel Refinery

The Sumitomo Metal Mining Co. (SMM) has developed a chlorine leach process similar to the one used in the Falconbridge Nikkelverk refinery which has been in commercial operation since 1992.[65, 66]

The SMM process (Figure 1.14) uses a similar leach-precipitation method to the Falconbridge CLP (Equation 1.43, Equation 1.44 and Equation 1.45). However, in the SMM process, some of the copper values remain in the pregnant leach solution and these are selectively removed via electrolysis as copper powder. Cobalt and iron are then precipitated from the leach liquor by simultaneous oxidation with chlorine gas and neutralisation with $NiCO_3$ according to the following equations (Equation 1.46 and Equation 1.47):[66]

**Equation 1.46**

$$2Co^{2+} + Cl_2 + 3NiCO_{3(s)} + 3H_2O \rightarrow 2Co(OH)_{3(s)} + 3Ni^{2+} + 2Cl^- + 3CO_{2(g)}$$

**Equation 1.47**

$$2Fe^{2+} + Cl_2 + 3NiCO_{3(s)} + 3H_2O \rightarrow 2Fe(OH)_{3(s)} + 3Ni^{2+} + 2Cl^- + 3CO_{2(g)}$$

The nickel remaining in the solution is electrowon to nickel metal. To separate the cobalt values from the iron in the hydroxide precipitate, the residue is treated with sulfuric acid and sodium sulfite, resulting in the selective leaching of cobalt over iron. After leaching, the resulting sulfate solution is neutralised with aqueous ammonia. Solvent extraction of cobalt from the solution with Versatic Acid 10 (Figure 1.13), followed by stripping with HCl, results in a cobalt chloride electrolyte for electrowinning (Equation 1.48 and Equation 1.49).[67]

**Equation 1.48**

$$2LH_{(org)} + CoSO_4 + 2NH_4OH \rightarrow L_2Co_{(org)} + (NH_4)_2SO_4 + H_2O$$

**Equation 1.49**

$$L_2Co_{(org)} + 2HCl \rightarrow 2LH_{(org)} + CoCl_2$$

(LH = Versatic Acid 10)

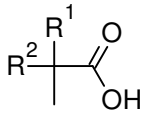


**Figure 1.13: Versatic Acid 10 (R = alkyl).**

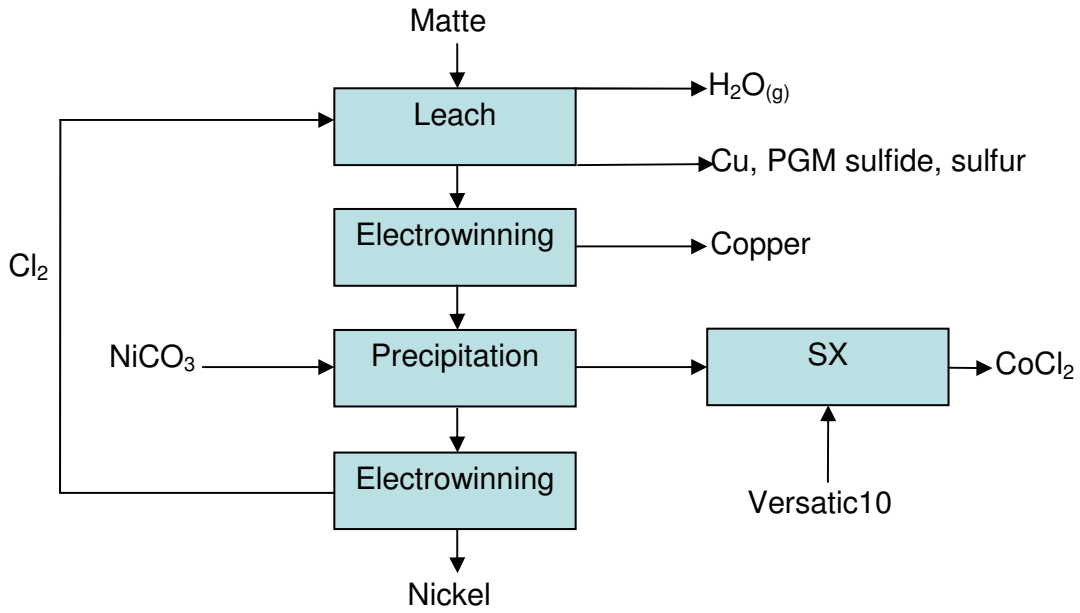


**Figure 1.14: A simplified diagram of the SMM process.**

## 1.7.4. Production of Nickel from Laterites

Lateritic nickel ores are nickel oxides (NiO) that also contain large quantities of other metal oxides, including cobalt (CoO), depending on the ore. The two principal lateritic nickel ores are the iron-containing (FeOOH) limonites and the magnesium-containing ($Mg_3Si_2O_5(OH)_4$) saprolites. It is estimated that about 72% of the worlds nickel resources exist as laterites, and yet these only account for 42% of nickel production.[68] The increasing demand for nickel, coupled with dwindling nickel sulfide resources and environmental pressures, has stimulated renewed interest in the hydrometallurgical processing of nickel laterite ores.[68]

Application of hydrometallurgy to the treatment of nickel laterites dates back seventy years with the patent of Hubler and Archibald (1938), referring to the use of HCl for the selective leaching of nickel oxide over iron.[69] Serious development of a commercial hydrometallurgical process for the treatment of lateritic nickel ores has been much more recent. Chesbar Resources (now Jaguar Nickel) have investigated and compared sulfate and chloride hydrometallurgical processes for the refining of lateritic nickel ore.[5] Leaching tests conducted on nickel-cobalt laterites revealed that

a 20% HCl leach at $80^0$C and atmospheric pressure achieved a comparable percentage nickel extraction to a sulfuric acid pressure leach at $250^0$C. It was found that iron was extracted in both cases, although a better solid-liquid separation was achieved when using HCl. The recycling of lixiviant and neutralising agents (necessary in both sulfate and chloride processes) was found to be more feasible in the chloride process. These initial tests conducted by Chesbar Resources prompted them to develop a chloride hydrometallurgical process, involving an acidic leach, for nickel laterite refining.

The acid leaching of nickel laterites proceeds via a dissociation mechanism according to Equation 1.50, Equation 1.51 and Equation 1.52.[70, 71]

**Equation 1.50**

$$NiO_{(s)} + 2H^+ \rightarrow Ni^{2+} + H_2O$$

**Equation 1.51**

$$FeOOH_{(s)} + 3H^+ \rightarrow Fe^{3+} + 2H_2O \text{ (for limonites)}$$

**Equation 1.52**

$$2Mg_3Si_2O_5(OH)_{4(s)} + 12H^+ \rightarrow 6Mg^{2+} + 4SiO_{2(s)} + 10H_2O \text{ (for saprolites)}$$

Without selective leaching of the nickel values over iron and magnesium, a large quantity of proton is consumed. By using magnesium chloride to make up the lixiviant brine, magnesium leaching from saprolitic ore is minimised, while iron can be precipitated as an oxide or hydroxide by careful pH control when leaching limonitic ore (Equation 1.53).[72] However, the chloride concentration must be maintained such that $FeCl_4^-$ does not form to any extent as this retards iron hydrolysis.[5]

**Equation 1.53**

$$2FeCl_3 + 3H_2O \rightarrow Fe_2O_{3(s)} + 6HCl$$

The process developed by Jaguar Nickel (summarised in Figure 1.15) claims to produce a saleable mixed nickel/cobalt hydroxide product from both limonite and saprolite ores using a process which is both cleaner and more efficient than existing processes.[73] A magnesium chloride lixiviant containing HCl is used to leach the lateritic nickel values into solution. Magnesia (MgO) is added to the leach liquor in

order to adjust the pH to selectively precipitate iron as hematite. After filtration, the resulting solution is treated with more magnesia to precipitate the nickel-cobalt hydroxide product. Acid and magnesia are regenerated by treating the Co/Ni depleted solutions with pyrohydrolysis (Equation 1.54).

**Equation 1.54**

$$MgCl_2 + H_2O \rightarrow MgO_{(s)} + 2HCl$$

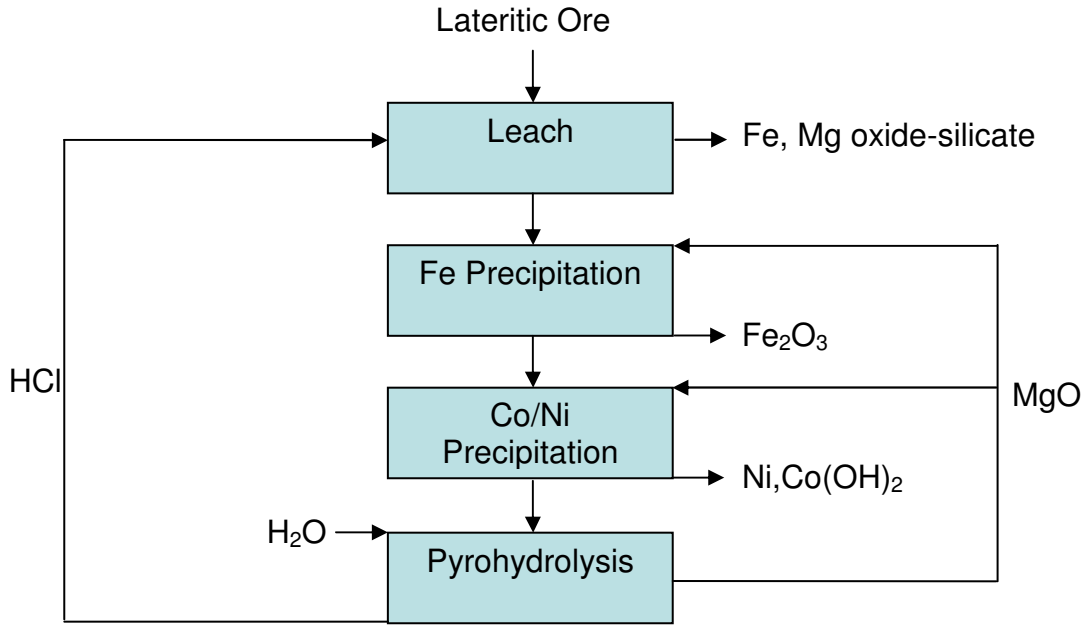


**Figure 1.15: A simplified diagram of a chloride hydrometallurgical process for the production of nickel developed by Jaguar Nickel.**

## 1.8. The Design of Extractants for New Anglo American Circuits for Zinc, Cobalt and Nickel Production

At the outset of the work described in this thesis, a meeting with Anglo Research in Johannesburg in July 2007[74] revealed the details of two new circuits for the production of zinc and cobalt/nickel using chloride hydrometallurgy and some of the specifications of the leach liquors from which solvent extraction of the desired metal values was to be performed.

### 1.8.1. General Circuit Details

Figure 1.16 summarises some of the features of the early Anglo American circuit for the production of zinc metal from sulfidic ores.[74]

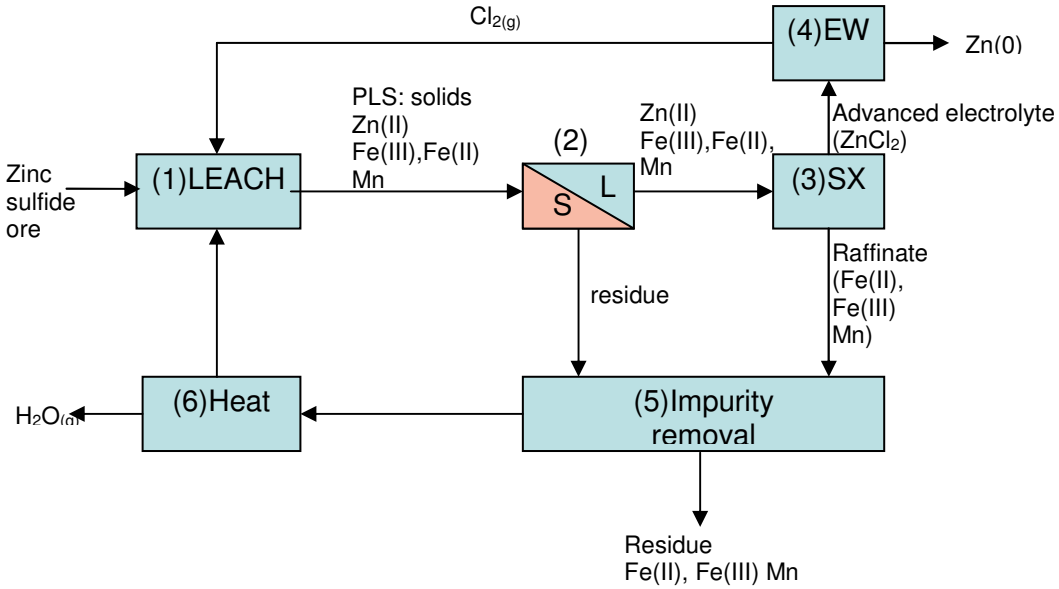


**Figure 1.16: An early draught of the circuit for zinc recovery from sulfide ore.[74]**

The ore is leached (1) into acid chloride media according to Equation 1.55 to produce a PLS of high acidity (about pH -0.7) and high chloride concentration (between 4 and 8 M), leaving elemental sulfur in the residue.

**Equation 1.55**

$ZnS_{(s)} + 2Cl_2 \rightarrow Zn^{2+} + 2Cl^- + S_{(s)}$

The PLS is then moved to the thickener (2) where the solids are removed, leaving the metal chlorides in solution. The zinc chloride is selectively extracted (3) and electrowon (4) with the liberated chlorine being recycled to regenerate the lixiviant. The waste residue and raffinate have all of the manganese and some iron removed in the 'impurity removal' step (5). The remaining solution is concentrated by evaporation of $H_2O$ (6) and recycled into the leaching step (1).

The Anglo American cobalt-nickel circuit is designed to treat lateritic ore bodies. The proposed circuit is similar to that devised by Jaguar Nickel (Figure 1.15), which involves iron removal via pH adjustment followed by the precipitation of nickel and cobalt hydroxide products via the addition of MgO. Anglo American have stated that the circuit could be improved if the nickel and cobalt values could be selectively recovered from the leach liquor via solvent extraction which would avoid the use of MgO to achieve the *concentration* and *separation* of the nickel and cobalt values as hydroxide products. The solvent extraction step for this circuit would be performed at similar chloride concentrations and pH to that in the zinc circuit, with a high selectivity required for the target metal value over ferric iron.

The central theme of this thesis is the development of new extractants to facilitate the *concentration* and *separation* of cobalt, nickel and zinc in the Anglo American circuits.

### 1.8.2. Extractant Design Criteria

When developing a new solvent extractant, certain design requirements must be met if it is to be industrially applicable. Successful reagents must be:

- cheap to synthesise;
- environmentally friendly to produce;
- stable under the required conditions for extraction and stripping;
- soluble exclusively in the organic phase;
- able to extract within a practicable time scale (i.e. show fast kinetics);

- able to extract in the pH range required; and
- selective for the required metal value(s) over other components in the PLS.

As previously discussed, the metal values can be extracted into an organic phase as cations, salts or anions (see Section 1.5). The use of a metal cation extractant would be disfavoured in both the Anglo American zinc and cobalt-nickel circuits as, according to Equation 1.13, the high proton activity in the acidic chloride feeds would make the deprotonation of a weakly acidic extractant unfavourable. A metal cation extractant would be particularly unattractive for use in the zinc circuit as one of the main requirements in the circuit is for the co-extraction of chloride.

In contrast, a metal salt extractant would recover a zinc chloride moiety as required in the circuit. However, the high proton activity in the leach liquor means that protons will compete effectively for the donor atoms in the metal cation binding site and would hinder the inner-sphere complex formation. Also, as metal salt extractants often contain ester functionality (see Table 1.2), the degradation of reagent via hydrolysis would be a risk.

The best solvent extraction mechanism for use in the cobalt-nickel and zinc circuits would appear to be anion exchange. This potentially provides a number of benefits. The complete separation of cobalt from the nickel values using an anion exchange reagent has been proven to be commercially viable in the Falconbridge Nikkelverk Refinery (see Section 1.7.3.1) and the high chloride concentration and acidity of the PLS would make the extraction of a cobalt or zinc chlorometallate moiety according to Equation 1.16 particularly favourable. Another potential advantage associated with anion exchange extraction is the fast kinetics offered by outer-sphere metal complex coordination.

Bearing these arguments in mind, it was decided to opt for the development of new anion exchange reagents and the central theme of this thesis is the design of new reagents to bind strongly and selectively to chlorometallate anions. The new reagents were investigated for the extraction of the base chlorometallate values, $CoCl_4^{2-}$ and

$ZnCl_4^{2-}$, and the major chlorometallate impurity, $FeCl_4^-$, in order to establish selectivity.

### 1.8.3. Anion Recognition

In the design of new anion exchange reagents for the selective recovery of chlorometallate anions in the new solvent extraction circuits, it is useful to consult the literature on anion recognition chemistry. The selective recognition of anions by molecular receptors is of great significance in biology, medicine, environmental science and industry.[75] Compared to cation recognition chemistry, anion recognition is a relatively new field which has its roots in the late 1960s and 1970s.[76-78] Studies by Lehn *et. al.* revealed the halide binding properties of nitrogen- and oxygen-containing cryptands of the type shown in Figure 1.17,[79] and work quickly expanded into guanidinium[80] and polyammonium[81] macrocyclic receptors.

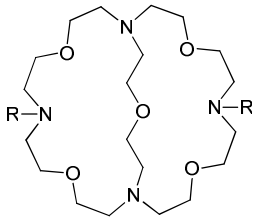


**Figure 1.17: An example of a cryptand investigated by Lehn *et. al.*[79] for anion recognition. Halide anions are bound in the central cavity by hydrogen bonding to the protonated amine groups (R = methyl or an ether 'strap' connecting the amine nitrogens).**

Since the early 1980s, the field of anion receptor chemistry has been enthusiastically developed and is extensively reviewed, with major interest stemming from biological systems, templating and anion sensing.[36, 82-84]

The chemical principles that govern anion recognition differ from those that govern cation recognition due to the difference in ion size, shape and ion-host interactions.[36, 85] Cations tend to be smaller than anions (see Table 1.4) and spherical in shape, whereas anions can be spherical ($F^-$, $Cl^-$, etc.), linear ($N_3^-$, $CN^-$, etc), trigonal planar ($NO_3^-$, $CO_3^{2-}$, etc.), tetrahedral ($FeCl_4^-$, $SO_4^{2-}$, etc.), square planar ($PdCl_4^{2-}$, $[Pt(CN)_4]^{2-}$, etc.), octahedral ($PF_6^-$, $CoCl_6^{2-}$, etc.) and many others.

| Cation | r / Å | Anion | r / Å |
|---|---|---|---|
| $Na^+$ | 0.95 | $F^-$ | 1.36 |
| $K^+$ | 1.33 | $Cl^-$ | 1.81 |
| $Rb^+$ | 1.48 | $Br^-$ | 1.95 |
| $Cs^+$ | 1.69 | $I^-$ | 2.16 |

**Table 1.4: The radius of some isoelectronic cations and anions.[86]**

Anions can bind to receptors via strong non-directional electrostatic ion-pairing forces provided that the receptor carries a positive charge, e.g. in ammonium, imidazolium, pyridinium or guanidinium groups.[85] Hydrogen bond donors are often used in anion receptor frameworks in order to achieve anion recognition through directional hydrogen bonding interactions.[87] A large range of hydrogen bond donor groups including amides, sulfonamides, ureas, thioureas, pyrroles, carbazoles, indoles and hydroxyls have been shown to act as effective anion receptor sites.[87, 88] Another important interaction in anion receptor chemistry is the Lewis acid-base interaction. As anions are Lewis bases, electron-deficient Lewis acidic centres with a low LUMO such as boron, mercury, germanium, silicon and tin may act as effective anion binding sites in receptors.[88]

A major challenge for chemists designing anion receptors is to make them selective for the target anion over other negatively charged species. Selective anion recognition can be achieved by designing a receptor with the shape and size that is complementary to the target anion. Schmidtchen *et. al.* have elegantly demonstrated how the cavity size of positively charged macrocycles (Figure 1.18) can be tuned in order to achieve selectivity between different halides.[89]

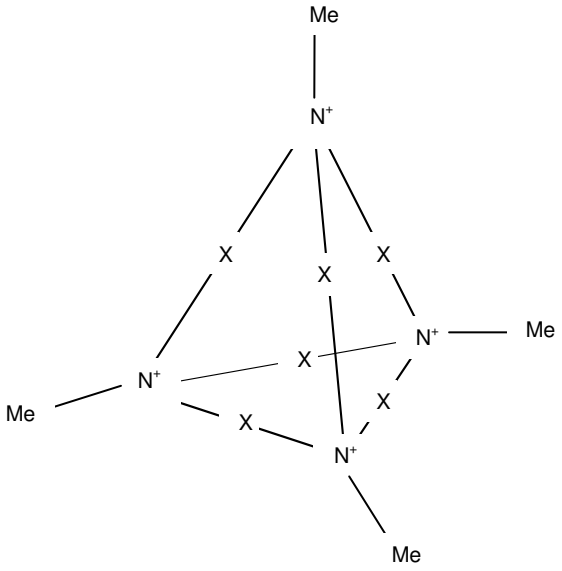


**Figure 1.18: An anion receptor with a positively charged cavity. When the spacer group ($X=(CH_2)_n$) is long the receptor prefers large halides and when short the receptor prefers small halides.[89]**

Lehn *et. al.* have shown that the ellipsoid-shaped hexaprotonated cryptand (Figure 1.19) is selective for linear anions such as azide ($N_3^-$) over other shapes such as tetrahedral perchlorate ($ClO_4^-$), trigonal nitrate ($NO_3^-$) and spherical halides.[77]

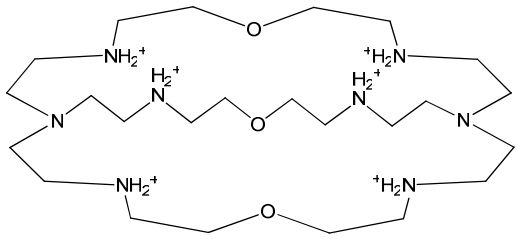


**Figure 1.19: An ellipsoid-shaped hexaprotonated cryptand found to be selective for linear anions.[77]**

In solvent extraction, of particular interest is the selective recognition of chlorometallate anions. The following sections, therefore, consider the design features associated with the development of new reagents for chlorometallate solvent extraction.

### 1.8.4. Hydrogen Bonding to Metal-Bound Halides

Metal-bound halides have been shown to be strong and directional hydrogen bond acceptors,[90, 91] with applications in the field of crystal engineering.[92-97] CH, NH and OH donors have been shown to form hydrogen bonds to metal-bound halides, with (D)H···X distances varying according to the trend: (C)H···X >> (N)H···X > (O)H···X.[91] The stronger NH and OH donors show more of an H···X-M angular preference than CH donors, as weaker bonds are more subject to deformation due to competition with other forces.[91, 98]

Both H···X-M angular preference and hydrogen bond distance is dependent on the halide.[91] The behaviour of metal fluoride acceptors differs from that of the other halogens, with metal fluorides forming much shorter hydrogen bonds than the other halogens according to the trend: H···F << H···Cl ≤ H···Br < H···I.[91] The preferential angle of approach for strong donors (NH) to fluoride (H···F-M = 120-160˚) is also distinct from that of the heavier halogens (H···X-M = 90-130˚).[91] Brammer *et. al.* have explored the origin of the trends in the preferred angular approach of H···X-M bonds by considering the electrostatic potential in the vicinity of the terminal halide ligand, X, in a series of model systems, *trans*-PdX($CH_3$)($PH_3$)$_2$, as calculated by Hartree-Fock methods.[91] Figure 1.20 shows the negative regions associated with this series of compounds and in each case the regions of greatest negative potential lie close to the halogen. The points of minima in the electrostatic potential should dictate the angular approach of hydrogen bond donors and this is in good agreement with crystallographic data.[91]

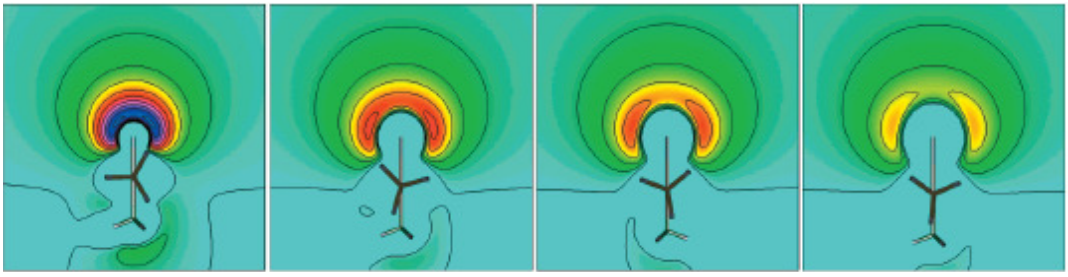

(a) (b) (c) (d)

**Figure 1.20: Negative electrostatic potential around *trans*-PdX($CH_3$)($PH_3$)$_2$ with the most negative areas shown in dark blue and red around the halogen. (a) X = F; (b) X = Cl; (c) X = Br; (d) X = I. Viewed down the Pd-C bond.[91]**

The varying areas of electrostatic potential shown in Figure 1.20 can be explained by referring to simple molecular orbital diagrams of the M-X σ-bond formed between the $p_z$ orbital of the halide and an appropriate metal d orbital (Figure 1.21).[91]

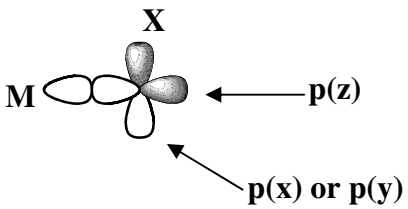


**Figure 1.21: Depiction of orbital overlap in a halogen-metal bond.**

For the M-F bond (Figure 1.22(a)), the bonding orbital will be mainly of fluoride character due to the large difference in electronegativity between the metal cation and fluoride. This means that there is little electron donation from the fluoride $p_z$ orbital to the metal cation so that the position on the bound halide *trans* to the metal ion remains electron dense (Figure 1.20(a)). In the other extreme, the bonding M-I orbital (Figure 1.22(b)) is more covalent in character and, therefore, is substantially metal and iodide in character so that significant electron donation from the iodide $p_z$ orbital occurs, thus depleting the electron density at the position on the halide *trans* to the metal ion (Figure 1.20(d)).

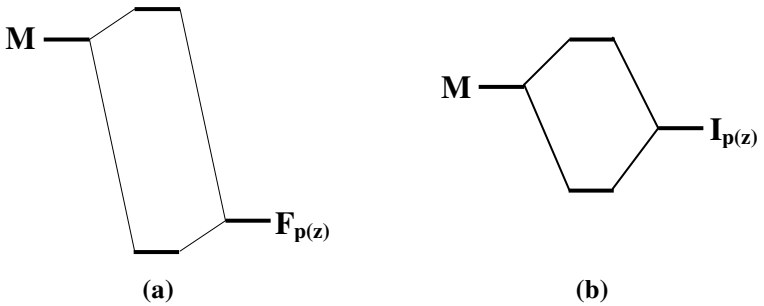


**Figure 1.22: Representations of MO diagrams comparing the M-F (a) and M-I (b) bonds.**

The hydrogen bond acceptor behavior of metal halides is important in the field of chloride hydrometallurgy as better anion exchange solvent extractant reagents could be developed by designing ligands with hydrogen bond donors positioned to interact

favourably with the areas of high electron density on the target chlorometallate anion.

### 1.8.5. Hydrogen Bond Donor Functionalised Reagents for Hexachloroplatinate Extraction

At the Universities of Edinburgh and Nottingham, principles which underpin anion recognition chemistry have been employed in the design of new reagents for the selective extraction of hexachloroplatinate over chloride.[38] DFT calculations and NMR spectroscopic studies on platinum group hexachlorometallates have shown that the areas of highest electron density are situated on the faces and edges of the octahedral complex (Figure 1.23).[94, 99]

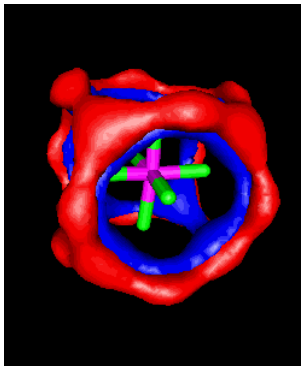

**Figure 1.23: The areas of high electron density on the hexachloroplatinate anion ($Pt^{4+}$ =pink, $Cl^-$ = green) are marked in red.[99]**

The Edinburgh and Nottingham teams designed tertiary amine-based extractants with amide and urea hydrogen bond donor functionality incorporated into the alkyl chains in order to address these areas of high electron density to effectively 'recognise' the $PtCl_6^{2-}$ anion (Figure 1.24).

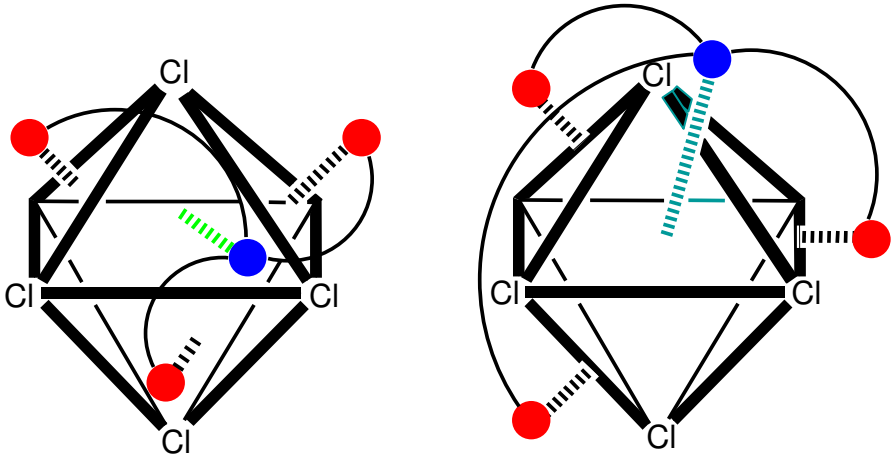


**Figure 1.24: A diagrammatic representation of how a hydrogen bond donor functionalised tertiary amine might protonate to recognise a $PtCl_6^{2-}$ anion. The protonated amine N (blue) forms a strong electrostatic interaction with the faces of the $PtCl_6^{2-}$ octahedron, while the hydrogen bond donors (red) 'wrap around' to address the faces or edges.**

The new extractants were based on tren (Figure 1.25) and they showed up to a ten-fold increase in selectivity for hexachloroplatinate over chloride relative to TOA.[38] This increased selectivity was attributed to the enhanced hexachloroplatinate anion recognition ability of the new ligands that stems from the extra hydrogen bond donor functionality.

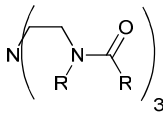


**Figure 1.25: The general structure of the new tren-based reagents designed for $PtCl_6^{2-}$ extraction.**

### 1.8.6. New Extractants for Chlorometallate Recovery in the Anglo American Circuits

In this thesis, a similar approach to that used in the design of the hexachloroplatinate extractants is employed in the development of new reagents for the *concentration* and *separation* of metal values in the Anglo American circuits. Like the hexachloroplatinate extractants, the new ligands were designed with a protonatable site in an organic framework containing hydrogen bond donor functionality that could address the areas of high electron density on the $MCl_4^{n-}$ anions. Espallargas *et. al.* have conducted DFT calculations to explore the electrostatic potential on the $CoCl_4^{2-}$ anion (Figure 1.26) and the areas of highest electron density were found to be situated on equatorial bands around each chloride approximately orthogonal to the Co-Cl bonds.[100] Like the hexachloroplatinate anion, this results in the areas of highest electron density residing on the edges and faces of the tetrahedron rather than on the vertices.

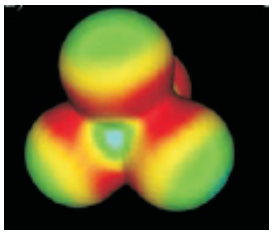

**Figure 1.26: Negative electrostatic potential around $CoCl_4^{2-}$ with the most negative areas shown in red.[100]**

Unlike hexachloroplatinate, the chlorometallates in the Anglo American circuits are labile. As shown in Scheme 1.3, the use of chloride activity and pH variation to control the loading and stripping of labile chlorometallates is associated with the problem that, at the higher pH and lower chloride activity used for stripping, the chloride ions may be replaced by the basic atoms in the extractant. Formation of inner-sphere complexes such as $[L_2MCl_2]$ suppresses stripping from the organic phase and prevents recycling the reagent.

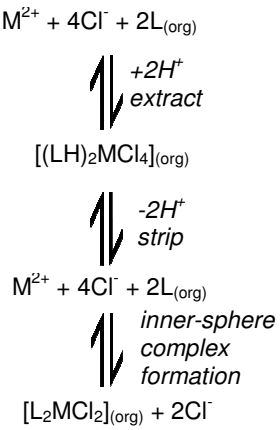


**Scheme 1.3: Inner-sphere complex formation by extractant lone pairs replacing chloride.**

Due to the risk of inner-sphere complex formation, many of the ligands presented in this thesis have design features that inhibit the coordination of basic lone-pairs to metal cationic centres.

## 1.9. General Thesis Aims and Outline

The main aims of this thesis are:

1. to gain insight into the fundamental chemistry that underpins chlorometallate solvent extraction, and
2. to design new solvent extractant reagents for use in the Anglo American circuits to facilitate the separation of cobalt and zinc chlorometallates from iron.

In Chapter 2, the methods used to achieve the above aims are examined. This includes a discussion on the solvent extraction and analytical techniques that were used to explore extractant *strength*, *selectivity* and *efficiency*; and the spectroscopic, crystallographic and theoretical methods that were employed in analysing the chlorometallate-extractant interactions that are involved in extraction.

Chapter 3 investigates a series of new pyridine-based ligands with varying amide and malonamide functionality for the solvent extraction of Zn(II), Co(II) and Fe(III) chlorometallates. Extractant performance was found to vary considerably across the

ligand series and the major hydrogen bonding interactions thought to be responsible for increased extractant performance were analysed in the solid, solution and gas phases.

Chapter 4 explores a series of new tertiary amine-based ligands with varying amide and malonamide functionality. Zn(II), Co(II) and Fe(III) chlorometallate extraction studies showed that the extractant performance varied across the series, with the amide and malonamide-functionalised ligands notably stronger than the tertiary alkyl amine standard. Pt(IV) extraction studies are also discussed, comparing the new tertiary amine ligands with the tren-based ligands of the previous study.[38] Solid state structures of ligand-chlorometallate complexes were used to explore hydrogen bonding interactions between the new tertiary amine ligands and chlorometallate anions.

Chapter 5 explores the possibility of using malonamide reagents for the selective extraction of Fe(III) from the Anglo American circuits. A series of new malonamide ligands with varying functionality were found to extract Fe(III) efficiently and with a high degree of selectivity over Zn(II) and Co(II).

## 1.10. References

1. Renner, H., Platinum Group Metals and Compounds. *Ullmann's Encyclopedia of Industrial Chemistry,* Wiley-VCH, **2005**, 7, 4.

2. McDonald, D., One hundred and fifty years. An anniversary review of Johnson Matthey's role in the economic history of platinum. *Platinum Met. Rev.,* **1967,** 11, (1), 18-29.

3. Dutrizac, J. E., The leaching of sulfide minerals in chloride media. *Hydrometallurgy,* **1992,** 29, (1-3), 1-45.

4. Flett, D. S., Chloride hydrometallurgy for complex sulphides: a review. *Chloride Metall. 2002: Pract. Theory Chloride/Met. Interact., Annu. Hydrometall. Meet., 32nd, Montreal, QC, Canada, Oct. 19-23, 2002,* **2002,** 1, 255-276.

5. Harris, B.; Magee, J., Atmospheric chloride leaching: the way forward for nickel laterites. *Hydrometall. 2003, Proc. Int. Symp., 5th, Vancouver, BC, Canada, Aug. 24-27, 2003* **2003,** 1, 501-515.

6. Winand, R., Chloride hydrometallurgy. *Hydrometallurgy,* **1991,** 27, (3), 285-316.

7. Habashi, F., *A Textbook of Hydrometallurgy,* Metallurgie Extractive: Quebec, **1993**.

8. Peters, E., Applications of chloride hydrometallurgy to treatment of sulfide minerals. *Chloride Hydrometall., Proc., [Int. Symp.],* **1977**, 1-36.

9. Awakura, Y.; Kamei, S.; Majima, H., A kinetic study of nonoxidative dissolution of galena in aqueous acid solution. *Metall. Trans., B,* **1980,** 11B, (3), 377-81.

10. Majima, H.; Awakura, Y.; Misaki, N., A kinetic study on nonoxidative dissolution of sphalerite in aqueous hydrochloric acid solutions. *Metall. Trans., B,* **1981,** 12B, (4), 645-9.

11. Sillen, L. G.; Martell, E. A., *Stability Constants of Metal-Ion Complexes. (Special Publication No. 17). 2nd ed.*, 1964, 754.

12. Sananayake, G., Review of theory and practice of measuring proton activity

and pH in concentrated chloride solutions and application to oxide leaching. *minerals engineering* **2007,** 20, 634-654.

13. Muir, D. M., Basic principles of chloride hydrometallurgy. *Chloride Metall. 2002: Pract. Theory Chloride/Met. Interact., Annu. Hydrometall. Meet., 32nd, Montreal, QC, Canada, Oct. 19-23, 2002,* **2002,** 2, 759-791.

14. Robinson, R. A.; Stokes, R. H., *Electrolyte Solutions. 2nd ed.* 1959, 572.

15. Senanayake, G.; Muir, D. M., Chloride processing of metal sulfides: review of fundamentals and applications. *Hydrometall. 2003, Proc. Int. Symp., 5th,, Vancouver, BC, Canada, Aug. 24-27, 2003,* **2003,** 1, 517-531.

16. Majima, H.; Awakura, Y., Measurement of the activity of electrolytes and the application of activity to hydrometallurgical studies. *Metall. Trans., B,* **1981,** 12B, (1), 141-7.

17. Dutrizac, J. E.; Chen, T. T., The effect of the elemental sulfur reaction product on the leaching of galena in ferric chloride media. *Metall. Trans. B,* **1990,** 21B, (6), 935-43.

18. Rath, P. C.; Paramguru, R. K.; Jena, P. K., Kinetics of dissolution of zinc sulfide in aqueous ferric chloride solution. *Hydrometallurgy,* **1981,** 6, (3-4), 219-25.

19. Lotens, J. P.; Wesker, E., The behavior of sulfur in the oxidative leaching of sulfidic minerals. *Hydrometallurgy,* **1987,** 18, (1), 39-54.

20. Crundwell, F. K., Effect of iron impurity in zinc sulfide concentrates on the rate of dissolution. *AIChE J.,* **1988,** 34, (7), 1128-34.

21. Crundwell, F. K., The influence of the electronic structure of solids on the anodic dissolution and leaching of semiconducting sulfide minerals. *Hydrometallurgy,* **1988,** 21, (2), 155-90.

22. Baker, R. D.; Cottam, S. M.; Day, H. E.; Griffith, W. A. Recovery of lead and silver from their sulfide ores by roasting and leaching. *US Patent,* 19750519, **1976**.

23. Berger, J. M.; Winand, R., Solubilities, densities and electrical conductivities of aqueous copper(I) and copper(II) chlorides in solutions containing other chloride such as iron, zinc, sodium and hydrogen chlorides. *Hydrometallurgy,* **1984,** 12, (1), 61-81.

24. Blitz-Raith, A. H.; Paimin, R.; Cattrall, R. W.; Kolev, S. D., Separation of cobalt(II) from nickel(II) by solid-phase extraction into Aliquat 336 chloride immobilized in poly(vinyl chloride). *Talanta,* **2007,** 71, (1), 419-423.

25. Muir, D. M.; Benari, M. D.; Clare, B. W.; Mangano, P.; Parker, A. J., Removal of iron and formation of copper(I) from solutions containing iron(II) and copper(II) by addition of chloride ion or acetonitrile. *Hydrometallurgy,* **1983,** 9, (3), 257-75.

26. Tasker, P. A.; Plieger, P. G.; West, L. C., Metal complexes for hydrometallurgy and extraction. *Comprehensive Coordination Chemistry II,* **2004,** 9, 759-808.

27. Szymanowski, J., Hydroximes and Copper Hydrometallurgy. *CRC Press,* **1993**.

28. Smith, A. G.; Tasker, P. A.; White, D. J., The structures of phenolic oximes and their complexes. *Coord. Chem. Rev.,* **2003,** 241, (1-2), 61-85.

29. Szymanowski, J., Physicochemical modification of extractants. *Crit. Rev. Anal. Chem.,* **1995,** 25, (3), 143-94.

30. Kordosky, G. A., Copper recovery using leach/solvent extraction/electrowinning technology: forty years of innovation, 2.2 million tons of copper annually. *Int. Solvent Extr. Conf., Cape Town, South Africa, Mar. 17-21, 2002,* **2002**, 853-862.

31. Sole, K. C.; Feather, A. M.; Cole, P. M., Solvent extraction in southern Africa: An update of some recent hydrometallurgical developments. *Hydrometallurgy,* **2005,** 78, (1-2), 52-78.

32. Nicol, M. J.; Fleming, C. A.; Preston, J. S., Application to Extractive Metallurgy. *Comprehensive Coordination Chemistry II,* **1987,** 6, 779-842.

33. Borowiak-Resterna, A.; Kyuchoukov, G.; Szymanowski, J., Options for copper(II) and zinc(II) extraction from chloride media with bi-functional extractants. *Int. Solvent Extr. Conf., Cape Town, South Africa, Mar. 17-21, 2002,* **2002**, 988-994.

34. Moyer, B. A.; Bonnesen, P. V., Physical factors in anion separations. *Supramol. Chem. Anions,* **1997**, 1-44.

35. Moyer, B. A.; Bonnesen, P. V.; Custelcean, R.; Delmau, L. H.; Hay, B. P., Strategies for using host-guest chemistry in the extractive separations of ionic guests. *Kem. Ind.,* **2005,** 54, (2), 65-87.

36. Bianchi, A.; Bowman-James, K.; Garcia-Espana, E.; Editors, *Supramolecular Chemistry of Anions,* **1997**, 461.

37. Barrett, J., *Inorganic Chemistry in Aqueous Solution. (Tutorial Chemistry Texts, Volume 21.),* **2003**, 184.

38. Bell Katherine, J.; Westra Arjan, N.; Warr Rebecca, J.; Chartres, J.; Ellis, R.; Tong Christine, C.; Blake Alexander, J.; Tasker Peter, A.; Schroder, M., Outer-sphere coordination chemistry: selective extraction and transport of the [PtCl6]2- anion. *Angew Chem Int Ed Engl,* **2008,** 47, (9), 1745-8.

39. Ellis, R. J.; Chartres, J.; Sole, K. C.; Simmance, T. G.; Tong, C. C.; White, F. J.; Schröder, M.; Tasker, P. A., Outer-sphere amidopyridyl extractants for zinc(II) and cobalt(II) chlorometallates. *Chem. Commun.,* **2008**.

40. Philip, H. I.; Nicol, M. J., The kinetics and mechanism of the deposition of nickel from chloride solutions. *Chloride Hydrometall., Proc., [Int. Symp.],* **1977**, 250-69.

41. Albert, L.; Winand, R., Copper electrowinning in chloride aqueous solutions. *Chloride Electrometall., Proc. Symp.,* **1982**, 189-202.

42. Mackinnon, D. J.; Brannen, J. M.; Lakshmanan, V. I., Zinc deposit structures obtained from synthetic zinc chloride electrolyte. *J. Appl. Electrochem.,* **1979,** 9, (5), 603-13.

43. Senanayake, G.; Muir, D. M., Speciation and reduction potentials of metal ions in concentrated chloride and sulfate solutions relevant to processing base metal sulfides. *Metall. Trans. B,* **1988,** 19B, (1), 37-45.

44. Szymanowski, J., Copper hydrometallurgy and extraction from chloride media. *J. Radioanal. Nucl. Chem.,* **1996,** 208, (1), 183-194.

45. Eccleston, E. C.; Bunk, S. A., Development of fluidized bed pyrohydrolysis processes for iron and nickel chloride solutions. *Chloride Metall. 2002: Pract. Theory Chloride/Met. Interact., Annu. Hydrometall. Meet., 32nd, Montreal, QC, Canada, Oct. 19-23, 2002,* **2002,** 2, 713-725.

46. Coscia, C.; Kozinski, J. A., Pyrohydrolysis of an Al-Fe-Mg-Cl solution - characterization of the transformation process. *Chloride Metall. 2002: Pract. Theory Chloride/Met. Interact., Annu. Hydrometall. Meet., 32nd, Montreal, QC, Canada, Oct. 19-23, 2002,* **2002,** 2, 683-698.

47. Swaddle, T. W.; Editor, *Inorganic Chemistry: An Industrial and Environmental Perspective,* **1996**, 488.

48. Greenwood, N. N.; Earnshaw, A., *Chemistry of the Elements, 2nd Edition,* **1997**.

49. Atwood, G. E.; Curtis, C. H. Hydrometallurgical production of copper. *Fr. Demande,* 19750114., **1975**.

50. Dalton, R. F.; Price, R.; Hermana, E.; Hoffman, B., Cuprex process. A new chloride-based hydrometallurgical process for copper recovery from sulfide ores. *Ingenieria Quimica,* **1987,** 19, (215), 115-120.

51. Fletcher, A. W.; Sudderth, R. B.; Olafson, S. M., Combining sulfate electrowinning with chloride leaching. Reply to comments. *JOM,* **1992,** 44, (3), 56-7.

52. Nogueira, E. D.; Regife, J. M.; Viegas, M. P., Design features and operating experience of the Quimigal ZINCEX plant. *Chloride Electrometall., Proc. Symp.,* **1982**, 59-76.

53. Martin, D.; Diaz, G.; Garcia, M. A.; Sanchez, F., Extending zinc production possibilities through solvent extraction. *Int. Solvent Extr. Conf., Cape Town, South Africa, Mar. 17-21, 2002,* **2002**, 1045-1051.

54. Diaz, G.; Martin, D.; Frias, C.; Sanchez, F., Emerging applications of ZINCEX and PLACID technologies. *JOM,* **2001,** 53, (12), 30-31.

55. Diaz, G.; Martin, D.; Frias, C.; Perez, O., Updated available solvent extraction technologies. *Solvent Extr. 21st Century, Proc. ISEC '99, Barcelona, Spain, July 11-16, 1999,* **2001,** 2, 1449-1454.

56. Beutier, D.; Burzynski, J. P.; Torre, Y., Iron elimination by oxygen in acid cuprous chloride solutions: the case of the Minemet process. *Iron Control Hydrometall., [Int. Symp.],* **1986**, 640-56.

57. Demarthe, J. M.; Gandon, L.; Georgeaux, A., A new hydrometallurgical process for copper. *Extr. Metall. Copper, Int. Symp.,* **1976,** 2, 825-48.

58. Craigen, W. J. S.; Kelly, F. J.; Bell, D. H.; Wells, J. A., Evaluation of the CANMET Ferric Chloride Leach (FCL) process for treatment of complex base-metal sulfide ores. *Sulphide Deposits,* **1990**, 255-69.

59. Stensholt, E. O.; Dotterud, O. M.; Henriksen, E. E.; Ramsdal, P. O.; Stalesen, F.; Thune, E., Development and practice of the Falconbridge chlorine leach process. *CIM Bull.,* **2001,** 94, (1051), 101-104.

60. Archibald, F. R., The Kristiansand nickel refinery. *J. Met.,* **1962,** 14, 648-52.

61. Stensholt, E. O.; Zachariasen, H.; Lund, J. H., Falconbridge chlorine leach process. *Trans. - Inst. Min. Metall., Sect. C,* **1986,** 95.

62. Stensholt, E. O.; Zachariasen, H.; Lund, J. H.; Thornhill, P. G., Recent improvements in the Falconbridge nickel refinery. *Extr. Metall. Nickel Cobalt, Proc. Symp. 117th TMS Annu. Meet.,* **1988**, 403-12.

63. Thornhill, P. G.; Wigstol, E.; Van Weert, G., Falconbridge matte leach process. *J. Metals,* **1971,** 23, (7), 13-18.

64. Van Weert, G., Some observations on the chloride-based treatment of nickel-copper-cobalt mattes. *Chloride Metall. 2002: Pract. Theory Chloride/Met. Interact., Annu. Hydrometall. Meet., 32nd, Montreal, QC, Canada, Oct. 19-23, 2002,* **2002,** 1, 277-298.

65. Ishikawa, Y.; Tsuchida, N.; Sugiura, T.; Esaki, S., The development of matte chlorine leach electrowinning in Sumitomo Nickel Refinery. *EPD Congr. 1992, Proc. Symp. TMS Annu. Meet.,* **1992**, 713-27.

66. Makino, S.; Sugimoto, M.; Yano, F.; Matsumoto, N., Operation of the MCLE (Matte Chlorine Leach Electrowinning) plant for nickel refining at Sumitomo Metal Mining Co., Ltd. *EPD Congr. 1996, Proc. Sess. Symp. TMS Annu. Meet., Anaheim, Calif., Feb. 4-9, 1996,* **1996**, 299-311.

67. Inami, T.; Toyabe, K.; Kanai, T., Cobalt refining process at Sumitomo Niihama nickel refinery. *Metall. Rev. MMIJ,* **1984,** 1, (2), 125-37.

68. McDonald, R. G.; Whittington, B. I., Atmospheric acid leaching of nickel laterites review. *Hydrometallurgy,* **2008,** 91, (1-4), 35-55.

69. Hubler, W. G.; Archibald, F. R. Treating lateritic ores. *US Patent,* 2105456, **1938**.

70. Rice, N. M.; Strong, L. W., Leaching of lateritic nickel ores in hydrochloric acid. *Can. Metall. Q.,* **1974,** 13, (3), 485-93.

71. Rubisov, D. H.; Krowinkel, J. M.; Papangelakis, V. G., Sulphuric acid pressure leaching of laterites - universal kinetics of nickel dissolution for limonites and limonitic/saprolitic blends. *Hydrometallurgy,* **2000,** 58, (1), 1-11.

72. Harris, B., A New Approach to the High Concentration Chloride Leaching of Nickel Laterites. *ALTA 2006 Nickel/Cobalt 11, Melbourne,* **2006**.

73. Harris, G. B.; Lakshmanan, V. I.; Sridhar, R. Leaching of laterite ores with acidic chloride solutions for recovery of metal values. *US Patent,* 2004228783, 2004.

74. Tasker, P. A.; Ellis, R. J.; Sole, K. C.; Smit, J. T.; Steyl, J.; Viljoen, K.; Vatta, L., *Private Communication,* Technical Visit Report*, Johannesburg,* **2007**.

75. Gloe, K.; Stephan, H.; Grotjahn, M., Where is the anion extraction going? *Chem. Eng. Technol.,* **2003,** 26, (11), 1107-1117.

76. Cram, D. J.; Cram, J. M., Host-guest chemistry. *Science,* **1974,** 183, (4127), 803-9.

77. Lehn, J. M.; Sonveaux, E.; Willard, A. K., Molecular recognition. Anion cryptates of a macrobicyclic receptor molecule for linear triatomic species. *J. Am. Chem. Soc.,* **1978,** 100, (15), 4914-16.

78. Pedersen, C. J., Cyclic polyethers and their complexes with metal salts. *J. Amer. Chem. Soc.,* **1967,** 89, (26), 7017-36.

79. Graf, E.; Lehn, J. M., Anion cryptates: highly stable and selective macrotricyclic anion inclusion complexes. *J. Am. Chem. Soc.,* **1976,** 98, (20), 6403-5.

80. Dietrich, B.; Fyles, T. M.; Lehn, J. M.; Pease, L. G.; Fyles, D. L., Anion receptor molecules. Synthesis and some anion binding properties of macrocyclic guanidinium salts. *J. Chem. Soc., Chem. Commun.,* **1978**, (21), 934-6.

81. Dietrich, B.; Hosseini, M. W.; Lehn, J. M.; Sessions, R. B., Anion receptor molecules. Synthesis and anion-binding properties of polyammonium macrocycles. *J. Am. Chem. Soc.,* **1981,** 103, (5), 1282-3.

82. Gale, P. A., Anion receptor chemistry: highlights from 1999. *Coord. Chem. Rev.,* **2001,** 213, 79-128.

83. Gale, P. A., Anion and ion-pair receptor chemistry: highlights from 2000 and 2001. *Coord. Chem. Rev.,* **2003,** 240, (1-2), 191-221.

84. Gale, P. A.; Garcia-Garrido, S. E.; Garric, J., Anion receptors based on organic frameworks: highlights from 2005 and 2006. *Chem. Soc. Rev.,* **2008,** 37, (1), 151-190.

85. Garcia-Espana, E.; Diaz, P.; Llinares, J. M.; Bianchi, A., Anion coordination chemistry in aqueous solution of polyammonium receptors. *Coord. Chem. Rev.,* **2006,** 250, 2952-2986.

86. Shriver, D. F.; Atkins, P. W., *Inorganic Chemistry*. Oxford University Press: Oxford, **1999**.

87. Bates, G. W.; Gale, P. A., An introduction to anion receptors based on organic frameworks. *Struct. Bonding,* **2008,** 129, 1-44.

88. Beer, P. D.; Gale, P. A., Anion recognition and sensing: the state of the art and future perspectives. *Angew. Chem., Int. Ed.,* **2001,** 40, (3), 486-516.

89. Schmidtchen, F. P., Inclusion of anions in macrotricyclic quaternary ammonium salts. *Angewandte Chemie,* **1977,** 89, (10), 751-2.

90. Aullon, G.; Bellamy, D.; Orpen, A. G.; Brammer, L.; Bruton, E. A., Metal-bound chlorine often accepts hydrogen bonds. *Chem. Commun. (Cambridge),* **1998**, (6), 653-654.

91. Brammer, L.; Bruton, E. A.; Sherwood, P., Understanding the Behavior of Halogens as Hydrogen Bond Acceptors. *Cryst. Growth Des.,* **2001,** 1, (4), 277-290.

92. Angeloni, A.; Orpen, A. G., Control of hydrogen bond network dimensionality in tetrachloroplatinate salts. *Chem. Commun.,* **2001**, (4), 343-344.

93. Balamurugan, V.; Hundal, M. S.; Mukherjee, R., First systematic investigation of C-H...Cl hydrogen bonding using inorganic supramolecular synthons: lamellar, stitched stair-case, linked-ladder, and helical structures. *Chem.--Eur. J.,* **2004,** 10, (7), 1683-1690.

94. Brammer, L.; Swearingen John, K.; Bruton Eric, A.; Sherwood, P., Hydrogen bonding and perhalometallate ions: a supramolecular synthetic strategy for new inorganic materials. *Proc Natl Acad Sci U S A,* **2002,** 99, (8), 4956-61.

95. Gillon, A. L.; Lewis, G. R.; Orpen, A. G.; Rotter, S.; Starbuck, J.; Wang, X.-M.; Rodriguez-Martin, Y.; Ruiz-Perez, C., Organic-inorganic hybrid solids: control of perhalometallate solid state structures. *Dalton,* **2000**, (21), 3897-3905.

96. Lewis, G. R.; Orpen, A. G., A metal-containing synthon for crystal engineering: synthesis of the hydrogen bond ribbon polymer [4,4'-H2bipy][MCl4] (M = Pd, Pt). *Chem. Commun.,* **1998**, (17), 1873-1874.

97. Rivas, J. C. M.; Brammer, L., Self-Assembly of 1-D Chains of Different Topologies Using the Hydrogen-Bonded Inorganic Supramolecular Synthons N-H...Cl2M or N-H...Cl3M. *Inorg. Chem.,* **1998,** 37, (19), 4756-4757.

98. Desiraju, G.; Steiner, T., *The Weak Hydrogen Bond: Applications to Structural Chemistry and Biology*. Oxford University Press: Oxford, **1999**, 528.

99. Naidoo, K. J.; Klatt, G.; Koch, K. R.; Robinson, D. J., Geometric Hydration Shells for Anionic Platinum Group Metal Chloro Complexes. *Inorg. Chem.,* **2002,** 41, (7), 1845-1849.

100. Espallargas, G. M.; Brammer, L.; Sherwood, P., Designing intermolecular interactions between halogenated peripheries of inorganic and organic molecules: Electrostatically directed M-X...X'-C halogen bonds. *Angewandte Chemie, International Edition,* **2006,** 45, (3), 435-440.

# CHAPTER 2

# METHODOLOGIES

## 2.1. Introduction

The general approach used in this study for the development new solvent extractant reagents for use in the proposed Anglo American circuits is summarised below in Figure 2.1.

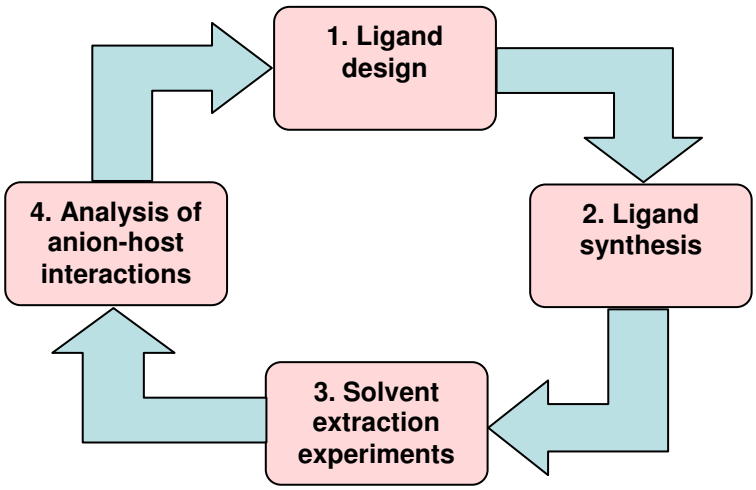


**Figure 2.1: A summary of the general methodology used in this thesis.**

The general methodology involved first designing a new series of chlorometallate extractants (1). After synthetic routes to the new reagents were explored (2), they were investigated for chlorometallate extraction in terms of *efficiency*, *strength* and *selectivity* (3). The ligands that performed the best in terms of their potential application to the Anglo American circuits were investigated further in order to study the major interactions between chlorometallate and extractant that might be responsible for their enhanced extraction performance (4), and this was considered in the design of the next series of extractants (1).

## 2.2. Ligand Design and Synthesis

The ligands presented in this thesis were designed to be proton selective in order to transport proton into a water immiscible organic phase to form neutral ligand-chlorometallate ion pair complexes, without replacing any ligands in the inner coordination sphere of the metal cation (as described in Chapter 1, Section 1.8.6), according to Equation 2.1.

**Equation 2.1**

$$nL_{(org)} + nH^+ + MCl_x^{n-} = [(LH)_nMCl_x]_{(org)}$$

Extensive alkyl chain functionality was incorporated into all of the ligands to ensure exclusive solubility in the organic phase. Amide and malonamide groups were also incorporated into many of the ligands to investigate the importance of hydrogen bond donors in the extraction of chlorometallate anions.

The preparation of individual target molecules within each ligand series is described in the 'Synthesis' sections in the corresponding chapters. Most synthetic routes followed the general method of forming a base-ester (B-E) intermediate from the basic starting material (B), followed by aminolysis of the ester to form an amide or malonamide functionalised organic base product (B-A) (Equation 2.2).

**Equation 2.2**

$$B \rightarrow B\text{-}E \rightarrow B\text{-}A$$

Progression of these reactions could be conveniently monitored by $^1H$ NMR as the ester -OR peaks and the amide NH peaks are easily distinguished. There are various methods described in the literature that can be used to form amides from ester starting materials.[1]

## 2.3. Solvent Extraction Experiments

Solvent extraction experiments were designed to investigate the equilibria shown in Equation 2.3 and Equation 2.4 which result in the transfer of the metallate anion into the water immiscible phase.

**Equation 2.3**

$$M^{2+} + 4Cl^- + 2H^+ + 2L_{(org)} \rightleftharpoons [(LH)_2MCl_4]_{(org)}$$

(when M = Co(II) or Zn(II)

**Equation 2.4**

$$Fe^{3+} + 4Cl^- + H^+ + L_{(org)} \rightleftharpoons [(LH)FeCl_4]_{(org)}$$

The extractive properties of individual ligands can be investigated by independently varying the concentration of the different species on the left hand side of the equilibria in Equation 2.3 and Equation 2.4 and observing the effect that this has on metal transfer into the water immiscible organic phase.

### 2.3.1. General Solvent Extraction Experimental Method

The experimental procedures that were used to study the behaviour of the new extractants were adapted from existing procedures used at the University of Edinburgh[2, 3] to model the requirements of the new Anglo American circuits. The general method used for the solvent extraction experiments is summarised in Figure 2.2.

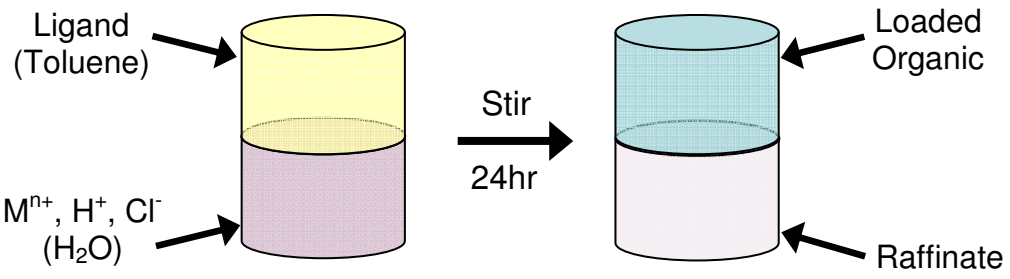


**Figure 2.2: A pictorial representation of the general solvent extraction procedure used in this study.**

The high solubility of polar organic molecules in chloroform has led to its use as the water immiscible solvent in many extraction studies carried out at the University of Edinburgh.[2-4] In this thesis, however, toluene is most frequently used as it has a history of use in industrial processes involving base chlorometallate extraction and is a good model for the aromatic hydrocarbon solvents that are used in existing processes.[5] The aqueous phase is often highly acidic with high chloride ion concentrations to resemble the conditions in the PLS produced in the Anglo American circuits. The ligand concentrations in the organic phase and metal concentrations in the aqueous phase were similar to procedures used recently at the University of Edinburgh to allow comparison of results with other work within the group and to produce aliquots with optimal metal concentrations for analysis. Experimental details such as size and type of extraction chamber, stirring method, system temperature and contact time were the same as in previous chlorometallate extraction studies performed at the University of Edinburgh.[2]

### 2.3.2. Metal Content Analysis

In this study, a robust and reliable method for measuring metal content in aqueous and organic solvents is essential. There are myriad methods used to analyse for metal ions, including atomic absorption spectroscopy (AAS) and UV-Vis spectroscopy, but for this study ICP-OES (inductively coupled plasma optical emission spectroscopy) was chosen. ICP-OES is a versatile method that can be used to accurately analyse the metal content in both organic and aqueous solutions, with detection limits as low as parts-per-billion.[6] The sample is passed as an aerosol through a plasma at temperatures exceeding 6500 K, which atomises, vaporises and excites the elements

in the sample into high energy states. As they relax back to lower energy states, the excited atoms and ions emit photons in the UV and visible regions at specific wavelengths, depending on the element. Wavelengths specific to the element under analysis can then be detected and the intensity of emission is proportional to the element concentration in the analyte. Initial calibration of the spectrometer with samples containing known concentrations of analyte can then be used to allow for accurate determination of the concentration of the element under analysis.

Previous studies within the group have revealed that the ICP-OES spectrometer gives optimal results at analyte concentrations between 0 and 250 ppm so samples in this study were made up for analysis within this concentration range.[2, 4] Organic phase analysis using the ICP-OES spectrometer requires adjustment of the machine to cope with the viscosity of the organic solvent. Organic solvents with low volatility are preferred in order to minimise evaporation before entering the plasma so butan-1-ol is routinely used as an effective organic solvent matrix.[7]

### 2.3.3. pH Dependence of Metal Loadings

According to Equation 2.3 and Equation 2.4, metal loading into the organic phase is dependent on the pH of the aqueous phase. By varying the proton concentration in the aqueous phase and observing the transport of metal value into the organic phase, the pH loading range, or the extractant *strength*, can be compared across a ligand series. The *strength* of an individual extractant is related to its ability to stabilise the $nH^+ \cdot MCl_x^{n-}$ ion pair in the organic phase, i.e. the ligand's ability to coordinate both a proton (related to it's basicity) and the metallate anion (related to the binding constant of the anion in the receptor site).

In order to study the pH dependence of chlorometallate extraction by mechanisms similar to that shown in Equation 2.3 and Equation 2.4, a method was developed that involved changing proton concentration in the aqueous phase while attempting to keep all other parameters constant. In order to keep chloride concentration in the aqueous phase constant while varying the concentration of HCl, it was necessary to

use a non-acidic 'innocent' chloride source. Alkali metal chloride salts are ideal sources of chloride for our studies as the alkali metal cations do not form anionic chlorometallate complexes in aqueous solution that would compete with the loading of the chlorometallate complexes of the target metal ion. In the work represented in this thesis, we used lithium chloride as it has a high solubility in water and has also been used as a non-acidic chloride source in similar studies.[8] By mixing LiCl and HCl solutions, it was possible to assemble acidic chloride solutions that contained the target metal ion with constant chloride concentration and variable proton concentration. These solutions were contacted with toluene phases that contained a constant concentration of extractant after which the equilibrium pH in the aqueous phase and the metal content in the organic phase were recorded. The results were then used to construct graphs showing how percentage loading of metal in the organic phase varies with equilibrium pH. These typically show an 'S-profile' as described in Figure 2.3.

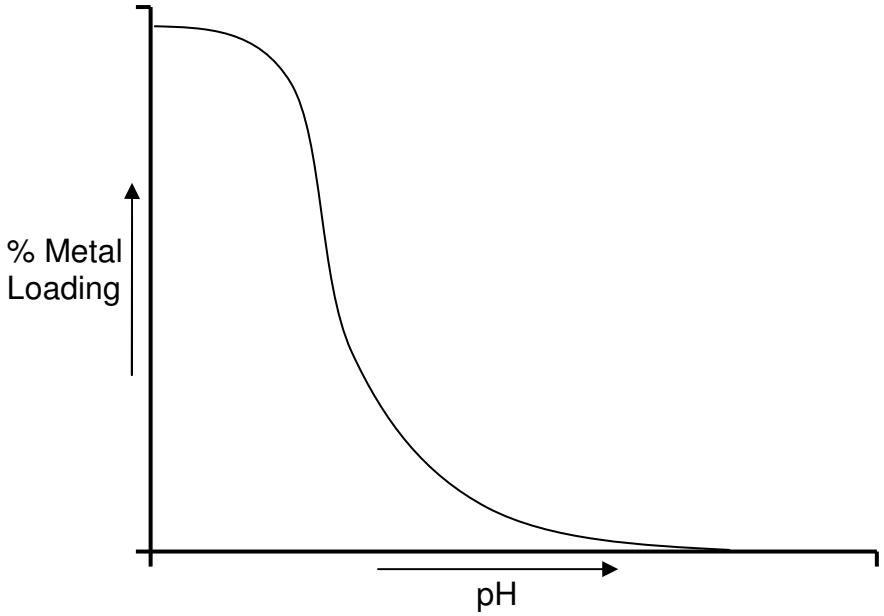


**Figure 2.3: A representation of a pH loading curve for the extraction of chlorometallate by organic base.**

The percentage loading is the calculated percentage of ligand loaded with chlorometallate assuming that the ligand is mono-protonated and overall charge-

neutral assemblies are present in the organic phase. Consequently, 2:1 ligand:chlorometallate species are assumed for Zn(II) and Co(II) loading (as $[(LH)_2MCl_4]$) and 1:1 species are assumed for Fe(III) loading (as $[(LH)MCl_4]$). This approach is supported by literature that usually reports $ZnCl_4^{2-}$, $CoCl_4^{2-}$ and $FeCl_4^-$ as the major extracted species when using anion exchange reagents.[9-12] However, other species with different anionic charge have also been reported to extract, such as $HCoCl_4^-$ and $CoCl_3^-$,[13-15] which would not form 2:1 complexes. Nevertheless, for a direct comparison of ligand extraction *strength* across a series, a definition of the precise speciation of the extracted chlorometallate anions is not essential.

It is important to study the pH dependence of chlorometallate extraction as the loading and stripping of metal values by pH adjustment is common in many industrial processes involving both metal cation and anion extraction.[16] Also, as different metals have different pH loading ranges, extraction selectivity between different metal values can be achieved by manipulating the pH in the aqueous phase. Adjusting the pH of leach liquors prior to solvent extraction is common in industrial processes as a method to prevent the extraction of unwanted metal values, particularly iron.[17, 18] As ferric iron is the main impurity in the new Anglo American circuits, it is important to compare the pH loading range of Zn(II) and Co(II) with Fe(III) in order to establish if any selectivity can be achieved with the new reagents.

## 2.3.4. Chloride Concentration Dependence of Metal Loadings

In chlorometallate extraction systems, the concentration of chloride ion in the aqueous phase has a large influence on metal extraction. Chloride concentration affects the speciation of the metal complexation and high chloride concentration favours the formation of extractable metal chloro-complexes, pushing the equilibrium in Equation 2.5 to the right.

**Equation 2.5**

$$M^{n+} + xCl^- \rightleftharpoons [MCl_x]^{n-x}$$

Generally, high chloride concentration favours chlorometallate extraction as the *Hofmeister bias* (see Chapter 1, Section 1.5.3) makes the extraction of

chlorometallate anion much more favourable than chloride so that the competitive equilibrium in Equation 2.6 lies far to the right.[19]

**Equation 2.6**

$$2LHCl_{(org)} + [MCl_4]^{2-} \rightleftharpoons [(LH)_2MCl_4]_{(org)} + 2Cl^-$$

However, some authors have observed that very high concentrations of HCl result in a decrease in metal extraction (Figure 2.4).[8, 20, 21]

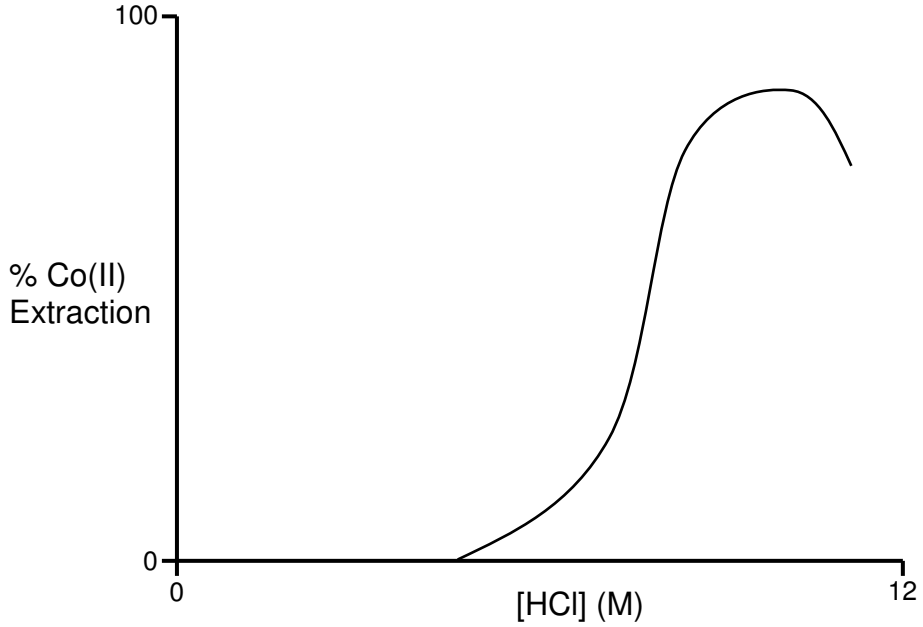


**Figure 2.4: A representation of a curve showing the dependence of cobalt(II) extraction with a trialkylamine on [HCl].[8, 20, 21]**

The decreased Co(II) extraction at high HCl concentrations was attributed to the formation and extraction of the hydrogen dichloride anion ($HCl_2^-$), which, being more charge diffuse and larger than chloride, competes more effectively with chlorometallate extraction (Equation 2.7).[8, 20]

**Equation 2.7**

$$[(LH)_2MCl_4]_{(org)} + 2HCl_2^- \rightleftharpoons 2LH{\cdot}HCl_{2(org)} + MCl_4^{2-}$$

Very high HCl concentrations are used in some industrial processes to achieve stripping. For example, $PtCl_6^{2-}$ is sometimes recovered from organic solvents by contacting with 12 M HCl (Equation 2.8) as an alternative to using a base (Equation 2.9).[22]

**Equation 2.8**

$$[(LH)_2PtCl_6]_{(org)} + 2HCl_2^- \rightleftharpoons 2LH{\cdot}HCl_{2(org)} + PtCl_6^{2-}$$

**Equation 2.9**

$$[(LH)_2PtCl_6]_{(org)} + 2OH^- \rightleftharpoons 2L_{(org)} + PtCl_6^{2-} + H_2O$$

Another way that high chloride concentrations can suppress loading is via the formation of more highly charged, and therefore less extractable, metallate species in the aqueous phase according to Equation 2.10.

**Equation 2.10**

$$MCl_4^{2-} + Cl^- \rightleftharpoons MCl_5^{3-}$$

This mechanism is likely to be the reason for the suppression of Cu(II) extraction by quaternary ammonium salts at high chloride concentration.[23]

To study the dependence of chlorometallate extraction on chloride concentration using the new reagents presented in this thesis, a method was developed that involved changing chloride concentration in the aqueous phase while attempting to keep other parameters constant. By mixing LiCl and HCl solutions, it was possible to produce acidic chloride solutions containing the target metal ion with constant proton concentration and varied chloride concentration. These solutions were contacted with toluene phases that contained a constant concentration of extractant, after which the metal content in the organic phase was established and graphs were plotted of the percentage loading (calculated in the same way as in the pH dependence experiments) against chloride concentration in the aqueous phase. It should be noted that, due to the significant dependence of the activity of proton on chloride concentration, chloride concentration is not a truly independent variable as the proton activity in solutions containing high chloride concentration will be significantly higher than that in solutions containing low chloride concentration.

The chloride concentration range in which ligands are able to extract metal value will depend largely on the *strength* of the particular ligand and its *selectivity* for chlorometallate over chloride. However, the speciation of the target metal value in the aqueous phase and the solvent extraction mechanism are also important factors. For example, ligands that are able to extract zinc according to the mechanism

described by Equation 2.11 could load at lower chloride concentrations than ligands that are only able to extract via the mechanism described by Equation 2.12 as $ZnCl_2$ forms at lower chloride concentrations than $ZnCl_4^{2-}$.[24]

**Equation 2.11**

$$ZnCl_2 + 2LHCl_{(org)} \rightleftharpoons [(LH)_2ZnCl_4]_{(org)}$$

**Equation 2.12**

$$[ZnCl_4]^{2-} + 2L_{(org)} + 2H^+ \rightleftharpoons [(LH)_2ZnCl_4]_{(org)}$$

It is important to study the affect that chloride concentration has on metal extraction as 'chloride swing' mechanisms are often used in industry to control the loading and stripping of metal chloro-complexes in solvent extraction processes. For example, the CUPREX process[25] and the Falconbridge chlorine leach process[18] (see Chapter 1, Section 1.7) involve extracting metal values from solutions containing high chloride concentration, which favours the formation of the extractable metal chloro-complexes, while stripping is achieved by contacting the loaded organic with a solution containing low chloride concentration, which disassembles the coordinated metal chloro-complex, releasing the metal value back into the aqueous phase.

Selectivity between different metal ions may also be achieved by manipulating chloride concentration as different chlorometallates often have different chloride concentration loading ranges. For this reason, it is beneficial to compare the chloride concentration loading ranges of the new ligands for the target metal ions, Zn(II) and Co(II), with the main impurity, Fe(III), to establish if any selectivity can be achieved.

### 2.3.5. Chlorometallate Extraction Efficiency

It is clear from Equation 2.3 and Equation 2.4 that more ligand in the organic phase would increase metal loading. By varying the concentration of ligand in the organic phase while keeping the conditions in the aqueous phase constant, the dependence of metal loading on extractant concentration can be established across a ligand series. Ligands that are able to extract more metal value at lower concentrations are more *efficient*.

In order to study ligand extraction *efficiency*, a procedure used in $PtCl_6^{2-}$ extraction studies[2] was adapted to suit the requirements for base metal recovery in the Anglo American circuits. The procedure involved contacting metal-containing aqueous phases, of acidity and chloride concentration resembling that likely to be found in the Anglo American circuits, with organic phases containing varying quantities of ligand. The metal content of the aqueous phase was analysed before and after extraction and the percentage of metal extracted from the aqueous phase was plotted against the ligand excess in the organic phase relative to the total metal (ligand excess = $[L]/[M]_{total}$). In this way, solvent extraction *efficiency* can be compared across a ligand series. The ligands which are the most *efficient* at extracting metal value are more attractive to commercial application.

### 2.3.6. Stripping Experiments

When assessing the commercial viability of new solvent extractant reagents, it is important to demonstrate quantitative recovery of the metal value from the organic phase and the effective reuse of the extractant in subsequent load-strip cycles. Retention of the metal value in the organic phase may indicate the formation of inner-sphere complexes (see Chapter 1, Section 1.8.6). In order to establish this, three successive load-strip cycles were performed. Loading involved contacting ligand-toluene solutions with highly acidic chloride aqueous phases containing Co(II), Zn(II) or Fe(III). Stripping involved contacting the loaded organic phases with equal volumes of deionised water. Three successive load-strip cycles were performed and the metal content of the organic phase was determined after each load or strip stage so that any loss of extractant activity could be monitored.

### 2.3.7. Analysis of Total Chloride and Metal Concentrations in the Loaded Organic Phases

In commercial processes that involve the solvent extraction of neutral metal chloride or chlorometallate anion complexes, it is important to determine the relative amount of chloride to metal ion that is extracted. This is particularly important in anion

exchange solvent extraction due to the ability of organic bases to transport more than one mole of HCl into the organic phase per mole of extractant (Equation 2.13).[26] Extra chloride that is transported across a circuit would build up in the electrolyte, resulting in poor materials balance.

**Equation 2.13**

$$L.HCl_{org} + HCl = L.HCl.HCl_{(org)}$$

For this reason, it was deemed necessary to develop a method for analysing the total number of moles of chloride that is extracted per mole of metal. ICP-OES is not effective for chloride analysis as the emission lines do not fall in the correct detection range of 160 to 900 nm.[27]

#### 2.3.7.1. Mohr's Method for Chloride Concentration Determination

A convenient method for the determination for chloride concentration in aqueous samples is via a *chloride electrode* which is often favoured as it does not require chemically altering the analyte. However, to determine chloride concentration in the presence of zinc or cobalt, a different method must be used due to complications arising from the formation of metal chloro-complexes.[28]

Chloride can be analysed gravimetrically by adding an excess of $AgNO_3$ to the solution. The number of moles of chloride in the analyte is equal to the number of moles of AgCl precipitate formed (Equation 2.14). This method for the determination of chloride concentration is known as 'Mohr's Method'.

**Equation 2.14**

$$Ag^+ + Cl^- \rightarrow AgCl_{(s)}$$

Instead of using the mass of precipitate to establish the amount of AgCl (and hence chloride concentration in the analyte), ICP-OES can be used to determine the concentration of Ag(I) in solution before and after precipitation with chloride, so that chloride concentration can be inferred (Equation 2.15).[28]

**Equation 2.15**

$$MCl_x^{y-} + zAg^+ \rightarrow xAgCl_{(s)} + M^{x-y} + (z-x)Ag^+$$

### 2.3.7.2. Analysis of Metal and Total Chloride Loading for Co(II), Zn(II) or Fe(III) Extraction

To determine the total metal and chloride transported into the organic phase, it is necessary to strip all of the extracted species into an aqueous phase prior to chloride analysis. This was done by adapting a method developed in the group previously[28] and involved contacting the loaded organic phase with an aqueous solution containing an excess of strong base (NaOH) which deprotonates all of the ligand, releasing all of the extracted species into the aqueous phase. The adaptation of Mohr's method was then used to establish chloride concentration in the stripped electrolyte. ICP-OES analysis was used to directly determine the amount of metal in the organic phase. The method used for the simultaneous analysis of chloride and metal loading is summarised in Figure 2.5.

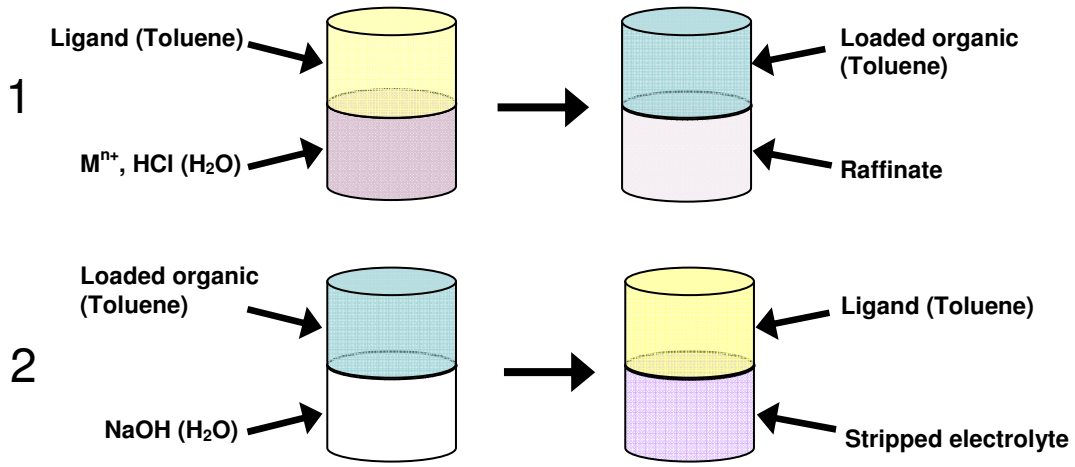


**Figure 2.5: The general procedure used for analysing metal ($M^{n+}$ = Co(II)/Zn(II)/Fe(III)) and chloride loading. Stage 1: Aqueous phases of high HCl concentration containing the target metal ion were contacted with an organic phase (toluene) containing the ligand. Stage 2: After separating from the raffinate, the loaded organic was contacted with an aqueous phase containing excess NaOH. Chloride concentration in the stripped electrolyte was determined using an adaptation of Mohr's method[28] and [$M^{n+}$] loaded was determined by analysing the loaded organic phase using ICP-OES.**

As stripping the loaded organic phase with excess base results in the precipitation of the zinc, cobalt or iron value as an oxide or hydroxide, there is a possibility that

chloride may be entrained in the solid and thus removed from solution. In order to test the accuracy of the method described in Figure 2.5, a control experiment was performed that involved testing a previously characterised ligand-chlorometallate complex, $[(L^2H)_2ZnCl_4]$ (see Chapter 3, Section 3.8.3). This involved dissolving the complex in toluene and analysing for zinc in the organic phase using ICP-OES and the theoretical concentration of chloride was calculated using $[Cl^-]_{theo} = 4 \times [Zn^{2+}]$. The method described in Figure 2.5 was used to experimentally define chloride concentration ($[Cl]_{exp}$) and the results for this are displayed in Table 2.1. A deviation of -2.7% was realised, which is acceptable for this study.

| [Zn] | $[Cl]_{theo}$ | $[Cl]_{exp}$ | % Deviation |
|---|---|---|---|
| (mM) | (mM) | (mM) | $([Cl]_{exp} - [Cl]_{theo})/[Cl]_{theo}*100$ |
| 5.330 | 21.320 | 20.751 | -2.7 |

**Table 2.1: Comparing the calculated $[Cl^-]$ in the organic phase with the $[Cl^-]$ determined using the experiment summarised in Figure 2.5 .**

### 2.3.7.3. Analysis of $PtCl_6^{2-}$ and Chloride Loading

As some of the ligands investigated in this study were tested as potential $PtCl_6^{2-}$ extractants, a method for establishing the total platinum and chloride loadings was developed.

When excess $AgNO_3$ was added to samples for chloride concentration analysis in the presence of $PtCl_6^{2-}$, a yellow precipitate (thought to be the $Ag_2PtCl_6$ complex)[29], was formed so that $Ag^+$ is removed both by $Cl^-$ and $PtCl_6^{2-}$. Assuming that only $Ag_2PtCl_6$ and AgCl precipitates form, and as $[Pt^{4+}]$ in the analyte prior to $AgNO_3$ addition can be determined accurately using ICP-OES, then the amount of $Ag_2PtCl_6$ can be inferred which leaves extra reduction in $[Ag^+]$ the result of AgCl formation. Thus chloride concentration in the presence of $PtCl_6^{2-}$ can be determined using both $[Pt^{4+}]$ and $[Ag^+]$ which can be established using ICP-OES (Equation 2.16).

**Equation 2.16**

$$xAg^+ + yCl^- + zPtCl_6^{2-} \rightarrow yAgCl_{(s)} + zAg_2PtCl_{6(s)} + (x-y-2z)Ag^+$$

$$\text{so } [Ag^+]_{remaining} = [Ag^+]_{initial} - [AgCl] - 2[Ag_2PtCl_6]$$

$$\text{if } [Ag_2PtCl_6] = [Pt^{4+}] \text{ and } [AgCl] = [Cl^-]$$

then $[Cl^-] = [Ag^+]_{initial} - 2[Pt^{4+}] - [Ag^+]_{remaining}$

An experiment was conducted to determine free chloride concentration in samples containing $PtCl_6^{2-}$ by the addition of excess $AgNO_3$ and using the theory described in Equation 2.16 (the results and method for this experiment are presented in appendix 2.1). The results show that this technique overestimates chloride concentration in samples that contain $PtCl_6^{2-}$, which may be due to extra silver ions being precipitated by the transfer of chloride from the platinum complex to $Ag^+$, (Equation 2.17) resulting in a lower than expected $[Ag^+]$ in solution and thus a higher estimation of chloride concentration. Taking this into account, and assuming total transfer of chloride from $Pt^{4+}$ to $Ag^+$, a lower than expected value for total chloride concentration is obtained. These results suggest a *partial* transfer of chloride from $Pt^{4+}$ to $Ag^+$, making accurate determination of chloride using this method impossible.

**Equation 2.17**

$$6Ag^+ + PtCl_6^{2-} \rightarrow 6AgCl_{(s)} + Pt^{4+}$$

For accurate chloride concentration determination in platinum back extraction samples, it is necessary to remove $PtCl_6^{2-}$ from solution. One way of doing this, suggested by D. Robertson from Anglo Platinum,[30] is by reducing $Pt^{4+}$ to $Pt^0$ using hydrazine (Equation 2.18).

**Equation 2.18**

$$PtCl_6^{2-} + N_2H_4 \rightarrow Pt_{(s)} + N_{2(g)} + 4H^+ + 6Cl^-$$

As hydrazine reduces $Ag^+$ and may damage the sensitive chloride electrode, the removal of residual hydrazine from treated samples is necessary for accurate chloride concentration determination. Various methods were attempted to achieve this, including evaporation, reacting with an oxidising agent, extracting into a separate phase and catalytic degradation (see appendix 2.2), but none of these techniques successfully allowed for accurate determination of total chloride concentration in $PtCl_6^{2-}$ solutions.

R. Grant and S. Belair from Johnson Matthey analyse the additional chloride in the presence of $PtCl_6^{2-}$ by removing the latter from back extraction solutions by

precipitation on adding excess $CsNO_3$ (Equation 2.19) leaving the free chloride in solution.[22]

**Equation 2.19**

$$2CsNO_3 + [PtCl_6]^{2-} = Cs_2PtCl_{6(s)} + 2NO_3^-$$

To test this method, a control experiment was performed which involved adding $CsNO_3$ to solutions containing known quantities of $PtCl_6^{2-}$ and NaCl of concentrations that may be expected in back extraction samples. The adaptation of Mohrs method was used to analyse the free chloride remaining in solution and the results for this are presented in Table 2.2. A deviation of -2.7% was realised for the lowest concentration of free chloride which is acceptable for this study.

| Free $[Cl]_{theo}$ (mM) | Free $[Cl]_{exp}$ (mM) | % deviation |
|---|---|---|
| | | $([Cl]_{exp} - [Cl]_{theo})/[Cl]_{theo}*100$ |
| 0.112 | 0.109 | -2.7 |
| 3.213 | 3.221 | 0.3 |
| 5.004 | 5.010 | 0.1 |

**Table 2.2: Chloride concentration in $H_2PtCl_6$ and NaCl solutions. Comparing the theoretical free chloride concentration based on [NaCl] ($[Cl]_{theo}$) with the free chloride concentration determined using the adaptation of Mohr's method ($[Cl]_{exp}$).**

## 2.4. Analysis of Anion-Host Interactions

One of the aims of the work in this thesis involves probing the major anion-host interactions that are responsible for the extraction of chlorometallate anions into organic solvents. This area of solvent extraction chemistry remains largely unexplored as electrostatic attraction and individual outer-sphere coordination interactions are often bundled together and referred to as 'ion-pairing'.[16] By having a more in-depth understanding of the structure of the extracted species and the major interactions, the development of better reagents for chlorometallate extraction may be realised.

A dominant force in chlorometallate extraction is the electrostatic attraction between the cationic host and the anionic guest. However, recent studies have suggested that hydrogen bonding interactions may also play an important role.[2] There are a number of methods that can be used to investigate hydrogen bonding interactions in anion binding including IR spectroscopy, NMR, X-ray crystallography and computational modelling. This section discusses the viability of using these techniques to study ligand-chlorometallate hydrogen bonding interactions.

### 2.4.1. X-Ray Crystallography

Brammer and Orpen have conducted leading research on solid state ligand-chlorometallate hydrogen bonding interactions for application in the field of inorganic crystal engineering (see Chapter 1, Section 1.8.4).[31-36] In this thesis, solid state structures of ligand-chlorometallate complexes were analysed using X-ray crystallography to examine the hydrogen bonding interactions that might be important in solvent extraction.

X-ray crystallography has become an increasingly popular technique for analysing hydrogen bonding interactions because of the increasingly accessible and powerful diffractometers and computational facilities.[37] However, there are certain

disadvantages associated with using X-ray crystallography as a tool for investigating interactions between ligand and chlorometallate in solvent extraction systems. One such disadvantage stems from the difficulties associated with the placement of hydrogen atoms which is vital for establishing potential hydrogen bonding interactions. X-rays interact with electron density and, in most cases, the nucleus of a particular atom can be found at the centre of the electron shell. However, when hydrogen atoms are covalently bonded to an atom of higher electronegativity, the average position of the single electron of the hydrogen atom is displaced towards the other atom and is, therefore, not representative of the position of the hydrogen nucleus.[38] In order to find a more representative position for hydrogen atoms, without resorting to neutron-diffraction techniques, it has become common practice to theoretically place the hydrogen atoms.[39] This can be done by using standard X-H bond lengths that have been previously determined using neutron diffraction. The problem with this practice is that it does not always take into account the angular distortion or elongation of the X-H bond that can arise from hydrogen bonding.[39]

Another problem with using X-ray crystallography to investigate ligand-chlorometallate interactions in the new systems is the difficulty associated with growing crystals. All of the extractants investigated in this study have long alkyl chain functionality that have a high degree of flexibility which does not allow for easy crystallisation, forming instead as oil or amorphous solids. This made it impossible to analyse the solid state structures of many of the ligand-chlorometallate complexes. To circumvent this problem, analogues of some of the most important ligands in this study were synthesised with shorter alkyl chains or with functionality designed to aid crystallisation. Crystalline ligand-chlorometallate complexes of these analogues were analysed using X-ray crystallography and the major interactions were assumed to be representative of the original extractant molecule.

Perhaps the biggest problem associated with using X-ray crystallography to analyse the ligand-chlorometallate interactions that are important in solvent extraction is that it is a solid state technique, whereas solvent extraction systems are in solution. Crystal packing forces only exist in the solid state and they can distort the structure

so that it is not representative of the solution state structure. In the solution phase, a major factor in complex stability may arise from solvation by non-polar molecules, which is not taken into account in crystal structure analysis. For this reason, it is desirable to compare X-ray crystal structures with solution phase analysis to verify whether the perceived solid-state interactions also exist in solution.

### 2.4.2. Solution Phase Techniques

IR and NMR spectroscopy are both standard techniques that can be used for the study of hydrogen bonding interactions in the solution phase.[40] In IR spectroscopy, the D-H stretching frequency is sensitive to hydrogen bonding, with red shifting of the band proportional to the strength of the interaction. Band overlap, however, makes a detailed analysis of hydrogen bonding interactions using this technique difficult.[39]

There are several NMR techniques that can be used to investigate solution phase structure and hydrogen bonding interactions.[41] As zinc is diamagnetic, NMR spectroscopy is an ideal method to study the interactions between the new reagents and the tetrachlorozincate complex in organic solvent. In $^{1}$H NMR spectroscopy, hydrogen bonding interactions cause the proton to be deshielded, resulting in a downfield shift that correlates with the distance between donor and acceptor atoms.[39, 42] By comparing the $^{1}$H NMR spectra for the free ligand with the ligand-chlorometallate and ligand-chloride complexes, protons that are involved in hydrogen bonding with the anions can be identified by their relative shifts. Large down-field shifts are good evidence for hydrogen bonding interactions and this data can be compared with the interactions observed in the crystal structure.

Nuclear Overhauser effect (NOE) spectroscopy is a useful method for investigating the structure of compounds in the solution phase.[41] The NOE refers to the phenomenon that when one of two nuclei in close proximity is irradiated, the NMR signal of the other nucleus becomes weaker or more intense, arising from the two nuclei relaxing each other over the short distance.[41, 43] Unlike spin coupling, the NOE

is observed through space, not through bonds, and thus provides information on the molecular geometry. In this study, 1D NOE difference spectroscopy was used to investigate the solution phase structure of the ligand-tetrachlorozincate complexes. 1D NOE difference spectra are obtained by subtracting the normal $^{1}H$ NMR spectrum from a spectrum taken with the irradiating signal on.[41] The resulting spectra shows the peak corresponding to the irradiated proton signal and other peaks corresponding to protons in close proximity.

One problem encountered when analysing the ligand-chlorometallate interactions using NMR spectroscopy was the difficulty associated with obtaining a conformationally pure product. If the complex is not conformationally pure, then some peaks in the spectra lose their multiplicity and are difficult to assign. Figure 2.6 shows the $^{1}H$ NMR spectra for TOA and the protonated TOA-chloride and TOA-tetrachlorozincate complexes and it can be seen that, upon ion-pair formation, the peaks corresponding to the protons most involved in interaction with the anion (protons A) lose their multiplicity and appear as broad singlets, making them difficult to assign. Conformationally pure ligand-anion complexes can be produced by crystallisation which, owing to the flexible nature of the ligands, was challenging.

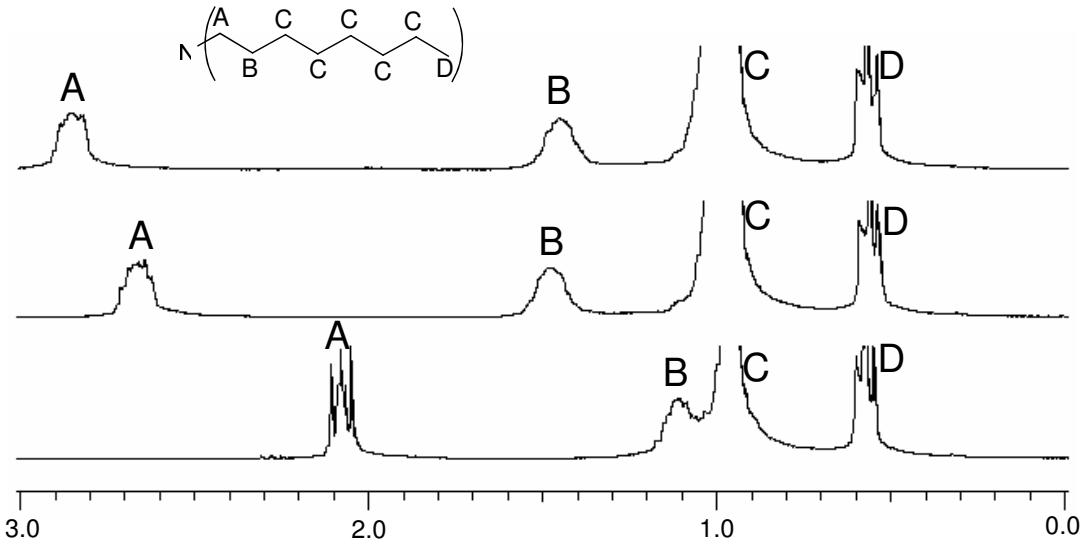


**Figure 2.6: The NMR spectra of TOA (bottom), TOA·HCl (middle) and $(TOA·H)_2ZnCl_4$ (top).**

### 2.4.3. Computational Methods

An attractive complement to the experimental techniques is the use of theoretical methods, which can be used to study a wide range of chemical systems, in the gas, solution and solid phases. Computational methods can be especially beneficial for cases where experimental data is unavailable.[44]

There are many different computational approaches available, the choice of which is determined by the size of the system and the property of interest. *Ab initio* computational methods are currently the most reliable, and provide a description of the properties and electronic structure of a molecule that is based purely on quantum mechanics, with no empirical parameters. They have proven useful for studying both inter- and intra-molecular interactions and have been employed extensively for the study of hydrogen bonding systems.[45] However, the most accurate *ab initio* calculations come at a high computational cost and are thus unsuitable for the study of the relatively large systems involved in this investigation.

Density Functional Theory (DFT) is a more recent, but increasingly popular, method that can be employed in simulating molecular interactions.[46, 47] By mapping the electron density with the electronic wave function, DFT calculations decrease the number of variables that need to be considered, which results in much more efficient calculations without significant loss of accuracy. It employs a conceptually different approach to wavefunction-based *ab initio* calculations, and instead focuses on the electron density of the system. The electronic energy is said to be a functional of the electron density, in that for each electron density there is a corresponding energy. As with *ab initio* methods, the proper inclusion of the exchange and correlation energy is also of paramount importance in DFT. As the electronic energy has been shown to be a functional of the electron density, so too is the exchange-correlation energy, although the functional form is unknown. Many different functionals have, therefore, been developed to attempt to describe the exchange and correlation interactions. Some are pure functionals, with no empirical parameters, others are described as hybrid functionals, and may contain parameters derived from *ab initio* methods or experiment.

Similarly to the wavefunction in *ab initio* methods, the electron density in DFT is constructed from a *basis set*, of known functions, of which there are many different types with varying degrees of complexity.[46] In this work, a 6-31g(d,p) basis set[48] is used, which is a split valance basis constructed from Gaussian functions. The core electrons are each described by one Gaussian function, which is itself built from six primitive Gaussian functions. The valence electrons are each described by two Gaussian functions, one built from three primitives and one which is a single primitive. The basis set is augmented with polarisation functions (d,p) – p functions on hydrogen and d functions on the heavier atoms.

The functional used was B3LYP, a hybrid functional (Becke's three-parameter exchange functional (B3)[49] and the correlation functional of Lee, Yang and Parr (LYP)[50]).

At this level of theory, optimised structures and relative interaction energies were calculated across a ligand series (Chapter 3, Section 3.6.3). This allowed for the study of ligands that were not investigated using the afore mentioned spectroscopic and crystallographic techniques.

The computational work described herein relates to the gas phase structures of the ligand-metallate complexes, which are likely to be more representative of the structures in the very poorly coordinating solvents used in this work, rather than the crystallographically determined solid state structures.

All calculations were performed on the EaStCHEM Research Computing Facility using Gaussian 03[51] with the assistance and guidance of Dr Patricia Richardson.

## 2.5. General Experimental Details

As many of the methods regarding chemicals and instrumentation, and solvent extraction experiments were similar in Chapters 3, 4 and 5, some of the procedures and experimental details are given here to avoid repetition.

### 2.5.1. Chemicals and Instrumentation

All solvents and reagents were acquired from Fisher, Aldrich or Acros. $^{1}H$ and $^{13}C$ NMR were obtained using a Bruker AC250 spectrometer at ambient temperature unless otherwise stated. Chemical shifts (δ) are reported in parts per million (ppm) relative to internal standards. CHN analytical data were obtained by the University of St Andrews Microanalytical Service on a CE-440 Elemental Analyzer. Mass spectrometry was performed on a Micromass ZMD instrument with a z-spray ESI source.

### 2.5.2. Solvent Extraction Experiments

ICP-OES analysis was performed on a Perkin Elmer Optima 5300DV spectrometer and standards were purchased from Alfa Asar. All volumes were measured using 5, 2.5, 1 and 0.25 mL pipettes. Samples were filtered using 0.45 μm syringe filters. The measurements of pH were carried out using a Sartorius PP-50 pH meter. All extractions were performed by vigorously stirring solutions with magnetic stirrer bars in sealed 100 mL Schott bottles overnight at room temperature.

#### 2.5.2.1. Control Experiment Analysing for Zn(II) and Chloride

A solution of $[(L^{2}H)_{2}ZnCl_{4}]$ in toluene (10 mL, 5.33 mM) was prepared by weighing the previously characterised crystalline solid (see Chapter 3, section 3.8.3) (0.06 g, 0.05 mmol) into a 10 mL volumetric flask and diluting to the mark with toluene. An aliquot (1 mL) of the organic phase was transferred into a 5 mL volumetric flask, evaporated *in vacuo* and diluted to the mark with butan-1-ol for ICP-OES analysis. An aliquot (3 mL) of the toluene solution was stirred with aqueous NaOH solution (3

mL, 0.05 M) for 30 mins. The phases were separated and the aqueous phase was filtered. An aliquot of the filtrate (0.5 mL) was stirred, in a darkened box, with 0.5 mL of an aqueous solution of $AgNO_3$ (0.03 M) in $HNO_3$ (1 M) for 5 mins. The resulting AgCl precipitate was filtered off and a 0.5 mL aliquot of the filtrate was transferred into a 5 mL volumetric flask and made up to the mark with 1 M $HNO_3$ for Ag(I) analysis by ICP-OES.

#### 2.5.2.2. Control Experiment Analysing for Chloride in the Presence of $PtCl_6^{2-}$

Five aqueous solutions of $H_2PtCl_6$ (5 mL, 0.65 mM) containing variable NaCl (0.11-5.00 mM) were prepared. Aliquots (2.5 mL) of each solution were transferred into vials containing $CsNO_3$ (0.01 g, 0.51 mmol) and stirred for 5 mins. To each aqueous phase, a 2.5 mL aliquot of $AgNO_3$ solution (6.00 mM) in $HNO_3$ (1 M) was added and stirred in a darkend box for 5 mins. The precipitate was filtered off and a 0.5 mL aliquot of the filtrate was transferred into a 5 mL volumetric flask and made up to the mark with 1 M $HNO_3$ for Ag(I) analysis by ICP-OES.

#### 2.5.2.3. Dependence of M(II) Loading on pH

Aqueous metal chloride solutions (0.01 M $MCl_n$, 6 M $Cl^-$) of acidity ranging between pH -2 and 6 were prepared by measuring 2.5 mL of $MCl_n$ solution (0.02 M $MCl_n$ in 6 M LiCl) into 5 mL volumetric flasks and adding variable quantities of HCl solution (6 M HCl or 0.1 M HCl in 6 M LiCl) and diluting to the mark with 6 M LiCl solution. The aqueous phase aliquots were extracted with ligand solutions in toluene (5 mL, 0.01 M) and the phases were separated. Aliquots (1 mL) of the organic phases were transferred into 5 mL volumetric flasks, evaporated *in vacuo* and diluted to the mark with butan-1-ol for ICP-OES analysis and the pH of the aqueous phases were recorded.

#### 2.5.2.4. Dependence of M(II) Loading on Chloride Concentration

Aqueous metal chloride solutions (0.01 M $MCl_n$, 0.1 M $H^+$) of chloride concentrations ranging between 0.1 M and 8 M were prepared by measuring

0.0625 mL of $MCl_n$ solution (0.8 M $MCl_n$ in 8 M HCl) into 5 mL volumetric flasks and adding varying quantities of 8 M LiCl solution and diluting to the mark with deionised water. The metal chloride solutions were extracted with ligand solution in toluene (5 mL, 0.01M) and the phases were separated. Aliquots (1 mL) of the organic phases were transferred into 5 mL volumetric flasks, evaporated *in vacuo* and diluted to the mark with butan-1-ol for ICP-OES analysis.

#### 2.5.2.5. Dependence of M(II) Loading on Ligand Concentration

Solutions of ligand were prepared at varying concentrations between 0.0005 - 0.05 M by weighing aliquots of 0.05 M ligand stock solution in toluene into 5 mL volumetric flasks and diluting to the mark with toluene. The ligand solutions were extracted with metal chloride solutions (250 ppm M(II) in one part 6 M LiCl to one part 6 M HCl). Aqueous samples for ICP-OES analysis were prepared by weighing 2 mL of the aqueous phase into 5 mL volumetric flasks and diluting to the mark with deionised water.

#### 2.5.2.6. Stripping and Reagent Reuse

An aqueous metal chloride solution (15 mL, 0.01 M $MCl_2$, 6 M HCl) was extracted with an equal volume of 0.01 M ligand solution in toluene. The phases were separated and an aliquot (1 mL) of the organic phase was transferred into a 5 mL volumetric flask, evaporated *in vacuo* and diluted to the mark with butan-1-ol for ICP-OES analysis. The remaining organic phase was stirred for 30 mins with an equal volume of deionised water, after which the phases were separated and an aliquot (1 mL) of the organic phase was transferred into a 5 mL volumetric flask, evaporated *in vacuo* and diluted to the mark with butan-1-ol for ICP-OES analysis. The remaining organic phase was subjected to two more load strip cycles as described above.

#### 2.5.2.7. Analysis for Zn(II) or Co(II) and Total Chloride Loading

An aqueous metal chloride solution (5 mL, 0.01 M $MCl_2$, 6 M HCl) was extracted with ligand solution in toluene (5 mL, 0.01 M) and the phases were separated. An aliquot (1 mL) of the organic phase was transferred into a 5 mL volumetric flask, evaporated *in vacuo* and diluted to the mark with butan-1-ol for ICP-OES analysis. An aliquot (3 mL) of the organic phase was stirred with aqueous NaOH solution (3 mL, 0.05 M) for 30 mins. The phases were separated and the aqueous phase was filtered. An aliquot of the filtrate (0.5 mL) was stirred, in a darkened box, with 0.5 mL of an aqueous solution of $AgNO_3$ (0.04 M) in $HNO_3$ (1 M) for 5 mins. The resulting AgCl precipitate was filtered off and a 0.5 mL aliquot of the filtrate was transferred into a 5 mL volumetric flask and made up to the mark with 1 M $HNO_3$ for Ag(I) analysis by ICP-OES.

## 2.6. References

1. Montalbetti, C. A. G. N.; Falque, V., Amide bond formation and peptide coupling. *Tetrahedron,* **2005,** 61, (46), 10827-10852.

2. Bell Katherine, J.; Westra Arjan, N.; Warr Rebecca, J.; Chartres, J.; Ellis, R.; Tong Christine, C.; Blake Alexander, J.; Tasker Peter, A.; Schroder, M., Outer-sphere coordination chemistry: selective extraction and transport of the [PtCl6]2- anion. *Angew Chem Int Ed Engl,* **2008,** 47, (9), 1745-8.

3. Forgan, R. S., *Ph.D Thesis*, Modification of Phenolic Oximes for Copper Extraction. University of Edinburgh, **2008**.

4. Gordon, R. J., *Ph.D Thesis*, Improved mass transportation efficiency in copper solvent extraction. University of Edinburgh, **2008**.

5. Bacon, G.; Mihaylov, I., Solvent extraction as an enabling technology in the nickel industry. *Int. Solvent Extr. Conf., Cape Town, South Africa, Mar. 17-21, 2002,* **2002**, 1-13.

6. Varnes, A. W., Inductively coupled plasma mass spectrometry. *Handb. Instrum. Tech. Anal. Chem.,* **1997**, 419-439.

7. Boorn, A. W.; Browner, R. F., Effects of organic solvents in inductively coupled plasma atomic emission spectrometry. *Anal. Chem.,* **1982,** 54, (8), 1402-10.

8. Good, M. L.; Bryan, S. E.; Holland, F. F., Jr.; Maus, G. J., Nature of the hydrogen ion effect on the extraction of Co(II) from aqueous chloride media by substituted ammonium chlorides of high molecular weight. *J. Inorg. Nucl. Chem.,* **1963,** 25, (9), 1167-73.

9. Haesebroek, G.; De Schepper, A.; Van Peteghem, A., Solvent extraction of iron and zinc from concentrated cobalt(II) chloride solutions at Metallurgie Hoboken-Overpelt. *Extr. Metall. Nickel Cobalt, Proc. Symp. 117th TMS Annu. Meet.,* **1988**, 463-77.

10. Miller, J. D.; Fuerstenau, M. C., Hydration effects in quaternary amine extraction systems. *Met. Trans.,* **1970,** 1, 2531-5.

11. Sato, T.; Shimomura, T.; Murakami, S.; Maeda, T.; Nakamura, T., Liquid-liquid extraction of divalent manganese, cobalt, copper, zinc and cadmium from

aqueous chloride solutions by tricaprylmethylammonium chloride. *Hydrometallurgy,* **1984,** 12, (2), 245-54.

12. Wassink, B.; Dreisinger, D.; Howard, J., Solvent extraction separation of zinc and cadmium from nickel and cobalt using Aliquat 336, a strong base anion exchanger, in the chloride and thiocyanate forms. *Hydrometallurgy* **2000,** 57, (3), 235-252.

13. Blitz-Raith, A. H.; Paimin, R.; Cattrall, R. W.; Kolev, S. D., Separation of cobalt(II) from nickel(II) by solid-phase extraction into Aliquat 336 chloride immobilized in poly(vinyl chloride). *Talanta,* **2007,** 71, (1), 419-423.

14. Paimin, R.; Cattrall, R. W., The extraction of cobalt(II) from lithium chloride solutions by Aliquat 336 dissolved in chloroform. *Aust. J. Chem.,* **1982,** 35, (11), 2345-51.

15. Paimin, R.; Cattrall, R. W., The extraction of cobalt(II) from hydrochloric acid solutions by Aliquat 336R dissolved in chloroform. *Aust. J. Chem.,* **1983,** 36, (5), 1017-20.

16. Tasker, P. A.; Plieger, P. G.; West, L. C., Metal complexes for hydrometallurgy and extraction. *Comprehensive Coordination Chemistry II,* **2004,** 9, 759-808.

17. Harris, G. B.; Lakshmanan, V. I.; Sridhar, R. Leaching of laterite ores with acidic chloride solutions for recovery of metal values, *US Patent,* 2004228783, **2004**.

18. Stensholt, E. O.; Dotterud, O. M.; Henriksen, E. E.; Ramsdal, P. O.; Stalesen, F.; Thune, E., Development and practice of the Falconbridge chlorine leach process. *CIM Bull.,* **2001,** 94, (1051), 101-104.

19. Moyer, B. A.; Bonnesen, P. V.; Custelcean, R.; Delmau, L. H.; Hay, B. P., Strategies for using host-guest chemistry in the extractive separations of ionic guests. *Kem. Ind.,* **2005,** 54, (2), 65-87.

20. Good, M. L.; Bryan, S. E., Extraction of Group VIII metals by long-chain alkyl amines. II. Cobalt(II)-hydrochloric acid systems. *J. Inorg. Nucl. Chem.,* **1961,** 20, 140-6.

21. Sato, T., The extraction of cobalt(II) from hydrochloric acid solution by tri-n-octylamine. *J. Inorg. Nucl. Chem.,* **1967,** 29, (2), 547-53.

22. Grant, R.; Belair; S., Refinery 2020, *Personal Communication*, Next Generation PM Solvex (Confidential), **2009**.

23. du Preez, J. G. H., Recent advances in amines as separating agents for metal ions. *Solvent Extr. Ion Exch.,* **2000,** 18, (4), 679-701.

24. Sato, T.; Nakamura, T., The stability constants of the aqueous chloro complexes of divalent zinc, cadmium and mercury determined by solvent extraction with tri-n-octylphosphine oxide. *Hydrometallurgy,* **1980,** 6, (1-2), 3-12.

25. Dalton, R. F.; Price, R.; Hermana, E.; Hoffman, B., Cuprex process. A new chloride-based hydrometallurgical process for copper recovery from sulfide ores. *Ingenieria Quimica,* **1987,** 19, (215), 115-120.

26. Borowiak-Resterna, A.; Kyuchoukov, G.; Szymanowski, J., Options for copper(II) and zinc(II) extraction from chloride media with bi-functional extractants. *Int. Solvent Extr. Conf., Cape Town, South Africa, Mar. 17-21, 2002* **2002**, 988-994.

27. Varnes, A. W., *Inductively Coupled Plasma Atomic Emission Spectroscopy*. Prentice Hall, New Jersey, **1997**.

28. Lin, T., *Ph.D Thesis*, Strength, transport efficiency and selectivity of novel extractants for the recovery of base metals. University of Edinburgh, **2009**.

29. Vogel, A., *A Textbook of Macro and Semimacro Qualitative Inorganic Analysis*., Longman: New York, 5, **1979**.

30. Westra Arjan, N.; Chartres, J.; Ellis, R.; Robertson, D.; Tasker Peter, A., *Private Communication,* Meeting Proceedings, *Edinburgh*, **2006**.

31. Angeloni, A.; Orpen, A. G., Control of hydrogen bond network dimensionality in tetrachloroplatinate salts. *Chem. Commun.,* **2001**, (4), 343-344.

32. Balamurugan, V.; Hundal, M. S.; Mukherjee, R., First systematic investigation of C-H...Cl hydrogen bonding using inorganic supramolecular synthons: lamellar, stitched stair-case, linked-ladder, and helical structures. *Chem.--Eur. J.,* **2004,** 10, (7), 1683-1690.

33. Brammer, L.; Swearingen John, K.; Bruton Eric, A.; Sherwood, P., Hydrogen bonding and perhalometallate ions: a supramolecular synthetic strategy for new inorganic materials. *Proc Natl Acad Sci U S A,* **2002,** 99, (8), 4956-61.

34. Gillon, A. L.; Lewis, G. R.; Orpen, A. G.; Rotter, S.; Starbuck, J.; Wang, X.-M.; Rodriguez-Martin, Y.; Ruiz-Perez, C., Organic-inorganic hybrid solids: control of perhalometallate solid state structures. *Dalton,* **2000**, (21), 3897-3905.

35. Lewis, G. R.; Orpen, A. G., A metal-containing synthon for crystal engineering: synthesis of the hydrogen bond ribbon polymer [4,4'-H2bipy][MCl4] (M = Pd, Pt). *Chem. Commun.,* **1998**, (17), 1873-1874.

36. Rivas, J. C. M.; Brammer, L., Self-Assembly of 1-D Chains of Different Topologies Using the Hydrogen-Bonded Inorganic Supramolecular Synthons N-H...Cl2M or N-H...Cl3M. *Inorg. Chem.,* **1998,** 37, (19), 4756-4757.

37. Desiraju, G.; Steiner, T., *The Weak Hydrogen Bond: Applications to Structural Chemistry and Biology*. Oxford University Press, Oxford, **1999**, 528.

38. Schuster, P.; Zundel, G.; Sandorfy, C., *The Hydrogen Bond: Recent Developments in Theory and Experiments, Vol. 3: Dynamics, Thermodynamics, and Special Systems*. **1976**, 662.

39. Steiner, T., The hydrogen bond in the solid state. *Angew Chem Int Ed Engl,* **2002,** 41, (1), 49-76.

40. Jeffrey, G. A., *An Introduction to Hydrogen Bonding*. **1997**, 272.

41. Williams, D. H.; Fleming, I., *Spectroscopic Methods in Organic Chemistry. 4th Ed*. **1990**, 302.

42. Connors, K. A., *Binding Constants: The Measurements of Molecular Complex Stability*, **1987**, 350.

43. Mason, J.; Editor, *Multinuclear NMR*. **1987**, 639.

44. Gillan, M. J., The virtual matter laboratory. *Contemp. Phys.,* **1997,** 38, (2), 115-130.

45. Del Bene, J. E.; Jordan, M. J. T., What a difference a decade makes: progress in ab initio studies of the hydrogen bond. *THEOCHEM,* **2001,** 573, 11-23.

46. Riley, K. E.; Op't Holt, B. T.; Merz, K. M., Jr., Critical Assessment of the Performance of Density Functional Methods for Several Atomic and Molecular Properties. *J. Chem. Theory Comput.,* **2007,** 3, (2), 407-433.

47. Ziegler, T.; Tschinke, V., Density functional theory as a practical tool in organometallic energetics and dynamics. *Density Funct. Methods Chem.,* **1991**, 139-54.

48. Hariharan, P. C.; Pople, J. A., Influence of polarization functions on MO hydrogenation energies. *Theor. Chim. Acta.,* **1973,** 28, (3), 213-22.

49. Becke, A. D., A new mixing of Hartree-Fock and local-density-functional theories. *J. Chem. Phys.,* **1993,** 98, (2), 1372-7.

50. Lee, C.; Yang, W.; Parr, R. G., Development of the Colle-Salvetti correlation-energy formula into a functional of the electron density. *Phys. Rev. B: Condens. Matter,* **1988,** 37, (2), 785-9.

51. Frisch, M. J.; Trucks, G. W.; Schlegel, H. B.; Scuseria,G. E.; Robb, M. A.; Cheeseman, J. R.; Montgomery, J. A.; Vreven,Jr., T.; Kudin, K. N.; Burant, J. C.; Millam, J. M.; Iyengar, S. S.; Tomasi, J.;Barone, V.; Mennucci, B.; Cossi, M.; Scalmani, G.; Rega,N.; Petersson, G. A.; Nakatsuji, H.; Hada, M.; Ehara, M.; Toyota, K.; Fukuda, R.; Hasegawa, J.; Ishida, M.; Nakajima, T.; Honda, Y.; Kitao, O.;Nakai, H.; Klene, M.; Li, X.; Knox, J. E.; Hratchian, H. P.; Cross, J. B.;Bakken, V.; Adamo, C.; Jaramillo, J.; Gomperts, R.; Stratmann, R. E.;Yazyev, O.; Austin, A. J.; Cammi, R.; Pomelli, C.; Ochterski, J. W.; Ayala, P. Y.; Morokuma, K.; Voth, G. A.; Salvador, P.; Dannenberg, J. J.; Zakrzewski, V.G.; Dapprich, S.; Daniels, A. D.; Strain, M. C.; Farkas, O.; Malick, D. K.; Rabuck, A. D.; Raghavachari, K.; Foresman, J. B.; Ortiz, J. V.; Cui, Q.; Baboul, A. G.; Clifford, S.; Cioslowski, J.; Stefanov, B. B.; Liu, G.; Liashenko, A.; Piskorz, P.;Komaromi, I.; Martin, R. L.; Fox, D. J.; Keith, T.; Al-Laham, M. A.; Peng, C. Y.; Nanayakkara, A.; Challacombe, M.; Gill, P. M. W.; Johnson, B.; Chen, W.; Wong, M. W.; Gonzalez, C.; Pople, J. A., *Gaussian 03, Revision E.01*, Gaussian, Inc., Wallingford CT, **2004**.

# CHAPTER 3

# AMIDO-FUNCTIONALISED STERICALLY HINDERED PYRIDINES

## 3.1 Aims

The aim of the work described in this chapter was to design, synthesise and study the extractive properties of a series of new amido-functionalised sterically hindered alkyl pyridine extractants with varying hydrogen bond donor/acceptor functionality.

## 3.2 Functionalised Pyridines in Base Metal Extraction

In the late 1980s, a division of ICI (now Cytec) patented a new process for the treatment of sulfidic copper ore in acidic chloride media known as the CUPREX process (see Chapter 1, Section 1.7.1),[1, 2] which produces a highly concentrated acidic copper chloride pregnant leach solution. Well established chelating copper extractants, such as the hydroximes,[3] cannot be used to recover the chloro-copper species that form in such solutions and they also produce acid which must be neutralised. ICI proposed an extractant known as ACORGA CLX-50 which selectively recovers $CuCl_2$ from the pregnant leach solution and is responsible for the efficient materials balance in the CUPREX process (see Chapter 1, Section 1.7.1, Scheme 1.1). The active component in ACORGA CLX-50 is diisodecyl pyridine-3,5-dicarboxylate (Figure 3.1).

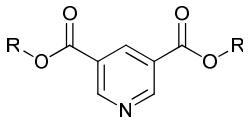


**Figure 3.1: Diisodecyl pyridine-3,5-dicarboxylate, the active component of ACORGA CLX-50 (R = isodecyl).**

Since the inception of the CUPREX process, a range of both ester and amide substituted pyridine ligands have been investigated for copper extraction from chloride feeds.[4-10] The extractive properties of substituted pyridine reagents are dependent on the nucleophilicity of the pyridyl nitrogen, which can be tuned by various substituents at different positions. ACORGA CLX-50, for example, is of optimum nucleophilicity to selectively extract $CuCl_2$ over other metals and chloro-

complexes from about 4 M HCl, whilst allowing for easy stripping with water.[7] Electron-withdrawing groups, such as amides and esters, draw electron density away from the pyridine ring through the inductive effect, thus making the pyridyl nitrogen lone-pairs less nucleophilic. The closer the electron withdrawing group is to the pyridyl nitrogen the larger the effect, so that ligands with substituents on position 2 are less nucleophilic than those with substituents on positions 3 and 4.

Converse to electron-withdrawing groups, the incorporation of electron donating groups increases the basicity of the pyridyl nitrogen. Alkyl groups significantly increase reagent basicity through induction. The position of alkyl substituents relative to the pyridyl nitrogen only has a moderate effect so that reagents with substituents on the 2 and 4 positions are only slightly more basic than those with substituents on the 3 position.[7]

## 3.3 The Design of New Amidopyridyl Ligands for Chlorometallate Extraction in the Anglo American Circuits

Amide and ester substituted pyridine extractants are usually designed to target base metal chloride salts by coordination of the pyridyl nitrogen to the inner-sphere of the metal chloride complex. However, outer-sphere chlorometallate extraction mechanisms resulting from protonation of the pyridyl nitrogen on amido-substituted pyridines (Figure 3.2) have recently been reported for palladium[11] and cadmium[12] chlorometallates at high acid concentrations according to Equation 3.1 (M = Pd(II) or Cd(II):

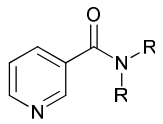


**Figure 3.2: An example of an amido-substituted pyridine reagent shown to extract $CdCl_4^{2-}$[12] and $PdCl_4^{2-}$[11] anions. R = n-hexyl**

**Equation 3.1**

$$2L_{(org)} + 2H^+ + [MCl_4]^{2-} = [(LH)_2MCL_4]_{(org)}$$

The designing of amidopyridyl reagents specifically for chlorometallate solvent extraction is novel. Base metal chlorometallate solvent extractants must be organic soluble as well as selective for proton over metal cation to prevent substitution of chloride during stripping (see Chapter 1, Section 1.8.6). 2,6-Lutidine (Figure 3.3) has been shown to be selective for the extraction of low coordination number cations such as $Ag^{+}$[13] and also has been used as a non-coordinating buffer in aqueous solutions of metal ions.[14] The reagents shown in Figure 3.4 incorporate a 2-*tert*-butyl substituted pyridine unit to act as a protonatable site which will not readily bond to base metal cations. The *tert*-butyl groups also have the advantage of increasing the basicity of the pyridyl nitrogen as well as increasing solubility in the organic phase. The amide and malonamide groups in **L$^{1}$-L$^{4}$** (Figure 3.4) were incorporated to address the outer coordination spheres of chlorometallate ions as such groups are chemically robust and have been used extensively in anion recognition chemistry.[15].

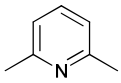


**Figure 3.3: 2,6-Lutidine**

One of the aims of this work was to define what benefits in terms of strength of extraction and selectivity over chloride and between chlorometallates ($FeCl_4^-$, $CoCl_4^{2-}$ and $ZnCl_4^{2-}$ in particular) accrues from the incorporation of the hydrogen bond donor amide and malonamide functionalities. This can be done by using **L$^{0}$** (Figure 3.4) as a control because, in conventional terms, this has only an 'ion-pairing' capability. The ligands **L$^{0}$-L$^{4}$** (Figure 3.4) have varying degrees of amide and malonamide hydrogen bond donor functionality to promote outer-sphere complex formation.

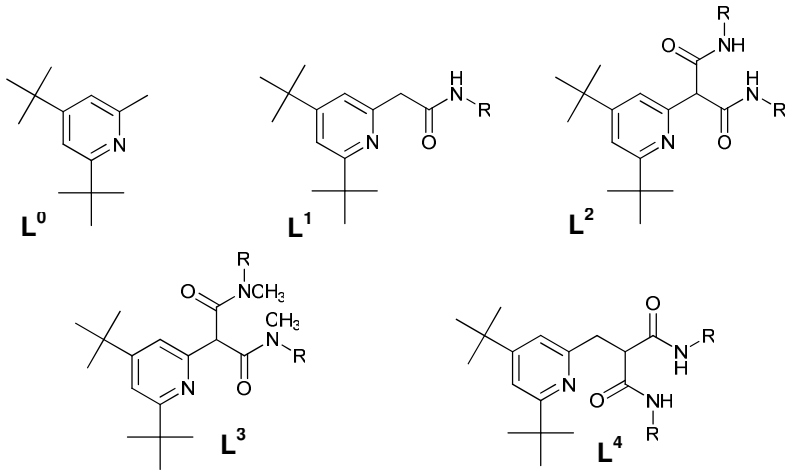


**Figure 3.4: The series of new sterically pyridyl extractants with varying degrees of amide and malonamide functionality (R=n-hexyl).**

## 3.4 Exploration of Synthetic Methods

The ligand $\mathbf{L^0}$ was developed in 71% yield by reacting α-picoline with *tert*-butyl lithium. The synthesis of $\mathbf{L^1}$, $\mathbf{L^2}$ and $\mathbf{L^3}$ proceeded via the same malonic ester intermediate, dimethyl (4,6-di-*tert*-butylpyridin-2-yl)malonate (**1**), which was made in 60% yield by first reacting α-picoline with *tert*-butyl lithium and then with dimethyl carbonate (Figure 3.5). Reacting the malonic ester, **1**, with a 1.3 molar excess of hexylamine yielded $\mathbf{L^2}$ and a mono-substituted product, **2**, in 43% and 55% yields respectively. By subjecting **2** to hydrolysing conditions, $\mathbf{L^1}$ was evolved in 95% yield. The preparation of $\mathbf{L^3}$ was achieved in 70% yield by reacting the malonic ester with *N*-methylhexylamine (Figure 3.6).

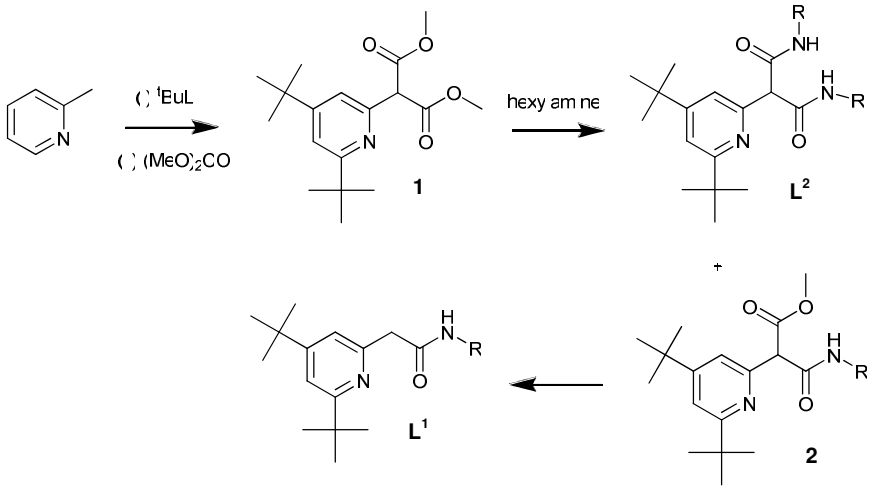


**Figure 3.5: Synthetic route to the amidopyridyl ligands $\mathbf{L^1}$ and $\mathbf{L^2}$ (R=n-hexyl).**

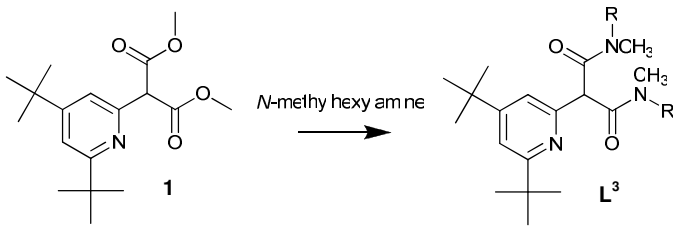


**Figure 3.6: Synthetic route to $L^3$. (R = n-hexyl)**

Figure 3.7 summarises the synthesis of $\mathbf{L^4}$, which involved bromination of $\mathbf{L^0}$ at the benzylic position to produce the bromo-pyridyl product, **3**, in 53% yield. The bromo-pyridyl product was then added to a solution of methyl malonate carbanion (produced by reacting methyl malonate with NaH) to evolve a malonic ester intermediate, **4**, in 77% yield. This was then reacted with hexylamine to develop $\mathbf{L^4}$ in 80% yield.

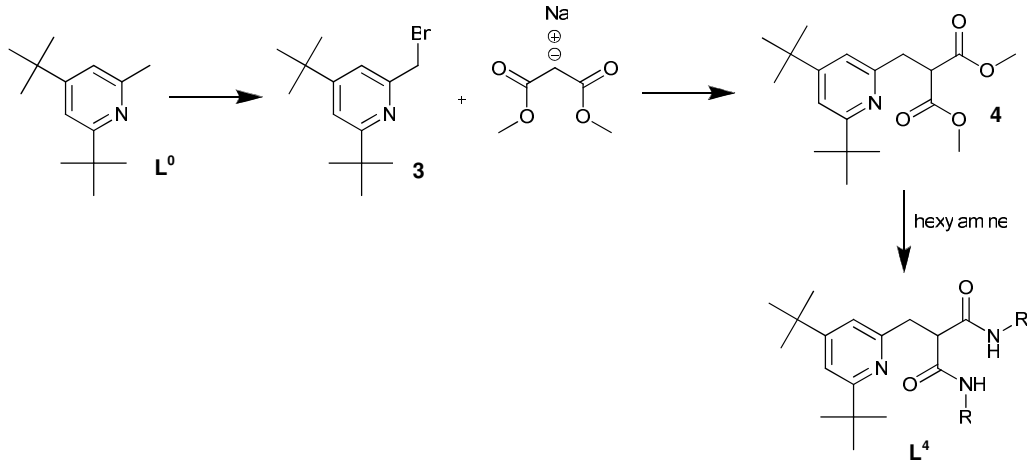


**Figure 3.7: Synthetic route to the amidpyridyl ligand $L^4$ (R=n-hexyl).**

The synthetic methods for all of the ligands are generally high yielding. However, the use of α-picoline and *tert*-butyl lithium as feed-stocks would make the large-scale production of these ligands expensive so that alternative routes should be found for potential commercial application.

## 3.5 Solvent Extraction Experiments

The main aim of the studies reported in this section was to define how the variation of hydrogen bond donor/acceptor functionality in the series of reagents shown in Figure 3.4 affects the *strength* and *selectivity* of chlorometallate extraction; focusing on the extraction of Co(II), Zn(II) and Fe(III) from acidic chloride solutions. The extractants $\mathbf{L^0}$-$\mathbf{L^4}$ all showed sufficient solubility in toluene, both as neutral and protonated species, to allow solvent extraction experiments to be performed readily. All solvent extraction data discussed in this chapter are presented in Appendices 3.1, 3.2 and 3.3.

### 3.5.1 pH Dependence of Metal Loadings

The main aim of the pH dependence experiments was to examine how extractant *strength* varies across the ligand series and to identify the optimum loading pH range for Zn(II) and Co(II) while exploring any conditions that might result in selectivity for the base metals over Fe(III).

When 0.01 M solutions of ligands in toluene were contacted with aqueous solutions of 0.01 M $CoCl_2$ or $ZnCl_2$ containing variable amounts of HCl and an excess of chloride (6 M), metal uptake into the toluene solution showed a marked dependence on the equilibrium pH of the aqueous phase (Figure 3.8). For both Co(II) and Zn(II) extraction, the order of strength of the ligands is: $\mathbf{L^2 > L^4 > L^1 > L^3 >> L^0}$, and $\mathbf{L^0}$, the 'control', which has no amido groups, shows no metal uptake. High Fe(III) loadings were observed for all of the ligands at pH values <1.8 (apart from $\mathbf{L^0}$ which formed an emulsion on contact with acidic ferric chloride solution). Above this pH, Fe(III) precipitates as oxide/hydroxide species. The regions of high iron loading are marked as a red box in Figure 3.8. The ligands $\mathbf{L^2}$ and $\mathbf{L^4}$ are able to extract significant quantities of Zn(II) at pH values at which Fe(III) precipitates. The high *strength* of $\mathbf{L^2}$ and $\mathbf{L^4}$ is significant for commercial application as this could allow for the recovery of Zn(II) from iron-depleted solutions of high pH without the need to re-acidify.

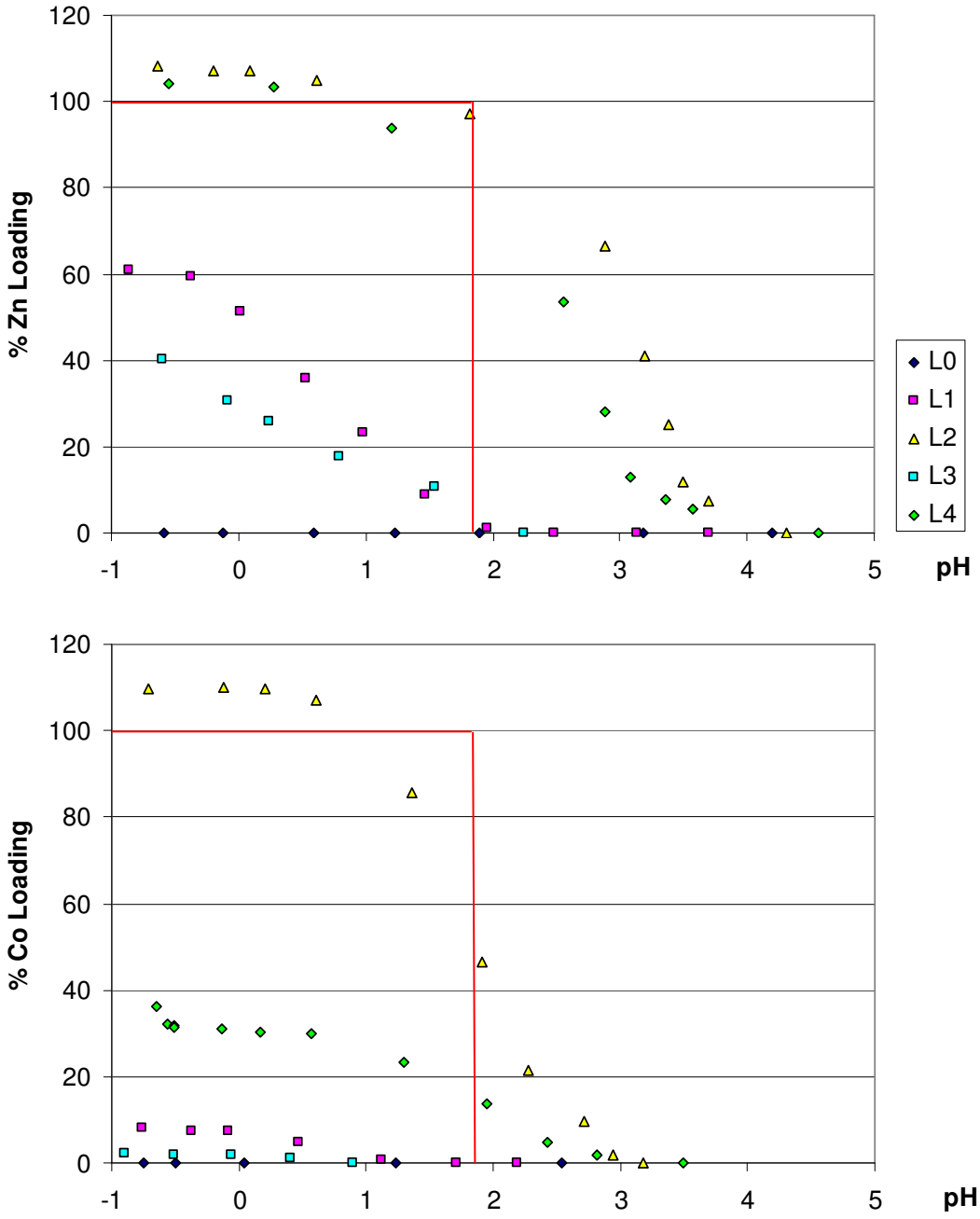


**Figure 3.8: The pH dependence of Zn(II) or Co(II) loading* by 0.01 M toluene solutions of $L^0$, $L^1$, $L^2$, $L^3$ or $L^4$ after contacting with an equal volume of an aqueous chloride ($[Cl^-]$ = 6 M) solution of $CoCl_2$ or $ZnCl_2$ (0.01 M). High Fe(III) loadings are observed inside the red box.**
***Based on formation of $[(LH)_2MCl_4]$**

For all of the ligands, Zn(II) is extracted more readily than Co(II) (lower proton concentrations in the aqueous phase are required to ensure high loadings). This can be ascribed mainly to the overall formation constants for $MCl_x^{n-}$ complexes in aqueous solutions being larger for Zn(II), and the resulting increased activity of

$ZnCl_4^{2-}$ favours extraction. Data on the step-wise formation constants for a large range of metal ions in various oxidation states, according to Equation 3.2, are provided by Sillen and Martell.[16, 17]

**Equation 3.2**

$$M^{z+} + nCl^- = MCl_n^{z-n}$$

$$\beta_n = [MCl_n^{z-n}]/[M^{z+}][Cl^-]^n$$

The reported values for $\beta_n$ have been determined under a variety of conditions using different techniques such as ion exchange, conductivity, solubility, polarography and distribution between two phases and, as a result, vary significantly. These data have been reviewed by Muir who quotes $\log\beta_4$ values for $CoCl_4^{2-}$ and $ZnCl_4^{2-}$ in high ionic strength aqueous chloride solutions as -2.82 and -1.22 respectively.[18] More details of the speciation of metal chloro-complexes with respect to chloride concentration are given in Chapter 1, Section 1.4.

The observation that the Zn(II) loadings of $\mathbf{L^2}$ and $\mathbf{L^3}$ and the cobalt loading of $\mathbf{L^2}$ exceeds 100% at low pH values implies that species can be formed in the organic phase which have lower L:M stoichiometries than the 2:1 value for $[(LH)_2MCl_4]$, e.g. $[(LH)MCl_3]$ or $[(LH)_2M_2Cl_6]$,[19, 20] , or that some double protonation of the ligand can occur to give a dicationic form of the extractant and neutral assemblies with formulae $[(LH_2)MCl_4]$.[21]

## 3.5.2 Chloride Concentration Dependence of Metal Loadings

The main aim of the chloride concentration dependence experiments was to define the optimum aqueous chloride concentrations for the loadings of Zn(II) and Co(II) across the ligand series and to explore any conditions that might result in selectivity for the base metals over Fe(III).

When 0.01 M solutions of ligands in toluene were contacted with aqueous solutions of 0.01 M $FeCl_3$, $CoCl_2$ or $ZnCl_2$ containing variable concentrations of chloride and constant proton (0.1 M), the metal uptake into the organic phase showed a marked dependence on chloride concentration in the aqueous phase (Figure 3.9). It is clear

from the plots in Figure 3.9 that it would be possible to control metal loading and stripping by manipulating chloride concentration in the aqueous phase. Increasing chloride concentration results in increased metal loadings and Zn(II) extracts at lower chloride concentrations than Fe(III), while Co(II) is least readily extracted. This can be attributed to the relative formation constants of the chlorometallate anions (see above), as metal ions which form extractable anionic species more readily (such as Zn(II)) are expected to extract at lower chloride concentrations. The amido-functionalised ligands, $\mathbf{L^1}$-$\mathbf{L^4}$, all extract Zn(II) at a lower chloride concentrations than Fe(III), suggesting that, in solutions that contain moderate concentrations of chloride, the new amido-functionalised ligands may be effective for separating these two metals.

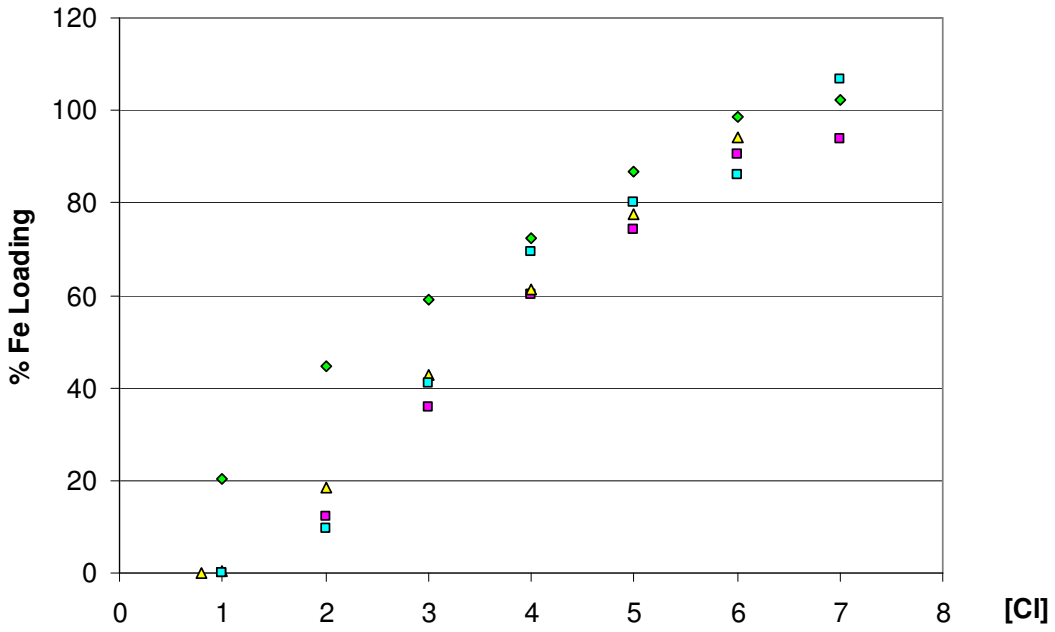

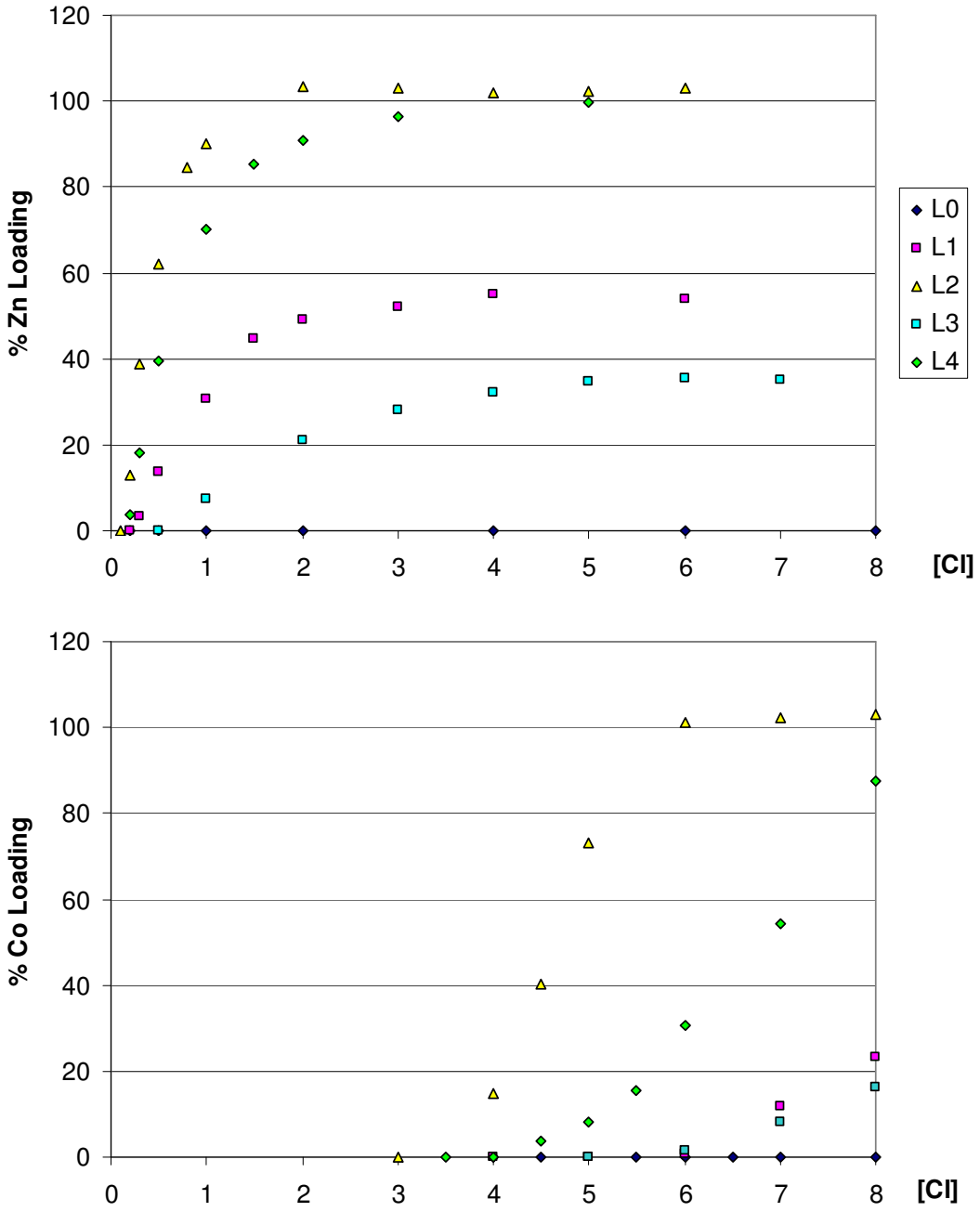


**Figure 3.9: The chloride concentration dependence loadings* of Fe(III), Zn(II) or Co(II) by 0.01 M toluene solutions of $L^0$, $L^1$, $L^2$, $L^3$ or $L^4$ after contacting with an equal volume of an aqueous chloride solution of $FeCl_3$, $CoCl_2$ or $ZnCl_2$ (0.01 M, $[H^+]$ = 0.1 M).**

***based on formation of $[(LH)_2MCl_4]$ for M = Co(II) or Zn(II) and $[(LH)FeCl_4]$.**

### 3.5.3 Extraction Efficiency from Model Pregnant Leach Solutions

This section compares the efficiencies of the new extractants in recovery of Co(II) and Zn(II) from strong acid chloride solutions with compositions chosen to resemble those expected in the pregnant leach solutions of the new Anglo American circuits.

When toluene solutions containing different concentrations of the extractants [L] were contacted with aqueous solutions of 250 ppm Co(II) or Zn(II), 6 M chloride and 3 M proton, metal uptake into the organic phase showed a marked dependence on [L] (Figure 3.10). For both cobalt and zinc extraction, the order of *efficiency* of the ligands resembles the order of *strength*: $\mathbf{L^2 > L^4 > L^1 > L^3 >> L^0}$, and $\mathbf{L^0}$, the 'control', which has no amido groups, shows no metal uptake.

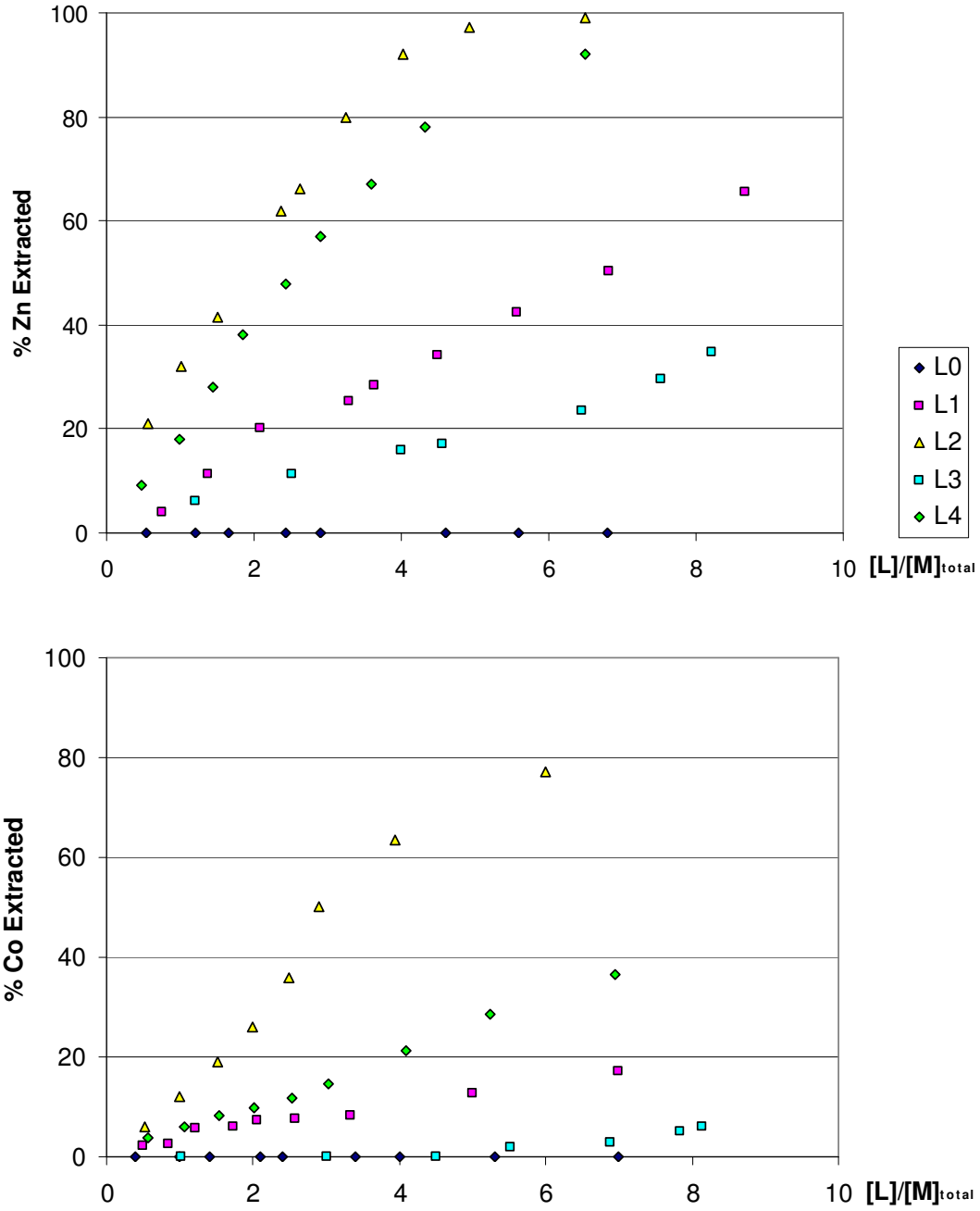


**Figure 3.10: The extraction of Zn(II) and Co(II) into toluene solutions containing different concentrations of reagent after contacting with an equal volume of an aqueous solution of $CoCl_2$ or $ZnCl_2$ (250 ppm M(II), $[H^+]$ = 3 M, $[Cl^-]$ = 6 M). The charts record $[L]_{org}/[M]_{total}$ values.**

### 3.5.4 Stripping

Solvent extraction technology requires the complete recovery of metal value from the water immiscible phase and the subsequent reuse of extractant. This can be demonstrated by the experiment described in Chapter 2, Section 2.3.6. Retention of the metal value in the organic phase may indicate the formation of inner-sphere complexes (discussed in Chapter 1, Section 1.8.6). According to Figure 3.8 and Figure 3.9, contacting a loaded ligand-toluene solution with an aqueous solution of high pH and low chloride concentraiton should facilitate the complete recovery of metal value. The complete recovery of both Co(II) and Zn(II) from loaded solutions of the *strongest* and most *efficient* ligand, $\mathbf{L^2}$, was demonstrated (Figure 3.11) by contacting loaded organic phases with deionised water and comparable loadings in subsequent load-strip cycles indicated no inner-sphere coordination or significant loss in reagent activity.

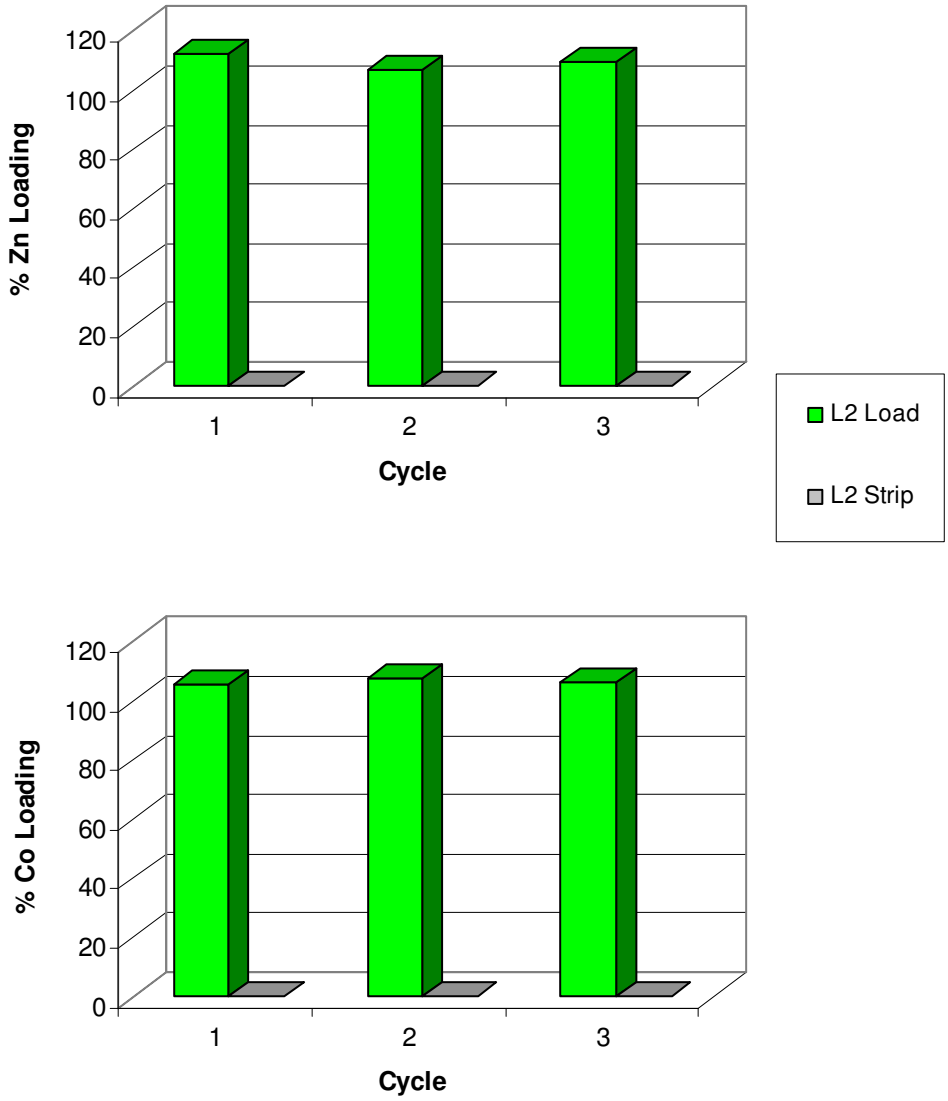


**Figure 3.11: Percentage metal loadings* of 0.01 M toluene solutions of $L^2$ during three successive load-strip cycles. Loading involved the contact of 0.01 M ligand-toluene solutions with 6 M HCl solutions containing 0.01 M Zn(II) or Co(II), and stripping the contact of the loaded organic with an equal volume of deionised water.**

***based on formation of $[(LH)_2MCl_4]$ for M = Co(II) or Zn(II).**

### 3.5.5 Analysis of Metal and Total Chloride Loading of Organic Extractant

It is helpful to know the ratios of chloride to metal ion present in the loaded organic phase to define the mode of action of metallate extraction (see Chapter 2, Section 2.3.7). For $\mathbf{L^2}$, the chloride and Zn(II) or Co(II) concentrations in the toluene were determined under conditions which lead to high loadings; 0.01 M Co(II) or Zn(II) in 6 M HCl. The loaded organic phase was collected and contacted with an alkali aqueous solution to ensure complete stripping and the concentration of stripped chloride was determined as described in Chapter 2, Section 2.3.7.

Table 3.1 displays the results for the [M(II)]/[$Cl^-$] analysis experiment and calculates the relative concentrations of metal-bound chloride (assuming [$Cl^-$] bound = 4 x [$M^{2+}$]) and hence the concentration of free chloride in the organic phase ([$Cl^-$] free = [$Cl^-$] total – [$Cl^-$] bound).

| Metal | [L] | [$M^{2+}$] | % Loading | [$Cl^-$] total | [$Cl^-$] bound | [$Cl^-$] free |
|---|---|---|---|---|---|---|
| | (mM) | (mM) | | (mM) | (mM) | (mM) |
| Co | 6.88 | 3.73 | 108.41 | 23.33 | 14.92 | 8.40 |
| Zn | 6.88 | 3.90 | 113.41 | 19.35 | 15.61 | 3.73 |

**Table 3.1: Total analysis for [M(II)] and [$Cl^-$] loading in toluene solutions containing $\mathbf{L^2}$.**

Table 3.1 shows that the fully loaded organic phase is transporting a significant quantity of 'free' chloride in addition to the chloride bound to the metal ion. This may arise from the transportation of additional HCl as described in Chapter 2, Section 2.3.7, which would be possible by the multiple protonation of $\mathbf{L^2}$. Support for this is provided by evidence that malonamido oxygens can be protonated (see Chapter 5). The multiple protonation of $\mathbf{L^2}$ may also account for the >100% loadings by the formation of 1:1 species such as [($\mathbf{L^2}H_2$)$MCl_4$] as described above at the end of Section 3.5.1.

## 3.6 Analysis of Anion-Host Interactions

The origins of the higher *strength* and *efficiency* of metallate uptake shown by $\mathbf{L^2}$ are of interest. The following sections discuss the major interactions in the solid, solution and gas phase structures of the ligands and their complexes, focussing on $\mathbf{L^2}$.

### 3.6.1 Analysis of $L^2$-Chlorometallate Complexes in the Solid State

At the outset, it was assumed that, on protonation, $\mathbf{L^2}$ would present a tripodal arrangment of the pyridinium and the two amido N-H groups to address the three edges of a face of an $MCl_4^{2-}$ anion as shown in Figure 3.12. The formation of pyridinium hydrogen bonds to chlorometallates is well documented,[22, 23] and for tetrahedral species this typically involves asymmetric bifurcated N-H···$Cl_2M$ linkages.[22] In practice, in the solid state structures of $[(\mathbf{L^2}H)_2CoCl_4]$ and $[(\mathbf{L^2}H)_2ZnCl_4]$ (Figure 3.13), the proton on the pyridinium nitrogen, H1A, shows a preference for interacting with the malonamide oxygen atoms. This effectively locks the ligand in a conformation which allows four separate hydrogen atoms to interact with the outer-coordination sphere of the $MCl_4^{2-}$ anion (Figure 3.13(b)). The central C-H bond of the malonamide unit approaches the centre of the face [Cl1A, Cl2, Cl2A] and, in addition, the two amido and the pyridinium C-H hydrogen atoms, H241, H242 and H3, align with the edges of the same face, forming weak and asymmetric bifurcated hydrogen bonds. These interactions are summarised in Table 3.2.

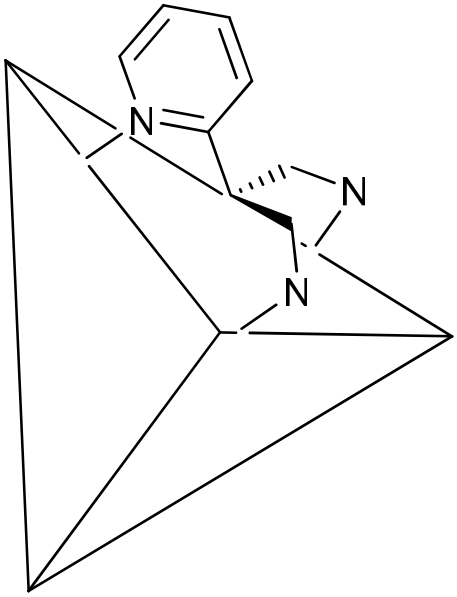


**Figure 3.12: A sketch showing the assumed tripodal N-H donor interactions between $L^2$ and the edges of the $MCl_4^{2-}$ tetrahedron.**

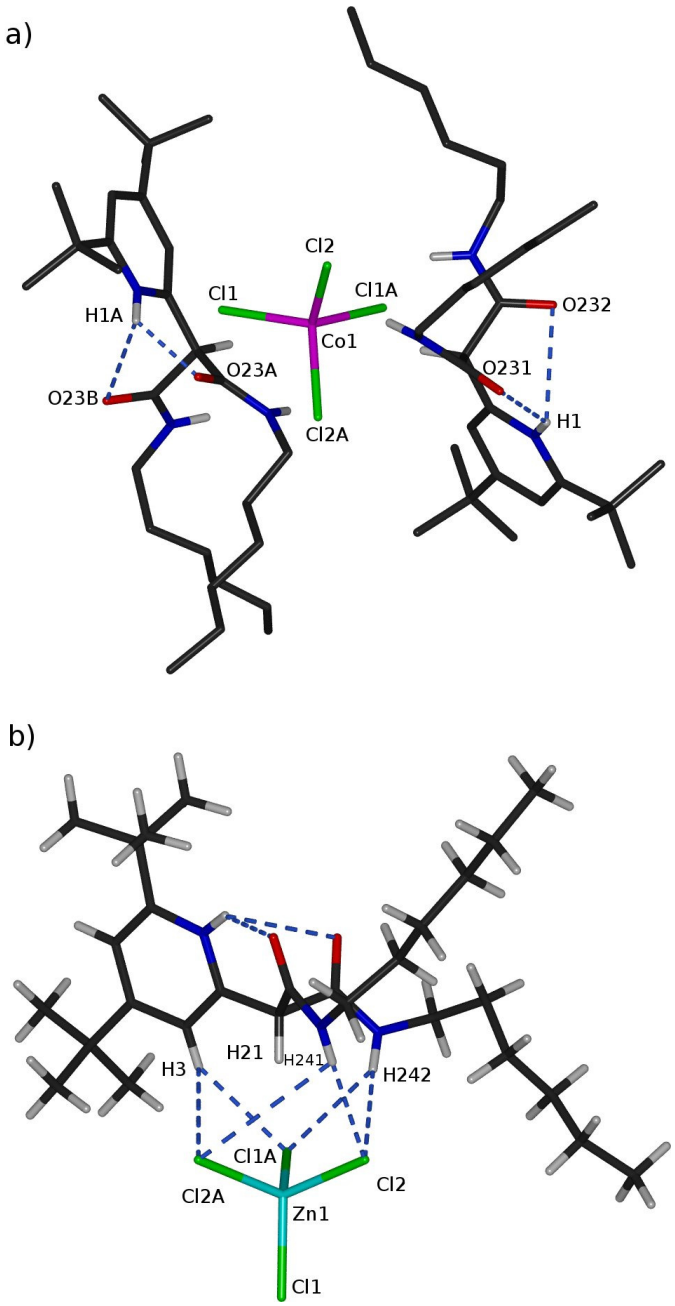


**Figure 3.13: (a) The solid-state structure* of $[(L^2H)_2CoCl_4]$ showing the pyridinium N-H contacts with the malonamide carbonyl groups, H1 to O231 and O232 of 1.978 and 2.831 Å, respectively and (b) the outer sphere contacts in $[(L^2H)_2ZnCl_4]$, H3···Cl1A, H3···Cl2A, H241···Cl2, H241···Cl2A, H242···Cl2 and H242···Cl1A distances are 2.764, 3.219, 2.46, 3.78, 2.60 and 3.05 Å. In addition, the H21 atom makes contacts of 3.104, 2.923, 3.018 and 2.979 Å to Cl1A, Cl2A, Cl2 and Zn.**

***With the exception of the proton attached to the pyridinium nitrogen atom and the malonamide N-H and C-H donors, all hydrogen atoms have been omitted for clarity.**

| Distance | $[(L^2H)_2CoCl_4]$ | $[(L^2H)_2ZnCl_4]$ |
|---|---|---|
| H241-Cl2 | 2.47 | 2.46 |
| H241-C2A | 3.73 | 3.78 |
| H242-Cl2 | 2.596 | 2.60 |
| H242-Cl1A | 3.03 | 3.05 |
| H21-Cl2 | 3.021 | 3.018 |
| H21-Cl1A | 3.112 | 3.104 |
| H21-Cl2A | 2.945 | 2.923 |
| H3-Cl1A | 2.766 | 2.764 |
| H3-Cl2A | 3.223 | 3.219 |
| H1-O232 | 2.831 | 2.892 |
| H1-O231 | 1.978 | 1.889 |

**Table 3.2: The N-H···O, N-H···Cl and C-H···Cl contact distances (Å) for the $[(L^2H)_2MCl_4]$ complexes in Figure 3.13.**

In contrast to the structures of $CoCl_4^{2-}$ salts of 4-halopyridinium cations,[22] formation of $[(\mathbf{L^2}H)_2CoCl_4]$ is accompanied by only small distortions of the metallate anion from idealized tetrahedral geometry (Table 3.3). The two faces of the $CoCl_4^{2-}$ tetrahedron addressed by the $\mathbf{L^2}H^+$ cations show only a small compression (ΣCl-M-Cl; 323.45(7)° c.f. 328.4°) relative to a regular tetrahedron and the other two faces show the consequent identical expansion (ΣCl-M-Cl; 332.98(7)° c.f. 328.4°). A comparison of the cobalt and zinc structures suggests that $\mathbf{L^2}H^+$ interacts slightly more strongly with the $ZnCl_4^{2-}$ ion because there is a larger distortion from tetrahedral geometry. This could contribute to the observed greater strength of extraction of zinc by $\mathbf{L^2}H^+$, but is unlikely to be the major factor (see below).

| Bond lengths and contact distances/ Å and bond and torsion angles/° | M = Co | M = Zn | M = Co | M = Zn |
|---|---|---|---|---|
| M-Cl1 | 2.2405(8) | 2.2292(12) | 2.301 | 2.285 |
| M-Cl2 | 2.2971(8) | 2.3051(13) | 2.342 | 2.348 |
| | | | | |
| Cl1-M-Cl1A | 115.02(5) | 115.89(7) | 119.29 | 118.48 |
| Cl1-M-Cl2 | 108.21(3) | 108.32(5) | 107.60 | 107.65 |
| Cl1-M-Cl2A | 109.75(3) | 109.73(4) | 107.99 | 108.60 |
| Cl2-M-Cl1A | 109.75(3) | 109.73(4) | 108.00 | 108.60 |
| Cl2-M-Cl2A | 105.49(5) | 104.2(8) | 105.57 | 105.07 |
| ΣCl-M-Cl interacting face[a] | 323.45(7) | 322.25(10) | 321.17 | 321.32 |
| ΣCl-M-Cl non-interacting face[b] | 332.98(7) | 333.94(10) | 334.89 | 334.73 |
| | | | | |
| N241-C221-C21-C2 | 150.7(3) | 149.7(4) | | |
| N242-C222-C21-C2 | -134.9(3) | -135.9(4) | | |
| | | | | |
| Cl1···Cl2 | 3.6761(11) | 3.6761(17) | 3.747 | 3.739 |
| Cl1···Cl1A | 3.7798(14) | 3.779(2) | 3.972 | 3.927 |
| Cl1···Cl2A | 3.7114(10) | 3.7084(17) | 3.756 | 3.762 |
| Cl2···Cl1A | 3.7114(10) | 3.7084(17) | 3.756 | 3.762 |
| Cl2···Cl2A | 3.6567(16) | 3.638(3) | 3.730 | 3.727 |
| ΣCl···Cl interacting face[a] | 11.044(2) | 11.022(2) | 11.23 | 11.23 |
| ΣCl···Cl non-interacting face[b] | 11.167(2) | 11.164(2) | 11.45 | 11.42 |

**Table 3.3: Bond lengths, contact distances/Å and torsion angles/° in the inner- and outer-coordination spheres of the cobalt and zinc complexes, $[(L^2H)_2MCl_4]$. Values in the third and forth columns are those from the B3LYP/6-31g(d,p) calculated structures of $[(L^2H)_2ZnCl_4]$ and $[(L^2H)_2CoCl_4]$, respectively (see Section 3.6.3).**

**[a] defined by Cl1,Cl2,Cl2A**

**[b] defined by Cl1,Cl2,Cl1A**

There are many examples of the formation hydrogen bonds, often quite weak, to anions which involve similar C-H donors to those in $\mathbf{L^2}H^+$,[24-26] and C-H···Cl contacts similar to those found in $[(\mathbf{L^2}H)_2CoCl_4]$ and $[(\mathbf{L^2}H)_2ZnCl_4]$ are a feature of many of the structures of the hexachloroplatinate(IV) assemblies formed by the tren-based ligands studied previously (see Chapter 1, Section 1.8.5).[27] The significance of the

contributions from the C-H···Cl contacts to the binding enthalpy of the assemblies is considered in more detail in Section 3.6.3 using density functional theory (DFT) calculations on gas phase structures.

### 3.6.2 Analysis of $L^2$-Chlorometallate Complexes in Organic Solvent

In interpreting the origins of the increased strength and selectivity of $\mathbf{L^2}$ as an extractant for $CoCl_4^{2-}$ and $ZnCl_4^{2-}$, it is important to define whether the mode of interaction of $\mathbf{L^2}H^+$ with the outer-coordination sphere in water-immiscible solvents is similar to that observed in the solid state. NMR spectra of the free ligand $\mathbf{L^2}$ and the salts, $[(\mathbf{L^2}H)Cl]$ and $[(\mathbf{L^2}H)_2ZnCl_4]$, (Figure 3.14 to Figure 3.18) provide evidence that protonation causes both an increase in rigidity and adoption of a particular conformation.

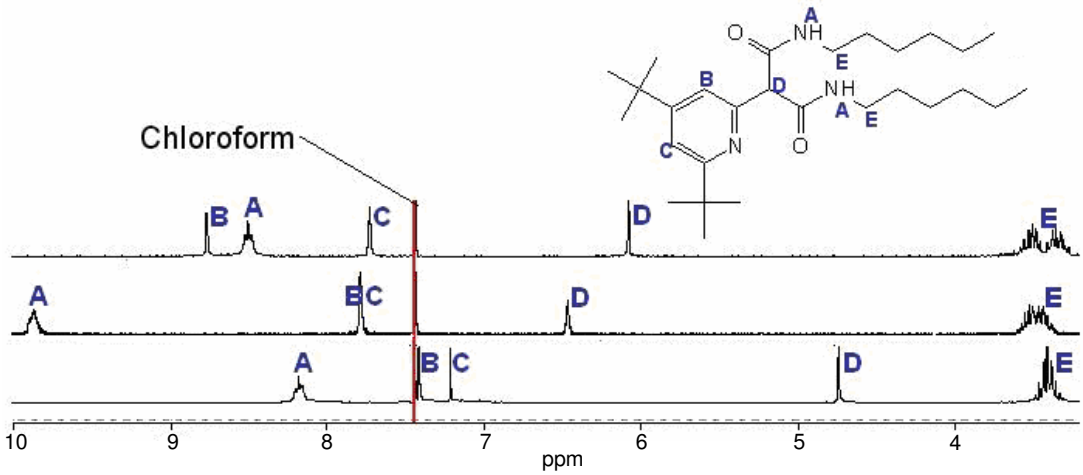


**Figure 3.14: 1D $^1$H NMR spectra for $L^2$ (bottom) and the complexes $[(L^2H)_2ZnCl_4]$ (top) and $[L^2HCl]$ (middle). Solvent = chloroform.**

As expected, the chemical shifts of the groups which form hydrogen bonds in the solid state structure of $[(\mathbf{L^2}H)_2ZnCl_4]$ are very dependent on the nature of the conjugate anion in the $^1$H NMR spectra of $[(\mathbf{L^2}H)Cl]$ and $[(\mathbf{L^2}H)_2ZnCl_4]$ (see signals A, B and D in Figure 3.14). Retention of a 'chelated' structure for the pyridinium N-H proton, located between the two amido oxygen atoms in the solid state (see Figure 3.13) is consistent with its signal in chloroform solution being

observed at very low field (14.80 ppm) in the 600 MHz spectrum (Figure 3.15).

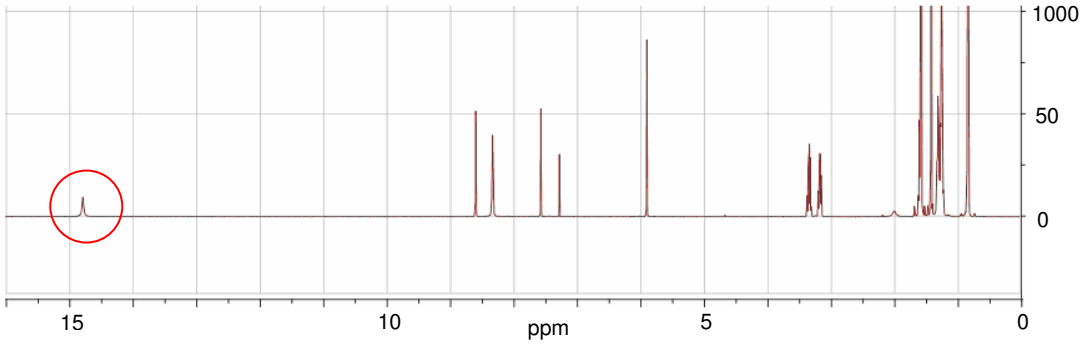


**Figure 3.15: The 600 MHz 1D $^{1}$H NMR spectrum of $[(L^{2}H)_2ZnCl_4]$, showing the pyridinium NH proton at 14.80 ppm. Solvent = chloroform.**

Assignment of signals B and C in the spectrum of $[(\mathbf{L}^{2}H)_2ZnCl_4]$ in Figure 3.14 as C-H pyridinium protons, rather than N-H protons, is confirmed by cross coupling to $^{13}$C in an HSQC NMR experiment (see Figure 3.16).

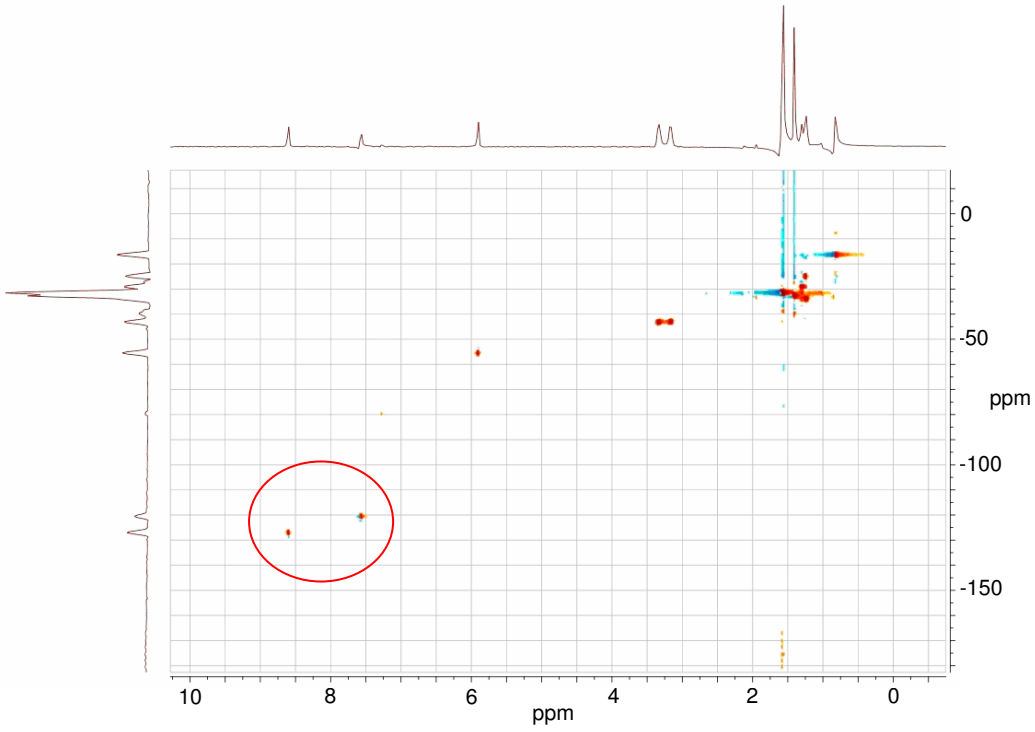


**Figure 3.16: The HSQC spectrum of $[(L^{2}H)_2ZnCl_4]$ showing the low field aromatic proton signals on the x-axis cross coupling with the low field aromatic $^{13}$C signals on the y-axis, confirming the assignment of peaks B and C on the 1D $^{1}$H NMR spectra as aromatic C-H protons. Solvent = chloroform.**

Assignment of signal C in the spectrum of $[(\mathbf{L}^{2}\mathrm{H})_2\mathrm{ZnCl_4}]$ in Figure 3.14 as the 5-H pyridinium proton was established by a 1D NOE difference spectrum (see Figure 3.17). Irradiation of the signal at 7.59 ppm confirmed that the proton is close to *both* the *tert*-butyl groups.

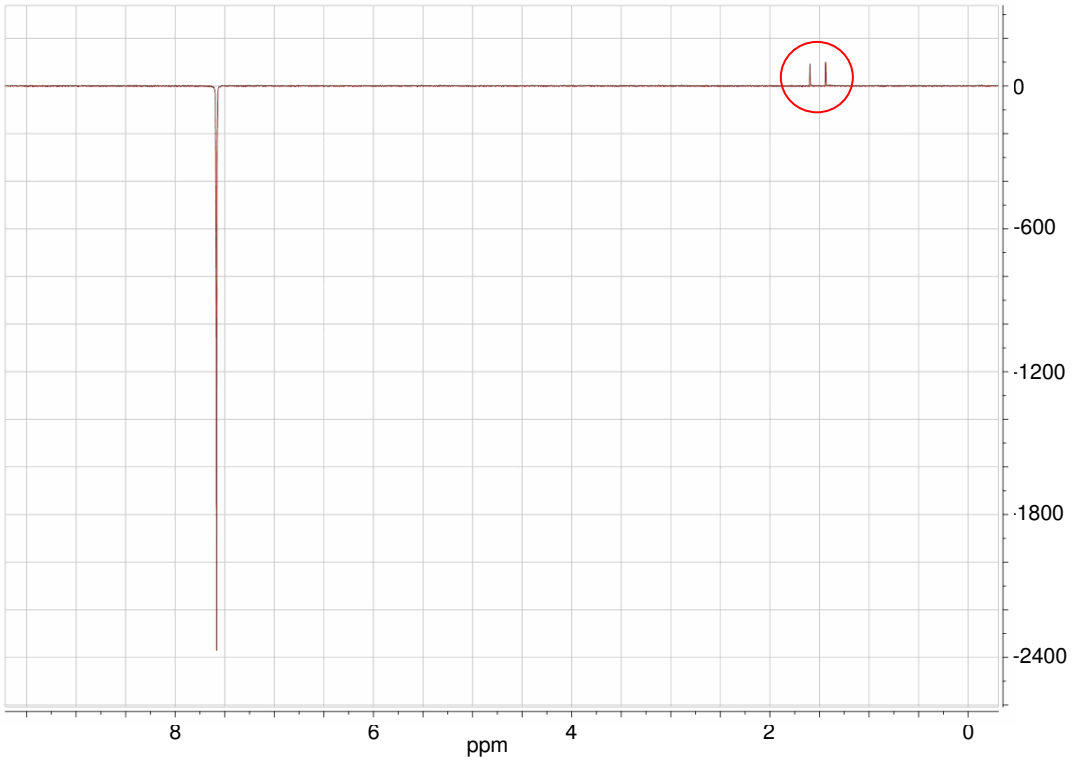


**Figure 3.17: A 1D NOE spectrum of $[(\mathbf{L}^{2}\mathrm{H})_2\mathrm{ZnCl_4}]$, irradiating the signal at 7.59 ppm. Solvent = chloroform.**

Incorporation of the 3-pyridino C-H group into the outer-coordination sphere of $\mathrm{ZnCl_4^{2-}}$ is consistent with its proton signal (see B in Figure 3.14) occurring at much lower field, 8.77 ppm, than in the free ligand and the hydrochloride salt. Protonation of the pyridine ring causes a smaller shift of the 5-H proton signal (see C in Figure 3.14) relative to that in the free ligand and the resulting signals occur at similar shifts in the spectra of $[(\mathbf{L}^{2}\mathrm{H})\mathrm{Cl}]$ and $[(\mathbf{L}^{2}\mathrm{H})_2\mathrm{ZnCl_4}]$ (at 7.81 and 7.72 ppm), which is consistent with this hydrogen atom, in contrast with the 3-H atom, being well separated from the conjugate anion in solution.

To further explore the conformation of $[(\mathbf{L}^{2}\mathrm{H})_2ZnCl_4]$ in organic solvent, a 1D NOE difference spectrum was taken irradiating the signal at 5.87 ppm assigned to the malonamide C-H proton (signal D in Figure 3.14). This spectrum (Figure 3.18) shows peaks at 8.31 and 8.62 ppm that correspond to the amide N-H and the 5-H pyridinium C-H (signals A and B in Figure 3.14) protons. This confirms that the central malonamide C-H and N-H donors and the 5-H pyridinium C-H donor are in close proximity in solution phase, which would arise from a conformation similar to the crystal structure shown in Figure 3.13. This suggests that the solid state structure of $[(\mathbf{L}^{2}\mathrm{H})_2ZnCl_4]$ is representative of the solution phase structure that would occur in the solvent extraction process.

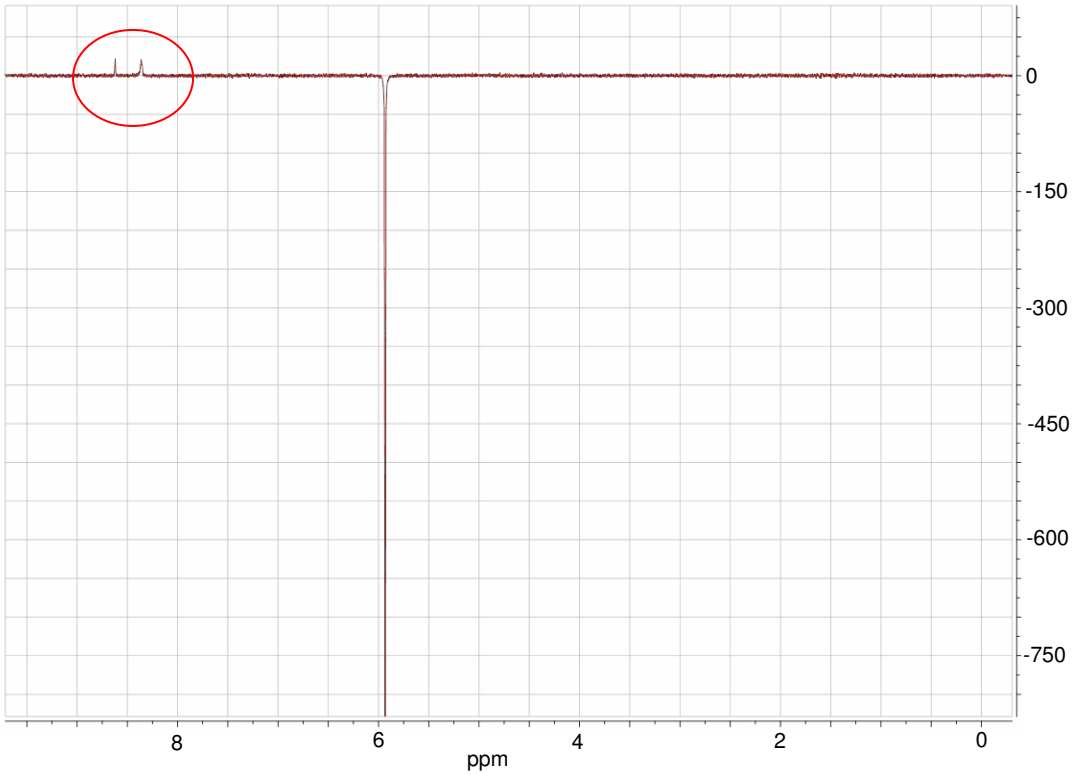


**Figure 3.18: A 1D NOE spectrum of $[(\mathbf{L}^{2}\mathrm{H})_2ZnCl_4]$, irradiating the signal at 5.87 ppm. Solvent = chloroform.**

## 3.6.3 Density Functional Theory Calculations

Density functional theory (DFT) calculations were performed to compare the energy-minimised structures: (i) of the ligands before and after protonation and (ii) of the assemblies formed by the protontated ligands with tetrachlorometallate or chloride anions, in order to investigate the anion binding mechanisms across the ligand series. Most of the discussion below focus on $\mathbf{L^2}$ because it is possible to compare results with the X-ray structures and NMR spectra obtained for its complexes (see Figure 3.13 to Figure 3.18) and also because it is the most efficient chlorometallate extractant. Where possible the atom labelling follows that used for the X-ray structures (see Figure 3.13).

### 3.6.3.1 Proton Affinity

The calculated structures of the neutral and protonated forms of $\mathbf{L^2}$ are shown in Figure 3.19. In both species, intra-molecular hydrogen bonding interactions determine the orientation of the malonamide arms relative to the pyridine ring. In the neutral molecule, the dominant interaction is between the pyridyl nitrogen lone pair and an N-H group on a malonamide arm. Similar interactions are also observed in the calculated structures of $\mathbf{L^1}$ and $\mathbf{L^4}$ (see appendix 3.6). For $\mathbf{L^3}$, however, the presence of the amide methyl groups precludes any such hydrogen bonding interaction (see appendix 3.6). For $\mathbf{L^2}$ and $\mathbf{L^4}$, an additional weaker intra-arm hydrogen bonding interaction is also seen between an amide hydrogen and an oxygen on the opposite arm, which effectively locks the relative orientation of the arms as shown in Figure 3.19(a). The strong N-H···N hydrogen bonding interactions between the amide and pyridyl groups in $\mathbf{L^1}$, $\mathbf{L^2}$ and $\mathbf{L^4}$ contributes to the stabilisation of the neutral ligands, with the strongest interaction associated with $\mathbf{L^2}$. The intra-atomic distances and the Natural Bond Orbital (NBO) derived stabilisation energies, *E(2)*, associated with the hydrogen bonding interactions in each neutral ligand are summarised at the end of this Section in Table 3.4.

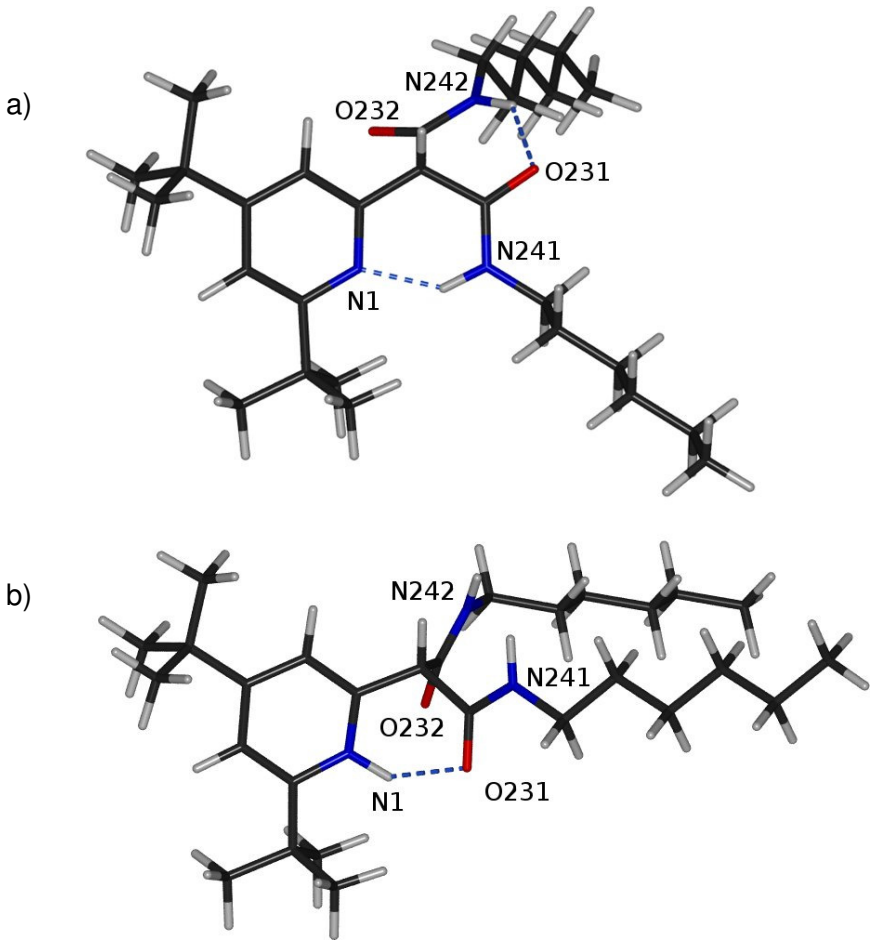


**Figure 3.19: The B3LYP/6-31g(d,p) calculated structures of (a) $L^2$ and (b) $L^2H^+$ with the intra-molecular hydrogen bonding interactions highlighted.**

As might be expected, the conformation of each ligand changes significantly on protonation. The hydrogen on the pyridinium nitrogen is now able to interact with the oxygen atoms of the malonamide unit. In the calculated structure of $\mathbf{L^2H^+}$ (Figure 3.19(b)), two non-equivalent hydrogen bonds are formed between the hydrogen on the pyridinium nitrogen and O231 (1.956 Å) and O232 (2.415 Å). The calculated structure of $\mathbf{L^2H^+}$ agrees very well with that determined from the crystal structure of $[(\mathbf{L^2H})_2ZnCl_4]$, where a similar asymmetric N-H···O hydrogen bonding motif is evident. The hydrogen bonding interactions in the protonated species lock the molecule into an arrangement that aligns both of the amide N-H bonds, the central C-H bond of the malonamide unit and the 3-CH bond of the pyridinium unit on the same side of the molecule. Similar structural features are also evident in the protonated forms of the ligands $\mathbf{L^1}$, $\mathbf{L^3}$ and $\mathbf{L^4}$ (see appendix 3.6), with the formation

of an array of N-H and C-H hydrogen bond donors on the opposite side of the molecule relative to the pyridinium nitrogen. The calculated inter-atomic distances and NBO derived stabilisation energies for the dominant N-H···O hydrogen bonding interaction for each ligand are summarised in Table 3.4. The N-H···O interactions are calculated to be strongly stabilising in the protonated forms and would be expected to increase the basicity of the ligands, an important factor in determining their efficacy as metal extractants.

The proton affinity, PA, can be used as a measure of the gas phase basicity of a molecule, and can be calculated from Equation 3.3:

**Equation 3.3**

$$PA = \{E[LH^+] + ZPE\} - \{E[L] + ZPE\}$$

where $E[LH^+]$ and $E[L]$ are the electronic energies of the protonated and neutral forms of the ligands, and the ZPE are the associated zero point energy corrections. The calculated proton affinities for $\mathbf{L^0}$-$\mathbf{L^4}$ are given in Table 3.4. Experimental gas or solution phase proton affinity data is unavailable for $\mathbf{L^0}$-$\mathbf{L^4}$, however, the gas phase proton affinity of pyridine and 2,4,6-trimethyl pyridine have been determined experimentally to be around 222 $kcalmol^{-1}$ and 230 $kcalmol^{-1}$, respectively.[28] It is expected that the proton affinities of $\mathbf{L^0}$-$\mathbf{L^4}$ would be higher than that of both pyridine and 2,4,6-trimethyl pyridine due to the combination of electron donation from *tert*-butyl groups into the ring and stabilisation of the pyridinium proton via intra-molecular hydrogen bonding interactions with the malonamide arms.

The calculated proton affinity order, $\mathbf{L^3 > L^1 > L^4 > L^2 > L^0}$ does not match that of the measured extractant *strength* of the ligands. Instead, it correlates with the changes in intra-molecular hydrogen bonding between the neutral and protonated forms of each ligand. The low proton affinity of $\mathbf{L^2}$ can be linked to the strong hydrogen bonding interactions in the neutral molecule, which are lost on protonation. In contrast, the highest proton affinity is calculated for $\mathbf{L^3}$, which can form strong N-H···O bonds in the protonated form, but has no N-H···N bonding interactions in the neutral molecule to overcome. The lowest proton affinity is calculated for $\mathbf{L^0}$ which, without

malonamide arms, cannot stabilise its protonated form by hydrogen bonding interactions.

### 3.6.3.2 Ligand-Anion Complexation

The calculated minimum energy structures for the 1:1 complexes of the mono-protonated ligands, $\mathbf{L^0}H^+$ etc., with a $ZnCl_4^{2-}$ anion are shown in Figure 3.20. With the exception of $[(\mathbf{L^0}H)ZnCl_4]^-$, the minimum energy structures for all of the $[(\mathbf{L}H)ZnCl_4]^-$ complexes has the tetrachlorozincate lying on the *opposite* side of the ligand from the location of the formal positive charge on the pyridinium group. The arrangements are comparable to that in the crystal structure of $[(\mathbf{L^2}H)_2ZnCl_4]$ (Figure 3.13) and are consistent with its $^1$H NMR data (see Section 3.6.2), suggesting that in the gas phase, solid state and solution the electrostatic attraction between the cationic ligands, $\mathbf{L^1}H^+$-$\mathbf{L^4}H^+$, and the metallate anion is **not** the dominant factor in determining structure of the 'ion-pair'. A similar trend is seen in the energy-minimised structures of the neutral 2:1 complexes with tetrachlorozincate, $[(\mathbf{L}H)_2ZnCl_4]$ (Figure 3.21 andFigure 3.23), and of the 1:1 complexes with chloride, $[(\mathbf{L}H)Cl]$, (Figure 3.22). In all cases, the anion approaches to the hydrogen bond donor groups, and only when there are no such groups present, in $\mathbf{L^0}H^+$, does the anion associate closely with the pyridinium unit (see Figure 3.20(a), Figure 3.21(a) andFigure 3.22(a)).

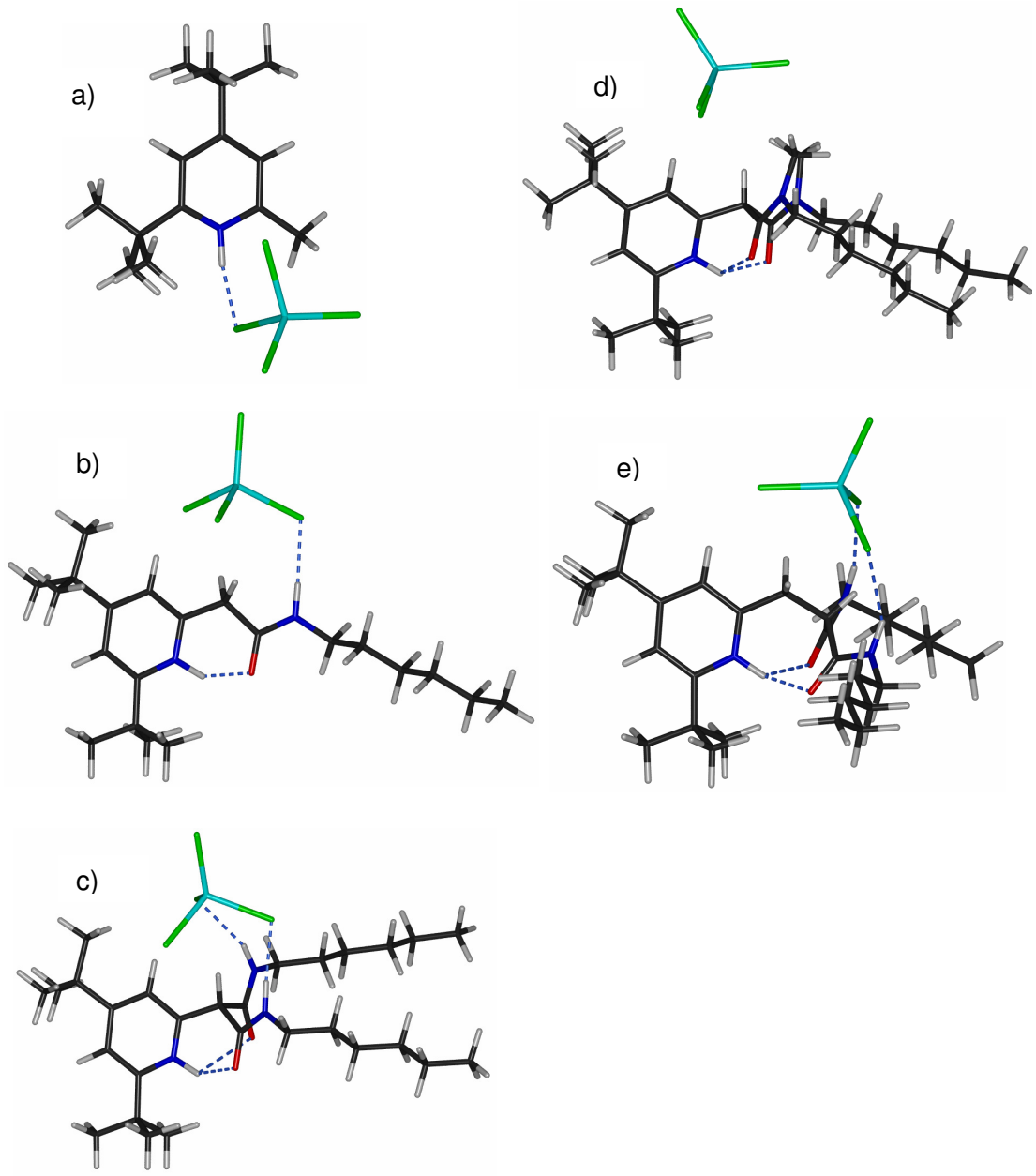


**Figure 3.20: The B3LYP/6-31g(d,p) calculated structures of the 1:1 complexes $[(LH)ZnCl_4]^-$, (a) $L^0$, (b) $L^1$, (c) $L^2$, (d) $L^3$, (e) $L^4$.**

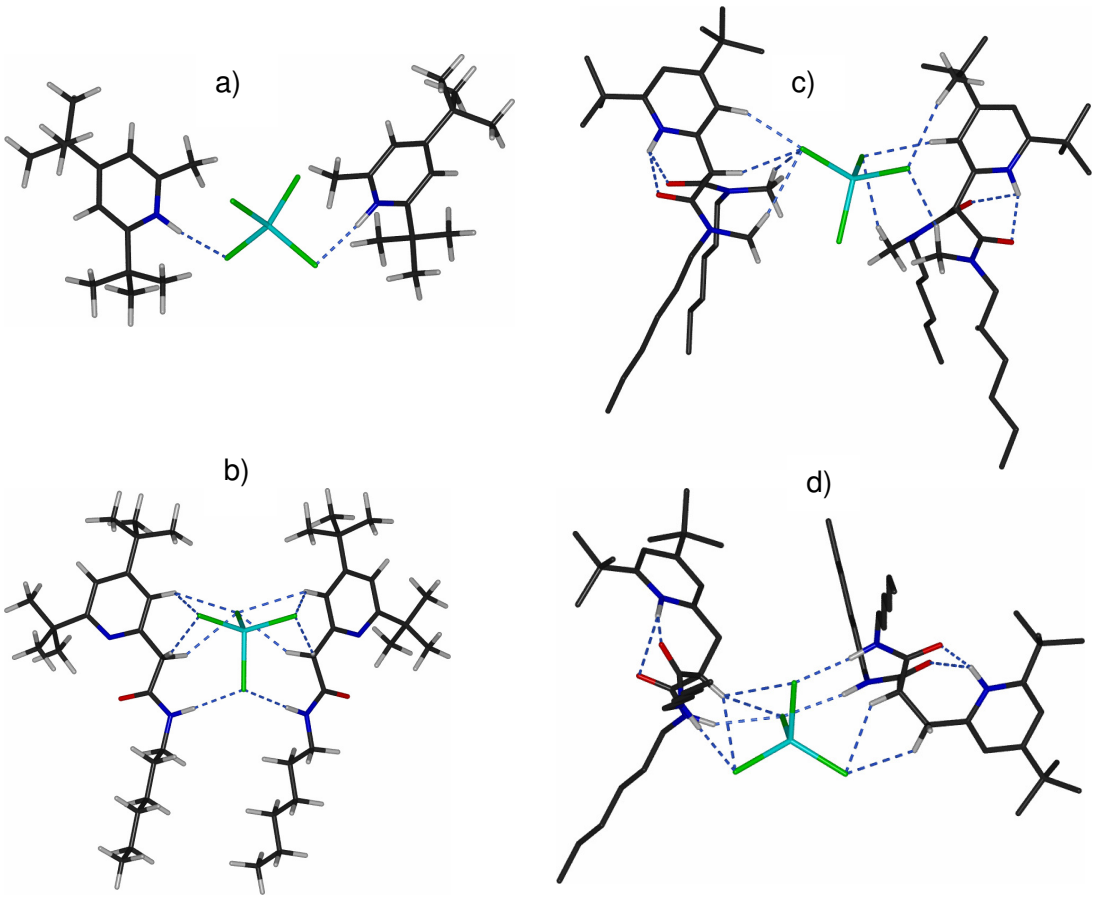


**Figure 3.21: The B3LYP/6-31g(d,p) calculated structures of the 2:1 complexes $[(LH)_2ZnCl_4]$, (a) $L^0$, (b) $L^1$, (c) $L^3$, (d) $L^4$.**

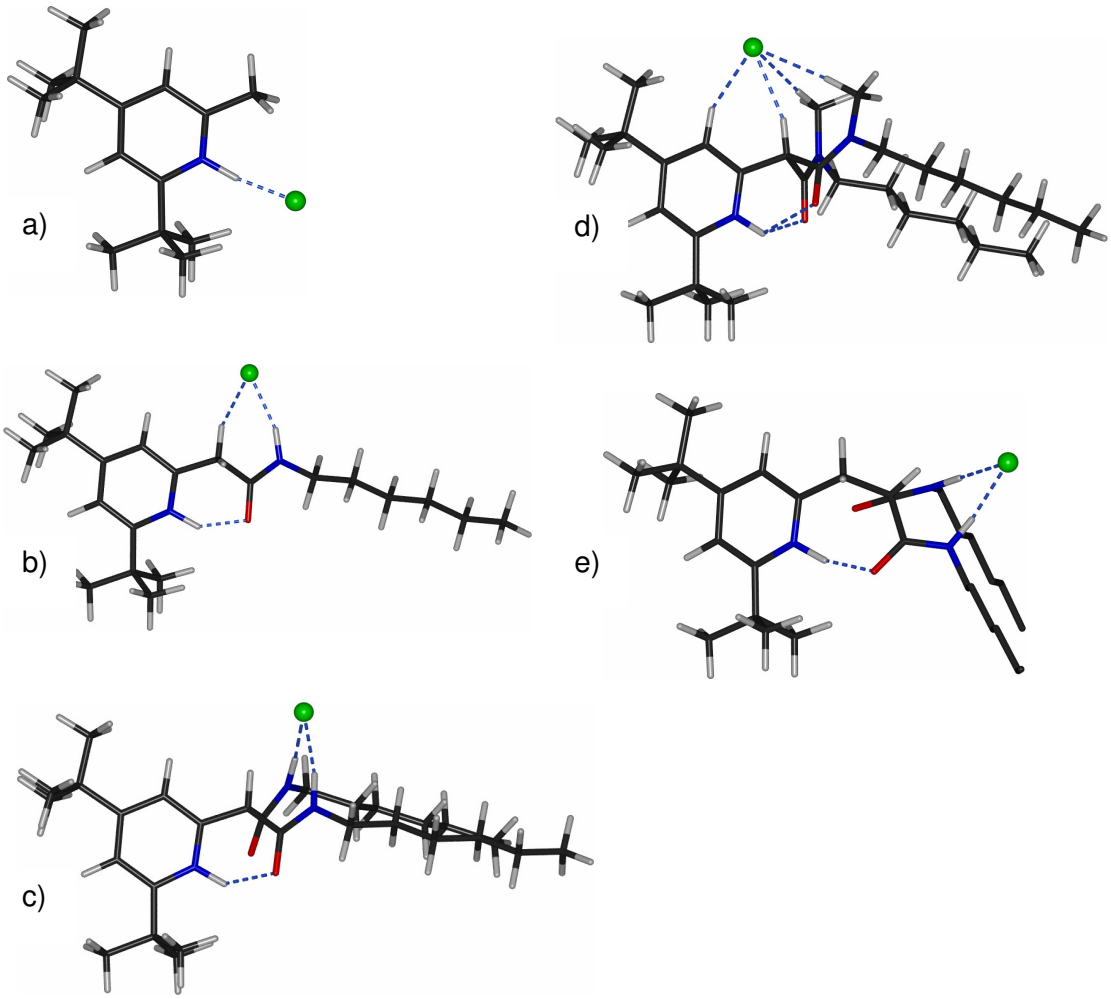


**Figure 3.22: The B3LYP/6-31g(d,p) calculated structures of the 1:1 complexes [(LH)Cl] , (a) $L^0$, (b) $L^1$, (c) $L^2$ (d) $L^3$, (e) $L^4$.**

The calculated structure of $[(\mathbf{L^2}H)_2ZnCl_4]$ (Figure 3.23) is similar to the solid state structure (Figure 3.13) in that it shows a 'proton-chelating' interaction between one of the malonamide oxygens and the pyridine nitrogen, and the ligands interact with the outer-sphere of the chlorometallate anion via several weak hydrogen bonding interactions involving the central malonamide C-H and N-H donors and the 5-H pyridinium C-H donor. In the calculated structure, one of the pendant *n*-hexyl groups in each ligand has a similar conformation to that in the solid state, but the other folds back around the tetrachlorozincate anion, generating a more hydrophobic assembly which may better represent that which exists in the extraction process. The calculated

structure for [($\mathbf{L}^2$H)Cl] (Figure 3.22(c)) corroborates well with solution phase analysis as it shows the chloride positioned close to the malonamide N-H and central C-H donors, which is reflected in the chemical shifts of the corresponding peaks in the $^1$H NMR spectrum (Figure 3.14).

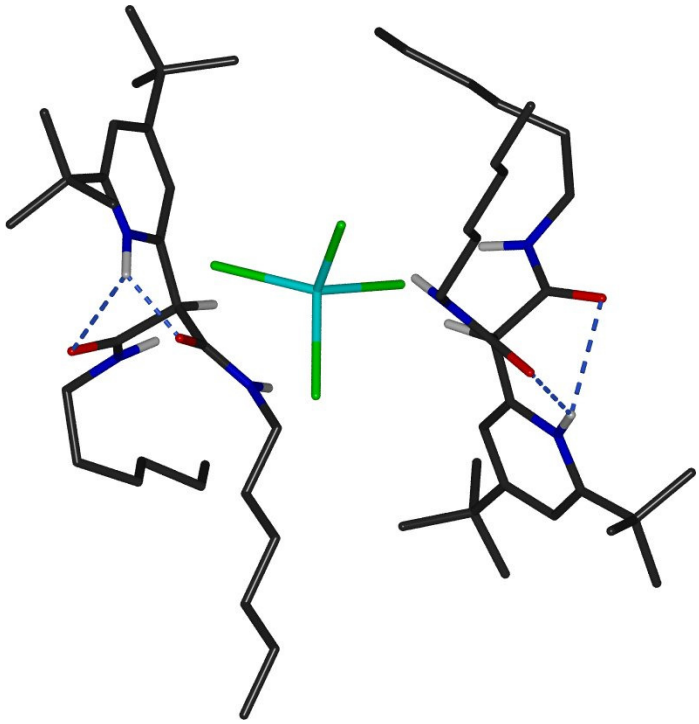

**Figure 3.23: The B3LYP/6-31g(d,p) calculated structure of the 2:1 complex [($\mathbf{L}^2$H)$_2$ZnCl$_4$].**

### 3.6.3.3 Natural Bond Order Analysis

Natural Bond Order (NBO) analysis of the natural charges indicated, as would be expected, that the partial charges on the chloride atoms in tetrachlorozincate are always lower than in the free chloride anion, and that electron donation from the anion occurs towards C-H and N-H acceptors on the ligand. Electron donation into N-H anti-bonding orbitals makes a larger contribution to complex stability than into C-H anti-bonding orbitals; the strongest N-H···Cl interaction, at -18.8 kcal mol$^{-1}$, occurs in [($\mathbf{L}^4$H)$_2$ZnCl$_4$], whilst the strongest C-H···Cl interaction is -5.4 kcal mol$^{-1}$ in [($\mathbf{L}^1$H)$_2$ZnCl$_4$]. Though interactions with C-H bonds are weaker, falling in the range -2.4 to -5.4 kcal mol$^{-1}$, a feature of the ligands $\mathbf{L}^1$H$^+$-$\mathbf{L}^4$H$^+$ is that they all can provide two strongly polarised C-H donors (the 3-H and 2-CH substituent of the pyridinium

unit) to complement the amide N-H to chlorometallate interactions and thus enhance complex stability. The partial positive charges are calculated to be slightly greater on the 2-CH hydrogen atom (0.29-0.32) than on the pyridinium 3-H atom (0.27-0.30) with values being approximately half those on the amide N-H hydrogen atoms (0.62-0.64).

NBO analysis also showed a significant charge-transfer interaction (around -2.4 kcal $mol^{-1}$) from a lone pair orbital located on the zinc into an anti-bonding orbital on the C-H bond that points directly at the centre of the metallate face. The corresponding stabilisation energy in $[(\mathbf{L^2}H)_2CoCl_4]$ is <-1 $kcalmol^{-1}$, below the threshold conventionally used to determine whether an interaction is of charge-transfer (i.e. hydrogen bonding) nature or dominated by dispersion or electrostatic interactions.[29] A theoretical study of the metal-based hydrogen bond accepting properties of $d^{10}$ $Co(CO)_4^-$ and $Ni(CO)_4$ complexes involving an NBO analysis similar to that which is presented in this study has been conducted by Alkorta *et. al.*.[30] The strength of the D-H···M interactions were found to vary significantly with the metal and type of hydrogen bond donor with interactions ranging between -9.83 and -86.89 kcal $mol^{-1}$ for the $Co(CO)_4^-$ complexes and 0.09 and -2.74 kcal $mol^{-1}$ for the $Ni(CO)_4$ complexes.

D-H···M interactions between hydrogen bond donors and metal centres have been observed in the solid state for a range of compounds, for example in $[(EtNH)Co(CO)_4]$ (Figure 3.24).[31-37] The characteristics of such interactions, outlined by Brammer *et. al.*,[32] include a protonic bridging hydrogen (typically an X-C-H or N-H donor), an electron rich metal centre with filled d orbitals (usually $d^8$ or $d^{10}$) to facilitate 3c-4e interaction and approximately linear D-H···M geometry. These characteristics are largely observed in the $[(\mathbf{L^2}H)_2ZnCl_4]$ solid state structure which has a C-H···Zn angle of 172.3°.

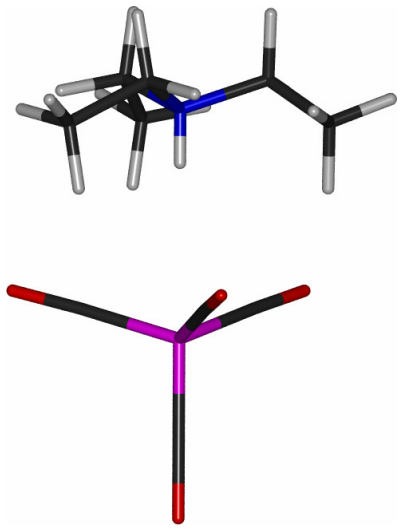

**Figure 3.24: The solid state structure of $[(EtNH)Co(CO)_4]$.[32]**

The perceived C-H···Zn interaction in the calculations for the $[(\mathbf{L^2}H)_2ZnCl_4]$ complex is likely to be a consequence of the C-H···Cl and N-H···Cl interactions which forcibly aligns the central malonamide C-H donor with the centre of the face of the tetrachlorozincate tetrahedron, bringing it close to the metal centre. This results in a favourable interaction with the lone-pair in the $dx^2$-$y^2$ orbital which may contribute to the overall stability of the complex.

### 3.6.3.4 Anion Binding Energies

Gas phase binding energies for the 2:1 ligand-anion complexes were calculated using Equation 3.4 and are summarised in Table 3.4.

**Equation 3.4**

$$BE[(LH)_2MCl_4] = \{E[(LH)_2MCl_4] + ZPE\} - 2\{E[LH^+] + ZPE\} - \{E[MCl_4^{2-}] + ZPE\}$$

$E[(LH)_2MCl_4]$ is the energy of the complex, $E[LH^+]$ is the energy of the protonated ligand and $E[MCl_4^{2-}]$ is the energy of the chlorometallate. The ZPE are the appropriate zero-point energy corrections for each component.

With the exception of $\mathbf{L^0}$, the trend in the calculated binding energies of the $[(LH)_2ZnCl_4]$ complexes, $\mathbf{L^2 > L^0 > L^4 > L^1 > L^3}$, correlates well with the observed trend in extractant *strengths*, $\mathbf{L^2 > L^4 > L^1 > L^3 > L^0}$ (Figure 3.8). The high binding energy for $[(\mathbf{L^0}H)_2ZnCl_4]$ may arise from the higher Coulombic contribution as the

anion approaches the cationic pyridinium N-H unit rather than the amide hydrogen bond donors (as in $\mathbf{L^1}$-$\mathbf{L^4}$). The binding energies for the zinc and cobalt complexes of $\mathbf{L^2}$, $[(\mathbf{L^2}H)_2ZnCl_4]$ and $[(\mathbf{L^2}H)_2CoCl_4]$, are very similar, differing by less than 1.5 kcal $mol^{-1}$. The difference in the extraction *strength* and *efficiency* of cobalt and zinc complexes is, therefore, not likely to be due to the binding energies of the two complexes, but rather the speciation in the aqueous phase (see Section 3.5).

An estimate of the contribution that van der Waals, dipole-dipole and hydrogen bonding interactions make to the binding energy of each complex was made using Equation 3.5,

**Equation 3.5**

$$BE[L_2MCl_4^{2-}] = E[L_2MCl_4^{2-}] - 2E[L] - E[MCl_4^{2-}]$$

where, $E[L_2MCl_4^{2-}]$ is the energy of the complex formed between two neutral ligands and the negatively charged anion in the geometry of the energy minimised $[(LH)_2MCl_4]$ ion-pair, E[L] is the energy of the neutral ligand in the geometry of the energy minimised $[(LH)_2MCl_4]$ ion-pair and $E[MCl_4^{2-}]$ is the energy of the chlorometallate. Although the electron density on the pyridyl rings in the neutral and protonated ligands will differ, the change in natural charges is similar for each ligand, so the trends in the binding energies, $BE[L_2MCl_4^{2-}]$, should still provide a relative measure of how structural differences between each ligand affects the strength of hydrogen bonding interactions with the metal anions.

The calculated binding energies in the complexes following the removal of the dominant electrostatic interaction, $BE[L_2MCl_4^{2-}]$ are summarised in Table 3.4. As expected, $\mathbf{L^2}$ and $\mathbf{L^4}$, which each have two polar N-H bonds, have the strongest binding energies, and $\mathbf{L^0}$, which, whilst deprotonated cannot support a strong Coulombic interaction with the metal anion, has the lowest. $\mathbf{L^3}$, with no N-H electron acceptors, and $\mathbf{L^1}$, with only one, have comparable binding energies; the sum of the multiple weaker C-H acceptor interactions in $\mathbf{L^3}$ equating to that of the stronger N-H interaction in $\mathbf{L^1}$.

The trend in the binding energies of the $[L_2MCl_4^{2-}]$ assemblies, $\mathbf{L^2 > L^4 > L^1 > L^3 > L^0}$, is the same as the trend in extractant strength (Figure 3.8). This suggests that the varying hydrogen bond donor functionality in the ligands $\mathbf{L^0}$-$\mathbf{L^4}$ is an important factor in determining their relative strengths.

### 3.6.3.5 Interaction Energy

One of the aims of this study was to develop a theoretical model that explains the variation in solvent extraction performance across the ligand series. Although the gas phase binding energy is an important factor in determining the strength of each ligand as a metal extractant, the contribution from the basicity of each ligand cannot be overlooked. We have, therefore, defined an interaction energy, IE, for each ligand, which is the sum of the proton affinity of each ligand and the binding energy of the complex (Equation 3.6), in a rudimentary attempt to model extractant strength.

**Equation 3.6**

$$IE = BE[(LH)_2MCl_4] + 2PA$$

It should be noted that, by convention, the proton affinities are given as positive numbers, though in fact, as exogenic processes, the associated energy is actually negative, as for the binding energies.

The calculated interaction energies for the $[(LH)_2ZnCl_4]$ ligand complexes are given in Table 3.4. The ordering of the interaction energy: $\mathbf{L^2 > L^4 > L^3 > L^1 > L^0}$, is in reasonable agreement with the experimentally observed extractant strengths. The low proton affinity of $\mathbf{L^0}$ is in opposition to its high binding energy, resulting in a low interaction energy and, therefore, low extractant strength. In contrast, for $\mathbf{L^2}$, the strongest metal extractant, a low calculated proton affinity arising from strong intra-molecular hydrogen bonding interactions is overcome by a high calculated binding energy.

Interaction energy is a very rudimentary model for extractant strength and does not take into account the many complex factors that affect the solvent extraction of chlorometallate complexes. However, it does illustrate the importance of anion binding and proton affinity in chlorometallate solvent extraction.

| | Ligand | | | | |
|---|---|---|---|---|---|
| | **0** | **1** | **2** | **3** | **4** |
| **$E_p$ / Ha** | -602.56 | -1007.17 | -1411.77 | -1490.38 | -1451.09 |
| **$ZPE_p$ / Ha** | 0.34 | 0.54 | 0.74 | 0.79 | 0.77 |
| **N-H…O E(2) / kcalmol$^{-1}$** | - | -34.85 | -16.96 | -10.15 | -47.69 |
| **N-H…O / Å** | - | -1.611 | -1.776 | -1.867 | -1.542 |
| **$E_n$ / Ha** | -602.15 | -1006.76 | -1411.36 | -1489.96 | -1450.68 |
| **$ZPE_n$ / Ha** | 0.36 | 0.55 | 0.75 | 0.81 | 0.78 |
| **N…H-N *E(2)* / kcalmol$^{-1}$** | - | -6.49 | -16.57 | - | -11.32 |
| **N…H-N / Å** | - | -2.118 | -1.890 | - | -1.988 |
| **PA / kcalmol$^{-1}$** | 242.5 | 251.2 | 249.3 | 257.0 | 250.6 |
| **BE**[$(L_2ZnCl_4^{2-}$] / **kcalmol$^{-1}$** | 5.325 | -56.513 | -86.603 | -56.180 | -79.962 |
| **BE**[$(LH)_2ZnCl_4$] / **kcalmol$^{-1}$** | -241.9 | -232.82 | -246.44 | -224.7 | -238.99 |
| **BE**[$(LH)_2CoCl_4$] / **kcalmol$^{-1}$** | | | -244.99 | | |
| **IE**[$(LH)_2ZnCl_4$] / **kcalmol$^{-1}$** | **-726.92** | **-735.28** | **-745.19** | **-738.61** | **-740.09** |

**Table 3.4: B3LYP/6-31g(d,p) calculated energies, E, zero point energies, ZPE, inter-atomic hydrogen bonding distances for N···H-N and N-H···O interactions, NBO derived stabilisation energies, *E(2),* proton affinities, PA, binding energies, BE, and interaction energis, IE, for the protonated and neutral forms of the ligands $L^0$-$L^4$. The subscripts n and p refer to the neutral and protonated species, respectively.**

## 3.7 Conclusions

The comparison of $\mathbf{L^0}$-$\mathbf{L^4}$ as extractants for tetrachlorometallates and the interpretation of the structure and bonding in the complexes formed in solution, in the solid state and in the gas phase has demonstrated the importance of outer-coordination sphere chemistry in chlorometallate solvent extraction systems.

Chlorometallates such as $CoCl_4^{2-}$ and $ZnCl_4^{2-}$ are *soft anions* and the high strength of extraction by $\mathbf{L^1}H^+$-$\mathbf{L^4}H^+$ arise, in part, because these ligands are able to provide *several* hydrogen bond donor groups to address regions of negative charge density on the faces and edges of the tetrahedra. An important feature of the new extractants is that they provide positively polarised C-H bonds to address the outer-coordination sphere of the chlorometallates and, whilst the resulting interactions are not as strong as those from the amido N-H units, they significantly enhance the overall binding energy. The hydrogen bonding from the array of C-H and N-H interactions contributes significantly to the binding energy in the $[(LH)_2MCl_4]$ assemblies, complementing the electrostatic 'ion-pair' type bonding between the pyridinium unit and the chlorometallate anion.

The work carried out in this chapter is summarised in the following conclusions:

- The new reagents, $\mathbf{L^0}$-$\mathbf{L^4}$, can be prepared on gram scales using facile, high yielding methods.
- The amido-functionalised pyridines, $\mathbf{L^1}$-$\mathbf{L^4}$, extract zinc or cobalt within the pH and chloride concentration ranges specified by Anglo American.
- The malonamide, $\mathbf{L^2}$, was the most efficient ligand for zinc or cobalt extraction into toluene.
- Quantitative stripping of both zinc and cobalt is possible from $\mathbf{L^2}$-toluene solutions using distilled water, suggesting that the incorporation of a bulky *tert*-butyl group adjacent to the pyridino nitrogen atom is completely effective in preventing coordination to the inner-sphere of the zinc and cobalt

ions under the conditions used for loading and stripping their chlorometallates.

- Analysis of the $[(\mathbf{L^2}H)_2MCl_4]$ (M = Co(II) or Zn(II)) structures in the solid, solution and gas phases showed 'proton chelation' between the carbonyl oxygens and bridge-head amine nitrogen. This would increase reagent basicity and, therefore, *strength* and resulted in a pre-organised array of C-H and N-H donors for interaction with the chlorometallate anion which was attributed to the higher extraction *efficiency* of $\mathbf{L^2}$.
- Analysis of the calculated gas-phase structures of $\mathbf{L^1}$-$\mathbf{L^4}$ showed preferential approach of the chlorometallate and chloride anions to hydrogen bond donors rather than the cationic charge, suggesting that the structure of ligand-chlorometallate complexes formed in the solvent extraction process is determined by hydrogen bonding as opposed to coulombic interactions.
- The calculated binding energies of the $\mathbf{L^0}$-$\mathbf{L^4}$ complexes demonstrated the importance of hydrogen bonding interactions in complex stability.
- An interaction energy, consisting of the sum of proton affinities and binding energy, was used to describe extractant *strength*, and this compared reasonably well with the observed trend across the ligand series.

The development of hydrogen bond donor functionalised sterically hindered pyridine reagents for chlorometallate extraction was novel, and analysis of the ligand-chlorometallate interactions in the solid, solution and gas phases gave insight into the extraction mechanism. However, the commercial viability of the pyridine-based ligands to the Anglo American circuits will be limited by the cost of the reagents which arises from expensive pyridine precursors and the need for working with unstable air-sensitive reagents such as *tert*-butyl lithium. For this reason, extractants containing an alternative type of organic base were considered and the successful design features in the pyridine-based ligands were applied in the development of a new series of solvent extractants, namely the amido-functionalised tertiary alkylamines presented in Chapter 4.

# 3.8 Experimental

General experimental details are given in Chapter 2, Section 2.5.

## 3.8.1 Ligand Synthesis

### 3.8.1.1 2,4-Di-*tert*-butyl-6-methylpyridine $L^{038}$

In a 500 mL, two-necked round bottomed flask, α-picoline (6.0 g, 65 mmol) dissolved in dry *n*-heptane (100 mL) was cooled, under $N_2$, to -75°C using an acetone-dry ice bath. The solution was stirred under $N_2$ for 1 h, after which 1.5 M *tert*-butyllithium in pentane (215 mL) was carefully added using a pressure compensating addition funnel, resulting in the colourless solution turning bright yellow. The pentane was distilled off under $N_2$ and the remaining solution was refluxed for 1 h, over which time the colour changed from yellow to deep red. The reaction mixture was then cooled to 0°C in an ice bath and quenched by cautiously adding water (100 mL). The aqueous layer was extracted using hexane (3 x 100 mL) and the combined organic layers were dried over magnesium sulfate and then concentrated on a rotary evaporator to give. The crude product was purified by column chromatography on silica gel using 5% diethyl ether in hexane as eluent to give $\mathbf{L^0}$ (9.4 g, 71%) as a red-brown oil; $\delta_H$ (250 MHz; $CDCl_3$) 1.18 (s, 9H, $^t$Bu), 1.29 (s, 9H, $^t$Bu), 2.43 (s, 3H, 6-Me), 6.82 (s, 1H, 3-H), 7.02 (s, 1H, 5-H); $\delta_C$ (63 MHz; $CDCl_3$) 25.5, 31.0, 31.1, 35.0, 38.5, 113.7, 116.1, 157.2, 160.2, 168.5.

### 3.8.1.2 Dimethyl (4,6-di-*tert*-butylpyridin-2-yl)malonate 1

In a 500 mL, two-necked round bottomed flask, α-picoline (2.9 g, 31.2 mmol) dissolved in dry *n*-heptane (100 mL) was cooled, under $N_2$, to -75°C using an acetone-dry ice bath. The solution was stirred under $N_2$ for 1 h, after which 1.5 M *tert*-butyllithium in pentane (104 mL) was carefully added using a pressure compensating addition funnel, resulting in the colourless solution turning bright yellow. The pentane was distilled off under $N_2$ and the remaining solution was refluxed for 1 h, over which the colour changed from yellow to deep red. The

reaction mixture was then cooled in an ice bath to 0°C and dimethyl carbonate (14.5 g, 161 mmol) was added drop-wise, causing the mixture to effervesce and solidify. The residue was re-dissolved in ether and ammonium chloride (10 g) was cautiously added followed by water (100 mL). The aqueous layer was extracted with ethyl acetate (3 x 150 mL), and the combined organic layers were dried over magnesium sulfate, filtered and concentrated on a rotary evaporator. The crude product was purified by column chromatography on silica gel using 5% then 10% diethyl ether in hexane as eluent to give the malonate **1** (6.0 g, 60%) as a bright yellow crystalline solid; $\nu_{max}$(KBr disc)/cm$^{-1}$ 2962-2871 (C-H stretch), 1756 (C=O stretch); $\delta_H$ (250 MHz; DMSO-$d_6$) 1.25 (s, 18H, $^t$Bu), 3.64 (s, 6H, $OCH_3$), 5.52 (s, 1H, CHCO), 7.19 (s 1H, 5-H), 7.28 (s 1H, 3-H); $\delta_C$ (63 MHz; $CDCl_3$) 28.4, 30.5, 31.3, 35.8, 38.1, 53.3, 61.0, 115.6, 118.0, 151.9, 161.1, 169.1; *m/z* (ES) 322 ($M+H^+$).

### 3.8.1.3 Methyl 2-(4,6-di-*tert*-butylpyridin-2-yl)-3-(hexylamino)-3-oxopropanoate 2 and 2-(4,6-di-*tert*-butylpyridin-2-yl)-*N*,*N*'-dihexylmalonamide $L^2$

Dimethyl (4,6-di-*tert*-butylpyridin-2-yl)malonate **1** (3.0 g, 9.3 mmol) and *n*-hexylamine (1.19 g, 11.8 mmol) were refluxed in a 500 mL round bottomed flask in toluene (250 mL) for 24 h. The reaction mixture was concentrated on a rotary evaporator and then purified by column chromatography on silica gel using 40% then 50% diethyl ether in hexane as elutent. The low $R_f$ product was isolated to give $\mathbf{L^2}$ (1.9 g, 43%) as a pale brown oil (Found: C, 72.9; H, 10.7; N, 9.10. $C_{28}H_{49}N_3O_2$ requires C, 73.2; H, 10.7; N, 9.14); $\nu_{max}$(KBr disc)/cm$^{-1}$ 3324 (N-H stretch), 3029-2864 (C-H stretch), 1688 (C=O stretch); $\delta_H$ (250 MHz; $CDCl_3$) 0.95 (m, 6H, $CH_3CH_2$), 1.35 (m, 12H, $CH_3CH_2CH_2CH_2$), 1.40 (s, 9H, $^t$Bu), 1.50 (s, 9H, $^t$Bu), 1.66 (m, 4H, $NCH_2CH_2$), 3.24 (m, 4H, $NCH_2$), 4.65 (s, 1H, CHCO), 7.29 (s, 1H, 5-H), 7.40 (s, 1H, 3-H), 8.42 (t, 2H, NH); $\delta_C$ (63 MHz; $CDCl_3$) 14.6, 23.1, 27.3, 29.8, 30.0, 31.3, 32.0, 35.1, 38.1, 40.3, 62.4, 115.5, 119.4, 154.1, 162.6, 168.2, 169.4; *m/z* (ES) 430.6 ($M+H^+$).

The high $R_f$ product was isolated to give **2** (2.0 g, 55%) as a pale brown oil; $\delta_H$

(250 MHz; $CDCl_3$) 1.00 (m, 6H, C*H*$_3$CH$_2$), 1.37 (m, 6H, CH$_3$C*H*$_2$C*H*$_2$C*H*$_2$), 1.42 (s, 9H, 2-$^t$Bu), 1.49 (s, 9H, $^t$Bu), 1.65 (m, 2H, NCH$_2$C*H*$_2$), 3.42 (m, 2H, NCH$_2$), 3.86 (s, 3H, CH$_3$O), 4.80 (s, 1H, CHCO), 7.27 (s, 1H, 5-H), 7.41 (s, 1H, 3-H), 8.35 (t, 1H, NH); $\delta_C$ (63 MHz; $CDCl_3$) 14.1, 22.8, 26.9, 28.8, 30.1, 31.4, 32.3, 34.9, 37.0, 41.3, 53.5, 60.0, 114.5, 118.7, 153.7, 161.2, 169.1, 170.0; *m/z* (ES) 376.5 ($M+H^+$).

### 3.8.1.4 2-(4,6-Di-*tert*-butylpyridin-2-yl)-*N*-hexylacetamide $L^1$

In a 250 mL round bottomed flask, **2** (1.0 g, 2.6 mmol) was dissolved in methanol (100 mL) and refluxed with 6M aqueous NaOH solution (2.1 mL) for 3 h after which 6 M aqueous HCl (4.3 mL) was added and stirring was continued for 1 h. The methanol was removed on a rotary evaporator and the product was extracted with ethyl acetate (3 x 100mL), dried over magnesium sulfate and concentrated on a rotary evaporator to give $\mathbf{L^1}$ (0.82 g, 95%) as a pale brown oil (Found: C, 75.4; H, 10.8; N, 8.49. $C_{21}H_{36}N_2O$ requires C, 75.9; H, 10.9; N, 8.42); $\nu_{max}$(KBr disc)/cm$^{-1}$ 3296 (N-H stretch), 2957-2864 (C-H stretch), 1652 (C=O stretch); $\delta_H$ (250 MHz; $CDCl_3$) 0.78 (m, 3H, C*H*$_3$CH$_2$), 1.15 (m, 6H, CH$_3$C*H*$_2$C*H*$_2$C*H*$_2$), 1.33 (s, 9H, $^t$Bu), 1.59 (s, 9H, $^t$Bu), 1.76 (m, 2H, NCH$_2$C*H*$_2$), 3.15 (q, 2H, NCH$_2$), 4.40 (s, 2H, CH$_2$CO), 7.45 (s, 1H, 5-H), 7.69 (s, 1H, 3-H), 8.82 (t, 1H, NH); $\delta_C$ (63 MHz, $CDCl_3$) 14.6, 23.1, 27.3, 30.1, 31.3, 32.1, 33.5, 35.2, 38.2, 40.1, 45.5, 114.6, 118.8, 154.8, 162.0, 168.9, 170.2; *m/z* (ES) 333 ($M+H^+$).

### 3.8.1.5 2-(4,6-Di-*tert*-butylpyridin-2-yl)-*N,N'*-dihexyl-*N,N'*-dimethylmalonamide $L^3$

Dimethyl (4,6-di-*tert*-butylpyridin-2-yl)malonate **1** (3.0 g, 9.3 mmol) and *n*-hexylmethylamine (5.4 g, 47 mmol) were heated at 80°C in a 100 mL round bottomed flask for 24 h. The reaction mixture was purified by column chromatography on silica gel using 50% then 67% diethyl ether in hexane as elutent to give $\mathbf{L^3}$ (3.2 g, 70%) as a pale brown oil (Found: C, 73.5; H, 11.7; N, 8.57 $C_{30}H_{53}N_3O_2$ requires C, 73.9; H, 11.0; N, 8.61); $\nu_{max}$(KBr disc)/cm$^{-1}$ 3026-2866 (C-H stretch), 1684 (C=O stretch); $\delta_H$ (250 MHz; $CDCl_3$) 0.76 (m, 6H,

C*H*$_3$CH$_2$), 1.15 (m, 12H, CH$_3$C*H*$_2$C*H*$_2$C*H*$_2$), 1.26 (s, 9H, $^t$Bu), 1.29 (s, 9H, $^t$Bu), 1.66 (m, 4H, NCH$_2$C*H*$_2$), 2.82 (s, 3H, NC*H*$_3$), 2.89 (s, 3H, NC*H*$_3$), 3.24 (m, 4H, NCH$_2$), 5.12 (s, 1H, CHCO), 7.10 (s, 1H, 5-H), 7.19 (s, 1H, 3-H); $\delta_C$ (63 MHz; CDCl$_3$) 168.0, 160.5, 153.9, 119.2, 114.4, 59.4, 50.3, 48.8, 37.6, 35.2, 33.9, 33.8, 32.1, 31.9, 31.0, 27.3, 22.9, 14.3; *m/z* (ES) 430.6 (M+H$^+$)**.**

### 3.8.1.6 2-(Bromomethyl)-4,6-di-*tert*-butylpyridine 3

To a solution of **L$^0$** (6.1 g, 30 mmol) in chloroform (150 mL) was added 1,1'-azobis(cyclohexanecarbonitrile) (0.37 g, 1.5 mmol) followed by *N*-bromosuccinimide (6.78 g, 39.0 mmol) and the mixture was irradiated with a 500 W visible light source in a 250 mL round bottomed flask. The heat from the lamp was sufficient to bring the reaction to reflux. After 7 h the lamp was turned off and the reaction mixture was concentrated on a rotary evaporator and then suspended in hexane. After the solid was filtered off, the filtrate was concentrated on a rotary evaporator and then purified by column chromatography on silica gel using 1 % diethyl ether in hexane as eluent to give 2-(bromomethyl)-4,6-di-*tert*-butylpyridine **3** (4.5 g, 53%) as a colourless oil; $\delta_H$ (250 MHz; CDCl$_3$) 1.22 (s, 9H, $^t$Bu), 1.28 (s, 9H, $_t$Bu), 4.45 (s, 2H, CH$_2$), 7.13 (s, 2H, CH); $\delta_C$ (63 MHz; CDCl$_3$) 30.4, 32.2, 35.6, 36.4, 37.9, 115.8, 117.7, 155.9, 162.2, 168.6.

### 3.8.1.7 Dimethyl [(4,6-di-*tert*-butylpyridin-2-yl)methyl]malonate 4

To a suspension of 60% sodium hydride in paraffin oil (1.3 g, 32 mmol) in THF (100 mL), dimethyl malonate (4.59 g, 40.2 mmol) was added causing evolution of hydrogen gas. Once the reaction had subsided, 2-(bromomethyl)-4,6-di-*tert*-butylpyridine **3** (7.6 g, 26.8 mmol) in THF (30 mL) was added and the mixture was refluxed for 30 min. The reaction mixture was allowed to cool to room temperature and was then concentrated on a rotary evaporator. The residue was suspended in hexane (200 mL) which was then washed with water (50 mL). The aqueous phase was re-extracted with DCM (100 mL) and the combined organic layers were dried over magnesium sulfate and concentrated on a rotary evaporator. The residue was purified by column chromatography using 10%

diethyl ether in hexane as eluent to give dimethyl [(4,6-di-*tert*-butylpyridin-2-yl)methyl]malonate **4** (6.9 g, 77% yield) as a pale yellow oil; $\delta_H$ (250 MHz; $CDCl_3$) 1.43 (s, 9H, $^tBu$), 1.46 (s, 9H, $^tBu$), 3.60 (d, 2H, $CH_2$), 3.91 (s, 6H, $CH_3O$), 4.42 (t, 1H, CHCO), 7.11 (s, 1H, 5-H), 7.26 (s, 1H, 3-H); $\delta_C$ (63 MHz; $CDCl_3$) 30.6, 32.0, 35.1, 32.5, 33.8, 51.4, 53.6, 114.1, 117.5, 156.0, 160.8, 167.6, 172.8.

#### 3.8.1.8 2-[(4,6-Di-*tert*-butylpyridin-2-yl)methyl]-*N*,*N*'-dihexylmalonamide $L^4$

Dimethyl [(4,6-di-*tert*-butylpyridin-2-yl)methyl]malonate (2.6 g, 7.8 mmol) was heated to 80°C in *n*-hexylamine (5.5 g, 54 mmol) for 48 h. The reaction mixture was purified by column chromatography on silica gel using 20% ethyl acetate in hexane as eluent to give $\mathbf{L}^4$ (2.9 g, 80%) as a brown solid; $\delta_H$ (250 MHz; $CDCl_3$) 0.75 (t, 6H, $CH_3CH_2$), 1.16 (m, 12H, $CH_3CH_2CH_2CH_2$), 1.15 (s, 9H, $^tBu$), 1.26 (s, 9H, $^tBu$), 1.35 (m, 4H, $CH_3CH_2CH_2$) 3.10 (q, 4H, $NCH_2$), 3.27 (d, 2H, $CH_2CH$), 3.75 (t, 1H, $CH_2CH$), 6.89 (s, 1H, 5-H), 7.09 (s, 1H, 3-H) 7.39 (t, 2H, NH); $\delta_C$ (63 MHz; $CDCl_3$) 30.6, 32.0, 35.1, 32.5, 33.8, 51.4, 53.6, 114.1, 117.5, 156.0, 160.8, 167.6, 172.8.

### 3.8.2 Solvent Extraction Experiments

Experiments determining the dependence of metal loading (M = Zn(II), Co(II) or Fe(III)) on pH, chloride concentration and ligand concentration, and the procedures used to evaluate metal recovery from the organic phase and the evaluation of metal and total chloride loading, were conducted according to the procedures described in Chapter 2, Section 2.5.

### 3.8.3 Complex Synthesis and Crystallography

The crystal structures of $L^2$-chlorometallate complexes were solved by Dr Fraser White at the University of Edinburgh Crystallography Service.

#### 3.8.3.1 $(L^2H)_2MCl_4$ (M = Co or Zn)

A 9 M aqueous HCl solution (10 mL) containing $MCl_2$ ($CoCl_2$: 0.20 g, 1.54 mmol; $ZnCl_2$: 0.20 g, 1.47mmol ) was stirred with a toluene solution (10 mL) of $\mathbf{L^2}$ (0.70 g, 1.54 mmol) in a 100 mL Schott bottle. After 3 h the phases were separated and the toluene phase was evaporated under vacuum leaving an oily residue, which was dissolved in a 50:50 diethyl ether-hexane mix (10 mL). Slow evaporation at 4°C over the course of 4 days gave crystals which were suitable for X-ray tructure determination.

**$(HL^2)_2CoCl_4$** was isolated as blue crystals (Found: C, 59.8; H, 8.86; N, 7.31. $C_{56}H_{100}Cl_4CoN_6O_4$ requires: C, 59.9; H, 8.98; N, 7.49.)

**$(HL^2)_2ZnCl_4$** was isolated as colourless crystals (Found C, 59.8; H. 8.93; N, 7.44. $C_{56}H_{100}Cl_4ZnN_6O_4$ requires: C, 59.6; H, 8.93; N, 7.45.)

#### 3.8.3.2 Crystal structure of $[(L^2H)_2CoCl_4]$

Data were collected on a blue block (0.33 x 0.26 x 0.21 mm) on a 3 circle Bruker Smart Apex CCD diffractometer with graphite-monochromated Mo-Kα radiation (λ = 0.71073 Å) equipped with an Oxford Cryosystems low temperature device operating at 150 K. The crystal was indexed using the Bruker Smart software[39] and found to be *I*-centred tetragonal with $a = b = 19.5947(3)$, $c = 33.4454(11)$ Å. From initial indexing a data collection strategy was used to collect fully complete data to a resolution of 61° in 2θ in as short a time as possible. In total 31199 reflections were collected and from these the space group was determined to be $I4_1/a$. Absorption correction was performed using a multi-scan method by

applying the SADABS[40] program, and data were merged according to the crystal system in SHELX[41] which gave 5662 unique reflections with a merging R-factor of 0.0972. After solution by direct methods with SHELXS[41] all atoms were refined anisotropically and hydrogen atoms were placed geometrically, riding on their host atoms. Some disorder was encountered in one of the alkyl chains which was refined as two components with the main component assigned a 0.6 site occupancy factor occupancy and the secondary component, 0.4. Full matrix least squares refinement was carried out against $F^2$ producing a final conventional R-Factor of 0.0493 based on 3794 reflections.

#### 3.8.3.3 Crystal structure of $[(L^2H)_2ZnCl_4]$

Data were collected on a colourless wedge (0.58 x 0.39 x 0.13 mm) using the same experimental setup, procedure and software as above with the exception of being optimised for 100% completeness to 53° in 2θ. The crystal was tetragonal, $I4_1/a$ with $a = b = 19.6101(4)$, $c = 33.3823(15)$ Å. In total 62514 reflections were collected and merged to give 5642 unique reflections and a merging R-factor of 0.0687. A final conventional R-Factor of 0.0874 was determined based on 5226 reflections.

### 3.8.4 NMR Complex Synthesis and Crystallography

The NMR spectra in Section 3.6.2 were recorded on a Bruker AC250, Bruker DPX360 or AVA600 spectrometer at 298 K, and chemical shifts (δ) are reported in parts per million (ppm) relative to TMS. NMR samples were prepared by dissolving 40 mg of the ligand or ligand complex in 0.6 ml $CDCl_3$. 1D NOE and HSQC spectra were carried out by Marika de Cremoux of the University of Edinburgh NMR service.

### 3.8.5 Computational and modelling work

Most of the DFT calculations were carried out by Dr Patricia Richardson who also contributed substantially in interpreting the results.

Density functional calculations were carried out with the Gaussian03[42] program using the B3LYP functional.[43, 44] Geometry optimisations were carried out at the 6-31g(d,p) level,[45] followed by frequency calculations, at the same level, to confirm structures were minima on the potential energy surface. A larger basis set containing diffuse functions, and a dispersion corrected functional would have been desirable, but not practically feasible, due to the size of the complexes under study and the available computational resource. The oft levelled criticism of the B3LYP functional is that dispersion is neglected. However in the complexes described herein the predominant intermolecular interactions observed are electrostatic and charge-transfer in nature (*vida infra*), both of which are described reasonably well with by B3LYP functional.

1:1 and 2:1 ligand-anion complexes were constructed from optimised units, based on the crystal structure of $L^2$, and subjected to further geometry optimisation and frequency calculations. Some exploration of the conformational space was achieved by placing the ligands at various positions with respect to the anions. For the 2:1 complexes multiple near-degenerate (energy separations less than 0.1 $kcalmol^{-1}$) conformational isomers were found for each compound, differing in the relative orientation of the ligands and the particular face that each was accessing, but broadly maintaining the characteristic binding motif for each ligand. In solution it is likely that the complexes will exist in a statistical distribution of these various conformers. The complex and ligand structures presented herein are those of the lowest energy minima that were found, and these structures were used in the calculation of binding energies. The difference in binding energies between the different ligands was, in all cases, significantly greater than the energetic difference between the conformational isomers of the individual ligands.

The counterpoise method of Boys and Bernardi[46] was employed to correct for basis set superposition errors in $E[(LH)_2MCl_4]$. Weinhold's natural bond orbital (NBO) method[47-49] was used to explore the atomic charge distribution in the complexes and study the strength and nature of individual hydrogen bonding interactions. The NBO

approach describes hydrogen bonding interactions within a framework of donor-acceptor charge-transfer interactions between idealised "Lewis" type orbitals. The energetic importance of each interaction can be estimated using a second-order pertubative approach. The stabilisation energy associated with delocalisation between each donor NBO (i) and acceptor NBO (j) can be estimated as

$$E(2) = \Delta E_{ij} = q_i \frac{F(i,j)^2}{\varepsilon_j - \varepsilon_i}$$

Where $q_i$ is the donor orbital occupancy, $\varepsilon_i$ and $\varepsilon_j$ are the orbital energies and *F(i,j)* is the off-diagonal NBO Fock matrix element.

## 3.9 References

1. Dalton, R. F.; Diaz, G.; Price, R.; Zunkel, A. D., The Cuprex metal extraction process: recovering copper from sulfide ores. *JOM* **1991,** 43, (8), 51-6.

2. Dalton, R. F.; Price, R.; Hermana, E.; Hoffman, B., Cuprex process. A new chloride-based hydrometallurgical process for copper recovery from sulfide ores. *Ingenieria Quimica* **1987,** 19, (215), 115-120.

3. Szymanowski, J., Hydroximes and Copper Hydrometallurgy. *CRC Press* **1993**.

4. Borowiak-Resterna, A., Extraction of copper from acid chloride solutions by N-alkyl- and N,N-dialkyl-3-pyridinecarboxamides. *Solvent Extr. Ion Exch.,* **1994,** 12, (3), 557-69.

5. Borowiak-Resterna, A., Extraction of copper(II) from acid chloride solutions by N-dodecyl- and N,N-dihexylpyridinecarboxamides. *Solvent Extr. Ion Exch.,* **1999,** 17, (1), 133-148.

6. Borowiak-Resterna, A.; Lenarcik, B., Effect of the Alkyl Chain Length in N,N-Dialkylpyridine-3-carboxamides upon their Extraction of Copper(II) from Aqueous Chloride Solutions. *Solvent Extr. Ion Exch.,* **2004,** 22, (6), 913-931.

7. Borowiak-Resterna, A.; Szymanowski, J.; Voelkel, A., Structure and nitrogen basicity of pyridine metal extractants. *J. Radioanal. Nucl. Chem.,* **1996,** 208, (1), 75-86.

8. Cote, G.; Jakubiak, A.; Bauer, D.; Szymanowski, J.; Mokili, B.; Poitrenaud, C., Modeling of extraction equilibrium for copper(II) extraction by pyridinecarboxylic acid esters from concentrated chloride solutions at constant water activity and constant total concentration of ionic or molecular species dissolved in the aqueous solution. *Solvent Extr. Ion Exch.,* **1994,** 12, (1), 99-120.

9. Soldenhoff, K. H., Solvent extraction of copper(II) from chloride solutions by some pyridine carboxylate esters. *Solvent Extr. Ion Exch.,* **1987,** 5, (5), 833-51.

10. Szymanowski, J.; Jakubiak, A.; Cote, G.; Bauer, D.; Cierpiszewski, R., Equilibrium and kinetic studies of copper extraction from chloride solutions with pyridine carboxylates. *Hydrometall. '94, Pap. Int. Symp.,* **1994**, 675-82.

11. Regel-Rosocka, M.; Wisniewski, M.; Borowiak-Resterna, A.; Cieszynska, A.; Sastre, A. M., Selective extraction of palladium(II) from hydrochloric acid solutions with pyridinecarboxamides and ACORGA LX50. *Sep. Purif. Technol.,* **2007,** 53, (3), 337-341.

12. Tomaszewska, M.; Borowiak-Resterna, A.; Olszanowski, A., Cadmium extraction from chloride solutions with model N-alkyl- and N,N-dialkyl-pyridine-carboxamides. *Hydrometallurgy,* **2007,** 85, (2-4), 116-126.

13. Elias, H.; Rass, U.; Wannowius, K. J., Complex formation of silver(I) with sterically hindered pyridine bases. *Inorganica Chimica Acta,* **1984,** 86, (2), L37-L38.

14. Bips, U.; Elias, H.; Hauroeder, M.; Kleinhans, G.; Pfeifer, S.; Wannowius, K. J., Lutidine buffers of very limited coordination power for the pH range 3-8. *Inorg. Chem.,* **1983,** 22, (26), 3862-5.

15. Kang Sung, O.; Begum Rowshan, A.; Bowman-James, K., Amide-based ligands for anion coordination. *Angew Chem Int Ed Engl,* **2006,** 45, (47), 7882-94.

16. Martell, A. E.; Sillen, L. G., Stability constants of metal-ion complexes. *Chem. Soc. (London), Spec. Publ.,* **1964,** 17, 754.

17. Sillen, L. G.; Martell, A. E., *Stability Constants of Metal-Ion Complexes. Supplement No. 1. Pt.: Inorganic Ligands. Part 2: Organic Including Macromolecule Ligands. (Special Publication No. 25. Supplement No. 1 to Special Publication No. 17).* 1971, 865.

18. Muir, D. M., Basic principles of chloride hydrometallurgy. *Chloride Metall. 2002: Pract. Theory Chloride/Met. Interact., Annu. Hydrometall. Meet., 32nd, Montreal, QC, Canada, Oct. 19-23, 2002,* **2002,** 2, 759-791.

19. Blitz-Raith, A. H.; Paimin, R.; Cattrall, R. W.; Kolev, S. D., Separation of cobalt(II) from nickel(II) by solid-phase extraction into Aliquat 336 chloride immobilized in poly(vinyl chloride). *Talanta,* **2007,** 71, (1), 419-423.

20. Paimin, R.; Cattrall, R. W., The extraction of cobalt(II) from hydrochloric acid solutions by Aliquat 336R dissolved in chloroform. *Aust. J. Chem.,* **1983,** 36, (5), 1017-20.

21. Bacon, G.; Mihaylov, I., Solvent extraction as an enabling technology in the nickel industry. *Int. Solvent Extr. Conf., Cape Town, South Africa, Mar. 17-21, 2002,* **2002**, 1-13.

22. Espallargas, G. M.; Brammer, L.; Sherwood, P., Designing intermolecular interactions between halogenated peripheries of inorganic and organic molecules: Electrostatically directed M-X...X'-C halogen bonds. *Angew Chem Int Ed Engl,* **2006,** 45, (3), 435-440.

23. Gillon, A. L.; Lewis, G. R.; Orpen, A. G.; Rotter, S.; Starbuck, J.; Wang, X.-M.; Rodriguez-Martin, Y.; Ruiz-Perez, C., Organic-inorganic hybrid solids: control of perhalometallate solid state structures. *Dalton,* **2000**, (21), 3897-3905.

24. Bernstein, J.; Davis, R. E.; Shimoni, L.; Chang, N.-L., Patterns in hydrogen bonding: functionality and graph set analysis in crystals. *Angew. Chem., Int. Ed. Engl.,* **1995,** 34, (15), 1555-73.

25. Glidewell, C.; Low, J. N.; Skakle, J. M. S.; Wardell, J. L., Diethyl 2-(4-nitrophenyl)malonate forms a hydrogen-bonded chain of rings. *Acta Crystallogr., Sect. E: Struct. Rep. Online,* **2004,** E60, (1), o60-o62.

26. Hay, B. P.; Bryantsev, V. S., Anion-arene adducts: C-H hydrogen bonding, anion-pi interaction, and carbon bonding motifs. *Chem. Commun.,* **2008**, (21), 2417-2428.

27. Warr, R. J.; Westra, A. N.; Bell, K. J.; Chartres, J.; Ellis, R.; Tong, C.; Simmance, T. G.; Gadzhieva, A.; Blake, A. J.; Tasker, P. A.; Schroder, M., Selective Extraction and Transport of the [PtCl6]2- Anion through Outer-Sphere Coordination Chemistry. *Chem.--Eur. J.,* **2009,** 15, (19), 4836-4850.

28. Choi, K. H.; Lee, H. J.; Karpfen, A.; Yoon, C. J.; Park, J.; Choi, Y. S., Hydrogen-bonding interaction of methyl-substituted pyridines with thioacetamide: steric hindrance of methyl group. *Chem. Phys. Lett.,* **2001,** 345, (3,4), 338-344.

29. Harris, C. D.; Holder, A. J.; Eick, J. D.; Chappelow, C. C., Natural Bond Orbital Evaluation of AM1-Predicted C-H-O Hydrogen Bonds in Dimers of 1,5,7,11-Tetraoxaspiro[5.5]Undecane. *Cryst. Growth Des.,* **2003,** 3, (2), 239-246.

30. Alkorta, I.; Rozas, I.; Elguero, J., Transition metals as hydrogen bond acceptors: a theoretical study. *THEOCHEM,* **2001,** 537, 139-150.

31. Brammer, L., Metals and hydrogen bonds. *Dalton Trans.,* **2003**, (16), 3145-3157.

32. Brammer, L.; McCann, M. C.; Bullock, R. M.; McMullan, R. K.; Sherwood, P., Et3NH+Co(CO)4-: hydrogen-bonded adduct or simple ion pair? Single-crystal neutron diffraction study at 15 K. *Organometallics,* **1992,** 11, (7), 2339-41.

33. Brammer, L.; Zhao, D., A Hydrogen-Bonded Chain Involving both N-H...N and N-H...Co Hydrogen Bonds. Low-Temperature X-ray Crystal Structure of [(NMP)3H2][Co(CO)4]2 (NMP = N-Methylpiperazine). *Organometallics,* **1994,** 13, (5), 1545-7.

34. Brammer, L.; Zhao, D., Low-temperature structures of [py2H]+[Co(CO)4]- (py = pyridine) and [(tmen)H]+[Co(CO)4]- (tmen = N,N,N',N'-tetramethylethylenediamine). *Acta Crystallogr., Sect. C: Cryst. Struct. Commun.,* **1995,** C51, (1), 45-8.

35. Calderazzo, F.; Fachinetti, G.; Marchetti, F.; Zanazzi, P. F., Preparation and crystal molecular structure of two trialkylamine adducts of tetracarbonylcobalt hydride showing a preferential trialkylammonium-tetracarbonylcobaltate interaction. *J. Chem. Soc., Chem. Commun.,* **1981**, (4), 181-3.

36. Martin, A., Hydrogen bonds involving transition metal centers acting as proton acceptors. *J. Chem. Educ.,* **1999,** 76, (4), 578-583.

37. Brammer, L.; Charnock, J. M.; Goggin, P. L.; Goodfellow, R. J.; Orpen, A. G.; Koetzle, T. F., The role of transition metal atoms as hydrogen bond acceptors: a neutron diffraction study of bis(tetra-n-propylammonium) tetrachloroplatinate(II)-cis-dichlorobis(methylamine)platinum(II) (1/1) at 20 K. *J. Chem. Soc., Dalton Trans.,* **1991**, (7), 1789-98.

38. Scalzi, F. V.; Golob, N. F., Alkylation of pyridine with tert-butyllithium. Convenient syntheses of 2,6-di-tert-butylpyridine and 2,4,6-tri-tert-butylpyridine. *J. Org. Chem.,* **1971,** 36, (17), 2541-2.

39. Bruker-Nonius, B.-A., Madison, Wisconsin, USA, Editon edn., **2002**.

40. G. M. Sheldrick, B.-A., Madison, Wisconsin, USA, Editon edn., **2004**.

41. G. M. Sheldrick, U. o. G., Germany and Bruker-AXS, Gottingen.

42. M. J. Frisch, G. W. T., H. B. Schlegel, G. E. Scuseria,; M. A. Robb, J. R. C., J. A. Montgomery, Jr., T. Vreven,; K. N. Kudin, J. C. B., J. M. Millam, S. S. Iyengar, J. Tomasi,; V. Barone, B. M., M. Cossi, G. Scalmani, N. Rega,; G. A. Petersson, H. N., M. Hada, M. Ehara, K. Toyota,; R. Fukuda, J. H., M. Ishida, T. Nakajima, Y.

Honda, O. Kitao,; H. Nakai, M. K., X. Li, J. E. Knox, H. P. Hratchian, J. B. Cross,; V. Bakken, C. A., J. Jaramillo, R. Gomperts, R. E. Stratmann,; O. Yazyev, A. J. A., R. Cammi, C. Pomelli, J. W. Ochterski,; P. Y. Ayala, K. M., G. A. Voth, P. Salvador, J. J. Dannenberg,; V. G. Zakrzewski, S. D., A. D. Daniels, M. C. Strain,; O. Farkas, D. K. M., A. D. Rabuck, K. Raghavachari,; J. B. Foresman, J. V. O., Q. Cui, A. G. Baboul, S. Clifford,; J. Cioslowski, B. B. S., G. Liu, A. Liashenko, P. Piskorz,; I. Komaromi, R. L. M., D. J. Fox, T. Keith, M. A. Al-Laham,; C. Y. Peng, A. N., M. Challacombe, P. M. W. Gill,; B. Johnson, W. C., M. W. Wong, C. Gonzalez, and J. A. Pople *Gaussian 03, Revision E.01*, Gaussian, Inc.: Wallingford CT, **2004**.

43. Becke, A. D., A new mixing of Hartree-Fock and local-density-functional theories. *J. Chem. Phys.,* **1993,** 98, (2), 1372-7.

44. Lee, C.; Yang, W.; Parr, R. G., Development of the Colle-Salvetti correlation-energy formula into a functional of the electron density. *Phys. Rev. B: Condens. Matter,* **1988,** 37, (2), 785-9.

45. Hariharan, P. C.; Pople, J. A., Influence of polarization functions on MO hydrogenation energies. *Theor. Chim. Acta,* **1973,** 28, (3), 213-22.

46. Boys, S. F.; Bernardi, F., The calculation of small molecular interactions by the differences of separate total energies. Some procedures with reduced errors. *Mol. Phys.,* **1970,** 19, (4), 553-566.

47. Carpenter, J. E.; Weinhold, F., Transferability of natural bond orbitals. *J. Am. Chem. Soc.,* **1988,** 110, (2), 368-72.

48. Reed, A. E.; Curtiss, L. A.; Weinhold, F., Intermolecular interactions from a natural bond orbital, donor-acceptor viewpoint. *Chem. Rev.,* **1988,** 88, (6), 899-926.

49. Reed, A. E.; Weinstock, R. B.; Weinhold, F., Natural population analysis. *J. Chem. Phys.,* **1985,** 83, (2), 735-46.

# CHAPTER 4

# AMIDO-FUNCTIONALISED TERTIARY AMINES

## 4.1. Aims

The aim of the work described in this chapter was to design, synthesise and study the extractive properties of a series of new amido-functionalised tertiary amine extractants with varying hydrogen bond donor/acceptor functionality, focusing on 'proton chelating' and ligand-chlorometallate hydrogen bonding interactions.

## 4.2. Alkyl Amines in Solvent Extraction

Alkyl amines are good candidates as anion exchange extractants for metal complex recovery from acidic media as they are often relatively inert, cheap to manufacture, able to carry a positive charge and soluble in non-polar solvents.[1] Since the 1940s, a large amount of research and development has been conducted on alkylamine extractants and this body of work has been condensed and reviewed in journals and text books.[1, 2] As metallate anion extractants, alkylamines are divided into two main groups in terms of how they function in extraction processes, namely, secondary and tertiary alkylamines and quaternary alkylammonium cations.[2]

Quaternary alkylammonium extractants (for example the commercial Aliquat 336) are permanently cationic and extract metal complex anions via an exchange process with another anion according to:

**Equation 4.1**

$$n[(R_4N)Y]_{(org)} + [MX_x]^{n-} \rightleftharpoons [(R_4N)_n(MX_x)]_{(org)} + nY^-$$

The advantage of quaternary alkylammonium extractants is that they can transport metal values into the organic phase over a wide pH range and they have been investigated for the recovery and separation of various metal complex anions.[3] The disadvantage of using such reagents is that the stripping of the metal value from the organic phase is difficult and inefficient which limits their use in hydrometallurgy processes.[4]

Secondary and tertiary alkylamines (for example the commercial Alamine 336) extract metal complex anions via the generation of a protonated species in the organic phase according to:

**Equation 4.2**

$$nR_3N_{(org)} + [MX_x]^{n-} + nHY \rightleftharpoons [(R_3NH)_n(MX_x)]_{(org)} + nY^-$$

Steric crowding around the N atom in tertiary alkylamines makes them selective for proton over metal cation so that inner-sphere complex formation is unfavourable.[2]

Tertiary alkylamines were initially used commercially in the 1950's to recover uranium from acidic sulphate solutions produced from mines in the US according Equation 4.3 and Equation 4.4.[5]

**Equation 4.3**

$$2[(R_3NH)_2SO_4]_{(org)} + [UO_2(SO_4)_3]^{4-} \rightleftharpoons [(R_3NH)_4UO_2(SO_4)_3]_{(org)} + 2SO_4^{2-}$$

**Equation 4.4**

$$[(R_3NH)_2SO_4]_{(org)} + [UO_2(SO_4)_2]^{2-} \rightleftharpoons [(R_3NH)_2UO_2(SO_4)_2]_{(org)} + SO_4^{2-}$$

Since the late 1950's, secondary and tertiary alkylamines have been developed for the extraction of a large range of anionic metal complexes.[2]

Tertiary alkylamine extractants play a key role in the refining process for platinum group metals (PGMs) (Scheme 4.1) as they are used to extract the chlorometallate anions of platinum and iridium. Solvent extraction technology made the production of PGMs more economical as it replaced the complicated and inefficient precipitation processes that were used previously.[6]

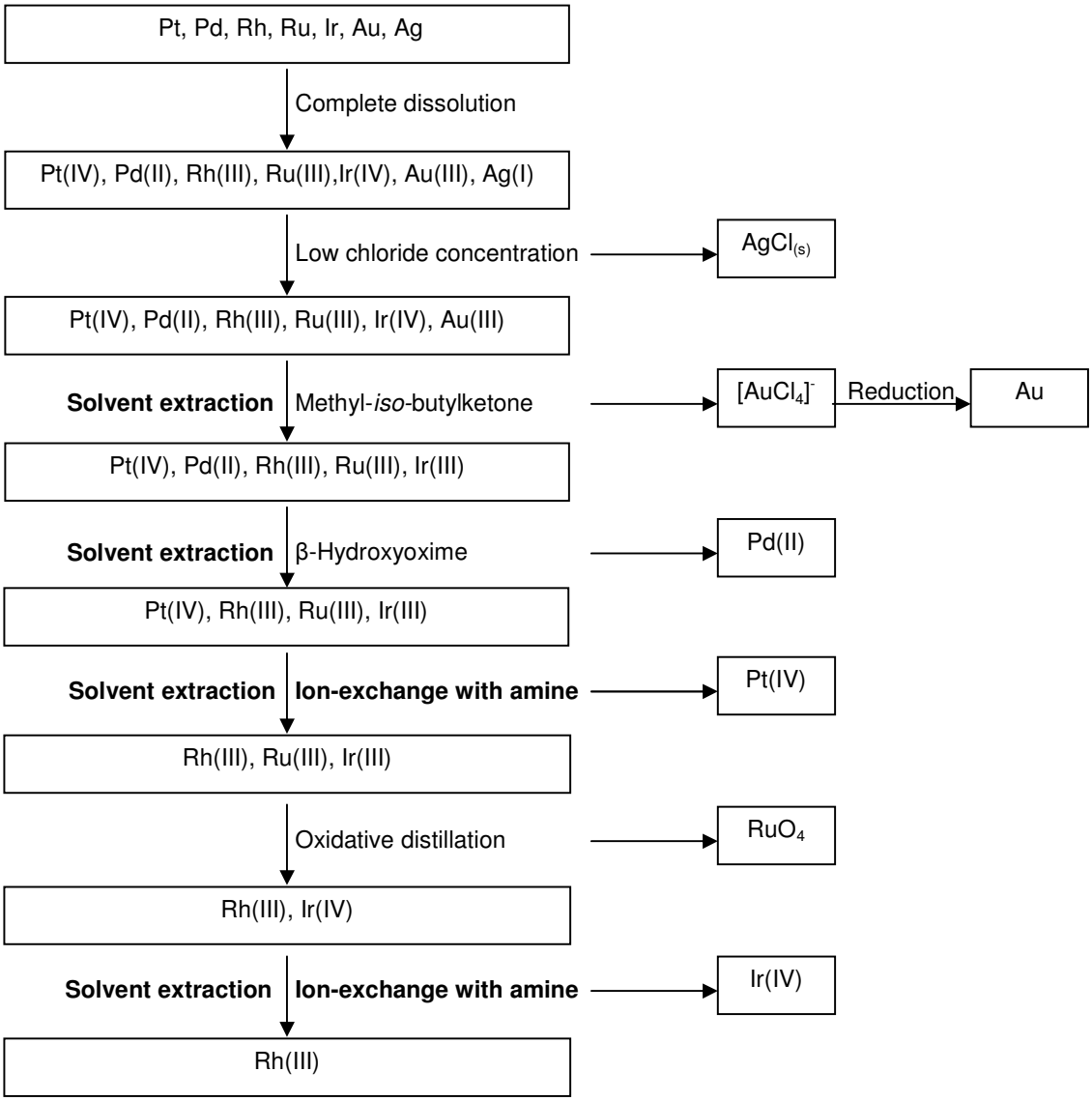


**Scheme 4.1: A representation of a modern PGM refining process with the two steps using tertiary alkylamines to recover chlorometallates shown in bold.[6]**

Secondary and tertiary alkylamines have also found application in commercial processes for the solvent extraction of base metal chlorometallates, such as for the separation of cobalt and nickel at the Falconbridge Nikkelverk refinery[7] and the extraction of zinc in the Zincex process[8] (see Chapter 1, sections 1.7.2 and 1.7.3.1). They have also been investigated as potential solvent extraction reagents for the recovery of other base metal chlorometallate complexes including copper, cadmium and manganese.[9, 10]

## 4.3. Design of New Tertiary Alkylamine Ligands for Chlorometallate Extraction in the Anglo American Circuits

Recent studies have shown that the extraction *efficiency* of tertiary alkylamine ligands may be enhanced by incorporating hydrogen bond donor groups into the alkyl chains (see Chapter 1, section 1.8.5).[11] In the pyridine-based ligands described in Chapter 3, it was found that extractant *strength* was increased when the hydrogen bond accepting carbonyl oxygen groups could form a six-membered 'proton chelating' ring with the protonated basic site (Figure 4.1).[12] On the assumption that formation of such a six-membered chelate ring will enhance the strength of complex formation with chlorometallates in other amido extractants by increasing proton affinity and pre-organising the amido and α-methylene protons, we set about the synthesis and testing of new extractants containing the component (b). These new ligands (see below) contain a different carbon-nitrogen sequence linking the protonatable tertiary nitrogen atom and the amide group from that in the reagents reported[11] for the recovery of hexachloroplatinate. The latter have carbonyl and nitrogen atoms of the amido group reversed (see (c) in Figure 4.1) and consequently comparable 'chelation of the proton' will generate a less favourable seven-membered ring.

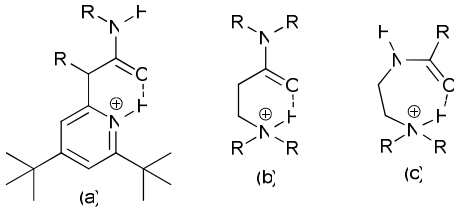


**Figure 4.1: 'Proton chelation' to form a six-membered ring (a) in the pyridine reagents $L^1$, $L^2$ and $L^3$ discussed in Chapter 3 and (b) used as a design criteria in this chapter, compared to the seven-membered ring (c) that could form in the previously investigated tren-based reagents.[11]**

The series of new tertiary alkylamine reagents discussed in this chapter are shown in Figure 4.2. In addition to the desired intra-molecular hydrogen bonding between the amine proton and pendant amide (see above) they were designed to be easily synthesised

from much cheaper starting materials than the ligands in Chapter 3, making them more commercially viable.

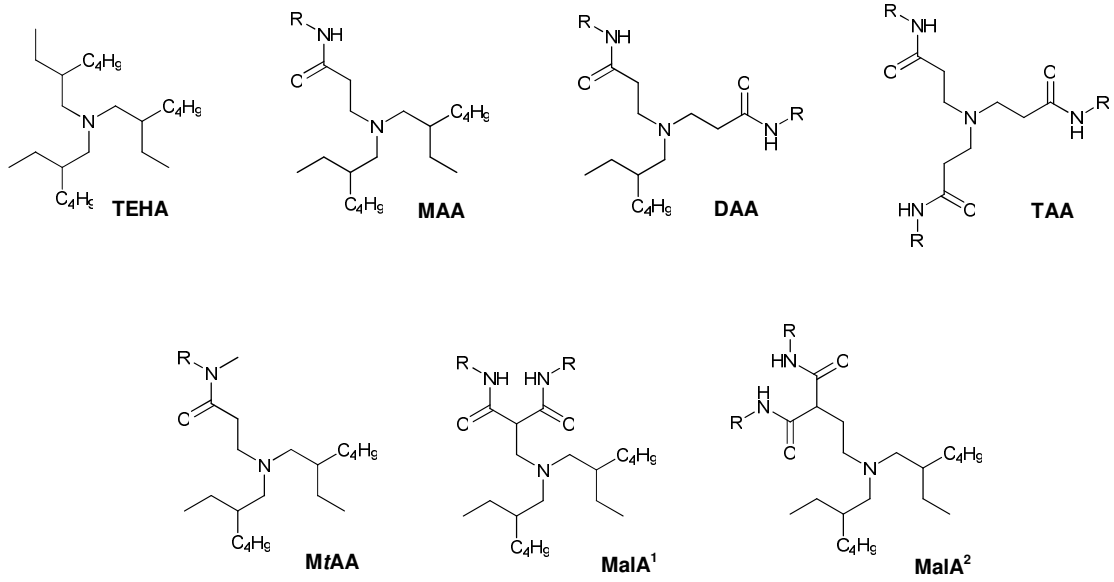


**Figure 4.2: The new series of tertiary alkylamine ligands with varying degrees of amide and malonamide functionality (R = n-hexyl).**

The new ligands contain branched octyl groups, frequently referred to in hydrometallurgy by the non-standard name '2-ethylhexyl groups'. These increase solubility in non-polar organic solvents and also provide steric hindrance around the nitrogen lone pair to discourage inner-sphere complexation with the metal cations. Tris(2-ethylhexyl)amine (**TEHA**) is an isomer of tri-*n*-octylamine (**TOA**), which has been used as a model for the commercial Alamine 336 reagent in previous studies.[11] The mono-amido (**MAA**), di-amido (**DAA**) and tri-amido (**TAA**) functionalised tertiary amines shown in Figure 4.2 are all capable of forming six-membered 'proton chelating' rings of the type shown in Figure 4.1(b).

Increasing the number of pendant amide groups with series **MAA < DAA < TAA** and the number of N-H hydrogen bond donors was expected to increase extractant *strength*, although they also likely make the molecules more polar and show intermolecular hydrogen bonding which is likely to decrease solubility in non-polar organic solvents.

The mono *tert*-amido functionalised alkylamine (**M*t*AA**) is analogous to **MAA** and, although it does not have amido N-H hydrogen bond donor capability, it does have potential C-H donors in α-methylene groups of the tertiary ammonium group which have also been shown to interact favourably with chlorometallate anions.[13]

The malonamide functionalised alkylamine, **MalA$^{1}$**, was designed to be capable of forming a six-membered proton chelating ring that could result in a pre-organised array of C-H and N-H donors analogous to the ligand **L$^{2}$** in Chapter 3. However, in practice synthesis proved impossible, so an alternative malonamide functionalised extractant, **MalA$^{2}$**, was designed which differs in having an extra $CH_2$ spacer group between the amine and malonamide functionality. Although solving the problems with synthesis, this malonamide cannot form a six-membered 'proton-chelating' ring.

## 4.4. Exploration of Synthetic Methods

Where possible, the main aim was to develop high yielding synthetic routes to the new tertiary alkylamine reagents that can be performed using cheap starting materials with stable, non-toxic intermediates and by-products as this would be most attractive for large-scale commercial production. However, as the most atom efficient synthetic routes were sometimes unsuccessful, a number of other methods were also attempted in the exploration of a working synthesis.

### 4.4.1. Synthesis of MAA, DAA and TAA

The general synthetic approach the ligands **MAA**, **DAA** and **TAA** proceeds via an ester intermediate (**5**, **6** or 7) as amino esters are stable and relatively easy to synthesise ( Figure 4.3).[14] The key feedstocks are methyl acrylate, ammonia and aliphatic amines, which are all readily available.

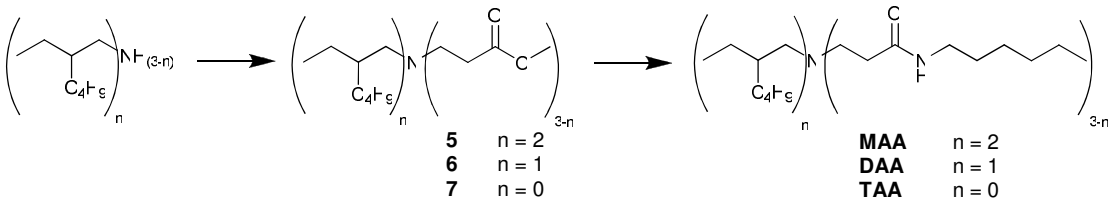


**Figure 4.3: The general synthetic approach to the amido-functionalised tertiary alkylamine reagents, MAA, DAA and TAA.**

### 4.4.1.1. Synthesis of Ester Intermediates

The ester intermediates (**5**, **6** and **7**) for the ligands **MAA**, **DAA** and **TAA** were all conveniently prepared from the amine starting materials via a Michael addition reaction with methyl acrylate (Figure 4.4) at ambient temperature in methanol.[14]

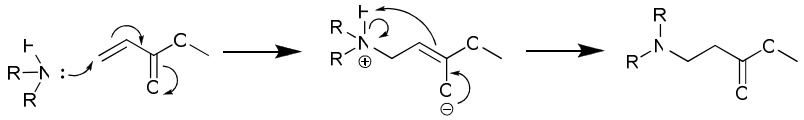

**Figure 4.4: The mechanism for the Michael addition of an alkyl amine to methyl acrylate.**

This method for amino-ester formation is attractive for commercial application as both methyl acrylate and the amine starting materials (ammonia, 2-ethylhexylamine and bis(2-ethyl)hexyalmine) are readily available and the reaction does not require aggressive conditions. The ester intermediates **5**, **6** and **7** were all isolated in good yields (67%, 74% and 42% respectively) after removing the starting materials and by-products *in vacuo* or by flash column chromatography.

### 4.4.1.2. Aminolysis

The ester-amide conversion was initially attempted directly by refluxing the ester, **5**, with hexylamine in toluene (see appendix 4.1). However, even after 3 days at reflux, no reaction had taken place so different methods were explored.

### 4.4.1.3. Aminolyis Via Improved Leaving Group Quality

Ester-amide conversions, as for all reactions involving nucleophilic substitution at the carbonyl group, depend on the quality of the electrophile (in this case the amino-ester **5**, **6** or **7** in Figure 4.3), the strength of the nucleophile (hexylamine) and the quality of the leaving group ($MeO^-$). A new approach to the aminolysis of **5**, **6** and **7** involved changing $MeO^-$ to a better leaving group. This involved first hydrolysing the ester to a carboxylic acid by reacting it with NaOH and then re-acidifying with HCl. The carboxylic acid can then be activated by the attachment of a leaving group (LG) before reacting with hexylamine (Scheme 4.2). A plethora of methods have been developed to achieve the activation of carboxylic acids in this way and many are reported in a review by Montalbetti and Falque.[15]

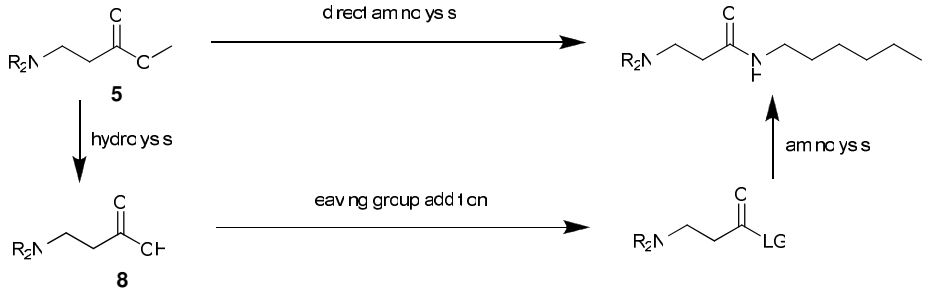


**Scheme 4.2: Synthesis of MAA from 5 by incorporation of a better leaving group (LG) (R = 2-ethylhexyl).**

### 4.4.1.4. Amide Formation via an Acyl Chloride Intermediate

Acid chlorides are more reactive towards nucleophiles than carboxylic acids and esters, and can be formed by a number of relatively simple procedures, some of which were attempted in this study (see appendix 4.2).

The most commercially attractive way of forming an acyl chloride from a carboxylic acid is by reacting it with thionyl chloride as this is a relatively cheap reagent that produces gaseous by-products (HCl and $SO_2$) that are easily removed from the reaction mixture.[15] However, when this method was applied to the synthesis of **MAA**, a number

of products were formed but not the amide, even after a number of attempts in different reaction conditions.

Cyanuric chloride is also a suitable reagent used for the synthesis of acyl chlorides from carboxylic acids in large-scale industrial processes (Figure 4.5).[16] This reagent is attractive for commercial use as only 0.33 molar equivalents relative to the carboxylic acid are required and the resulting cyanuric acid by-product can be easily removed via filtration. The application of this method to the synthesis of **MAA** yielded a number of products but not the amide.

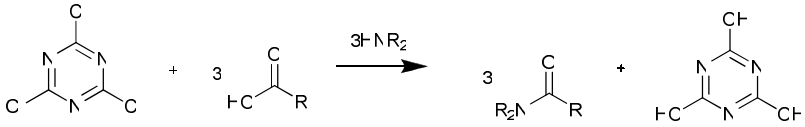

**Figure 4.5: Amide formation from a carboxylic acid using cyanuric chloride.**

An alternative, but more expensive, reagent that can be used to produce acyl chlorides from carboxylic acids is oxalyl chloride, which is reacted with the carboxylic acid in the presence of a catalytic amount of DMF. This method was also unsuccessful when applied to the synthesis of **MAA**, again yielding a mixture of products but not the desired amide.

The method of amide formation via an acyl chloride intermediate was abandoned in favour of exploring other techniques. It is likely that the method failed due to the high reactivity of acid chlorides which makes them susceptible to side reactions[17] as a large number of different products were developed in all cases.

#### 4.4.1.5. Amide Formation Using a Coupling Reagent

A good method for synthesising amides, that avoids going via an acyl chloride intermediate, is by forming an activated ester using a coupling reagent (Figure 4.6). A commonly used coupling reagent is 1-ethyl-3-(3-dimethylaminopropyl) carbodiimide (EDC), which converts carboxylic acids into amides in a one-pot synthesis.[17]

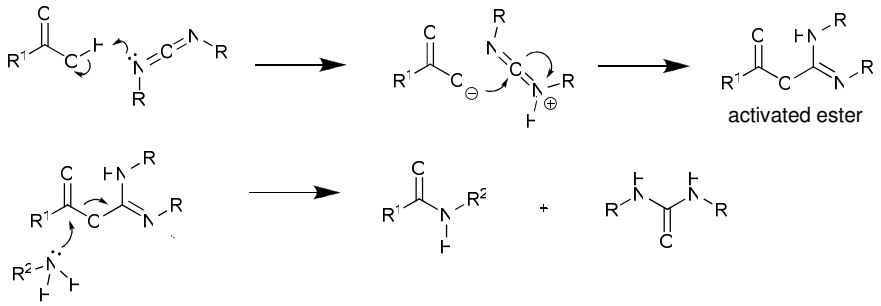


**Figure 4.6: The mechanism of amide formation by using a coupling reagent to form an activated ester.**

This method was attempted for the synthesis of **MAA** by reacting the carboxylic acid precursor, **8**, with one molar equivalent of hexylamine and EDC at ambient temperature for 24 hrs (see appendix 4.3). Analysis of the reaction mixture showed that no MAA had formed.

### 4.4.1.6. Forcing Methods

There are a great number of methods for amide formation that involve forming activated intermediates,[15] although these may not be appropriate for the large scale production of cheap reagents as they add extra stages to the synthesis and result in more by-products. Most convenient would be the direct aminolysis of the ester or carboxylic acid starting materials and, although this method was not initially successful for the synthesis of **MAA**, the reaction might be forced under more favourable conditions.

The first 'forcing method' that was attempted involved reacting the carboxylic acid precursor of **MAA** (**8**), with hexylamine. This method is intuitively unfavourable due to the formation of the stable carboxylic acid salt (Equation 4.5). However, the reaction might be driven at high temperature if water can be removed from the reaction mixture *in situ*.

**Equation 4.5**

$$R^1NH_2 + HOOCR^2 \rightleftharpoons [R^1NH_3^{+}\cdot^{-}OOCR^2] \rightleftharpoons R^1COONHR^2 + H_2O$$

To achieve this, the reaction was performed in toluene with a Dean-Stark trap fitted to the condenser in order to remove the water as a toluene azeotrope. This was successful in producing the target molecule **MAA** in 8% yield. Although this produced enough **MAA** for some solvent extraction experiments to be completed, a more high yielding synthesis was sought.

A simple way of forcing a reaction is by using a large excess of one of the starting materials. This concept was applied to the synthesis of **DAA** by heating **6** at $90^0$C with 7 molar equivalents of hexylamine. After 48 hours, **DAA** was successfully isolated from the reaction mixture by flash column chromatography in 66% yield. The ester starting material and hexylamine were also recovered from the column. This method was also adapted for the synthesis of **MAA** from **5**, resulting in a 68% yield. When this method was adapted for the synthesis of **TAA**, the crude product could not be purified by flash column chromatography as the highly polar tri-amide had a similar Rf value to the by-products. Instead, the ligand **TAA** was successfully separated as a white solid in 11% yield after washing the crude product with a hexane-ether mixture. The simplicity of this method, along with the successful recovery of starting materials and the relatively high product yield, makes it attractive for development for commercial application. Further development would aim to avoid chromatography as this would be expensive, preferring instead the purification of product via other methods, e.g. distillation.

### 4.4.2. Synthesis of M*t*AA

When the forcing method involving the use of a large concentration excess of alkylamine was applied to the synthesis of **M*t*AA** using the reaction of *N*-methylhexylamine with **5** (Scheme 4.3), it was found that the mono-ester precursor did not react (see appendix 4.4). This may be due to the poor nucleophilic quality of *N*-methylhexylamine compared to hexylamine which arises from the increased steric hindrance around the nitrogen atom.

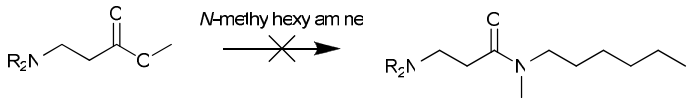


**Scheme 4.3: Synthesis of M*t*AA via direct aminolysis with *N*-methylhexylamine**

A different approach was, therefore, taken to find a route to the *tert*-amide reagent **M*t*AA**. This involved first assembling the *tert*-amide arm and then attaching it to the amine body. This was performed by synthesising an acrylic amide, **9**, by reacting *N*-methylhexylamine with acryloyl chloride and then performing a Michael addition with bis(2-ethyl)hexylamine to give **M*t*AA** in overall yield of 42% (Scheme 4.4).

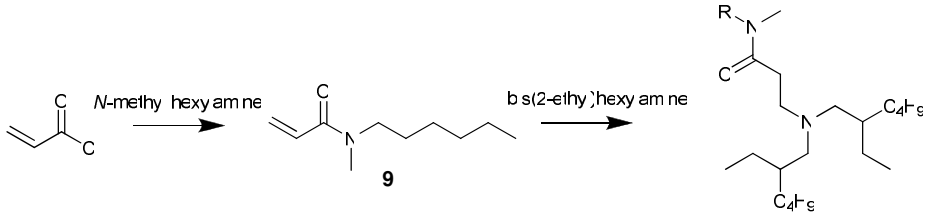


**9**

**Scheme 4.4: Synthesis of M*t*AA via an acrylic amide intermediate.**

The synthesis of **M*t*AA** using the method described in Scheme 4.4 is not as commercially attractive as the method used to produce the secondary amide ligands **MAA**, **DAA** and **TAA** as it uses acryloyl chloride as a starting material which is more expensive and less stable than methyl acrylate. However, the method is simple, does not require very expensive reagents and allows easy work-up of the product.

## 4.4.3. Synthesis of MalA[1]

The synthesis of the malonamide-functionalised alkylamine, **MalA[1]**, was attempted via a similar route to that for the secondary amido-ligands (involving a Michael addition with an acrylic ester, **10**, to form an amino-ester precursor, **11**, followed by direct aminolysis (Scheme 4.5)).

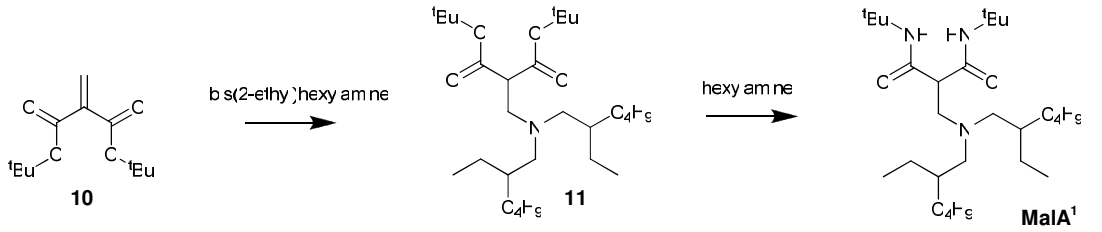


**Scheme 4.5: The proposed synthetic route to MalA[1].**

The first stage required preparation of the di-*tert*-butylmethylenemalonate starting material, **10**, as such a reagent is not available commercially. This was performed using a synthesis devised by Ballesteros *et. al.*,[18] yielding **10** in 48% yield. The next stage involved a Michael addition with bis(2-ethyl)hexylamine which, as with the previous Michael addition reactions, was performed in MeOH at ambient temperature and pressure (see appendix 4.5). Analysis of the reaction mixture after 24 hrs revealed a range of products, none of which was the desired malonate-functionalized alkylamine (**11** in Scheme 4.5). This was attributed to the high reactivity of the methylene malonate which may have resulted in attack by methanol as shown in Figure 4.7. Consequently, the reaction was repeated using diethyl ether as the solvent which yielded the desired malonate-functionalised alkylamine, **11**, in 67% yield.

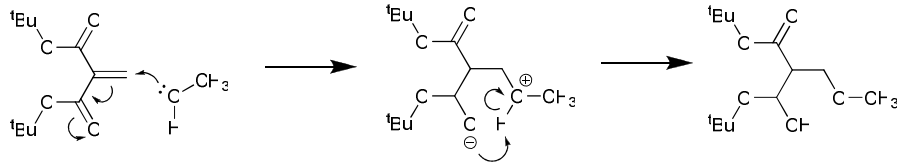

**Figure 4.7: A proposed reaction between methylene malonate and MeOH.**

The final stage of the synthesis of **MalA[1]** was the direct aminolysis of the malonate-functionalised alkylamine, **11**, by heating it in a large excess of hexylamine as previously described in section 4.4.1.6. After 24 hrs, analysis revealed that a mixture of products had formed which contained no **MalA[1]**.

Some of the problems in using the route described in Scheme 4.5 were attributed to the *tert*-butyl ester being a poor electrophile stemming from the steric hindrance around the

*tert*-butyl groups. When the synthesis devised by Ballesteros *et. al.* was adapted using methyl malonate as the starting material instead of *tert*-butyl malonate to generate methylmethylenemalonate, the desired product was not obtained, which was probably due to polymerisation of the starting materials as the reaction mixture had become a glassy-gel. This might be due to the higher reactivity of the methyl malonate starting material in comparison to the sterically hindered *tert*-butylmalonate.

In an attempt to convert the *tert*-butyl ester to a better leaving group, hydrolysis of **11** with NaOH in methanol was attempted, which produced a mixture of products but not the desired malonic acid material. It is possible that the presence of a base causes the degradation of the molecule via a reverse Michael addition reaction (Figure 4.8) as a significant quantity of bis(2-ethyl)hexylamine was detected in the reaction mixture.

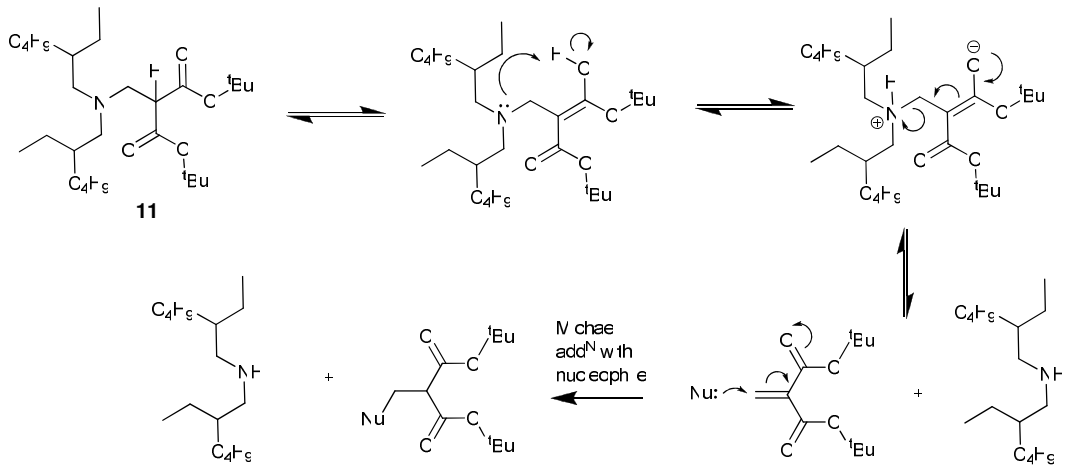


**Figure 4.8: A proposed reverse Michael addition reaction accounting for the reactivity of 11 towards base.**

The susceptibility of the malonic ester intermediate, **11**, to degradation suggests that the target extractant **MalA[1]** will also be unstable. Consequently, a homologue, **MalA[2]**, was targeted.

## 4.4.4. Synthesis of MalA[2]

**MalA[2]** ((3-(bis(2-ethylhexyl)amino)ethyl)-*N*-hexylmalonamide) has a similar basic nitrogen atom to malonamide carbonyl groups sequence to that in **L[4]** in Chapter 3. The extra $CH_2$ spacer group between the malonamide and the amine functionality over that in **MalA[1]** precludes the use of the Michael addition route outlined in Scheme 4.5. The alternative approach used is shown in Scheme 4.6 and involves constructing the malonic amino-ester intermediate, **14**, via an alkyl chloride derivative, **13**, followed by reaction with a large excess of hexylamine to produce the malonamide **MalA[2]** in a 27% overall yield. As the synthesis uses relatively cheap and commercially available starting materials, **MalA[2]** could be commercially viable if its extractive properties are good.

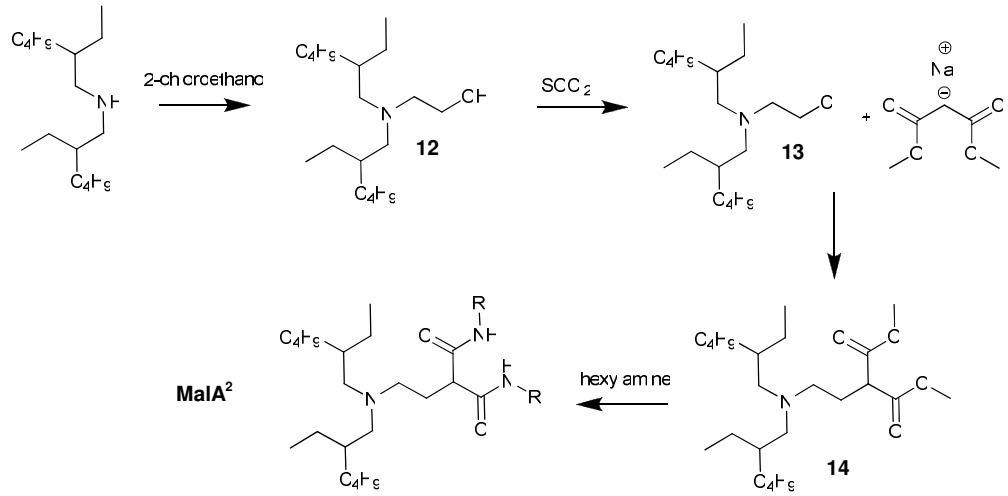


**Scheme 4.6: The synthetic route the ligand MalA[2].**

## 4.5. Solvent Extraction Studies

The main aim of the studies reported in this section was to define how the variation of hydrogen bond donor/acceptor functionality in the series of reagents shown in Figure 4.2 affects the *strength* and *selectivity* of chlorometallate extraction. This chapter focuses on the extraction of Co(II), Zn(II) and Fe(III) from acidic chloride solutions in order to assess the potential application of the new ligands to the Anglo American base metal recovery circuits. The extraction of $PtCl_6^{2-}$ from acid chloride solution was also investigated to compare performance with the tren-based extractants that were developed in a previous study.[11] All solvent extraction data discussed in this chapter are presented in appendices 4.9 to 4.15.

### 4.5.1. Zn(II), Co(II) and Fe(III) Extraction

The five extractants **TEHA**, **MAA**, **DAA**, **M*t*AA** and **MalA$^2$**, all showed sufficient solubility in toluene, both as neutral and protonated species, to allow solvent extraction experiments to be performed readily. Although TAA was insoluble in toluene, it showed sufficient solubility in chloroform to allow some extraction studies to be completed.

#### 4.5.1.1. pH Dependence of Metal Loadings

The main aim of the pH dependence experiments was to examine how extractant *strength* varies for each extractant and to identify the optimum loading pH range for Zn(II) and Co(II) chlorometallates while exploring any conditions that might result in selectivity for these base metals over Fe(III).

When 0.01 M solutions of ligands in toluene were contacted with aqueous solutions of 0.01 M $CoCl_2$ or $ZnCl_2$ containing variable amounts of HCl and an excess of chloride (6 M), metal uptake into the toluene solution showed a marked dependence on the

equilibrium pH of the aqueous phase (Figure 4.9). For both Co(II) and Zn(II) extraction, the order of strength of the ligands is: **DAA > MAA > M*t*AA > MalA$^2$ >> TEHA**. High ferric iron loadings were observed for all of the ligands at pH values <1.8. Above this pH iron precipitates as oxide/hydroxide species. The regions of high iron loadings are marked as a red box in Figure 4.9. For all of the ligands, Zn(II) is extracted more readily than Co(II) (lower proton concentrations in the aqueous phase are required to ensure high loadings). This is in agreement with the findings in the pyridyl ligand study (Chapter 3, section 3.5.1) where the possible reasons for higher Zn(II) loadings are discussed.

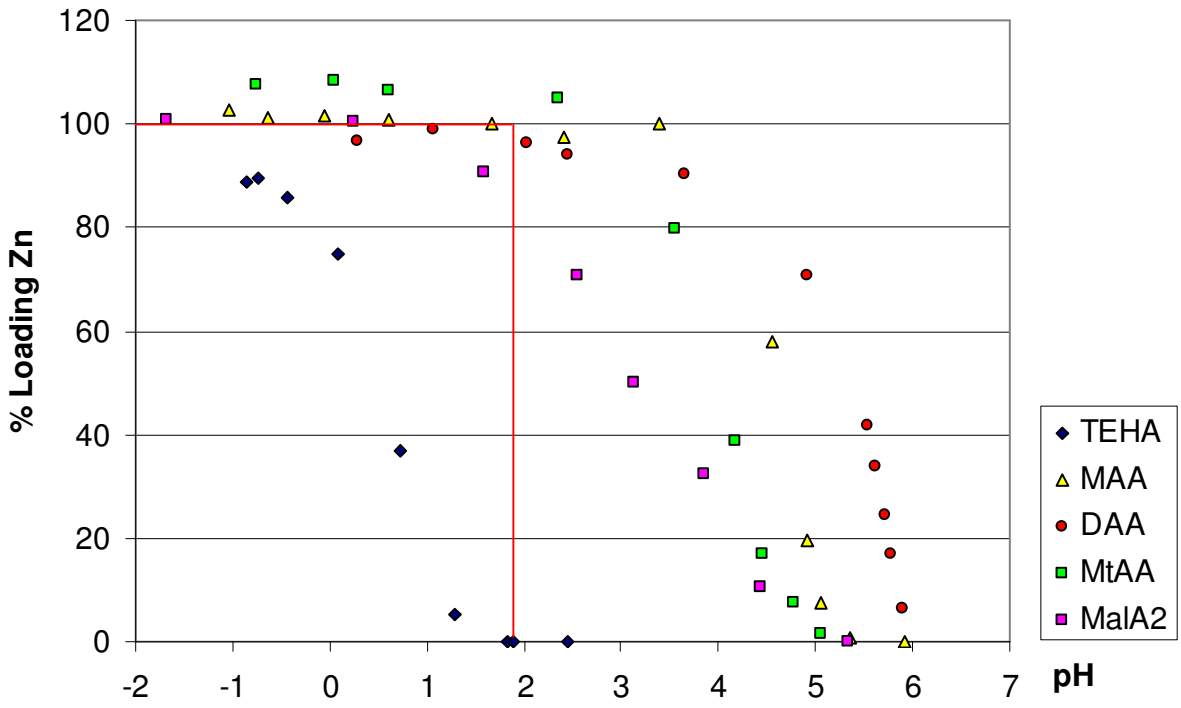

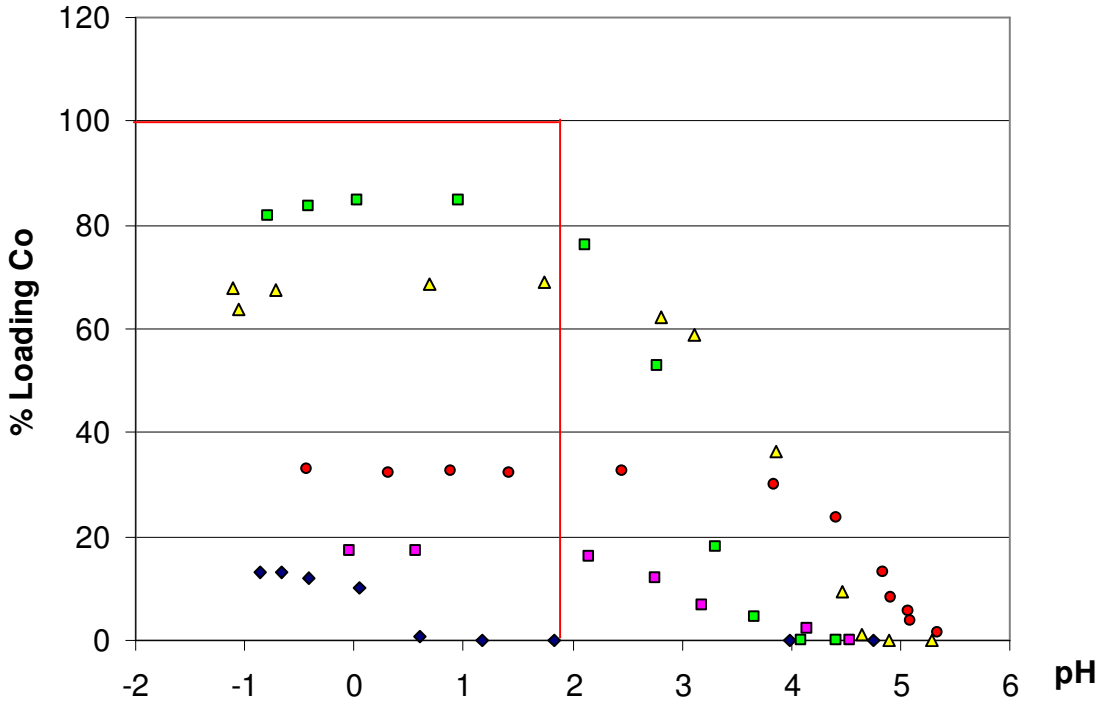


**Figure 4.9: The pH dependence of Zn(II) or Co(II) loading* by 0.01 M toluene solutions of TEHA, MAA, DAA, M*t*AA or MalA[2] after contacting with an equal volume of an aqueous chloride ($[Cl^-]$ = 6 M) solution of $CoCl_2$ or $ZnCl_2$ (0.01 M). High Fe(III) loadings are observed inside the red box.**
***Based on formation of $[(LH)_2MCl_4]$**

At high proton concentrations, ligand which is not loaded with chlorometallate can be assumed to be in the form of its hydrochloride salt and thus the pH loading profiles of the extractants are related to the *selectivity* of transport of chlorometallate anions over chloride (Equation 4.6).

**Equation 4.6**

$$[MCl_4]^{2-} + 2[(LH)Cl]_{(org)} \rightleftharpoons [(LH)_2MCl_4]_{(org)} + 2Cl^-$$

The observation that the ligand **M*t*AA** appears 'weaker' than **MAA** and **DAA** (a lower pH is needed to commence metal loading) yet reaches a higher maximum percentage loading implies that **M*t*AA** is less basic or has a lower affinity for anion but has a higher *selectivity* for chlorometallate over chloride so that Equation 4.6 lies further to the right

hand side. M*t*AA reaches a maximum loading of >100% and the possible reasons for this are discussed in Chapter 3, section 3.5.1.

Crucially, the amido-functionalised tertiary alkylamines are much stronger than **TEHA**, and they are able to extract significant quantities of Co(II) and Zn(II) at pH values at which iron precipitates. The high *strength* of the new amido-functionalised ligands is significant for commercial application as this could allow for the recovery of Co(II) or Zn(II) from iron-depleted solutions of high pH without the need to re-acidify.

#### 4.5.1.2. Chloride Concentration Dependence of Metal Loadings

The main aim of the chloride concentration dependence experiments was to define the optimum aqueous chloride concentrations for the loadings of Zn(II) and Co(II) across the ligand series and to explore any conditions that might result in selectivity for the base metals over Fe(III).

When 0.01 M solutions of ligands in toluene were contacted with aqueous solutions of 0.01 M $FeCl_3$, $CoCl_2$ or $ZnCl_2$ containing variable chloride concentration and constant proton concentration (0.1 M), the metal uptake into the organic phase showed a marked dependence on the concentration of chloride in the aqueous phase (Figure 4.10). For all of the ligands, increasing chloride concentration results in increased metal loadings and Zn(II) extracts at lower chloride concentrations than Fe(III), while Co(II) is least readily extracted. This is in agreement with the findings in Chapter 3, which discusses the origins of this phenomenon more detail (see Chapter 3, section 3.5.2).

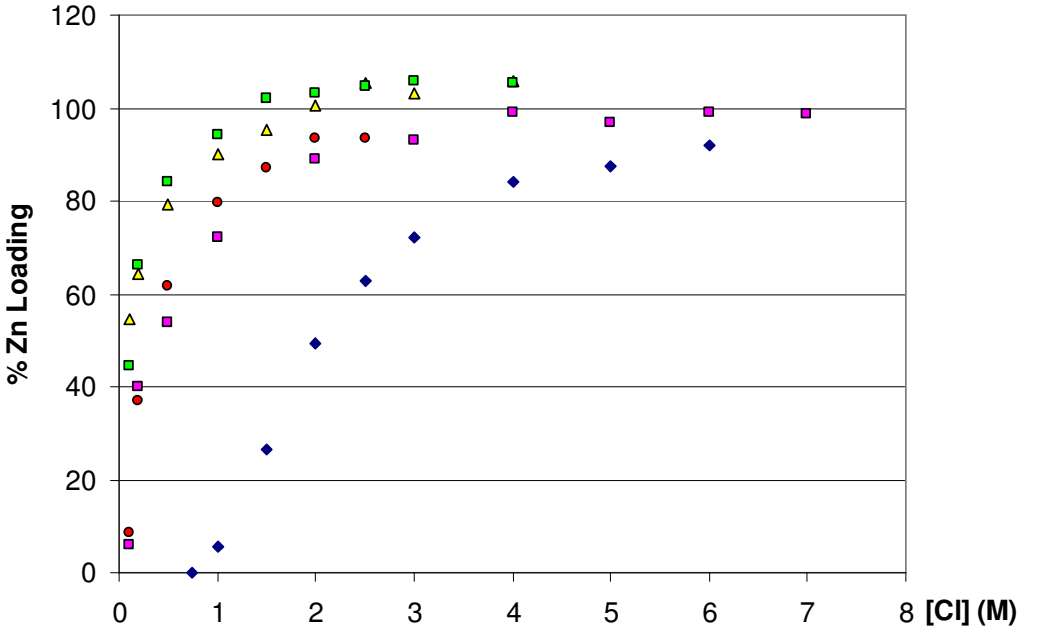
% Zn Loading
120
100
80
60
40
20
0
0
1
2
3
4
5
6
7
8
[Cl] (M)

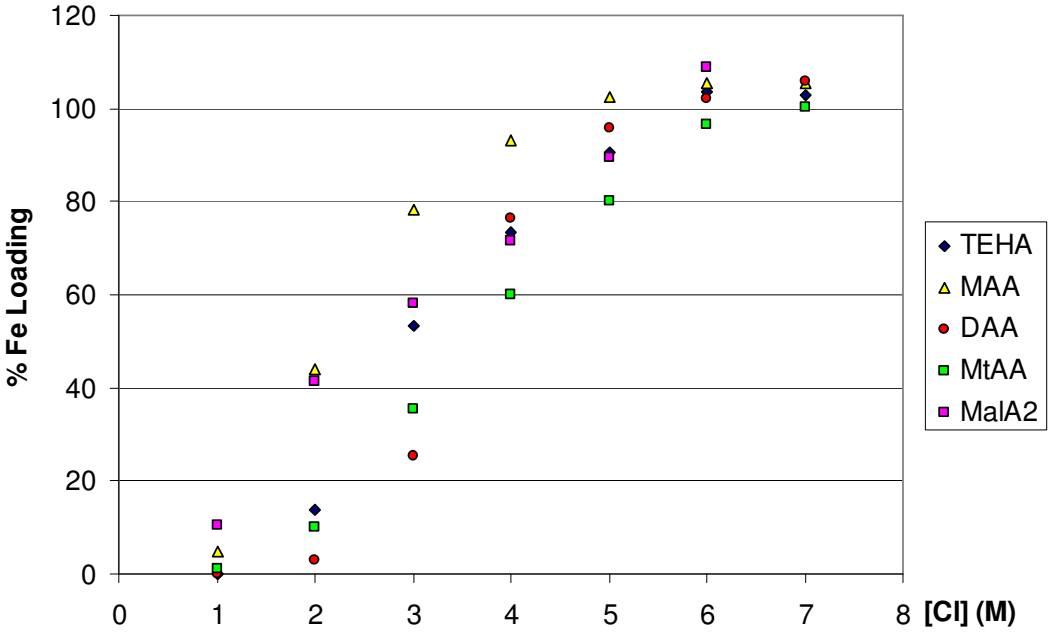
% Fe Loading
120
100
80
60
40
20
0
0
1
2
3
4
5
6
7
8
[Cl] (M)
TEHA
MAA
DAA
MtAA
MalA2

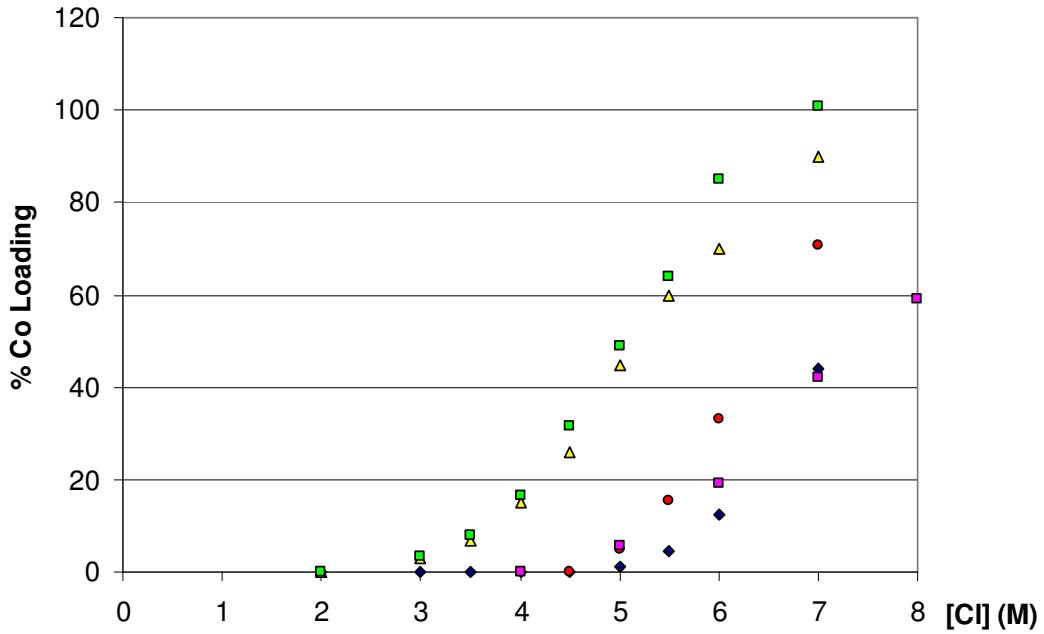


**Figure 4.10: The chloride concentration dependence of loadings* of Fe(III), Zn(II) or Co(II) by 0.01 M toluene solutions of TEHA, MAA, DAA, M*t*AA or MalA$^2$ after contacting with an equal volume of an aqueous solution of $FeCl_3$, $CoCl_2$ or $ZnCl_2$ (0.01 M, $[H^+]$ = 0.1 M).**
***based on formation of $[(LH)_2MCl_4]$ for M = Co(II) or Zn(II) and $[(LH)FeCl_4]$.**

The amido-functionalised ligands, **MAA**, **M*t*AA**, **DAA** and **MalA$^2$**, all extract zinc at lower chloride concentrations (<1 M) than **TEHA**. In contrast, all of the ligands begin to extract iron at similar chloride concentrations (>1 M). These results suggest that, in solutions that contain moderate concentrations of chloride, the new amido-functionalised ligands will be more effective for separating Zn(II) from Fe(III) than **TEHA**. This is illustrated in Figure 4.11 which compares the loadings of Zn(II) and Fe(III) on **TEHA** with those on **M*t*AA**. The selective extraction of Zn(II) over Fe(III) at chloride concentrations of less than 1 M, although not useful for the new Anglo American circuits, does have potential application for Zn(II) recovery in other commercial chloride hydrometallurgical circuits, such as in the treatment of spent pickling solutions.[19]

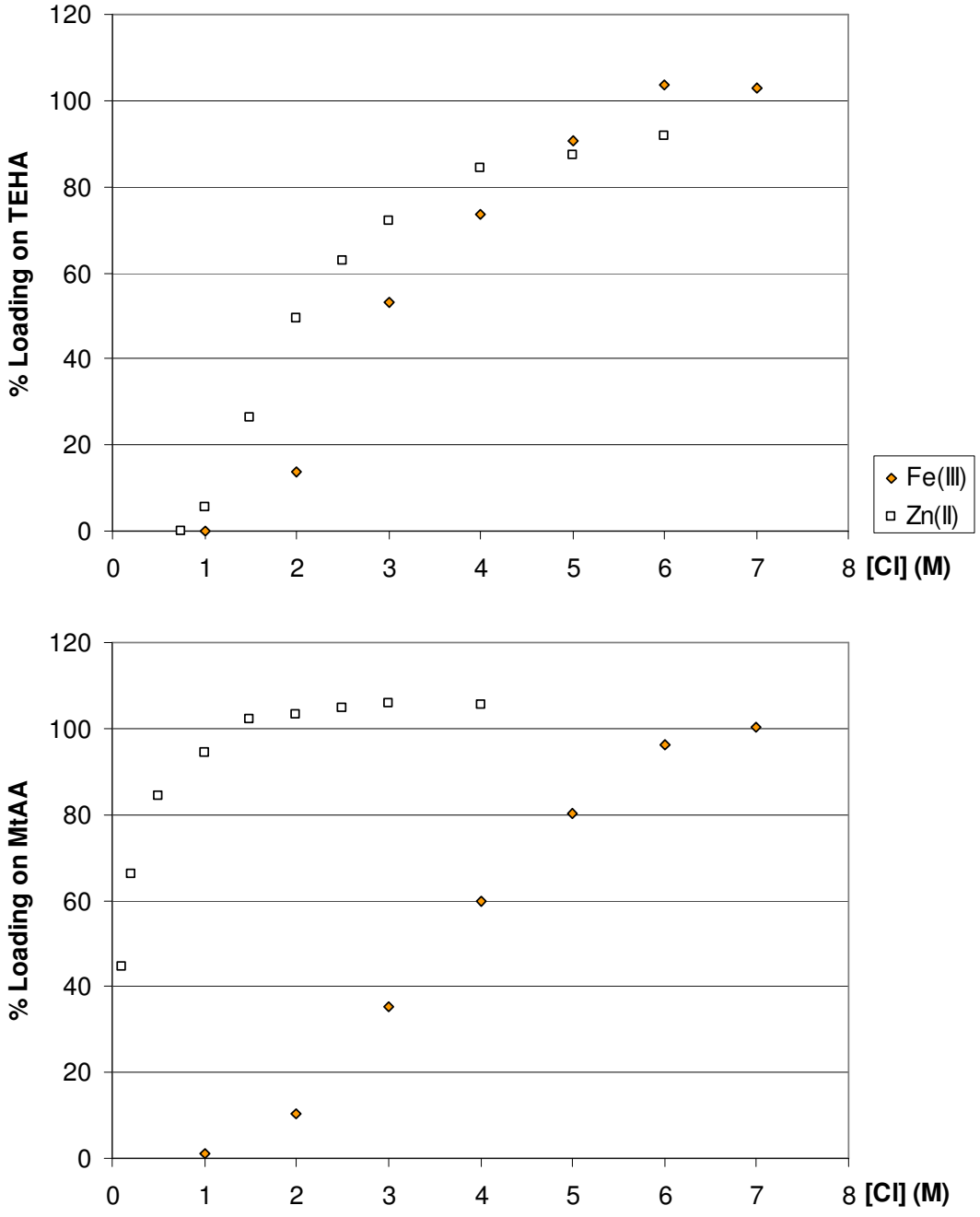


**Figure 4.11: The chloride concentration dependence of loadings* of Fe(III) and Zn(II) on TEHA and M*t*AA.**

***based on formation of $[(LH)_2ZnCl_4]$ and $[(LH)FeCl_4]$.**

#### 4.5.1.3. Extraction Efficiency from Model Pregnant Leach Solutions

This section compares the efficiencies of the new extractants and **TEHA** in recovery of Co(II) and Zn(II) from strong acid chloride solutions with compositions chosen to resemble those expected in the pregnant leach solutions of the new Anglo American circuits. Extractions were initially carried out using toluene solutions of the new reagents but were later extended to chloroform solutions to allow the efficiency of the tri-amide derivative (**TAA**), which has a very low solubility in toluene, to be assessed.

When toluene solutions containing different concentrations of the extractants [L] were contacted with aqueous solutions of 250 ppm Co(II) or Zn(II), 6 M chloride and 3 M proton, metal uptake into the organic phase showed a marked dependence on [L] (Figure 4.12).

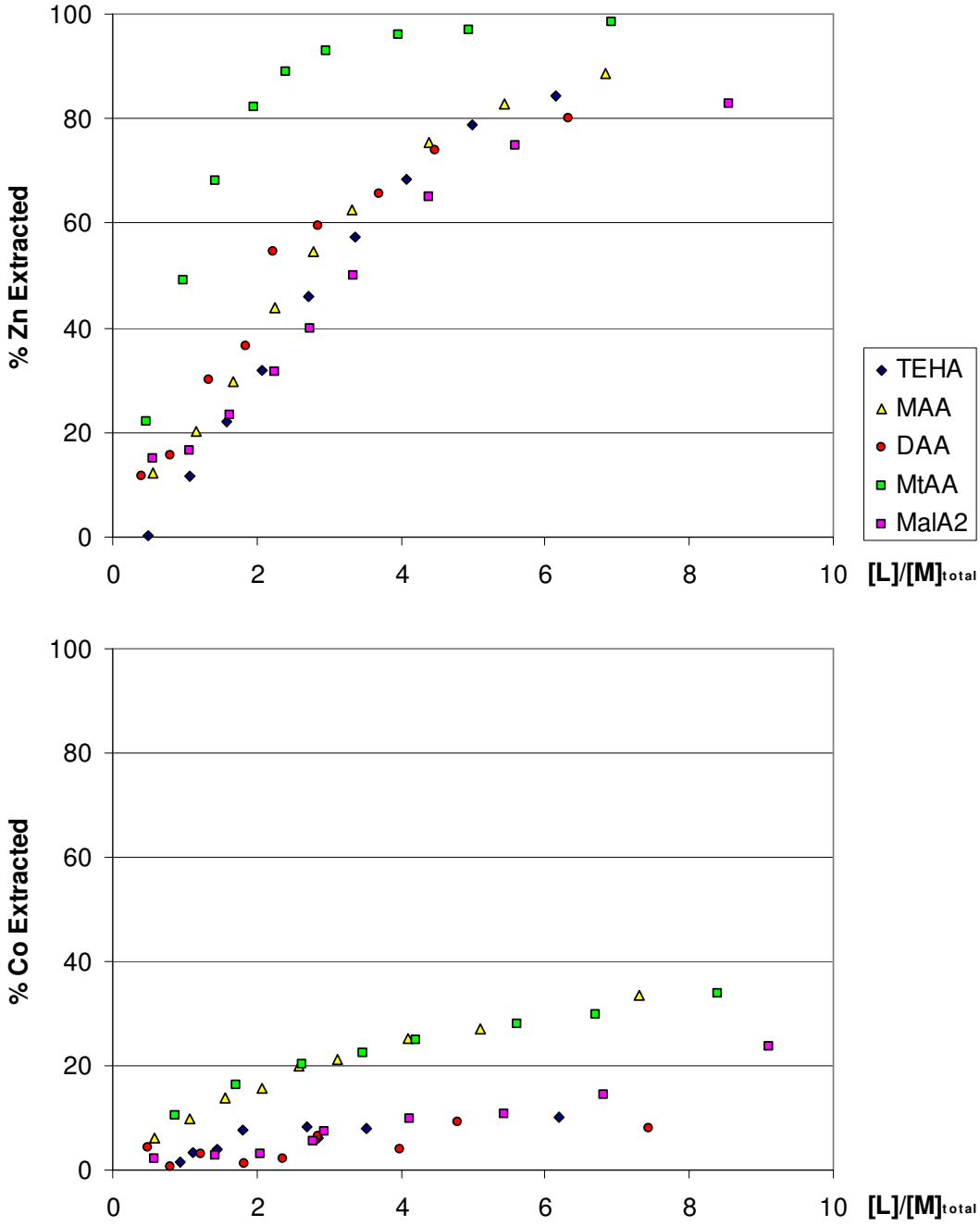


**Figure 4.12: The extraction of Zn(II) and Co(II) into toluene solutions containing different concentrations of reagent after contacting with an equal volume of an aqueous solution of $CoCl_2$ or $ZnCl_2$ (250 ppm M(II), $[H^+]$ = 3.2 M, $[Cl^-]$ = 6 M). The charts record $[L]_{org}/[M]_{total}$ values.**

**M*t*AA** is significantly more efficient at extracting Zn(II) into toluene than the other ligands which are similarly efficient. As expected from the results presented in Figure 4.9 and Figure 4.10, all of the ligands extract Co(II) less efficiently than Zn(II). **MAA** and **M*t*AA** are comparably efficient at extracting Co(II) and significantly more efficient than **MalA$^2$**, **DAA** and **TEHA**.

In general, when extracting into toluene from aqueous solution with compositions similar to those representing pregnant leach solutions from possible Anglo American circuits, the amide-functionality in the alkyl chains has a limited effect on extraction *efficiency*, with the exception of the tertiary amide, **M*t*AA**.

When extracting into chloroform solutions (Figure 4.13), all of the amido-functionalised ligands (**MAA**, **M*t*AA**, **DAA**, **TAA** and **MalA$^2$**) show much greater extraction efficiencies than **TEHA**. It is clear that the solvent system has a major affect on the extraction efficiency of **TEHA**, which extracts chlorometallates comparably well into toluene but very poorly into chloroform. This contrasts with the amido-functionalised reagents which also extract chlorometallates into chloroform, albeit with a much lower *efficiency* than into toluene.

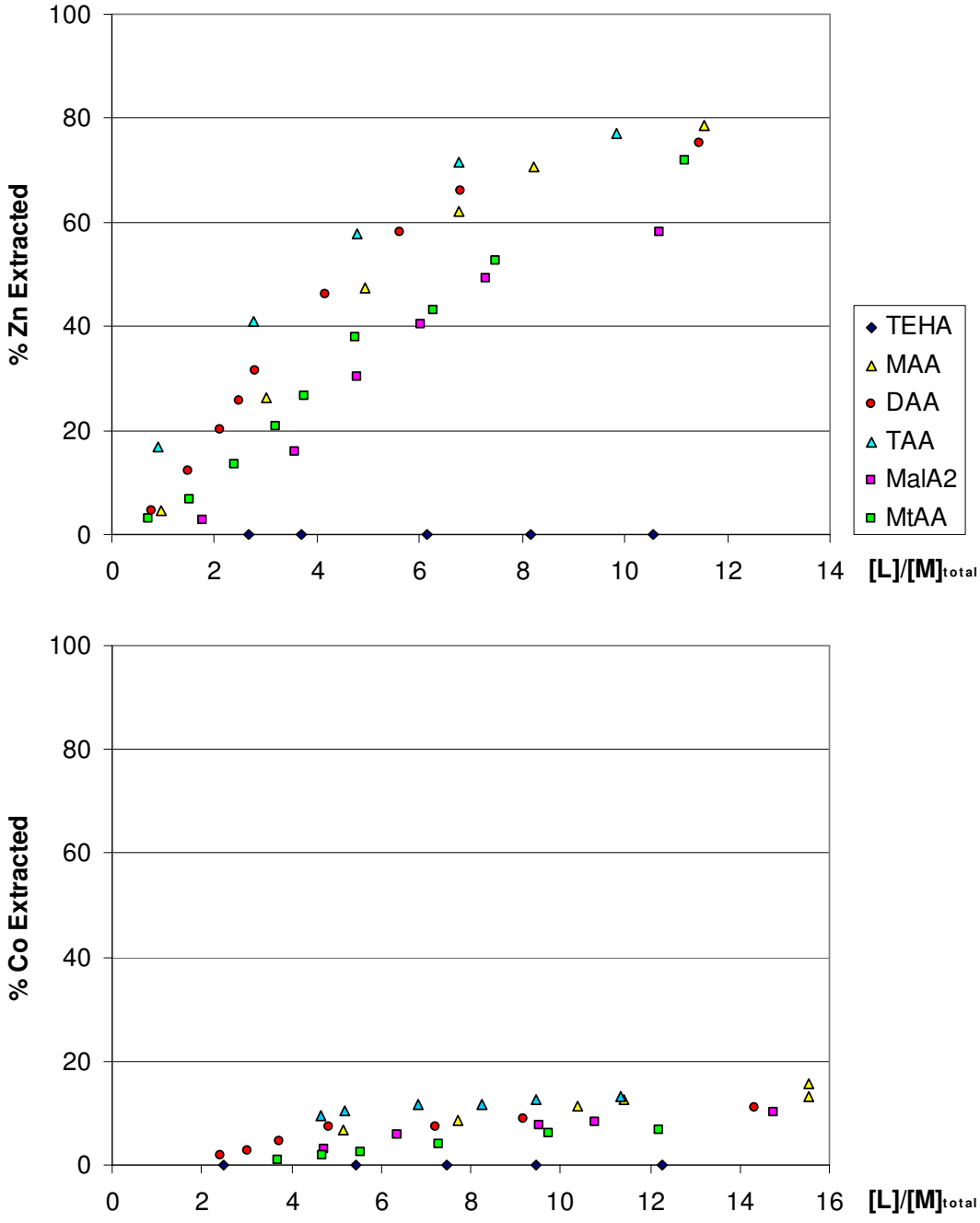


**Figure 4.13: The extraction of Zn(II) and Co(II) into chloroform solutions containing different concentrations of reagent after contacting with an equal volume of an aqueous solution of $CoCl_2$ or $ZnCl_2$ (250 ppm M(II), $[H^+]$ = 3.2 M, $[Cl^-]$ = 6 M). The charts record $[L]_{org}/[M]_{total}$ values.**

The effect that the extracting solvent has on the chlorometallate extraction *efficiency* is difficult to explain. An obvious difference between the two solvents is polarity, with chloroform having a higher dielectric constant than toluene.[20] Solvent polarity affects the *Hofmeister bias*, which implies that large and more charge diffuse anions (like chlorometallates) extract more readily into non-polar solvents than small and charge localised anions (like chloride) so that, in solvent extraction systems, extraction of chlorometallate is inherently more favourable than extraction of chloride (see Chapter 1, section 1.5.3). The *Hofmeister bias* is more pronounced in less polar organic solvents so that extraction into toluene would recover chlorometallate from the aqueous phase at a higher degree of *selectivity* over chloride (resulting in greater extraction *efficiency*) than when extracting into chloroform.

Good and Bryan have investigated the extraction of Co(II) from highly acidic chloride media with various alkylamines in a range of organic solvents and they found extraction efficiency to be *independent* from the dielectric constant of the solvent.[21] The authors observed that extraction of Co(II) was significantly decreased in hydrogen bond donor solvents, particularly the haloforms, and they argued that hydrogen bonding interactions between the amine N and the C-H donor in the solvent interferes with ion-pair formation, supporting their theory with some evidence from IR spectroscopic studies. This theory suggests a competition between proton and the haloform C-H donor for the basic amine N in the organic phase, implying that, in hydrogen bond donor solvents, only a fraction of the amine is protonated, which seems unlikely when in contact with highly acidic solutions and does not explain why the new amide and malonamide functionalised ligands presented in this study are less susceptible than **TEHA**.

An alternative explanation involves referring to solvation interactions between the hydrogen bond donor/acceptor groups on the ligand-chlorometallate assemblies and solvent molecules. Toluene may act as a hydrogen bond acceptor solvent so that weak ‘T-shaped’ hydrogen bonding interactions might form to satisfy C-H δ+ on the outer-coordination sphere of the whole ligand-chlorometallate assemblies in both the new

amide/malonamide functionalised ligands and **TEHA** as both have C-H donor functionality that would be exposed to the solvent environment (Figure 4.14). Such interactions have been observed previously by Steiner *et. al.*.[22, 23]

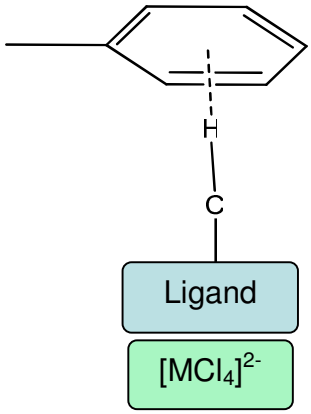


**Figure 4.14: A sketch of a possible stabilising 'T-shaped' hydrogen bonding interaction between a C-H donor on the ligand-chlorometallate assembly and toluene.**

In hydrogen bond donor solvents, such as chloroform, the reverse is possible, where solvent hydrogen bond donor functionality would interact unfavourably with C-H δ+ on the ligand-chlorometallate assemblies (Figure 4.15).

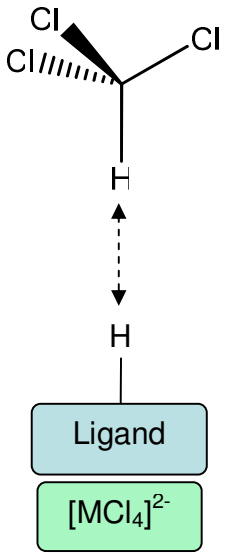


**Figure 4.15: A sketch of a possible destabilising interaction between a C-H donor on the ligand-chlorometallate assembly and a chloroform C-H donor.**

This interaction (Figure 4.15) may destabilise the ligand-chlorometallate assemblies and be responsible for the poor extraction efficiency of **TEHA** in chloroform. The new amide/malonamide functionalised ligands, however, also contain hydrogen bond acceptor carbonyl oxygens that may interact favourably with the C-H donor on chloroform (Figure 4.16).

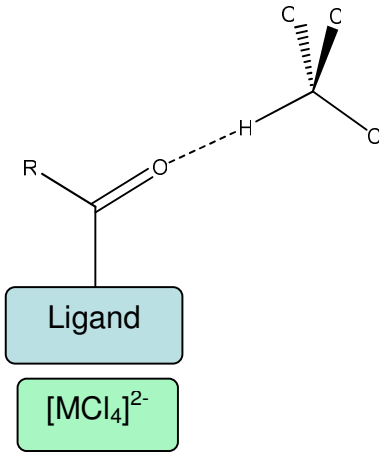


**Figure 4.16: A sketch of a possible stabilising interaction between a carbonyl hydrogen bond acceptor site on a 'MAA-type' ligand-chlorometallate assembly and a chloroform C-H donor.**

Such favourable CH···O interactions between the chloroform molecules and the ligand-chlorometallate assemblies may counteract the unfavourable interactions between the C-H δ+ around the ligand-chlorometallate complex and chloroform hydrogen bond donors, which would be possible in the amide/malonamide ligand-chlorometallate assemblies but not **TEHA**. This would account for the large difference in the extraction *efficiency* of the amide/malonamide functionalised ligands in chloroform relative to **TEHA**.

#### 4.5.1.4. Stripping

The new reagents show good extraction of cobalt and zinc chlorometallates with possible selectivity over ferric iron under certain conditions and this might meet the criteria needed for exploitation in the proposed new Anglo American circuits. To investigate the commercial viability of the new ligands further, it is important to demonstrate recoveries of the metals from the loaded organic solutions and effective reuse of the extractant in subsequent load-strip cycles. This can be achieved using the method described in Chapter 2, section 2.3.6.

**MAA** and **M*t*AA** both showed sufficiently rapid phase disengagement to allow load-strip cycles to be investigated. **DAA** formed an emulsion during stripping and consequently was not studied. Figure 4.17 shows that complete recovery of the metal value from the organic phase is possible by contacting with de-ionised water and comparable loadings in subsequent load-strip cycles indicated no inner-sphere coordination (discussed in Chapter 1, section 1.8.6) or significant loss in reagent activity.

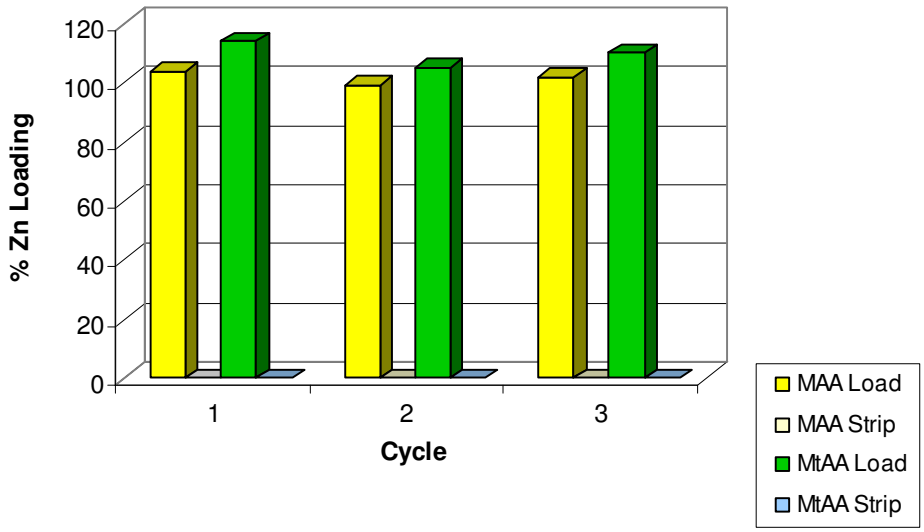

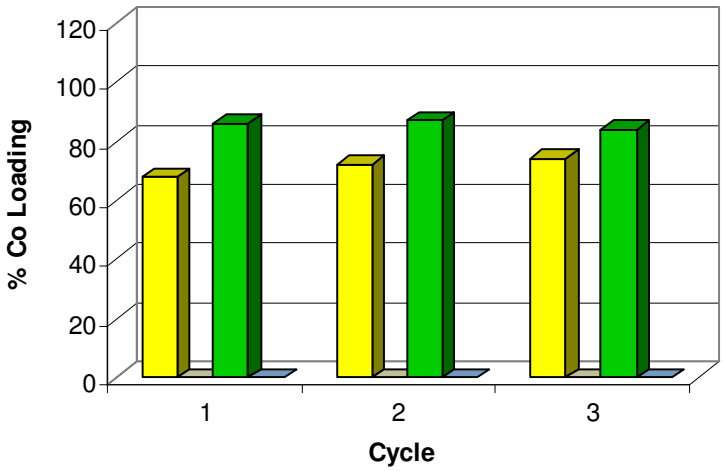


**Figure 4.17: Percentage metal loadings* of 0.01 M toluene solutions of MAA and M*t*AA during three successive load-strip cycles. Loading involved the contact of 0.01M ligand-toluene solutions with 6 M HCl solutions containing 0.01 M Zn(II) or Co(II), and stripping the contact of the loaded organic with an equal volume of deionised water.**

***based on formation of $[(LH)_2MCl_4]$ for M = Co(II) or Zn(II).**

### 4.5.1.5. Analysis of Metal and Total Chloride Loading of Organic Extractant

It is helpful to know the ratios of chloride to metal ion present in the loaded organic phase to define the mode of action of metallate extraction (see Chapter 2, section 2.3.7). In this work, for the most commercially viable ligands, **MAA** and **M*t*AA**, the chloride and the zinc or cobalt concentrations in the toluene were determined under conditions which lead to high loadings; 0.01 M Co(II) or Zn(II) in 6 M HCl. The loaded organic phase was collected and contacted with an alkali aqueous solution to ensure complete stripping and the concentration of stripped chloride was determined as described in Chapter 2 section 2.3.7.

Table 4.1 displays the results for the $[M(II)]/[Cl^-]$ analysis and calculates the relative concentrations of metal-bound chloride (assuming $[Cl^-]$ bound = 4 x $[M^{2+}]$) and hence

the concentration of free chloride in the organic phase ([$Cl^-$] free = [$Cl^-$] total – [$Cl^-$] bound).

| Ligand | Metal | [L] | [$M^{2+}$] | % Loading | [$Cl^-$] total | [$Cl^-$] bound | [$Cl^-$] free |
|---|---|---|---|---|---|---|---|
| | | (mM) | (mM) | | (mM) | (mM) | (mM) |
| MAA | Co | 12.31 | 3.89 | 63.22 | 18.27 | 15.56 | 2.71 |
| MAA | Zn | 12.31 | 6.05 | 98.33 | 20.49 | 24.20 | -3.71 |
| MtAA | Co | 10.77 | 4.23 | 79.76 | 18.00 | 17.18 | 0.82 |
| MtAA | Zn | 10.77 | 5.53 | 102.78 | 21.06 | 22.14 | -1.08 |

**Table 4.1: Total analysis for [M(II)] and [$Cl^-$] loading in toluene solutions containing MAA and M*t*AA.**

The calculated concentration of 'free' chloride in Table 4.1 for the loading of zinc on **MAA** and **MtAA** is a negative value. This could arise from the extraction of $ZnCl_3^-$ according to Equation 4.7, which would result in a lower total concentration of chloride in the organic phase. The extraction of such a species would also account for the >100% zinc loadings on M*t*AA as observed in Figure 4.9.

**Equation 4.7**

$$L_{(org)} + H^+ + [ZnCl_3]^- \rightleftharpoons [LHZnCl_3]_{(org)}$$

## 4.5.2. Pt(IV) Extraction

In previous work at the Universities of Edinburgh and Nottingham, hydrogen bond donor extractants containing the tris(2-amminoethyl)amine or 'tren' structure (Figure 4.18) were shown to extract $PtCl_6^{2-}$ much more efficiently than **TOA**.[11] The basic structure of these reagents differ from those presented in this study with respect to the atom sequence which links the amide group to the bridgehead nitrogen (Figure 4.18). It is of interest to establish whether the reversal of the amido N and carbonyl groups in **MAA** etc affects the efficiency of $PtCl_6^{2-}$ loading.

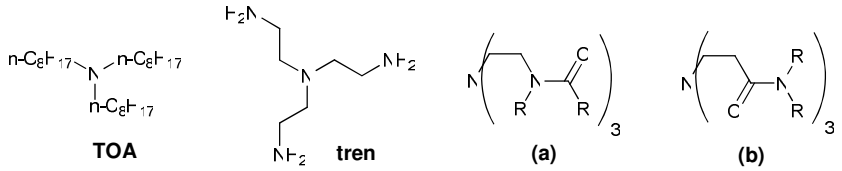


**Figure 4.18: The structures of the previously developed[11] tren-based extractants (a) compared with the reagents MAA etc (see Figure 4.2) presented in this study which have the general structure (b).**

### 4.5.2.1. Extraction into Chloroform

In order to compare the extractive behaviour of the new amido-functionalised tertiary alkylamines with the previously investigated tren-based derivatives, platinum extraction experiments were conducted with **MAA**, **M*t*AA**, **DAA**, **TAA** and **MalA**[2], using chloroform as the water immiscible solvent. **TOA** is included being a model for the Alamine-type reagents. Figure 4.20 compares the extraction efficiency curves for the new ligands with **TOA** and one of the best reagents from the previous platinum extraction study *N*,*N'*,*N"*-(nitrilotri-2,1-ethanediyl)tris(*N'*-3,4-dimethoxyphenyl urea) **15** (Figure 4.19).[11]

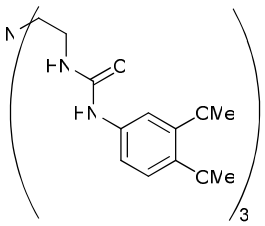

**Figure 4.19: Structure of the tren-based extractant, *N*,*N'*,*N"*-(nitrilotri-2,1 ethanediyl)tris(*N'*-3,4-dimethoxyphenyl urea) (15).[11]**

All of the amide functionalised reagents extract Pt(IV) into chloroform much more efficiently than **TOA**. The ligands **MAA**, **DAA** and **TAA** extract slightly more efficiently than the tren-based reagent, **15**, whereas the ligands **M*t*AA** and **MalA**[2] are less efficient.

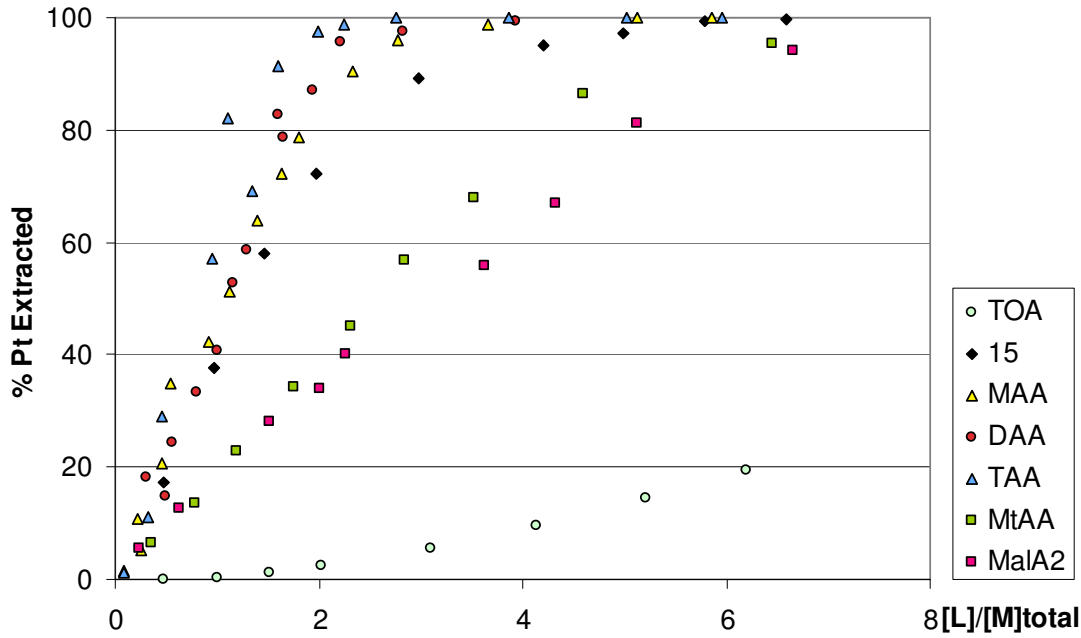


**Figure 4.20: The extraction of $PtCl_6^{2-}$ into chloroform solutions containing different concentrations of reagent after contacting with an equal volume of an aqueous solution of $H_2PtCl_6$ (250 ppm Pt(IV), [HCl] = 0.6 M). The charts record $[L]_{org}/[M]_{total}$ values.**

### 4.5.2.2. Extraction into Toluene

To further assess the commercial viability of the new ligands as potential platinum recovery reagents, the solvent extraction experiments were repeated using toluene as the organic solvent (Figure 4.21). **MAA** and **DAA** were slightly less efficient in toluene than they were in chloroform, whereas **M*t*AA** and **MalA$^2$** were a little more efficient. Most striking, however, is the performance of the industrial benchmark ligand, **TOA**, which is much more efficient in toluene than chloroform. This is comparable with the performance of **TEHA** in the base metal extraction study and the phenomenon is discussed further in section 4.5.1.3.

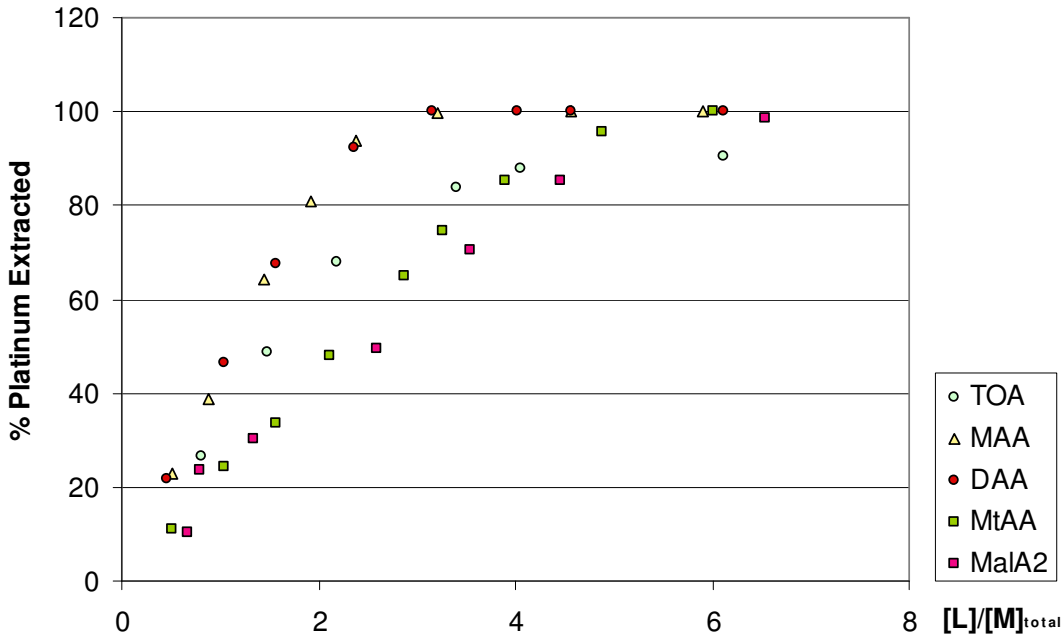


**Figure 4.21: The extraction of $PtCl_6^{2-}$ into toluene solutions containing different concentrations of reagent after contacting with an equal volume of an aqueous solution of $H_2PtCl_6$ (250 ppm Pt(IV), [HCl] = 0.6 M). The charts record $[L]_{org}/[M]_{total}$.**

To explore the overall $PtCl_6^{2-}$ vs $Cl^-$ *selectivity* of the ligand **MAA**, $[Pt^{4+}]/[Cl^-]$ total analysis experiments were performed as described in Chapter 2 section 2.3.7.3. Table 4.2 shows that the concentration of free chloride transported into the organic phase varies significantly with ligand molar excess. At a ligand molar excess of 1.66, 65% of the Pt(IV) is extracted from the aqueous phase with very little free chloride. A ligand molar excess of 2.51 extracts 92% of the Pt(IV) with a relatively small amount of free chloride. At a larger ligand molar excess of 4.16, 98% of the Pt(IV) is extracted from the aqueous phase with a significant quantity of free chloride. These results show that the ligand **MAA** is highly selective for the $PtCl_6^{2-}$ anion over chloride, which is encouraging for its potential commercial application as a platinum refining reagent.

| [L] (mM) | [L]/[$Pt^{4+}$] | % Pt Extracted | [$Cl^-$] (mM) |
|---|---|---|---|
| 2.13 | 1.66 | 65.27 | 0.02 |
| 3.21 | 2.51 | 91.97 | 0.25 |
| 4.28 | 3.34 | 98.25 | 0.96 |
| 5.33 | 4.16 | 100.00 | 1.54 |

**Table 4.2: Total analysis for $PtCl_6^{2-}$ and [$Cl^-$] loading.**

## 4.6. Analysis of Anion-Host Interactions

The origin of the enhanced extraction performance of the new reagents in Figure 4.2 relative to **TEHA** and **TOA** is of considerable interest, especially the increase in extractant *strength* as this is key to application of the new reagents in the selective extraction of Co(II) or Zn(II) over Fe(III) in the Anglo American circuits. In order to investigate the major interactions in the chlorometallate-ligand assemblies using the X-ray crystallography and NMR techniques described in Chapter 2, section 2.4, crystalline complexes are required. It did not prove possible to isolate crystals of ligand-chlorometallate complexes of sufficient quality for single crystal X-ray structure determination. This was not unexpected as the flexibility of the new ligands, stemming from the long alkyl chain functionalities, typically leads to formation of oils or greasy solids. To circumvent this problem, the ligand **MAAX** (Figure 4.22) was synthesised. **MAAX** is analogous to the extractant **MAA**, but with decreased alkyl chain length to aid crystallisation. As in **MAA**, the alkyl groups attached to the tertiary amine nitrogen atom are branched at the β-carbon atom, but in this case symmetrically.

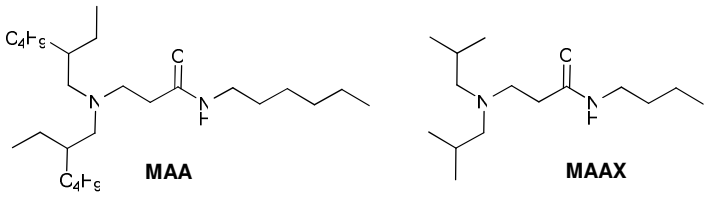


**Figure 4.22: Structure of MAA (left) and the crystallisable analogue MAAX (right). The hexyl chain attached to the amido nitrogen atom in MAA is replaced by an n-butyl group in MAAX.**

The [(**MAAX**H)$_2$ZnCl$_4$] and [(**MAAX**H)$_2$CoCl$_4$] crystal structures (Figure 4.23) have overall 2:1 ligand:chlorometallate stoichiometry. Unlike the **L$^2$**-chlorometallate crystal structures (Chapter 3, section 3.6.1), the **MAAX** structures are polymeric, with the ligands bridging between chlorometallate anions. Such polymeric structures are unlikely to be maintained in solution so that the solid state structures cannot be deemed as being representative of the solution state structures in the loaded organic phase. In both [(**MAAX**H)$_2$ZnCl$_4$] and [(**MAAX**H)$_2$CoCl$_4$] crystal structures, the ligand binds to the anion via many weak amide N-H and amide and ammonium α-carbon C-H hydrogen bonding interactions. This corroborates well with the **L$^2$**-chlorometallate complexes and anion recognition studies that show protonated polyamines interacting with large anions via numerous C-H and N-H donors as opposed to single localised hydrogen bonds.[13, 24, 25]

Like in the **L$^2$**-chlorometallate crystal structures, protonation of the amine nitrogen causes formation of a six-membered 'proton-chelating' ring. This has the effect of pre-organising the structure of the molecule so that the polar N-H and C-H donors associated with the amide and amine functionalities point away from each-other. This means that interaction with a single chlorometallate with a single protonated ligand becomes difficult. Consequentially, bridging structures are formed so that both groups of polar C-H and N-H donors may interact with an anion. Figure 4.23 shows an example of one such bridging unit for the [(**MAAX**H)$_2$ZnCl$_4$] and [(**MAAX**H)$_2$CoCl$_4$] crystal structures. In both structures the inter-molecular outer-sphere interactions are comparable (see Table 4.3) with H···Cl interactions ranging between 2.38 and 2.80 Å .

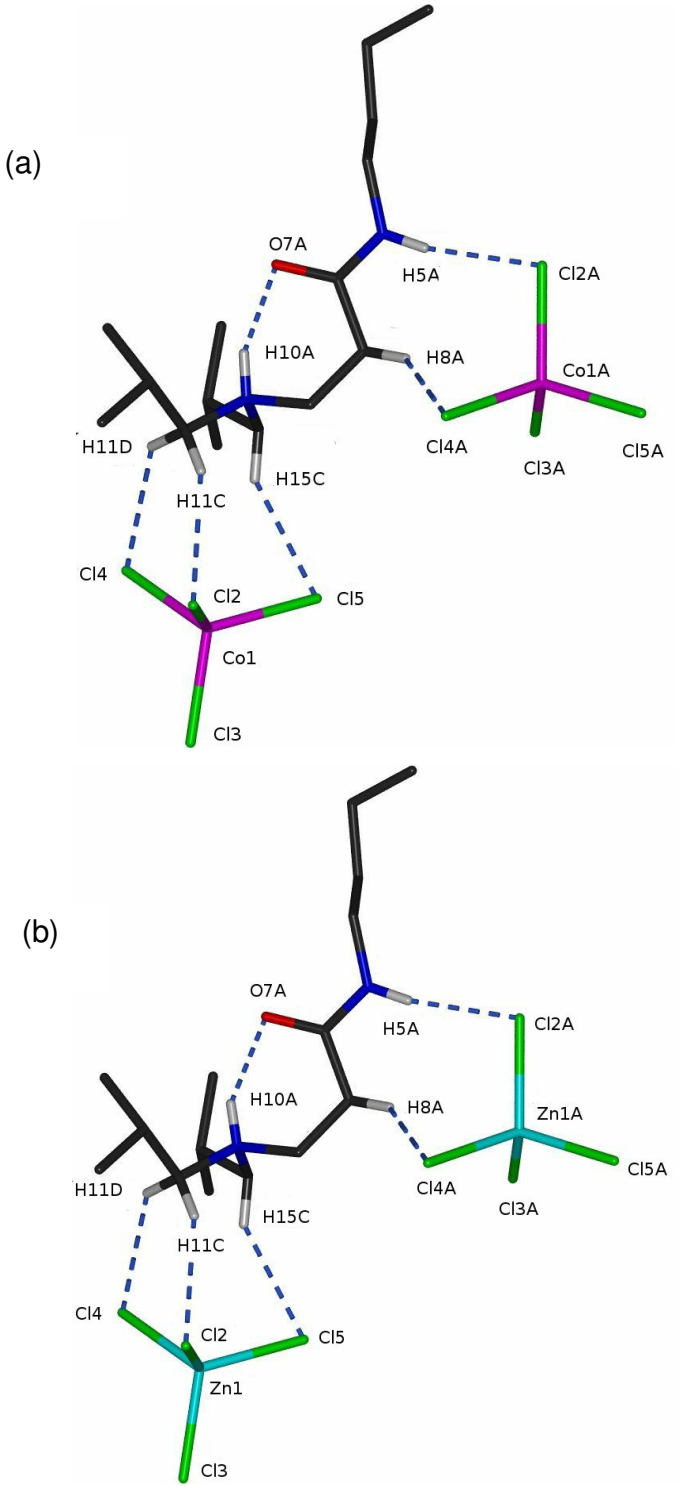


**Figure 4.23: An example of a bridging unit in the crystal structures for the $[(MAAXH)_2ZnCl_4]$ (a) and $[(MAAXH)_2CoCl_4]$ (b) complexes.**

| Contact distance/ Å | M = Co | M = Zn |
|---|---|---|
| H10A O7A | 1.92 | 2.00 |
| H5A Cl2A | 2.39 | 2.38 |
| H11C Cl2 | 2.80 | 2.80 |
| H11D Cl4 | 2.79 | 2.78 |
| H15C Cl5 | 2.71 | 2.72 |
| H8A Cl4A | 2.74 | 2.74 |

**Table 4.3: Contact distances/Å in the outer coordination spheres of the cobalt and zinc complexes, $[(\mathbf{MAAXH})_2MCl_4]$.**

Although the crystal structures for $[(\mathbf{MAAX}H)_2ZnCl_4]$ and $[(\mathbf{MAAX}H)_2CoCl_4]$ cannot be used as a reliable model for the solution phase moieties existing in solvent extraction conditions, some general observations can be made. Like in the $\mathbf{L^2}$-chlorometallate complexes, the intra-molecular six-membered 'proton chelating' ring, which allows close N-H···O contact with little strain, is expected to result in the stabilisation of the cationic charge, increasing ligand basicity and, therefore, increasing extractant *strength*. More proton chelation interactions would increase this effect, which may be the reason for the increased extractant *strength* of the diamide ligand, **DAA**, relative to the monoamide, **MAA**, (see section 4.5.1.1).

## 4.7. Conclusions

The successful design features established in Chapter 3 were applied to a group of new tertiary amine chlorometallate solvent extractants, **MAA**, **DAA**, **TAA**, **M*t*AA** and **MalA$^2$**, that are potentially cheap to manufacture and show marked improvements in *strength*, *selectivity* and *efficiency* with respect to the industrial benchmarks, **TOA** and **TEHA**.

The work carried out in this chapter is summarised in the following conclusions:

- The amido-functionalised tertiary amine ligands, **MAA**, **DAA**, **TAA**, **M*t*AA**, **MalA$^2$** and **MAAX**, can be prepared on gram scales using facile, high yielding methods and the synthetic strategies employed demonstrate the viability of large-scale synthesis for commercial application.
- The amido-functionalised tertiary amine ligands extract zinc or cobalt at much higher pH and zinc at much lower chloride concentrations than **TEHA**, so that selectivity over Fe(III) can be achieved.
- The tertiary amide **M*t*AA** was the most efficient ligand for zinc or cobalt extraction into toluene.
- Quantitative stripping of both zinc and cobalt is possible from toluene containing **M*t*AA** or **MAA** using distilled water and the concentration of free chloride in the loaded organic phase relative to chlorometallate was low, indicating high selectivity for chlorometallate extraction over chloride.
- The secondary amide ligands **MAA**, **DAA** and **TAA** were the most efficient for platinum extraction into chloroform, showing improved efficiency relative to the previously investigated tren-based reagents and much higher efficiency than **TOA**.[11]
- The amido-functionalised reagents **DAA** and **MAA** are more efficient than **TOA** when extracting platinum into toluene.

- **TOA** and **TEHA** are significantly more efficient when extracting cobalt, zinc or platinum into toluene than chloroform.
- Analysis of the solid-state structure of [(**MAAX**H)$_2$MCl$_4$] (M = Co(II) or Zn(II)) shows 'proton chelation' between the carbonyl oxygen and bridge-head amine nitrogen, which would increase reagent basicity and, therefore, strength; and interaction with the chlorometallate anion via a number of weak C-H and N-H donors, consistent with observations made in the solid state structures discussed in Chapter 3, section 3.6.

The potential for the amide-functionalised tertiary alkylamines described in this report to effect separation of Zn(II) or cobalt from Fe(III) in chloride feeds may have commercial value and Cytec have revealed that they are prepared to fund some further work in this area and to undertake protection of the IP. Johnson Matthey are funding further work into investigating the reagents for the refining of platinum group metals.

# 4.8. Experimental

General experimental details are given in Chapter 2, section 2.5.

## 4.8.1. Ligand Synthesis

### 4.8.1.1. Methyl 3-(di-2-ethylhexylamino)propanoate 5[14]

In a 250 mL round bottomed flask, di-2-ethylhexylamine (4.80 g, 19.89 mmol) and methyl acrylate (3.44 g, 39.98 mmol) dissolved in MeOH (100 mL) were stirred at ambient temperature for 24 hrs. The reaction mixture was then concentrated on a rotary evaporator and the crude product was purified by column chromatography on silica gel using 10% ethyl acetate in hexane as eluent to give the amino-ester **5** (4.40 g, 67% yield) as a clear oil. $\nu_{max}/cm^{-1}$ (thin film) 2957-2860 (C-H stretch), 1743 (C=O stretch), 1456-1400 (C-H bend), 1194 (N-C stretch), 1033 (O-Me stretch); $\delta_H$ (250 MHz, $CDCl_3$) 0.95-1.18 (m, 12H, C*H*$_3$), 1.35-1.67 (m, 18H, C*H*$_2$,C*H*, 2.34 (d, 4H, CHC*H*$_2$N), 2.63 (t, 2H, C*H*$_2$CO), 2.87 (t, 2H, NC*H*$_2$CH$_2$), 3.88 (s, 3H, OC*H*$_3$); $\delta_C$ (250 MHz, $CDCl_3$) 11.0, 14.4, 23.6, 24.6, 29.2, 31.5, 32.5, 37.7, 50.9, 51.6, 59.8, 173.7; *m/z* (ES) 328.08 ($M+H^+$).

### 4.8.1.2. Dimethyl 3,3'-(hexylimino)dipropanoate 6

In a 250 mL round bottomed flask, 2-ethylhexylamine (2.50 g, 19.36 mmol) and methyl acrylate (5.11 g, 59.39 mmol) dissolved in MeOH (100 mL) were stirred at ambient temperature for 24 hrs. The reaction mixture was then concentrated on a rotary evaporator and the crude product was purified by column chromatography on silica gel using 10% ethyl acetate in hexane as eluent to give the amino-ester **6** (4.25 g, 74% yield) as a clear oil. $\nu_{max}/cm^{-1}$ (thin film) 2956-2857 (C-H stretch), 1742 (C=O stretch), 1425-1436 (C-H bend), 1195 (N-C stretch), 1042 (O-Me stretch); $\delta_H$ (250 MHz, $CDCl_3$) 0.59-0.73 (m, 6H, C*H*$_3$), 0.93-1.24 (m, 9H, C*H*$_2$,C*H*), 2.00 (d, 2H, CHC*H*$_2$N), 2.22 (t, 4H,

C$H_2$CO), 2.54 (t, 4H, NC$H_2$C$H_2$), 3.44 (s, 6H, OC$H_3$); $\delta_C$ (250 MHz, $CDCl_3$) 10.9, 14.3, 23.4, 24.4, 29.0, 31.3, 32.7, 37.4, 50.1, 51.6, 58.8, 173.3; *m/z* (ES) 302.38 ($M+H^+$).

#### 4.8.1.3. Trimethyl 3,3',3''-nitrilotripropanoate 7

In a 250 mL round bottomed flask, 35% aqueous ammonia solution (1.02 g, 20.96 mmol) and methyl acrylate (14.50 g, 168.53 mmol) dissolved in MeOH (100 mL) were stirred at ambient temperature for 24 hrs. The reaction mixture was then concentrated on a rotary evaporator to give the amino-ester give **7** (2.45 g, 42% yield) as a clear liquid. $\nu_{max}/cm^{-1}$ (thin film) 2953-2842 (C-H stretch), 1733 (C=O stretch), 1437 (C-H bend), 1173 (N-C stretch), 1039 (O-Me stretch); $\delta_H$ (250 MHZ, $CDCl_3$) 2.38 (t, 6H, COC$H_2$), 2.72 (t, 6H, NC$H_2$), 3.62 (s, 9H, OC$H_3$); $\delta_C$ (250 MHz, $CDCl_3$) 32.8, 49.4, 51.6, 172.9; *m/z* (ES) 276.31 ($M+H^+$).

#### 4.8.1.4. 3-(di-2-ethylhexylamino)propanoic acid 8

In a 100 mL round bottomed flask, **5** (2.24 g, 6.83 mmol) and NaOH (0.81 g, 20.22 mmol) dissolved in MeOH (50 mL) were refluxed for 5 hrs. The reaction mixture was aloud to cool to ambient temperature and 6 M HCl solution (6.67 ml, 40 mmol) was added. The MeOH was removed on a rotary evaporator and the remaining solution was extracted with ethyl acetate (3 x 150 mL), and the combined organic layers were dried over magnesium sulfate, filtered and concentrated on a rotary evaporator to give **8** (2.03 g, 95%) as a clear oil. $\nu_{max}/cm^{-1}$ (thin film) 3000-2602 (O-H stretch), 2958-2869 (C-H stretch), 1734 (C=O stretch), 1464-1390 (C-H bend), 1201 (N-C stretch); $\delta_H$ ($CDCl_3$) 0.94-1.12 (m, 12H, C$H_3$), 1.33-1.68 (m, 18H, (C$H_2$)$_3$C$H$C$H_2$, 2.29 (d, 4H, CHC$H_2$N), 2.86 (t, 2H, C$H_2$CO), 2.87 (t, 2H, NC$H_2$C$H_2$), 3.18 (s, 3H, OC$H_3$); $\delta_C$ ($CDCl_3$) 12.0, 15.2, 24.4, 25.8, 30.4, 33.5, 34.3, 56.7, 59.2, 171.7; *m/z* (ES) 314.31 ($M+H^+$).

#### 4.8.1.5. 3-(di-2-ethylhexylamino)-*N*-hexylpropanamide MAA

***Method Involving the Azeotropic Removal of Water***

In a 250 mL round bottomed flask, **5** (2.13 g, 6.51 mmol), hexylamine (10.1 g, 13.02 mmol) were refluxed for 24 hrs under $N_2$ in toluene (100 mL) with a dean-stark trap fitted to the top of the condenser. The reaction mixture was then concentrated on a rotary evaporator and the crude product was purified by column chromatography on silica gel using 20% then 60% ethyl acetate in hexane to give the amide **MAA** (0.21 g, 8%) as a pale yellow oil (Found: C, 75.95; H, 14.96; N, 6.85. $C_{25}H_{52}N_2O$: C, 75.69; H, 13.21; N, 7.06); $\nu_{max}/cm^{-1}$ (thin film) 3290 (N-H stretch), 2957-2813 (C-H stretch), 1644 (C=O stretch), 1557 (N-H bend), 1462-1377 (C-H bend); $\delta_H$ 0.49-0.95 (m, 15H, C*H*$_3$), 0.95-1.30 (m, 24H, C*H*$_2$,C*H*), 1.30-1.50 (m, 2H, C*H*$_2$), 2.07 (t, 2H, COC*H*$_2$), 2.25 (d, 4H, NC*H*$_2$), 2.45 (t, 2H, NC*H*$_2$), 3.02-3.20 (m, 2H, NHC*H*$_2$), 7.85 (t, 1H, N*H*); $\delta_C$ (250 MHz, $CDCl_3$), 10.8, 14.3, 14.4, 22.9, 23.6, 24.6, 27.1, 29.1, 29.9, 31.6, 31.8, 33.6, 37.2, 39.8, 50.6, 58.7, 172.5; *m/z* (ES) 397.51 ($M+H^+$).

***Method Involving a Large Amine Concentration Excess***

In a 100 mL round bottomed flask, **5** (4.25 g, 12.99 mmol) and hexylamine (6.56 g, 64.87 mmol) were heated at 90$^o$C for 48 hrs. The reaction mixture was concentrated on a rotary evaporator and the crude product was purified by column chromatography on silica gel using 20% then 60% ethyl acetate in hexane to give the amide **MAA** (3.52 g, 68% yield) as a pale yellow oil (Found: C, 75.95; H, 14.96; N, 6.85. $C_{25}H_{52}N_2O$ requires C, 75.69; H, 13.21; N, 7.06); $\nu_{max}/cm^{-1}$ (thin film) 3290 (N-H stretch), 2957-2813 (C-H stretch), 1644 (C=O stretch), 1557 (N-H bend), 1462-1377 (C-H bend); $\delta_H$ 0.49-0.95 (m, 15H, C*H*$_3$), 0.95-1.30 (m, 24H, C*H*$_2$,C*H*), 1.30-1.50 (m, 2H, C*H*$_2$), 2.07 (t, 2H, COC*H*$_2$), 2.25 (d, 4H, NC*H*$_2$), 2.45 (t, 2H, NC*H*$_2$), 3.02-3.20 (m, 2H, NHC*H*$_2$), 7.85 (t, 1H, N*H*); $\delta_C$ (250 MHz, $CDCl_3$), 10.8, 14.3, 14.4, 22.9, 23.6, 24.6, 27.1, 29.1, 29.9, 31.6, 31.8, 33.6, 37.2, 39.8, 50.6, 58.7, 172.5; *m/z* (ES) 397.51 ($M+H^+$).

#### 4.8.1.6. 3,3'-(2-ethylhexylimino)bis(*N*-hexylpropanamide)·$H_2O$ DAA

In a 100 mL round bottomed flask, **6** (5.00 g, 16.60 mmol) and hexylamine (13.43 g, 132.81 mmol) were heated at 90$^o$C for 48 hrs. The reaction mixture was concentrated on

a rotary evaporator and the crude product was purified by column chromatography on silica gel using 2% then 10% methanol in ethyl acetate to give the amide **DAA** (4.79 g, 66 % yield) as a pale yellow oil (Found: C, 68.62; H, 14.29; N, 8.76. $C_{26}H_{55}N_3O_3$ requires C, 68.22; H, 12.11; N, 9.18); $\nu_{max}/cm^{-1}$ (thin film) 3289 (N-H stretch), 2928-2804 (C-H stretch), 1643 (C=O stretch), 1558 (N-H bend), 1458-1377 (C-H bend); $\delta_H$ (250 MHz, $CDCl_3$) 0.60-0.96 (m, 12H, C*H*$_3$), 0.96-1.30 (m, 21H, C*H*$_2$,C*H*), 1.30-1.48 (m, 4H, C*H*$_2$), 2.37 (t, 4H, COC*H*$_2$), 2.48 (d, 2H, NC*H*$_2$), 2.81 (t, 4H, NC*H*$_2$), 3.08-3.20 (m, 4H, NHC*H*$_2$), 7.89-8.03 (br, 2H, N*H*); $\delta_C$ (250 MHz, $CDCl_3$) 10.9, 14.3, 14.4, 22.8, 23.5, 24.9, 27.1, 29.1, 29.8, 31.5, 31.8, 33.4, 37.4, 39.7, 52.7, 58.9, 173.0; *m/z* (ES) 358.43 ($M+H^+$).

#### 4.8.1.7. 3,3',3''-Nitrilotris(*N*-hexylpropanamide)·½$NH_3$ TAA

In a 100 mL round bottomed flask, **7** (5.50 g, 19.99 mmol) and hexylamine (15.00 g, 148.34 mmol) were heated at 90°C for 48 hrs. The reaction mixture was concentrated on a rotary evaporator and then suspended in hexane. The solid was collected via filtration and washed with hexane to give the amide **TAA** (1.05 g, 11 % yield) as a white powder (Found: C, 66.15; H, 12.84; N, 12.97 $C_{58}H_{111}N_9O_6$ requires C, 66.01; H, 11.39; N, 12.83); $\nu_{max}/cm^{-1}$ (KBr disc) 3306 (N-H stretch), 2925-2749 (C-H stretch), 1635 (C=O stretch), 1547 (N-H bend), 1428-1378 (C-H bend); $\delta_H$ (250 MHz, $CDCl_3$) 0.99-1.10 (m, 9H, C*H*$_3$), 1.35-1.62 (m, 18H, C*H*$_2$), 1.62-1.80 (m, 6H, C*H*$_2$) 2.54 (t, 6H, COC*H*$_2$), 3.10 (t, 6H, NC*H*$_2$), 3.43 (q, 6H, NHC*H*$_2$), 6.88-7.03 (br, 3H, N*H*); $\delta_C$ (250 MHz, $CDCl_3$) 14.3, 22.8, 27.0, 29.8, 31.8, 35.9, 39.6, 45.6, 172.5; *m/z* (ES) 423.41 ($M+H^+$).

#### 4.8.1.8. *N*-Methylhexylacrylamide 9

In a 100 mL round bottomed flask, *N*-methylhexylamine (1.24 g, 10.77 mmol) and $Et_3N$ (1.63 g, 16.15 mmol) were dissolved in 40 mL DCM and cooled in an ice bath to 0 °C. Acryloyl chloride (1.01, 11.11 mmol) dissolved in 30 mL DCM was then cautiously added to the reaction mixture and stirred for 1 hr. Deionised water (40 mL) was then

cautiously added to the reaction mixture and the aqueous phase was washed with DCM (3 x 20 mL). The combined organic layers were dried with $MgSO_4$ and concentrated on a rotary evaporator to give the crude acrylic amide **9** (1.46g, 80.0% yield) as a yellow paste (the product was not further purified). $\delta_H$ (250 MHz, $CDCl_3$) 0.94-1.09 (m, 3H, C*H*$_3$), 1.34-1.51 (m, 6H, C*H*$_2$), 1.58-1.79 (m, 2H, C*H*$_2$), 3.15 (d, 3H, NC*H*$_3$), 3.41-3.60 (m, 2H, NC*H*$_2$), 5.74-5.85 (m, 1H, C*H*$_2$), 6.37-6.50 (m, 1H, C*H*$_2$), 6.65- 6.78 (m, 1H, C*H*); *m/z* (ES) 170.15 ($M+H^+$).

### 4.8.1.9. 3-(di-2-ethylhexylamino)-N-methylhexylpropanamide M*t*AA

In a 250 mL round bottomed flask, di-2-ethylhexylamine (4.80 g, 19.89 mmol) and **9** (3.08 g, 18.23 mmol) dissolved in MeOH (100 mL) were refluxed for 24 hrs. The reaction mixture was then concentrated on a rotary evaporator and the crude product was purified by column chromatography on silica gel using 4% ethyl acetate in hexane as eluent to give the amide **M*t*AA** (4.41 g, 59% yield) as a clear liquid (Found: C, 76.30; H, 12.94; N, 6.97 $C_{26}H_{54}N_2O$ requires C, 76.03; H, 13.25; N, 6.82); $\nu_{max}/cm^{-1}$ (thin film) 2956-2862 (C-H stretch), 1746 (C=O stretch), 1454-1401 (C-H bend), 1196 (N-C stretch), 1036 (O-Me stretch); $\delta_H$ (250 MHz, $CDCl_3$) 0.66-0.99 (m, 15H, C*H*$_3$), 1.05-1.67 (m, 18H, C*H*$_2$,C*H*), 2.09 (d, 4H, CHC*H*$_2$N), 2.30-2.45 (m, 2H, C*H*$_2$CO), 2.60-2.71 (m, 2H, NC*H*$_2$CH$_2$), 2.88 (d, 3H, NC*H*$_3$), 3.15-3.32 (m, NC*H*$_2$); $\delta_C$ (250 MHz, $CDCl_3$), 10.1, 13.3, 13.4, 23.9, 24.6, 25.3, 28.4, 30.7, 31.1, 31.9, 32.3, 33.7, 37.0, 39.8, 41.8, 53.6, 58.9, 173.1; *m/z* (ES) 411.53 ($M+H^+$).

#### 4.8.1.10. Di-*tert*-butyl-methylenemalonate 10

In a 250 mL round-bottomed flask, fitted with reflux condencer and calcium chloride drying tube, di-*tert*-butyl malonate (10.01 g, 46.31 mmol), paraformaldehyde (1.85 g, 92.00 mmol), potassium acetate (0.45 g, 4.61 mmol), cupric acetate monohydrate (0.46 g, 2.32 mmol) and glacial acetic acid (30 mL) were heated at 100°C for 2 hr. The reaction mixture was allowed to cool to room temperature and the reflux condenser was replaced with a short-path distillation apparatus with the vacuum outlet connected in sequence to a trap cooled in acetone–dry ice, a potassium hydroxide trap and another trap cooled in acetone–dry ice. The receiving flask was cooled in acetone–dry ice and the system was evacuated for 1 hr to remove acetic acid and other volatile material. The bath temperature was increased to 40–50°C for 15 min and then was rapidly raised to 140–150°C to drive over the malonic ester **10** (5.12 g, 48%), which was collected as a clear oil over a boiling-point range of 60–82°C. $\delta_H$ ($CDCl_3$) 1.64 (d, 18H, CC*H*$_3$), 6.41 (s, 2H, C*H*$_2$); *m/z* (ES) 229.16 ($M+H^+$).

#### 4.8.1.11. Di-*tert*-butyl 2 ((bis(2-ethylhexyl)amino)methyl)malonate 11

In a 100 mL round bottomed flask, **10** (1.37 g, 6.01 mmol) was stirred with bis(2-ethylhexyl)amine (2.89 g, 12.00 mmol) in diethyl ether (40 mL) for 24 h at ambient temperature. The reaction mixture was concentrated on a rotary evaporator and the crude product was purified by column chromatography on silica gel using DCM to give the amide amino malonate **11** (1.89 g, 67%) as a pale yellow oil. $\delta_H$ ($CDCl_3$) 0.70-0.86 (m, 12H, C*H*$_3$), 1.09-1.30 (m, 18H, C*H*$_2$,C*H*), 1.44 (s, 18H, CC*H*$_3$), 2.10 (d, 4H, NC*H*$_2$CH), 3.62-3.89 (m, 2H, NC*H*$_2$), 3.30 (t, 1H, C*H*); *m/z* (ES) 470.53 ($M+H^+$).

#### 4.8.1.12. 3-(di-2-ethylhexylamino)-*N*-ethanol 12

In a 250 mL round bottomed flask, potassium carbonate (20.70 g, 149.77 mmol) was added to a solution of bis(2-ethyl)hexylamine (24.15 g, 10.00 mmol) in 2-chloroethanol (40 mL) and the mixture was heated to $110^0$C for 72 hrs. The reaction mixture was

cooled to RT and DCM (150 mL) was added and the solids were filtered off. The filtrate was washed with water (3 x 100 mL) before being evaporated and dried under high vacuum. The residue was purified by column chromatography on silica gel with 0.1% $NH_4OH$ / 1% MeOH / DCM to 3% MeOH / DCM to give alcohol-functionalised alkylamine **12** (20.0g, 70%) as a colourless oil. $\delta_H$ 0.99-1.30 (m, 12H, C*H*$_3$), 1.25-1.90 (m, 18H, C*H*$_2$,C*H*), 2.41 (d, 4H, NC*H*$_2$), 2.72 (t, 2H, NC*H*$_2$), 3.75 (t, 4H, OC*H*$_2$); 12.8, 14.5, 23.4, 24.5, 28.6, 32.0, 37.1, 56.9, 58.2, 60.1; *m/z* (ES) 286.3 ($M+H^+$).

#### 4.8.1.13. 3-(di-2-ethylhexylamino)-*N*-chloroethane 13

In a 250 mL round bottomed flask thionyl chloride (9.42 g, 79.22 mmol) was cautiously added to a solution of **12** (18.80 g, 65.85 mmol) and a catalytic amount of DMF in chloroform (50 mL). The solution was refluxed for 2 hrs and then cooled. The reaction mixture was then concentrated on a rotary evaporator and place under high vacuum. The residue was dissolved in DCM (100 mL) and saturated aqueous sodium carbonate solution (100 mL) was cautiously added. The organic layer was dried over $MgSO_4$ and concentrated on a rotary evaporator to give the alkyl chloride **13** as a brown-orange oil (20.00 g, 100%). The product was not further purified. $\delta_H$ 0.77-1.13 (m, 12H, C*H*$_3$), 1.05-1.57 (m, 18H, C*H*$_2$,C*H*), 2.24 (d, 4H, NC*H*$_2$), 2.75 (t, 2H, NC*H*$_2$), 3.50 (t, 4H, OC*H*$_2$); *m/z* (ES) 205.3 ($M+H^+$).

#### 4.8.1.14. Methyl ((bis(2-ethylhexyl)amino)ethyl)malonate 14

A suspension of 60% sodium hydride in paraffin oil (0.96 g, 24.02 mmol) in THF (100 mL) was slowly added to a solution of dimethyl malonate (3.96 g, 30.20 mmol) in THF (30 mL) causing a vigorous reaction. Once addition was complete, a solution of **13** (6.08 g, 20.87 mmol) in THF (30 mL) was added and the reaction was refluxed for 72 hrs. The solvent was evaporated and the residue was partitioned between DCM (300 mL) and water (100 mL). The organic was washed with water (2 x 100 ml) before being dried over $MgSO_4$ and concentrated on a rotary evaporator. The residue was purified by column chromatography on silica gel with 20 % hexane in DCM then DCM then 1% MeOH in DCM to give the amino-malonate **14** (5.90 g, 74% yield). $\delta_H$ 0.87-1.15 (m, 12H, C*H*$_3$),

1.23-1.62 (m, 18H, C$H_2$,C*H*), 2.09-2.32 (m, 4H, C$H_2$C$H_2$), 2.50 (t, 2H, NC*H*), 3.89 (s, 3H, OC$H_3$); *m/z* (ES) 205.3 ($M+H^+$).

#### 4.8.1.15. 3-(di-2-ethylhexylamino)ethyl)-*N*-hexylmalonamide MalA$^2$

In a 100 mL round bottomed flask, **14** (2.12 g, 5.31 mmol) and hexylamine (2.69 g, 26.54 mmol) were heated at 90$^o$C for 48 hrs. The reaction mixture was concentrated on a rotary evaporator and the crude product was purified by column chromatography on silica gel using 20% then 60% ethyl acetate in hexane to give the amide **MalA$^2$** (1.54 g, 54% yield) as an orange paste (Found: C, 73.45; H, 12.96; N, 7.85. $C_{33}H_{67}N_3O_2$ requires C, 73.68; H, 12.55; N, 7.81); $\nu_{max}/cm^{-1}$ (thin film) 3297 (N-H stretch), 2951-2819 (C-H stretch), 1634 (C=O stretch), 1559 (N-H bend), 1442-1337 (C-H bend); $\delta_H$ 0.66-0.95 (m, 18H, C$H_3$), 0.99-1.50 (m, 34H, C$H_2$,C*H*), 1.83 (q, 2H, C$H_2$), 2.05 (d, 4H, C$H_2$), 2.19-2.30 (m, 2H, NC$H_2$), 2.91 (t, 1H, C*H*), 3.05-3.26 (m, 4H, NHC$H_2$), 6.46 (t, 2H, N*H*); $\delta_C$ (250 MHz, $CDCl_3$), 11.8, 14.2, 22.4, 23.4, 24.6, 26.7, 28.9, 29.2, 30.1, 30.9, 32.5, 32.6, 37.3, 39.9, 43.5, 44.1, 60.0, 171.2; *m/z* (ES) 538.65 ($M+H^+$).

#### 4.8.1.16. 3-(diisobutylamino)-*N*-butylpropanamide MAAX

In a 100 mL round bottomed flask, methyl acrylate (6.02 g, 70.01 mmol) and diisobutylamine (6.56 g, 64.87 mmol) were stirred at ambient temperature in methanol (50 mL) for 24 hrs. The reaction mixture was concentrated on a rotary evaporator and the residue was re-dissolved butylamine (25.55 g, 350 mmol) and heated at 90$^o$C for 48 hrs. The excess butylamine was removed *in vacuo* leaving the crude amide product **MAAX** (2.59 g, 78%) as a clear oil which was not further purified; $\nu_{max}/cm^{-1}$ (thin film) 3294 (N-H stretch), 2954-2813 (C-H stretch), 1645 (C=O stretch), 1559 (N-H bend), 1460-1373 (C-H bend); $\delta_H$ 0.44-0.91 (m, 15H, C$H_3$), 1.21-1.59 (m, 4H, C$H_2$), 1.71-1.89 (m, 2H, C*H*), 2.15-2.21 (m, 4H, C$H_2$), 2.35-2.46 (t, 2H, C$H_2$), 2.52-2.69 (t, 2H, C$H_2$), 3.20-3.31 (q, 2H, C$H_2$), 8.12 (t, 1H, N*H*); $\delta_C$ (250 MHz, $CDCl_3$), 14.8, 16.1, 16.6, 25.5, 30.6, 34.7, 35.9, 45.4, 52.9, 59.6, 179.7; *m/z* (ES) 256.35 ($M+H^+$).

## 4.8.2. Solvent Extraction Experiments

Experiments determining the dependence of metal loading (M = Zn(II), Co(II) or Fe(III)) on pH, chloride concentration and ligand concentration, and the procedures used to evaluate metal recovery from the organic phase and the evaluation of metal and total chloride loading, were conducted according to the procedures described in Chapter 2, section 2.5. The dependence of Pt(IV) loading on ligand concentration was determined using the procedure described by Bell *et. al*.[11]

### 4.8.2.1. Analysis for $PtCl_6^{2-}$ and Chloride Loading

Solutions of **MAA** were prepared at varying concentrations between 2.13 – 5.33 mM by weighing aliquots of 10.0 mM ligand stock solution in toluene into 5 mL volumetric flasks and diluting to the mark with toluene. Hexachloroplatinate solution (250 mL, 1.28 mM) was prepared by weighing $H_2PtCl_6{\cdot}6H_2O$ (0.066 g) into a 250 mL volumetric flask and diluting to the mark with 0.6 M HCl. Extractions were prepared by charging 100 mL Schott bottles containing a magnetic stirrer bar with 5 mL of the ligand solution and 5 mL of metal chloride solution. The extractions were stirred at 25ºC for 4 h, after which the phases were separated and 2 mL aliquots of the aqueous phases were weighed into 5 mL volumetric flasks and made up to the mark with 0.6 M HCl for Pt(IV) analysis using ICP-OES. An aliquots (4 mL) of each organic phase was stirred with analiquot (4 mL) of 0.05 M NaOH solution for 30 mins. The phases were separated and a 2.5 mL aliquot of each aqueous phase was transferred into vials containing $CsNO_3$ (0.01 g, 0.51 mmol) and stirred for 5 mins. To each aqueous phase, a 2.5 mL aliquot of $AgNO_3$ solution (6 mM) in $HNO_3$ (1 M) was added and stirred in a darkend box for 5 mins. The precipitate was filtered off using a filter syringe and a 0.5 mL aliquot of the filtrate was transferred into a 5 mL volumetric flask and made up to the mark with 1 M $HNO_3$ for Ag(I) analysis by ICP-OES.

### 4.8.3. Complex Synthesis and Crystallography

The crystal structures of **MAAX**-chlorometallate complexes were solved by Fraser White at the University of Edinburgh Crystallography Service.

**$(MAAXH)_2MCl_4$** (M = Co or Zn)

A 8 M aqueous HCl solution (10 mL) containing $MCl_2$ ($CoCl_2$: 0.20 g, 1.54 mmol; $ZnCl_2$: 0.20 g, 1.47mmol ) was stirred with a toluene solution (10 mL) of **MAAX** (0.39 g, 1.54 mmol) in a 100 mL Schotte bottle. After 3 h the phases were separated and the toluene phase was evaporated under vacuum leaving an oily residue, which was dissolved in a 50:50 diethyl ether-hexane mix (10 mL). Slow evaporation at 4°C over the course of 4 days gave crystals which were suitable for X-ray structure determination.

**$(MAAXH)_2CoCl_4$** was isolated as blue crystals (Found C, 50.25; H, 9.49; N, 7.84. $C_{30}H_{66}Cl_4CoN_4O_2$ requires: C, 50.35; H, 9.30; N, 7.83)

**$(MAAXH)_2ZnCl_4$** was isolated as colourless crystals (Found C, 49.85; H, 9.40; N, 7.77. $C_{30}H_{66}Cl_4ZnN_4O_2$ requires: C, 49.90; H, 9.21; N, 7.76)

**Crystal structure of [$(MAAXH)_2CoCl_4$]**

Data were collected on a blue lath (0.81 x 0.22 x 0.09 mm) using the same experimental setup, procedure and software as described in Chapter 3, section 3.8.3.2. The crystal was monoclinic $P2_1/c$ with $a$ = 13.3509(8), $b$ = 19.4903(11), $c$ = 16.4367(10)Å. In total 41498 reflections were collected and merged to give 5546 unique reflections and a merging R-factor of 0.0901. A final conventional R-Factor of 0.0983 was determined based on 5546 reflections.

**Crystal structure of $[(L^2H)_2ZnCl_4]$**

Data were collected on a colourless plate (0.64 x 0.13 x 0.09 mm) using the same experimental setup, procedure and software as described in Chapter 3, section 3.8.3.2. The crystal was monoclinic, $P2_1/c$ with $a$ = 13.3539(6), $b$ = 19.4875(9), $c$ = 16.4537(8)Å. In total 47550 reflections were collected and merged to give 8199 unique reflections and a merging R-factor of 0.0652. A final conventional R-Factor of 0.0526 was determined based on 8199 reflections.

## 4.9. References

1. Marcus, Y.; Kertes, A. S., *Ion Exchange and Solvent Extraction of Metal Complexes*. **1969**, 1037.

2. du Preez, J. G. H., Recent advances in amines as separating agents for metal ions. *Solvent Extr. Ion Exch.,* **2000,** 18, (4), 679-701.

3. Wassink, B.; Dreisinger, D.; Howard, J., Solvent extraction separation of zinc and cadmium from nickel and cobalt using Aliquat 336, a strong base anion exchanger, in the chloride and thiocyanate forms. *Hydrometallurgy,* **2000,** 57, (3), 235-252.

4. Bal, Y.; Bal, K. E.; Cote, G., Kinetics of the alkaline stripping of vanadium(V) previously extracted by Aliquat 336. *Minerals Engineering* **2002,** 15, (5), 377-379.

5. Mackenzie, J. M. W., Uranium Solvent Extraction using Tertiary Amines. *Uranium Ore Yellow Cake Seminar*, Melbourne, Australia, **1997**.

6. Bernardis, F. L.; Grant, R. A.; Sherrington, D. C., A review of methods of separation of the platinum-group metals through their chloro-complexes. *Reactive & Functional Polymers,* **2005,** 65, (3), 205-217.

7. Stensholt, E. O.; Dotterud, O. M.; Henriksen, E. E.; Ramsdal, P. O.; Stalesen, F.; Thune, E., Development and practice of the Falconbridge chlorine leach process. *CIM Bull.,* **2001,** 94, (1051), 101-104.

8. Nogueira, E. D.; Regife, J. M.; Viegas, M. P., Design features and operating experience of the Quimigal ZINCEX plant. *Chloride Electrometall., Proc. Symp.,* **1982**, 59-76.

9. Sato, T.; Adachi, K.; Kato, T.; Nakamura, T., The extraction of divalent manganese, cobalt, copper, zinc, and cadmium from hydrochloric acid solutions by tri-n-octylamine. *Sep. Sci. Technol.,* **1982,** 17, (13), 1565-76.

10. Sato, T.; Shimomura, T.; Murakami, S.; Maeda, T.; Nakamura, T., Liquid-liquid extraction of divalent manganese, cobalt, copper, zinc and cadmium from aqueous chloride solutions by tricaprylmethylammonium chloride. *Hydrometallurgy,* **1984,** 12, (2), 245-54.

11. Bell Katherine, J.; Westra Arjan, N.; Warr Rebecca, J.; Chartres, J.; Ellis, R.; Tong Christine, C.; Blake Alexander, J.; Tasker Peter, A.; Schroder, M., Outer-sphere coordination chemistry: selective extraction and transport of the [PtCl6]2- anion. *Angew Chem Int Ed Engl,* **2008,** 47, (9), 1745-8.

12. Ellis, R. J.; Chartres, J.; Sole, K. C.; Simmance, T. G.; Tong, C. C.; White, F. J.; Schröder, M.; Tasker, P. A., Outer-sphere amidopyridyl extractants for zinc(II) and cobalt(II) chlorometallates. *Chem. Commun.,* **2008**.

13. Wichmann, K.; Antonioli, B.; Soehnel, T.; Wenzel, M.; Gloe, K.; Gloe, K.; Price, J. R.; Lindoy, L. F.; Blake, A. J.; Schroeder, M., Polyamine-based anion receptors: Extraction and structural studies. *Coord. Chem. Rev.,* **2006,** 250, (23+24), 2987-3003.

14. Surendra, K.; Krishnaveni, N. S.; Sridhar, R.; Rao, K. R., beta -Cyclodextrin promoted aza-Michael addition of amines to conjugated alkenes in water. *Tetrahedron Lett.,* **2006,** 47, (13), 2125-2127.

15. Montalbetti, C. A. G. N.; Falque, V., Amide bond formation and peptide coupling. *Tetrahedron,* **2005,** 61, (46), 10827-10852.

16. Rayle, H. L.; Fellmeth, L., Development of a Process for Triazine-Promoted Amidation of Carboxylic Acids. *Org. Process Res. Dev.,* **1999,** 3, (3), 172-176.

17. Clayden, J.; Greeves, N.; Worthers, P.; Warren, S., *Organic Chemistry*. Oxford University Press, Oxford, **2001**.

18. Ballesteros, P.; Roberts, B. W., Di-tert-butyl methylenemalonate. *Org. Synth.,* **1986,** 64.

19. Mansur, M. B.; Rocha, S. D. F.; Magalhaes, F. S.; Benedetto, J. d. S., Selective extraction of zinc(II) over iron(II) from spent hydrochloric acid pickling effluents by liquid-liquid extraction. *J. Hazard. Mater.,* **2008,** 150, (3), 669-678.

20. Maryott, A. A.; Smith, E. R., Table of dielectric constants of pure liquids. *U. S. Dept. Commerce, Natl. Bur. Standards Circ.,* **1951,** No. 514, 44 pp.

21. Good, M. L.; Bryan, S. E., Extraction of Group VIII metals by long-chain alkyl amines. II. Cobalt(II)-hydrochloric acid systems. *J. Inorg. Nucl. Chem.,* **1961,** 20, 140-6.

22. Steiner, T.; Starikov, E. B.; Amado, A. M.; Teixeira-Dias, J. J. C., Weak hydrogen bonding. Part 2. The hydrogen bonding nature of short C-H...pi contacts:

crystallographic, spectroscopic and quantum mechanical studies of some terminal alkynes. *J. Chem. Soc., Perkin Trans. 2,* **1995**, (7), 1321-6.

23. Steiner, T.; Starikov, E. B.; Tamm, M., Weak hydrogen bonding. Part 3. A benzyl group accepting equally strong hydrogen bonds from O-H and C-H donors: 5-ethynyl-5H-dibenzo[a,d]cyclohepten-5-ol. *J. Chem. Soc., Perkin Trans. 2,* **1996**, (1), 67-71.

24. Antonioli, B.; Gloe, K.; Gloe, K.; Goretzki, G.; Grotjahn, M.; Hesske, H.; Langer, M.; Lindoy, L.; Mills, A. M.; Soehnel, T., Anion controlled supramolecular self-assembly of tetraprotonated tris[2-(benzylamino)ethyl]amine. *Z. Anorg. Allg. Chem.,* **2004,** 630, (7), 998-1006.

25. Ilioudis, C. A.; Hancock, K. S. B.; Georganopoulou, D. G.; Steed, J. W., Insights into supramolecular design from analysis of halide coordination geometry in a protonated polyamine matrix. *New J. Chem.,* **2000,** 24, (10), 787-798.

# CHAPTER 5

# MALONAMIDES

## 5.1. Aims

The aim of the work described in this chapter was to examine the Fe(III), Co(II) and Zn(II) chlorometallate anion extraction properties of a series of new alkyl-functionalised malonamide reagents.

## 5.2. Relevant Structural and Electronic Properties of Malonamides

Malonamides are a commercially viable type of reagent for use in solvent extraction processes as they are cheap to manufacture[1] and, due to their structural and electronic properties, are versatile, potentially acting as metal cation, anion or salt extractants.

One important property of malonamides is resonance (Figure 5.1). This causes partial N-C(O) double bond character, hindering rotation around this bond.[2, 3] The delocalisation of the nitrogen lone pair onto the carbonyl oxygens increases the polarity of the carbonyl group so that the oxygens are more nucleophilic. This has important implications in the solvent extraction of metal using malonamides.

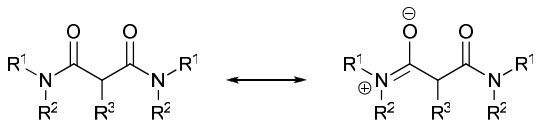

**Figure 5.1: Malonamide resonance structures (R = alkyl or H)**

Another important feature of malonamides is that they are subject to a tautomerisation (Figure 5.2), involving the migration of the central C-H proton onto a carbonyl oxygen.[4] This is a result of the acidic nature of the central C-H hydrogen, suggesting that it is well polarised and, therefore, a possible C-H donor of the type shown to be significant in the extraction of chlorometallate anions (see Chapter 3, Section 3.6).

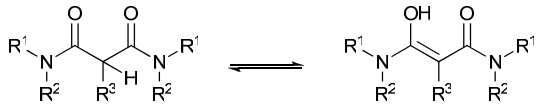

**Figure 5.2: Malonamide tautomers.**

## 5.3. Malonamides as Cation Exchange Extractants

Hiratani and co-workers have shown that a quinoyl-substituted malonamide ligand can be used to selectively extract Cu(II) over other base metal cations from solutions of above pH 3 (Figure 5.3).[5] The slight N-C(O) double bond character (see above), along with the steric hindrance of the n-butyl substituents, minimises bond rotation to provide a pre-organised square-planar cavity.

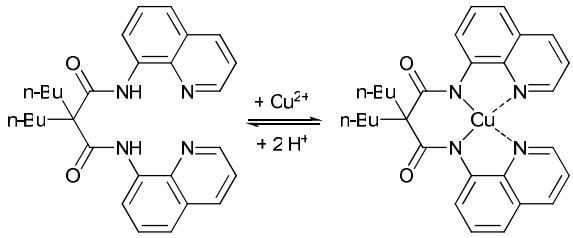

**Figure 5.3: Extraction of $Cu^{2+}$ by a quinoyl-substituted malonamide.[5]**

## 5.4. Malonamides as Metal Salt Extractants

In the late 1980s, various malonamides were investigated by Musikas and co-workers for the *concentration* and *separation* of trivalent lanthanides and actinides for the reprocessing of spent nuclear fuels in the DIAMEX process.[6-9] This work involved the design of malonamides to extract lanthanides and actinides from nitric acid solutions according to Equation 5.1. Extraction proceeds via interaction with the inner-sphere of the $M(NO_3)_3$ complex via the malonamide oxygens as shown in Figure 5.4.

**Equation 5.1**

$$M(NO_3)_3 + nL_{(org)} \rightleftharpoons M(NO_3)_3L_{n(org)}$$

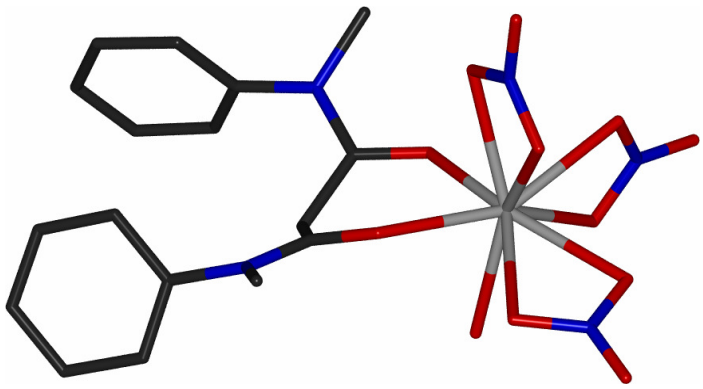

**Figure 5.4: Crystal structure of $[Yb(NO_3)_3L]$ (L = *N,N'*-dimethyl-*N,N'*-diphenylmalonamide).[10] (The hydrogens are omitted for clarity)**

## 5.5. Malonamides as Metal Anion Extractants

Malonamides for use in the DIAMEX process are designed to extract neutral $M(NO_3)_3$ lanthanide and actinide complexes, however, the extraction of anionic nitrato species according to Equation 5.2 has also been reported.[10] Extraction via this mechanism is thought to involve the protonation of the malonamide carbonyl oxygens and this is supported by IR spectroscopic studies[11] and *ab initio* calculations.[12]

**Equation 5.2**

$$M(NO_3)_4^- + LH^+_{(org)} \rightleftharpoons [(LH)M(NO_3)_4]_{(org)}$$

The use of malonamides to extract the $FeCl_4^-$ anion (Equation 5.3) from acid chloride solutions was first suggested by Costa *et. al.* as an alternative to Fe(III) removal by precipitation with pH adjustment as it does not consume base or result in the accumulation of complex iron residues that may cause environmental problems.[13-15] Costa and other authors have shown that alkyl-substituted malonamides extract Fe(III) from acid chloride feeds with high *efficiency* and *selectivity* over base metals such as Co(II), Cu(II), Zn(II), Ni(II) and Pb(II), with the $FeCl_4^-$ anion reported as being the dominant extracted species in most cases.[13-18] Although the downstream processing of the extracted Fe(III) is not discussed by the authors, it is possible that a ferric chloride solution of high purity could be produced by stripping into a solution of high pH and/or low chloride activity (Equation 5.4) which could be recycled as a

lixiviant or used as a feed-stock for the production of HCl by pyrohydrolysis (see Chapter 1, Sections 1.3.2 and 1.6.2).

**Equation 5.3**

$$FeCl_4^- + H^+ + L_{(org)} \rightleftharpoons [(LH)FeCl_4]_{(org)}$$

**Equation 5.4**

$$[(LH)FeCl_4]_{(org)} \rightleftharpoons FeCl_3 + HCl + L_{(org)}$$

## 5.6. The Design of New Alkyl-Functionalised Malonamides for $FeCl_4^-$ Extraction in the Anglo American Circuits

A new approach to the *concentration* and *separation* of metal values in the Anglo American circuits could involve the selective extraction of the major impurity, Fe(III), from the pregnant leach solutions using alkyl malonamide reagents. If $FeCl_4^-$ can be extracted with a high degree of *selectivity* and *efficiency* from the acid chloride feeds, then the remaining base metal values might be easier to refine. Figure 5.5 shows an idealised system where Fe(III) is extracted by a malonamide reagent to produce a stripped solution that is recycled into the lixiviant while leaving the 'target' base metal values in the raffinate. To apply this system to the Anglo American circuits, a new series of malonamide ligands was developed and investigated for the selective extraction of $FeCl_4^-$ over the other chlorometallates, $CoCl_4^{2-}$ and $ZnCl_4^{2-}$, from acid chloride solutions.

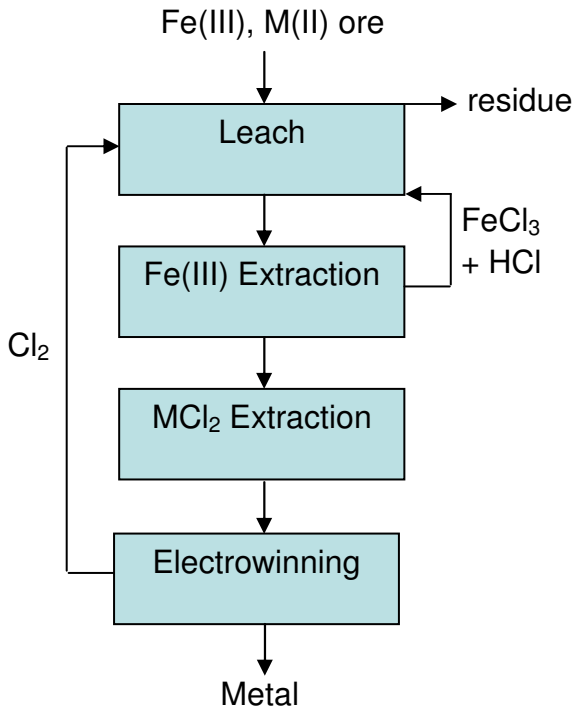


**Figure 5.5: An idealised system showing a chloride hydrometallurgical process involving Fe(III) extraction from the PLS prior to the extraction of the target metal ion M(II).**

When designing new malonamide ligands for $FeCl_4^-$ extraction from the Anglo American circuits, it is useful to consult the literature on reagent design for the DIAMEX process.[6, 10, 19] The general structure of malonamide reagents that are used to extract lanthanides and actinides in the DIAMEX process is shown in Figure 5.6, where the electronic and structural properties can be adjusted for optimal metal extraction by changing the nature of the substituents, $R^{1,2,3}$.

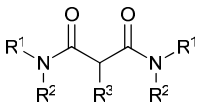


**Figure 5.6: The general structure of the malonamide reagents used in the DIAMEX process.[10, 19]**

$M(NO_3)_3$ extraction is optimal if $R^1$ is small (e.g. methyl) to limit steric hindrance for metal-ion coordination, while $R^2$ is large in order to maximise solubility in non-polar water immiscible organic solvent.[10] The substituent $R^3$ is usually a long alkyl chain to aid solubility in the organic phase and it was found that the best reagents have chains containing fourteen or more carbons substituted in this position.[6, 10] When

extracting $M(NO_3)_3$ from $HNO_3$ solution, proton competes with the metal salt for the nucleophilic site on the carbonyl groups so that $M(NO_3)_3$ extraction is optimised by low ligand basicity which can be accomplished by making the R groups electron withdrawing.[19] For $FeCl_4^-$ extraction, however, it might be more beneficial to have ligands with high basicity to promote protonation over inner-sphere complex formation to favour ion-pair formation.

The series of new malonamide extractants **M[1]-M[3]** (Figure 5.7) considered in this thesis have alkyl chain functionality designed to aid solubility in non-polar organic solvents and to increase basicity, while not hindering interaction with the chlorometallate anion. The substituents are varied across the ligand series in order to investigate how different C-H and N-H donor functionality affects solvent extraction performance. **M[1]** has tertiary amide groups, similar in structure to the malonamides used in the DIAMEX process. **M[2]** is similar to **M[1]** but with secondary amide groups in order to define the effect of the strong N-H hydrogen bond donors. **M[3]** is a piperidyl malonamide and was developed so that the effects of restricted flexibility around the nitrogens could be studied. In all cases, the central methylene carbon of the malonamide carries an n-pentadecyl to impart high solubility to the extractants, and thus complexes in non-polar, water immiscible solvents.

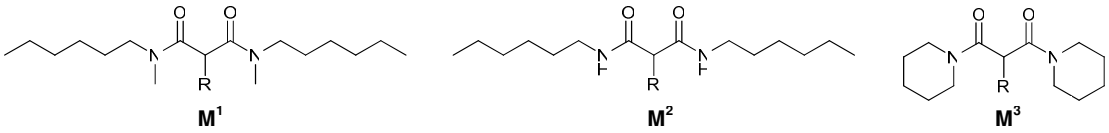


**Figure 5.7: The new series of alkyl-functionalised malonamide ligands for selective $FeCl_4^-$ extraction (R = n-pentadecyl).**

## 5.7. Exploration of Synthetic Methods

If solvent extraction is to be an economically viable method for the removal of Fe(III) from the Anglo American circuits, the extractant must be very cheap to manufacture in order to compete with the standard precipitation methods that are already used in industry.[20, 21]

In the synthesis of all three malonamides (see Scheme 5.1), methyl malonate was used as the starting material which is cheap, stable and readily available. For $\mathbf{M^1}$ and $\mathbf{M^3}$, direct aminolysis using a large excess of amine was applied to convert methyl malonate to the malonamide intermediates (**16** and **17**) followed by alkylation at the methylene position by first deprotonating with NaH and then adding n-pentadecyl bromide. When this approach was applied to the synthesis of $\mathbf{M^2}$, the hexyl malonamide intermediate, formed from aminolysis of methyl malonate with hexylamine, precipitated and it did not re-dissolved in THF. This insolubility is probably caused by the strong intermolecular hydrogen bonding N-H···O interactions between malonamide molecules. To circumvent this, methyl malonate was *first* alkylated to produce the intermediate ester, **18**, and *then* reacted with excess hexylamine to form the malonamide product $\mathbf{M^2}$ as shown at the bottom of Scheme 5.1.

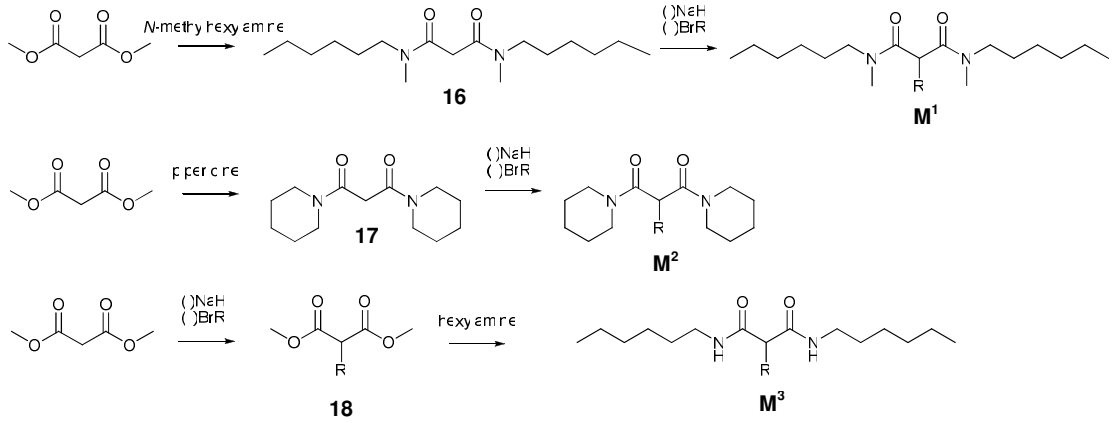


**Scheme 5.1: Synthetic routes to the new malonamide extractants $\mathbf{M^1}$, $\mathbf{M^2}$ and $\mathbf{M^3}$, which were prepared in 75, 79 and 76% yields respectively (R = n-pentadecyl).**

## 5.8. Solvent Extraction

The main aim of the studies reported in this section was to define how the variations in molecular structure of malonamides **M[1]**, **M[2]** and **M[3]** affects the *strength* and *selectivity* of chlorometallate extraction, focusing on the recovery of Fe(III), Co(II) and Zn(II) from acidic chloride solutions. All of the ligands showed sufficient solubility in toluene for a solvent extraction study, although it should be noted that the ligand **M[2]** was only sparingly soluble. All solvent extraction data discussed in this section are presented in Appendices 5.1, 5.2 and 5.3.

### 5.8.1. Dependence of Loading on Proton Concentration

The loadings of Fe(III), Co(II) and Zn(II) on the alkyl malonamide ligands were compared at variable proton concentration in order to evaluate extractant *strength* and *selectivity*. In order to facilitate Fe(III) separation in the Anglo American circuits, it is important that the malonamide ligands show very high selectivity for $FeCl_4^-$ over $ZnCl_4^{2-}$ and $CoCl_4^{2-}$. The chloride concentration in the aqueous phase was held constant at 8 M, which is the highest possible chloride concentration in the new circuits as defined by Anglo American and has been shown in previous studies (see Chapters 3 and 4) to favour the loadings of Zn(II) and Co(II) chlorometallates. Ligands that load Fe(III) but not Co(II) or Zn(II) in such favourable conditions can be said to be highly selective for Fe(III), so that the efficient separation of Fe(III) from the base metals might be realised. Proton concentration is used in this study instead of pH as the proton activity in 8 M chloride is so high that the pH can be very negative and out of calibration range of a pH electrode.

As expected, when 0.01 M solutions of **M[1]**-**M[3]** in toluene were contacted with aqueous solutions of 0.01 M $FeCl_3$, $CoCl_2$ or $ZnCl_2$ containing variable amounts of HCl and an excess of chloride (8 M), metal uptake into the toluene solution showed a marked dependence on the concentration of proton in the aqueous phase (Figure 5.8).

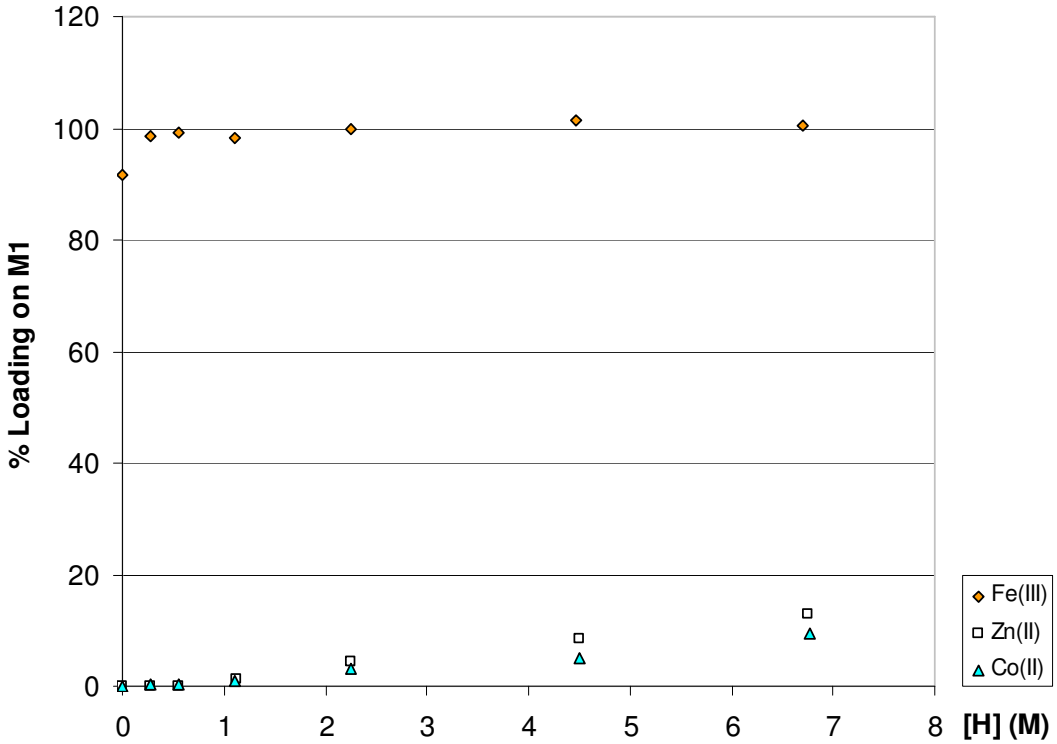
120
100
80
60
40
20
0
% Loading on M1
0
1
2
3
4
5
6
7
8
[H] (M)
Fe(III)
Zn(II)
Co(II)

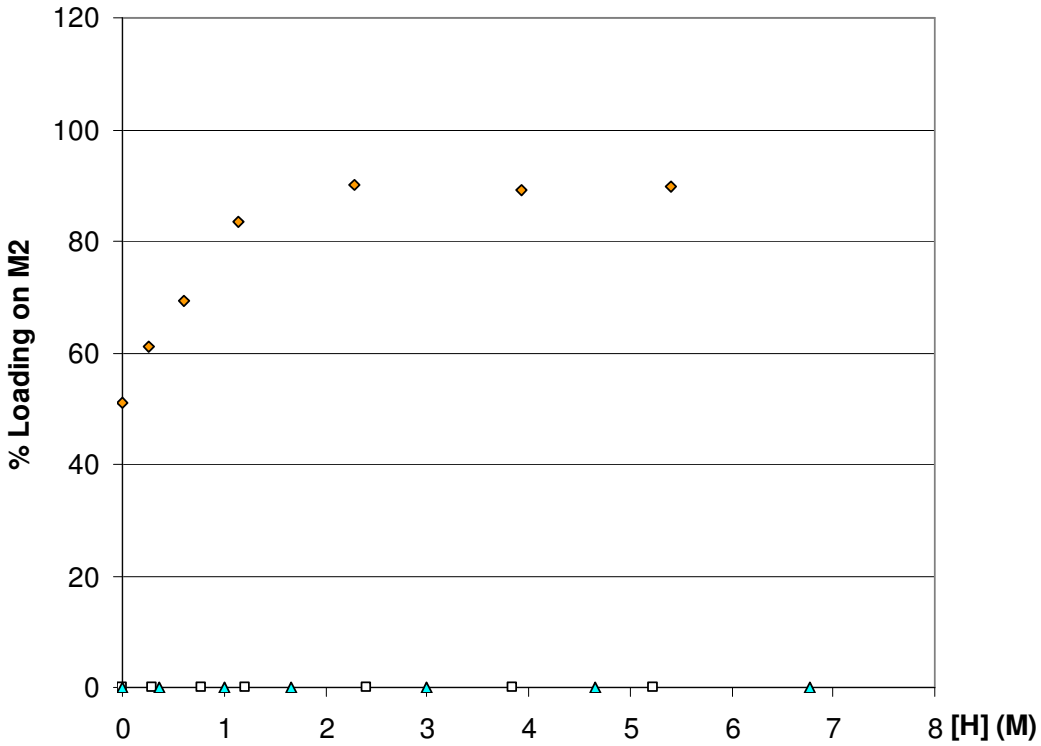
120
100
80
60
40
20
0
% Loading on M2
0
1
2
3
4
5
6
7
8
[H] (M)

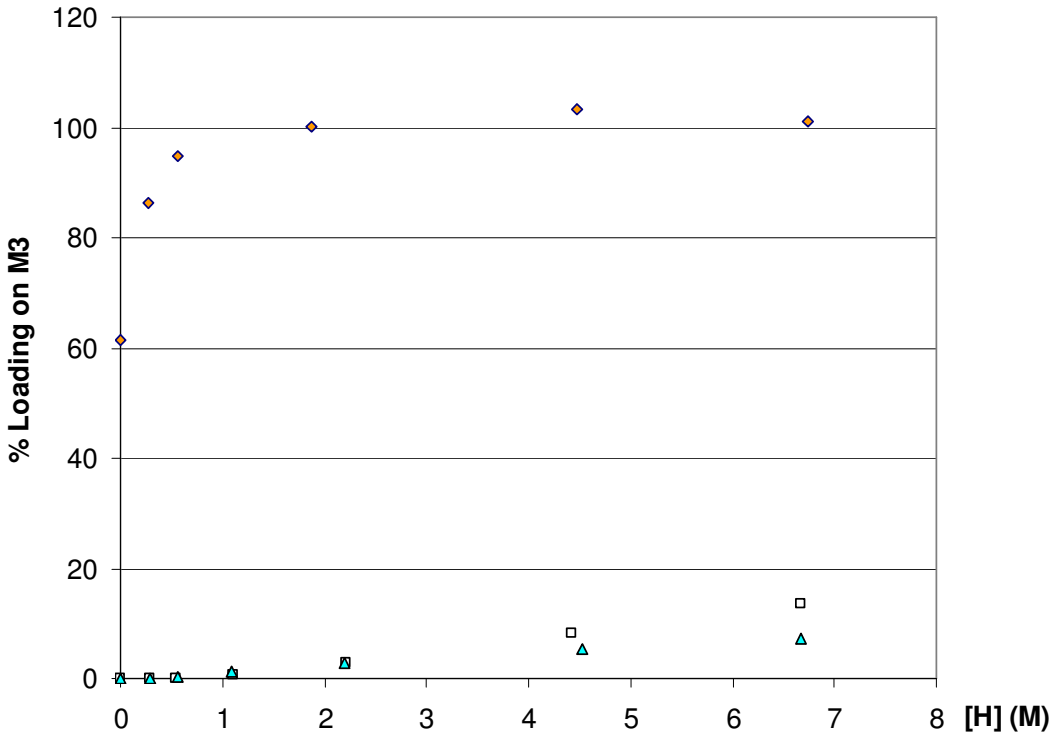


**Figure 5.8: The dependence of Fe(III), Zn(II) and Co(II) loadings* on proton concentrations, [H], in the feed solution by 0.01 M toluene solutions of $M^1$-$M^3$ after contact with an equal volume of aqueous chloride ($[Cl^-]$ = 8 M) solutions of 0.01 M $FeCl_3$, $CoCl_2$ or $ZnCl_2$.**
***based on the formation of $[(LH)FeCl_4]$ and $[(LH)_2MCl_4]$ (M = Co(II) or Zn(II))**

In all cases, the extractants $\mathbf{M^1}$-$\mathbf{M^3}$ show much higher loadings of Fe(III) than Zn(II) and Co(II). This can be ascribed at least in part to the *Hofmeister bias*[22, 23] (Chapter 1, Section 1.5.3), which implies that less highly charged monoanions, such as $FeCl_4^-$, are extracted more readily into non-polar water immiscible solvents than dianions, such as $CoCl_4^{2-}$ or $ZnCl_4^{2-}$.

At low proton concentrations, high Fe(III) loadings can be achieved without significant Co(II) or Zn(II) loading for all three ligands. At higher proton concentrations, only the secondary malonamide $\mathbf{M^2}$ shows total selectivity for Fe(III) over Zn(II) or Co(II). The observed maximum Fe(III) loading of only 90% for $\mathbf{M^2}$, as opposed to the 100% loadings observed for $\mathbf{M^1}$ and $\mathbf{M^3}$, is attributed to the lower selectivity of $\mathbf{M^2}$ for chlorometallate over chloride (see below).

## 5.8.2. Fe(III) Extraction and Transport Efficiency

If Fe(III) removal using the new malonamide reagents is to be viable, the ligands must show high extraction and transport *efficiency*. Figure 5.9 shows the extraction curves when aqueous solutions of 250 ppm Fe(III) in 8 M HCl are contacted with toluene solutions containing varying concentrations of $\mathbf{M^1}$-$\mathbf{M^3}$. The tertiary malonamides, $\mathbf{M^1}$ and $\mathbf{M^3}$, are highly efficient, both gaining ca. 95% Fe(III) extraction at a 1:1 ligand to Fe(III) ratio. The secondary malonamide, $\mathbf{M^2}$, is significantly less efficient, needing a 3:1 ligand to Fe(III) ratio to achieve comparable Fe(III) extraction. It is possible that this difference in solvent extraction *efficiency* between the secondary and tertiary malonamide ligands arises from the relative chloride vs chlorometallate *selectivities*.

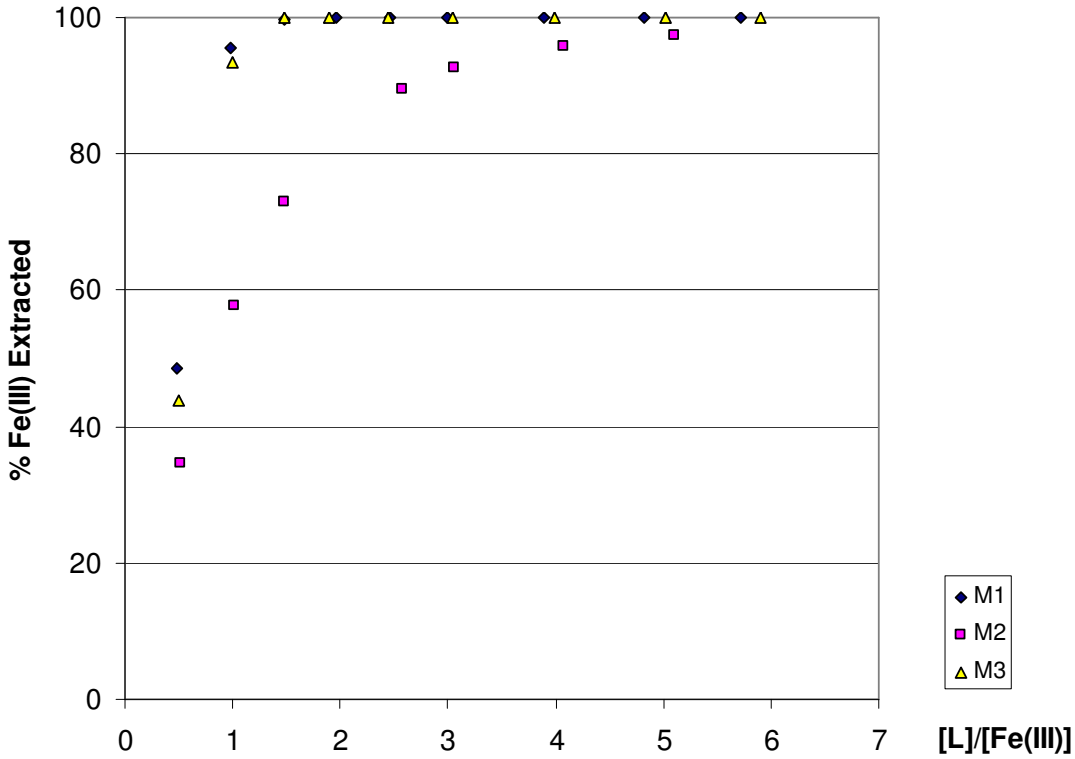


**Figure 5.9: The extraction of Fe(III) into toluene after contacting an equal volume of an aqueous solution of 250 ppm Fe(III) in 8 M HCl with toluene solutions of $\mathbf{M^1}$-$\mathbf{M^3}$ of ranging concentration.**

Conditions needed for stripping and recycling the reagents were investigated. As $\mathbf{M^1}$ is the *strongest* and most *efficient* extractant, this ligand was investigated in an

Fe(III) loading and stripping experiment. The results are shown in Figure 5.10 and it demonstrates that complete recovery of the metal value from the organic phase is possible by contacting with an equal volume of deionised water. High loadings of Fe(III) are maintained in consecutive load-strip cycles.

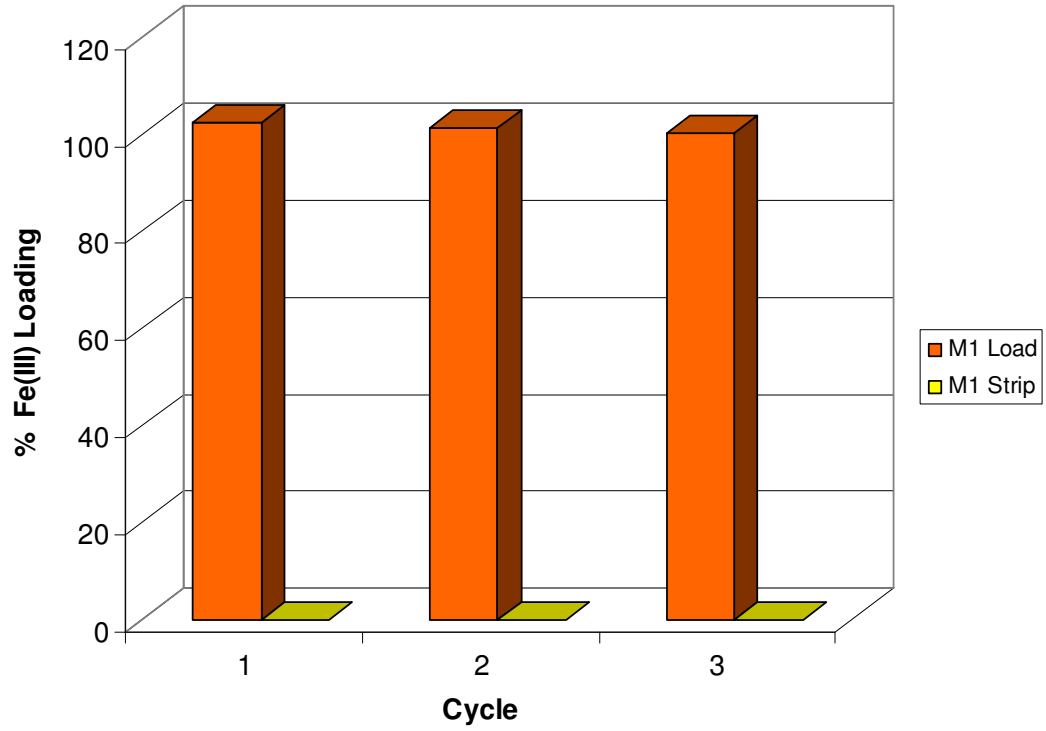


**Figure 5.10: Fe(III) loadings* before (orange) and after (yellow) stripping in three load-strip cycles for M[1]. Loading involved contacting 0.01 M ligand-toluene solutions with 8 M HCl solutions containing 0.01 M Fe(III) and stripping of the loaded organic contacting with an equal volume of deionised water.**

***based on the formation of [(LH)$FeCl_4$]**

## 5.8.3. Analysis of Iron and Chloride Loading on M[1]

Titration and $^1$H NMR studies undertaken by Costa *et. al.* have shown that addition of up to 4 protons per malonamide molecule is possible, so that 4 moles of HCl may be extracted per mole of malonamide.[13, 15] The extraction of a large excess of HCl would result in the depletion of HCl in the PLS and a build-up in the electrolyte, resulting in unfavourable materials balance. For this reason, the ratio of chloride to iron in the loaded organic phase needs to be defined. This involved contacting a 0.01

M solution of **M[1]** in toluene with an aqueous solution of 0.01 M Fe(III) in 8 M HCl, then separating the loaded organic phase and contacting it with NaOH solution to ensure complete stripping of all loaded species. The concentration of extracted metal and chloride was then established as described in Chapter 2, Section 2.3.7.

Table 5.1 displays the results for the [Fe(III)]/[$Cl^-$] analysis and calculates the concentrations of metal-bound chloride (assuming [$Cl^-$] bound = 4 x [Fe(III)]) and hence the concentration of 'free' chloride in the organic phase ([$Cl^-$] free = [$Cl^-$] total – [$Cl^-$] bound). Only a small amount of 'free' chloride is extracted relative to Fe(III), indicating a high selectivity of the ligand **M[1]** for $FeCl_4^-$ over $Cl^-$.

| [$M^1$] | [Fe(III)] | % loading | [$Cl^-$] total | [$Cl^-$] bound | [$Cl^-$] free |
|---|---|---|---|---|---|
| (mM) | (mM) | | (mM) | (mM) | (mM) |
| 9.33 | 9.37 | 100.43 | 37.90 | 37.46 | 0.44 |

**Table 5.1: Total analysis for [Fe(III)] and [$Cl^-$] loading on $M^1$.**

To further investigate the chloride vs $FeCl_4^-$ selectivity of **M[1]**, the dependence of chloride loading on proton concentration was monitored. This involved contacting 0.01 M solutions of **M[1]** in toluene with aqueous solutions containing variable amounts of HCl and an excess of chloride (8 M). The extracted chloride concentration was then analysed using the technique described in Chapter 2, Section 2.3.7.

Figure 5.11 compares the proton concentration dependence for chloride and $FeCl_4^-$ loadings. As expected, increased proton concentration results in increased chloride loadings. With no added proton (8 M LiCl solution), no chloride is loaded, while Fe(III) loading is above 90%, showing a high selectivity for $FeCl_4^-$ over chloride at low proton concentrations.

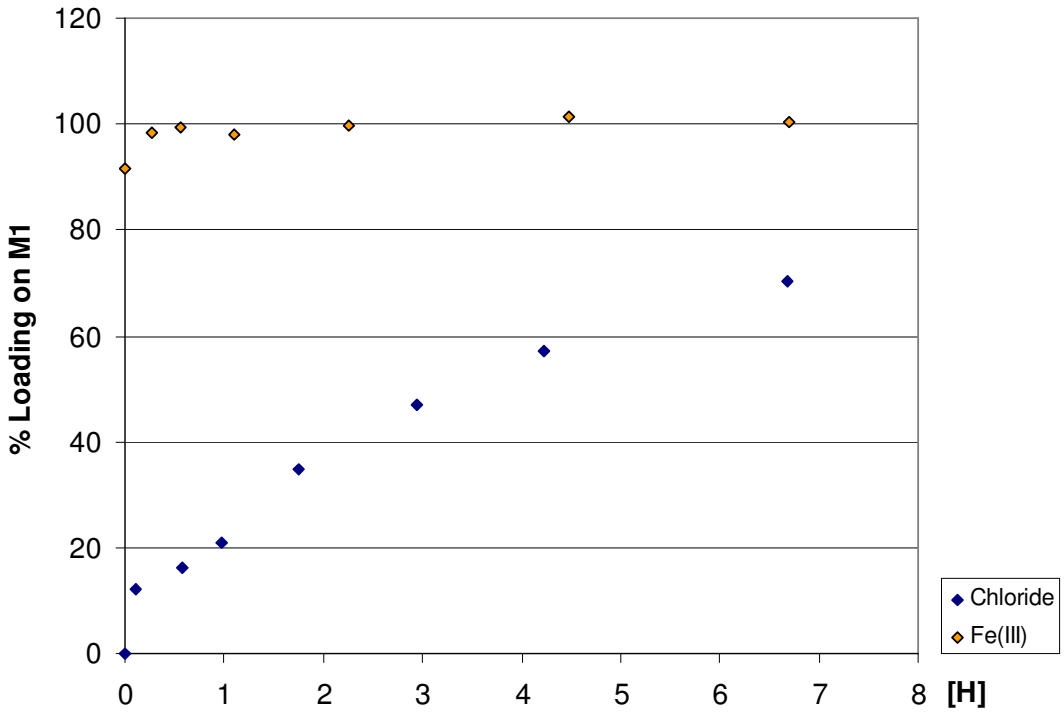


**Figure 5.11: The dependence of % loadings* of Fe(III) and $Cl^-$ on contacting toluene solutions of $M^1$ (0.01 M) with equal volumes of aqueous chloride solutions ($[Cl^-]$ = 8 M) or aqueous chloride solutions containing $FeCl_3$ (0.01 M, $[Cl^-]$ = 8 M).**

*** based on the formation of $[(LH)FeCl_4]$ and $[(LH)Cl]$**

## 5.9. Analysis of Anion-Host Interactions

The long alkyl chain functionality on the extractants **M$^1$**, **M$^2$** and **M$^3$** meant that crystallisation of extractant-chlorometallate complexes was not possible. In an attempt to circumvent this problem, a new malonamide **M$^3$X** (Figure 5.12), analogous to the extractant **M$^3$** but with a benzyl replacing the pentadecyl group, was used to aid crystallisation.

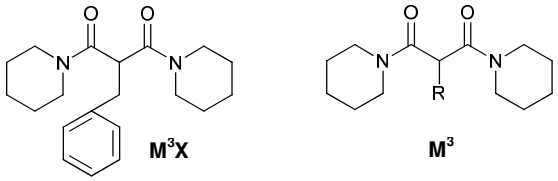


**Figure 5.12: The malonamide extractant analogues M$^3$X and M$^3$ (R = n-pentadecyl).**

Attempts to crystallise complexes of the type [(LH)$FeCl_4$] or [$(LH)_2MCl_4$] (M = Zn(II) or Co(II)) have so far been unsuccessful. A survey of the CSD yielded a structure of a protonated malonamide-tetrachlorocobaltate complex (Figure 5.13).[10] The authors discuss only the protonation of the malonamide and do not comment on the ligand-chlorometallate interaction. There are similarities to the structures of [(**L$^2$**H)$_2MCl_4$] (Chapter 3, Section 3.6) and [(**MAAX**H)$_2MCl_4$] (Chapter 4, Section 4.6) in that the proton interacts with both of the malonamide oxygens (although not equally strongly) and the ligand interacts with the outer-coordination sphere of the chlorometallate through an array of weak hydrogen bonds, namely C-H···Cl contacts. The strongest interaction between the malonamide and the $CoCl_4^{2-}$ is via a central malonamide C-H donor, which is consistent with its acidic nature shown by the tautomeric behaviour (see above).

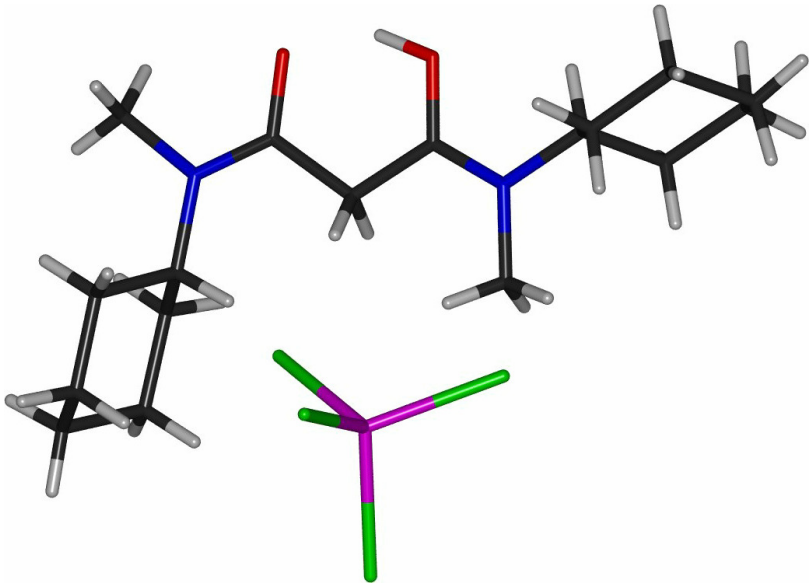

**Figure 5.13: The structure of $[(LH)_2CoCl_4]$ in the solid state where L = *N,N'*-dicyclohexyl-*N,N'*-dimethylmalonamide (the second ligand is omitted for clarity).[10]**

## 5.10. Conclusions and Future Work

We have shown that the extractants **M[1]**, **M[2]** and **M[3]** can be prepared on gram scales using facile, high yielding methods. The synthetic strategies employed have demonstrated the viability of large scale synthesis of malonamide extractants for commercial application.

Solvent extraction experiments have demonstrated that the reagents **M[1]**-**M[3]** have high selectivity for the recovery of Fe(III) over Zn(II) and Co(II) from acidic chloride feed solutions, with the greatest extraction *efficiency* and *strength* shown by **M[1]**. **M[1]** is highly selective for the $FeCl_4^-$ anion over chloride.

An analysis of the contacts in the solid state structure of a malonamide-tetrachlorocobaltate complex $[(LH)_2CoCl_4]$ (where L = *N,N'*-dicyclohexyl-*N,N'*-dimethylmalonamide)[10] confirms protonation of the malonamide oxygen atoms and interaction with the chlorometallate anion via a number of weak C-H hydrogen bond donors. This is consistent with the extractant-chlorometallate interactions observed in Chapters 3 and 4.

This preliminary study shows that the use of malonamides to recover Fe(III) from the Anglo American feeds might be a viable alternative to precipitation via pH adjustment if the resulting ferric chloride stripped solution is recycled. Future work in this area should focus on performing solvent extraction experiments on real feeds and assessing options for down-stream processing to further investigate the commercial viability of malonamides.

# 5.11. Experimental

General experimental details are given in Chapter 2, Section 2.5.

## 5.11.1. Synthesis

### 5.11.1.1. N,N'-dimethylhexylpentadecylmalonamide $M^1$

In a 100 mL round bottomed flask, methylhexylamine (4.32 g, 37.52 mmol) and methyl malonate (1.00 g, 7.50 mmol) were stirred at 90°C for 24 hrs then and concentrated on a rotary evaporator. To the residue, 60% NaH in mineral oil (0.32 g, 8.00 mmol) suspended in THF (100 mL) was cautiously added under $N_2$ via a pressure compensated addition funnel. The reaction mixture was stirred at ambient temperature and when hydrogen gas evolution had subsided 1-bromopentadecane (2.00 g, 6.89 mmol) in THF (30 mL) was added to the reaction mixture and refluxed for 3 hrs. The reaction mixture was concentrated on a rotary evaporator and the crude product was purified by column chromatography on silica gel using first 10 % and then 50 % diethyl ether in hexane to give the malonamide **$M^1$** (2.86 g, 75%) as a pale yellow oil. (Found: C, 75.95; H, 12.93; N, 5.95. $C_{33}H_{67}N_3O_2$ requires C, 75.53; H, 12.68; N, 5.51) $\delta_H$ (250 MHZ, $CDCl_3$) 1.01-1.19 (m, 9H, C*H*$_3$), 1.32-1.40 (m, 28H, C*H*$_2$), 1.62-1.86 (m, 4H, NCH$_2$C*H*$_2$), 2.06-2.19 (m, 2H, C*H*$_2$), 3.13 (s, 3H, C*H*$_3$), 3.21 (s, 3H, C*H*$_3$), 3.41-3.62 (m, 4H, NC*H*$_2$), 3.70-3.82 (m, 1H, C*H*); $\delta_C$ (250 MHz, $CDCl_3$) 14.2, 15.1, 16.4, 18.3, 23.4, 27.1, 29.6, 30.7, 32.1, 35.8, 36.6, 38.4, 49.3, 50.4, 170.7; *m/z* (ES) 509.83 ($M+H^+$).

### 5.11.1.2. *N,N'*-dihexylpentadecylmalonamide $M^2$

In a 250 mL round bottomed flask, 60% NaH in mineral oil (0.60 g, 15.00 mmol) was suspended in THF (100 mL) and methyl malonate (1.95 g, 14.74 mmol) was cautiously added under $N_2$ via a pressure compensated addition funnel. The reaction mixture was stirred at ambient temperature and, after hydrogen gas evolution had subsided, 1-bromopentadecane (4.33 g, 14.92 mmol) in THF (30 mL) was added to the reaction mixture and refluxed for 3 hrs. The reaction mixture was concentrated

on a rotary evaporator and the residue was dissolved in hexylamine (7.61 g, 75.23 mmol). The reaction mixture was stirred at 90°C for 24 hrs and then concentrated on a rotary evaporator. The crude product was purified by column chromatography on silica gel using 10% ether in hexane to give the malonamide **M2** (5.60 g, 79%) as a white solid. (Found: C, 75.25; H, 12.83; N, 5.33. $C_{33}H_{67}N_3O_2$ requires C, 74.94; H, 12.58; N, 5.83); $\delta_H$ (250 MHZ, $CDCl_3$) 0.81-0.97 (m, 9H, C*H*$_3$), 1.18-1.41 (m, 28H, C*H*$_2$), 1.41-1.60 (m, 4H, NCH$_2$C*H*$_2$), 1.75-1.90 (m, 2H, C*H*$_2$), 3.13 (t, 1H, C*H*), 3.21-3.30 (m, 4H, C*H*$_2$), 7.15 (t, 2H, N*H*); $\delta_C$ (250 MHz, $CDCl_3$) 14.7, 16.1, 16.6, 17.1, 18.4, 18.9, 22.4, 26.7, 27.9, 31.4, 33.2, 36.9, 37.2, 37.9, 48.6, 52.3, 171.9; *m/z* (ES) 481.65 ($M+H^+$).

### 5.11.1.3. *N,N*'-dipiperidylpentadecyl-malonamide $M^3$

In a 250 mL round bottomed flask, piperidine (9.00g, 105.88 mmol) and dimethyl malonate (2.74 g, 20.77 mmol) were stirred at 90°C for 24 hrs. The reaction mixture was concentrated on a rotary evaporator and to the residue 60% NaH in mineral oil (1.10 g, 27.50 mmol) suspended in THF (100 mL) was cautiously added under $N_2$ via a pressure compensated addition funnel. The reaction mixture was stirred at ambient temperature and, after hydrogen gas evolution had subsided, 1-bromopentadecane (7.29 g, 25.12 mmol) in THF (30 mL) was added to the reaction mixture and refluxed for 3 hrs. The reaction mixture was concentrated on a rotary evaporator and the crude product was purified by column chromatography on silica gel using first 10 % and then 50 % diethyl ether in hexane to give the malonamide $\mathbf{M^3}$ (7.08 g, 76%) as a pale yellow solid. (Found: C, 75.23; H, 12.13; N, 6.41. $C_{33}H_{67}N_3O_2$ requires C, 74.95; H, 11.68; N, 6.24); $\delta_H$ (250 MHZ, $CDCl_3$) 0.76-0.86 (m, 3H, C*H*$_3$), 1.12-1.33 (m, 30H, C*H*$_2$), 1.40-1.65 (m, 8H, NCH$_2$C*H*$_2$), 1.75-1.86 (m, 2H, C*H*$_2$), 3.25 (m, 9H, NC*H*$_2$, C*H*); $\delta_C$ (250 MHz, $CDCl_3$) 14.5, 19.5, 23.4, 25.6, 26.1, 27.6, 29.7, 30.3, 30.9, 32.3, 44.6, 47.9, 52.4, 169.6; *m/z* (ES) 449.35 ($M+H^+$).

### 5.11.1.4. *N,N*'-dipiperidylbenzyl-malonamide $M^3X$

In a 250 mL round bottomed flask, piperidine (9.04g, 106.22 mmol) and dimethyl malonate (2.51 g, 19.00 mmol) were stirred at 90°C for 24 hrs. The reaction mixture

was concentrated on a rotary evaporator and to the residue 60% NaH in mineral oil (1.10 g, 27.50 mmol) suspended in THF (100 mL) was cautiously added under $N_2$ via a pressure compensated addition funnel. The reaction mixture was stirred at ambient temperature and, after hydrogen gas evolution had subsided, benzyl bromide (7.89 g, 24.03 mmol) in THF (30 mL) was added to the reaction mixture and refluxed for 3 hrs. The reaction mixture was concentrated on a rotary evaporator and the crude product was purified by re-crystallisation from diethyl ether to give the malonamide **M$^3$X** (4.12 g, 66%) as white crystals. (Found: C, 73.16; H, 8.63; N, 8.51. $C_{33}H_{67}N_3O_2$ requires C, 73.14; H, 8.59; N, 8.53); $\delta_H$ (250 MHZ, $CDCl_3$) 1.19-1.40 (m, 12H, C*H*$_2$), 2.98-3.12 (m, 2H, NC*H*$_2$), 3.16 (d, 2H, CHC*H*$_2$), 3.20-3.35 (m, 4H, NC*H*$_2$), 3.51-3.65 (m, 2H, NC*H*$_2$), 3.86 (t, 1H, C*H*), 7.07-7.24 (m, 5H, Ar*H*); $\delta_C$ (250 MHz, $CDCl_3$) 24.7, 25.8, 26.3, 36.3, 43.6, 46.7, 50.5, 126.8, 128.8, 129.6, 139.8, 167.9; *m/z* (ES) 329.65 ($M+H^+$).

## 5.11.2. Solvent Extraction Experiments

### 5.11.2.1. Dependence of Loading on Proton Concentration

Aqueous metal chloride solutions (0.01 M $MCl_n$, 8 M $Cl^-$) of [$H^+$] ranging between 0 and 7 M were prepared by measuring 0.5 mL of $MCl_n$ solution (0.1 M $MCl_n$ in 8 M LiCl) into 5 mL volumetric flasks and adding variable quantities of 8 M HCl solution and diluting to the mark with 8 M LiCl solution. The aqueous phase aliquots were extracted with 0.01 M ligand solution in toluene and the phases were separated. Aliquots (1 mL) of the organic phases were transferred into 5 mL volumetric flasks, evaporated *in vacuo* and diluted to the mark with butan-1-ol for ICP-OES analysis.

### 5.11.2.2. Dependence of Fe(III) Loading on [L]

Ligand solutions were prepared as described in Chapter 2, Section 2.5.2.5. Ligand solutions were contacted with ferric chloride solution (250 ppm Fe(III), 8 M HCl). Aqueous samples for ICP-OES analysis were prepared by weighing 2 mL of the aqueous phase into 5 mL volumetric flasks diluted to the mark with deionised water.

#### 5.11.2.3. Fe(III) Load-Strip Experiment

The procedure outlined in Chapter 2, Section 2.5.2.6 was adapted to use an aqueous ferric chloride solution (15 mL, 0.01 M $FeCl_3$, 8 M HCl).

#### 5.11.2.4. Dependence of Chloride Loading on Proton Concentration

Aqueous metal chloride solutions (8 M $Cl^-$) of $[H^+]$ ranging between 0 and 7 M were prepared by measuring variable quantities of 8 M HCl solution into 5 mL volumetric flasks and diluting to the mark with 8 M LiCl solution. The aqueous phase aliquots were extracted with 0.01 M ligand solution in toluene and the phases were separated. Aliquots (3 mL) of the organic phases were stirred with aqueous NaOH solution (3 mL, 0.05 M) for 30 mins. The phases were separated and aliquots of the aqueous phases (0.5 mL) were mixed, in a darkened box, with aliquots (0.5 mL) of $AgNO_3$ (0.03 M) in $HNO_3$ (1 M) for 5 mins. The resulting AgCl precipitates were filtered off using a filter syringe and 0.5 mL aliquots of the filtrates were transferred into a 5 mL volumetric flasks and made up to the mark with 1 M $HNO_3$ for Ag(I) analysis by ICP-OES.

#### 5.11.2.5. Analysis for Fe(III) and Total Chloride Loadings

The procedure outlined in Chapter 2, Section 2.5.2.7 was adapted to use an aqueous ferric chloride solution (5 mL, 0.01 M Fe(III), 8 M HCl).

## 5.12. References

1. Sood, D. D.; Patil, S. K., Chemistry of nuclear fuel reprocessing: current status. *J. Radioanal. Nucl. Chem.,* **1996,** 203, (2), 547-573.

2. Pauling, L. C., *The Nature of the Chemical Bond and the Structure of Molecules and Crystals. An Introduction to Modern Structural Chemistry. 3rd ed.* **1960,** 644.

3. Tian, Q.; Hughes, M. A., Synthesis and characterization of diamide extractants for the extraction of neodymium. *Hydrometallurgy,* **1994,** 36, (1), 79-94.

4. Lefrancois, L.; Hebrant, M.; Tondre, C.; Delpuech, J.-J.; Berthon, C.; Madic, C., Z,E isomerism and hindered rotations in malonamides: an NMR study of N,N'-dimethyl-N,N'-dibutyl-2-tetradecyl-propane-1,3-diamidee. *J. Chem. Soc., Perkin Trans. 2,* **1999**, (10), 2231.

5. Hiratani, K.; Taguchi, K.; Ohhashi, K.; Nakayama, H., Highly selective solvent extraction of copper(II) from transition-metal ions with dibutyl N,N'-bis(8-quinolyl)malonamide. *Chem. Lett.,* **1989**, (11), 2073-6.

6. Musikas, C., Solvent extraction for the chemical separations of the 5f elements. *Inorg. Chim. Acta,* **1987,** 140, (1-2), 197-206.

7. Musikas, C.; Hubert, H., The extraction by N,N'-tetraalkylmalonamides. I. The perchloric and nitric acid extraction. *Solvent Extr. Ion Exch.,* **1987,** 5, (1), 151-74.

8. Musikas, C.; Hubert, H., Extraction by N,N'-tetraalkylmalonamides. II. Extraction of metallic ions. *Solvent Extr. Ion Exch.,* **1987,** 5, (5), 877-93.

9. Musikas, C.; Schulz, W. W.; Liljenzin, J.-O., Solvent extraction in nuclear science and technology. *Solvent Extr. Princ. Pract.,* **2004**, 507-557.

10. Chan, G. Y. S.; Drew, M. G. B.; Hudson, M. J.; Iveson, P. B.; Liljenzin, J.-O.; Skaalberg, M.; Spjuth, L.; Madic, C., Solvent extraction of metal ions from nitric acid solution using N,N'-substituted malonamides. Experimental and crystallographic evidence for two mechanisms of extraction, metal complexation and ion-pair formation. *J. Chem. Soc., Dalton Trans.,* **1997**, (4), 649-660.

11. Nigond, L.; Musikas, C.; Cuillerdier, C., Extraction by N,N,N',N'-tetraalkyl-2 alkyl propane-1,3 diamides. I. H2O, HNO3 and HClO4. *Solvent Extr. Ion Exch.,* **1994,** 12, (2), 261-96.

12. Spjuth, L.; Liljenzin, J. O.; Hudson, M. J.; Drew, M. G. B.; Iveson, P. B.; Madic, C., Extraction studies and ab initio calculations of some substituted malonamides. *Solvent Extr. 21st Century, Proc. ISEC '99, Barcelona, 1999,* **2001,** 1, 281-285.

13. Costa, M. C.; Carvalho, A.; Uryga, A.; Paiva, A. P., Solvent extraction of iron(III) from hydrochloric acid solutions using N,N'-dimethyl-N,N'-diphenylmalonamide and N,N'-dimethyl-N,N'-diphenyltetradecylmalonamide. *Solvent Extr. Ion Exch.,* **2003,** 21, (5), 653-686.

14. Costa, M. C.; Fernandes, C. E.; Hudson, M. J.; Iveson, P. B., Solvent extraction of base metal cations such as iron(III) from hydrochloric acid solutions using N,N'-substituted malonamides. *Solvent Extraction for the 21st Century, Proceedings of ISEC '99, Barcelona, 1999* **2001,** 1, 271-276.

15. Costa, M. C.; Martins, M.; Paiva, A. P., Solvent Extraction of Iron(III) from Acidic Chloride Media Using N,N'-Dimethyl-N,N'-dibutylmalonamide. *Separation Science and Technology* **2004,** 39, (15), 3573-3599.

16. Costa, M. C.; Peczek, I.; Sadowski, Z.; Natu, S.; Paiva, A. P., The Solvent Extraction of Iron(III) from Chloride Solutions by N,N'-Tetrasubstituted Malonamides: Structure-Activity Relationships. *Solvent Extr. Ion Exch.,* **2007,** 25, (4), 463-484.

17. Mowafy, E. A., Application of N,N'-Dimethyl-N,N'-Di(4-Chlorophenyl)Tetradecyl Malonamide for the Selective Recovery of Iron(III) from Concentrated Chloride Solutions. *Solvent Extr. Ion Exch.,* **2007,** 25, (6), 791-807.

18. Paiva, A. P.; Costa, M. C., Application of N,N'-tetrasubstituted malonamides to the recovery of iron(III) from chloride solutions. *Hydrometallurgy,* **2005,** 77, (1-2), 103-108.

19. Spjuth, L.; Liljenzin, J. O.; Hudson, M. J.; Drew, M. G. B.; Iveson, P. B.; Madic, C., Comparison of extraction behaviour and basicity of some substituted malonamides. *Solvent Extr. Ion Exch.,* **2000,** 18, (1), 1-23.

20. Harris, G. B.; Lakshmanan, V. I.; Sridhar, R. Leaching of laterite ores with acidic chloride solutions for recovery of metal values. *US Patent*, 2004228783, **2004**.

21. Stensholt, E. O.; Dotterud, O. M.; Henriksen, E. E.; Ramsdal, P. O.; Stalesen, F.; Thune, E., Development and practice of the Falconbridge chlorine leach process. *CIM Bull.,* **2001,** 94, (1051), 101-104.

22. Moyer, B. A.; Bonnesen, P. V., Physical factors in anion separations. *Supramol. Chem. Anions,* **1997**, 1-44.

23. Moyer, B. A.; Bonnesen, P. V.; Custelcean, R.; Delmau, L. H.; Hay, B. P., Strategies for using host-guest chemistry in the extractive separations of ionic guests. *Kem. Ind.,* **2005,** 54, (2), 65-87.

# CHAPTER 6

# CONCLUSIONS AND FUTURE WORK

At the outset of the work described in this thesis, the two main aims were:

1. to gain insight into the fundamental chemistry that underpins chlorometallate solvent extraction, and
2. to design new solvent extractant reagents for use in the Anglo American circuits to facilitate the separation of cobalt and zinc chlorometallates from iron.

To achieve the first, three series of new extractants were developed with different protonatable sites and varying hydrogen bond donor/acceptor functionality. The extractive properties were found to vary significantly across each ligand series and structural analysis in the solid state, in solution and by computational methods demonstrated the formation of outer-sphere complexes and that chlorometallate extraction is enhanced by

- the provision of a large number of weak hydrogen bond donors in the extractant rather than a smaller number of strong donors, and
- the stabilisation of the proton required to generate the cationic charge on the extractant through a 'chelate' interaction between the basic site and carbonyl oxygens present in amide groups.

This information was key to achieving the second aim and resulted in the development of the extractants **MAA** and **M*t*AA** (Chapter 4). These are considered to be best suited for use in the new Anglo American circuits as they,

- are easily synthesised from cheap and readily available starting materials,
- are soluble in toluene,
- can be stripped with water,
- have better *strength* and *efficiency* for $ZnCl_4^{2-}$ and $CoCl_4^{2-}$ extraction relative to the industrial bench mark **TEHA**, and
- show high $ZnCl_4^{2-}$ and $CoCl_4^{2-}$ loadings at pH above which Fe(III) precipitates.

The extractant **MAA** was shown to be the most effective ligand for $PtCl_6^{2-}$ extraction and ongoing studies have continued to reveal commercially useful features for this

reagent in the *concentration* and *separation* of PGMs.[1] The commercial potential for reagents of the MAA-type is demonstrated by interest from the reagent manufacturer Cytec and users, Anglo American and Johnson Matthey and has resulted in a patent application.

The new malonamide extractants, $\mathbf{M^1}$-$\mathbf{M^3}$ (Chapter 5), show high iron loadings across a range of proton concentrations while maintaining relatively low cobalt and zinc loadings and might, therefore, provide a viable alternative for iron removal to pH adjustment with new Anglo American flowsheets.

In achieving the aims outlined above, a greater understanding of the outer-sphere coordination chemistry was achieved. Of particular significance was the work involving the study of the series of pyridyl ligands $\mathbf{L^0}$-$\mathbf{L^4}$, which focused on the most efficient extractant $\mathbf{L^2}$. The solid state structure of $[(\mathbf{L^2}H)_2MCl_4]$ (M = Co(II) or Zn(II)) showed that 'proton chelation' involving the protonated pyridyl nitrogen and the malonamide oxygens results in a pre-organised array of two C-H and two N-H hydrogen bond donors that interact with a face of the tetrahedral anion. An NMR study of the zinc complex showed that this structure is maintained in the solution phase so that the 'proton chelation' and weak C-H and N-H interactions observed in the solid state are also present in solution and are, therefore, likely to be significant factors in the improved solvent extraction performance of $\mathbf{L^2}$ and other ligands in this study.

DFT calculations involving structural optimization and NBO calculations in the gas phase were used to explore further the properties of $\mathbf{L^0}$-$\mathbf{L^4}$. Calculations on the $[(\mathbf{L^2}H)_2MCl_4]$ (M = Co(II) or Zn(II)) complexes gave a similar structure to the solid state and confirmed the relative significance of the individual hydrogen bonding interactions. When other ligands in the series were studied in a similar way, it was found that the relative binding energies of the ligand-chlorometallate complexes provided a good model for predicting the relative *strengths* and *efficiencies* of the ligands.

The work presented in this thesis is of both academic and commercial significance and there are numerous possibilities for continued study. Of commercial interest would be the expansion of solvent extraction studies to define which reagents are best suited for development to meet the requirements of Anglo American flowsheets and 'real' feed solutions. This would involve working closely with the Anglo American team and preferably with reagent suppliers, such as Cytec, to develop a reagent which best meets the criterion defined in Chapter 1, section 1.8.2.

New tertiary amine reagents could be developed that might meet these criteria better. The work in this thesis shows that tertiary amide functionality (M*t*AA) gives the best *efficiency*, while additional carbonyl hydrogen bond acceptor functionality (DAA) gives the best *strength* when transporting base metal chlorometallates into water-immiscible organic solvents. Considering these factors, the ligand shown in Figure 1 is worthy of synthesis and testing.

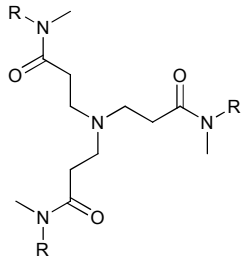

**Figure 1: Proposed new ligand T*t*AA (R = butyl).**

This ligand, T*t*AA, has three tertiary amide groups, presenting numerous C-H donors to interact with a chlorometallate anion. The tertiary amide functionality would also be expected to aid solubility. Synthesis could follow Scheme 1 which involves only volatile starting materials that may be removed *in vacuo* thus avoiding expensive chromatography or high temperature distillation. In addition, *N*-methylbutylamine is substantially cheaper than *N*-methylhexylamine (£37.97 for 1000 mL vs £50.33 for 10 mL)[2] T*t*AA may be expected to be *cheaper* to produce, *stronger*, more *efficient* and more *soluble* than the other tertiary amines presented in this thesis.

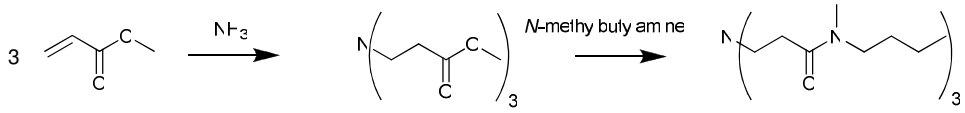


**Scheme 1: Suggested route to T*t*AA.**

The malonamide-ligands described in Chapter 5 could be developed further by expanding research into f-block metal extraction to assess their potential application in the DIAMEX process.[3] The malonamides may also be screened for their PGM chlorometallate extraction properties as amides are used for the *concentration* and *separation* of PGMs from highly acidic chloride solution by Johnson Matthey.[4]

The structural analysis of ligand-chlorometallate complexes in the solid, solution and gas phases is an area that should be extended more fully to the MAA-type and malonamide reagents in Chapters, 4 and 5. New solution-phase techniques, such as EDOR, might be used to further examine the ligand-chlorometallate assemblies in organic solvent.

A new methodology used in this thesis that might be developed further is the analysis of metallate extraction systems using computational modelling. The DFT calculations performed on the pyridyl ligands $\mathbf{L^0}$-$\mathbf{L^4}$ showed good agreement with experimental data, independently predicting the proton chelating interactions observed in the solid state structure of $[(\mathbf{L^2}H)_2MCl_4]$ (M = Co(II) or Zn(II)) and giving gas-phase interaction energies that reflect trends in extractant strength. The computational model used in this study to predict solvent extraction performance is simplistic and does not take into accounts many other factors, particularly solvation, which effect chlorometallate solvent extraction. Developing this model further, extending the software used to identify good anion receptors, e.g. HostDesigner,[5] could be an exciting area of academic and commercial interest in years to come.

# References

1. Henderson, D., *Unpublished Work,* University of Edinburgh, **2009**.

2. Aldrich, **2009**.

3. Musikas, C., Solvent extraction for the chemical separations of the 5f elements. *Inorg. Chim. Actam,* **1987,** 140, (1-2), 197-206.

4. Grant, R.; Belair; S., Refinery 2020, *Personal Communication*, Next Generation PM Solvex (Confidential), **2009**.

5. Hay Benjamin, P.; Firman Timothy, K., HostDesigner: a program for the de novo structure-based design of molecular receptors with binding sites that complement metal ion guests. *Inorg Chem,* **2002,** 41, (21), 5502-12.

# CHAPTER 7

# APPENDIX

The following files are located in the appendix CD.

**1.1:** Warr, R. J.; Westra, A. N.; Bell, K. J.; Chartres, J.; Ellis, R.; Tong, C.; Simmance, T. G.; Gadzhieva, A.; Blake, A. J.; Tasker, P. A.; Schroder, M., Selective Extraction and Transport of the $[PtCl_6]^{2-}$ Anion through Outer-Sphere Coordination Chemistry. *Chem.--Eur. J.,* **2009**, 15, (19), 4836-4850.

**1.2:** Ellis, R. J.; Chartres, J.; Sole, K. C.; Simmance, T. G.; Tong, C. C.; White, F. J.; Schröder, M.; Tasker, P. A., Outer-sphere amidopyridyl extractants for zinc(II) and cobalt(II) chlorometallates. *Chem. Commun.,* **2009**, (5), 583-5.

**1.3:** Bell Katherine, J.; Westra Arjan, N.; Warr Rebecca, J.; Chartres, J.; Ellis, R.; Tong Christine, C.; Blake Alexander, J.; Tasker Peter, A.; Schroder, M., Outer-sphere coordination chemistry: selective extraction and transport of the $[PtCl_6]^{2-}$ anion. *Angew Chem Int Ed Engl,* **2008**, 47, (9), 1745-8.

**2.1:** Determination of free chloride concentration in the presence of $PtCl_6^{2-}$ by Addition of $AgNO_3$

**2.2:** Hydrazine Removal

**2.2.1:** Procedure used to investigate the degradation of hydrazine by

different oxidising agents.

**2.2.2:** Procedure used to investigate removal of hydrazine into a different phase.

**2.2.3:** Procedure used to investigate the catalytic decomposition of hydrazine.

**2.2.4:** Procedure Used to Investigate the Removal of Hydrazine from Solution Using Evaporation.

**3.1:** pH Dependence Metal Loading Data for $\mathbf{L^0}$ to $\mathbf{L^4}$

**3.2:** Chloride Concentration Dependence Metal Loading Data for $\mathbf{L^0}$ to $\mathbf{L^4}$

**3.3:** Ligand Concentration Dependence Metal Loading Data for $\mathbf{L^0}$ to $\mathbf{L^4}$

**3.4:** Load-strip Data for $\mathbf{L^2}$

**3.5:** Crystal Structure Data for $[(L^2H)_2MCl_4]$

**3.6**: Data for DFT Calculated Optimised Structures of $L^0$-$L^4$

**4.1:** Attempted Synthesis of 3-(di-2-ethylhexylamino)-*N*-hexylpropanamide **MAA** via direct aminolysis of ester.

**4.2:** Attempted Synthesis of 3-(di-2-ethylhexylamino)-*N*-hexylpropanamide **MAA** via acyl chloride

**4.3:** Attempted Synthesis of 3-(di-2-ethylhexylamino)-*N*-hexylpropanamide **MAA** via Formation of Activated Ester using Coupling Reagent

**4.4:** Attempted Synthesis of 3-(di-2-ethylhexylamino)-N-methylhexylpropanamide **M*t*AA**

**4.5:** Attempted Synthesis of Di-*tert*-butyl-2-((bis(2-ethylhexyl)amino)methyl)malonate **11**

**4.6:** Attempted Synthesis of

3-(di-2-ethylhexylamino)methyl)-*N*-hexylmalonamide **MalA**[1]

**4.7:** Attempted Synthesis of Di-methyl-2-methylenemalonate

**4.8:** Attempted Synthesis of Di-*tert*-butyl-2-((di-2-ethylhexyl)amino)methyl)malonic acid

**4.9:** pH Dependence Metal Loading Data for **TEHA**, **MAA** etc

**4.10:** Chloride Concentration Dependence Metal Loading Data for **TEHA**, **MAA** etc

**4.11:** Ligand Concentration Dependence Metal Loading Data for **TEHA**, **MAA** etc in Toluene

**4.12:** Ligand Concentration Dependence Metal Loading Data for **TEHA**, **MAA** etc in Chloroform

**4.13:** Load-strip Data for **MAA** and **M*t*AA**

**4.14:** Ligand Concentration Dependence Pt(IV) Loading Data for

**TEHA**, **MAA** etc in Chloroform

**4.15:** Ligand Concentration Dependence Pt(IV) Loading Data for **TEHA**, **MAA** etc in Toluene

**4.16:** Crystal Structure Data for [(**MAAX**H)$_2$MCl$_4$]

**5.1:** Proton Concentration Dependence Metal Loading Data for **M**$^1$ to **M**$^3$

**5.2:** Ligand Concentration Dependence Fe(III) Loading Data for **M**$^1$ to **M**$^3$

**5.3:** Load-strip Data for **M**$^1$